



University of Kentucky  
UKnowledge

---

University of Kentucky Doctoral Dissertations

Graduate School

---

2006

## EFFECTS OF FOREST AND GRASS VEGETATION ON FLUVIOKARST HILLSLOPE HYDROLOGY, BOWMAN'S BEND, KENTUCKY

Linda Leann Martin  
*University of Kentucky*, [Linda.Geo@gmail.com](mailto:Linda.Geo@gmail.com)

[Right click to open a feedback form in a new tab to let us know how this document benefits you.](#)

---

### Recommended Citation

Martin, Linda Leann, "EFFECTS OF FOREST AND GRASS VEGETATION ON FLUVIOKARST HILLSLOPE HYDROLOGY, BOWMAN'S BEND, KENTUCKY" (2006). *University of Kentucky Doctoral Dissertations*. 362. [https://uknowledge.uky.edu/gradschool\\_diss/362](https://uknowledge.uky.edu/gradschool_diss/362)

This Dissertation is brought to you for free and open access by the Graduate School at UKnowledge. It has been accepted for inclusion in University of Kentucky Doctoral Dissertations by an authorized administrator of UKnowledge. For more information, please contact [UKnowledge@lsv.uky.edu](mailto:UKnowledge@lsv.uky.edu).

# ABSTRACT OF DISSERTATION

Linda Leann Martin

The Graduate School  
University of Kentucky

2006

EFFECTS OF FOREST AND GRASS VEGETATION  
ON FLUVIOKARST HILLSLOPE HYDROLOGY,  
BOWMAN'S BEND, KENTUCKY

---

ABSTRACT OF DISSERTATION

---

A dissertation submitted in partial fulfillment of the  
requirements for the degree of Doctor of Science in the  
College of Arts and Sciences  
at the University of Kentucky

By  
Linda Leann Martin

Lexington, Kentucky

Director: Dr. Jonathan D. Phillips, Professor of Geography

Lexington, Kentucky

2006

Copyright © Linda Leann Martin 2006

## ABSTRACT OF DISSERTATION

### EFFECTS OF FOREST AND GRASS VEGETATION ON FLUVIOKARST HILLSLOPE HYDROLOGY, BOWMAN'S BEND, KENTUCKY

Subsurface solutional pathways make limestone terrains sensitive to changes in soil properties that regulate flows to the epikarst. This study examines biogeomorphic factors responsible for changed water movements and erosion in fluviokarst slopes deforested 200 years ago along the Kentucky River, Kentucky. In this project, infiltration and water content data from forest and fescue grass soil profiles were analyzed within a detailed overview of system factors regulating hillslope hydrology. Results show that grass has growth and rooting characteristics that tend to create a larger volume of lateral water movement in upper soil layers than occurs under forests. This sets up the current emergent pattern of erosion in which water perches at grass slope bases and overwhelms pre-existing epikarst drainage.

Tree roots are able to cause solution at multiple discrete points of entry into fractures and bedding planes, increasing storage capacity and releasing sediment over time. Grass roots do not enter bedrock, and their rooting depth limits diffuse vertical preferential flow in root channels to above one meter. In the area's dense clay soils, flow under grass is conducted sideways either through the regolith or at the bedrock surface. Rapid flow along rock faces in hillslope benches likely moves fines via subsurface routes from the hillslope shoulders, causing the exposure of flat outcrops under grass. Lower growing season evapotranspiration also promotes higher grass summer flow volumes. Gullying occurs at sensitive points where cutters pass from the uphill grassed area into the forest, or where flow across the bedrock surface crosses grass/forest boundaries oriented vertical to the slope. At these locations, loss of the protective grass root mat, coupled with instigation of tree root preferential flow in saturated soils, causes soil pipes to develop.

Fluviokarst land management decisions should be based on site-specific slope, soil depth, and epkarst drainage conditions, since zones sensitive to erosion are formed by spatial and temporal conjunctions of a large number of lithologic, karst, soil, climate, and vegetation factors. This study shows that it is the composite of differing influences created by forest and grass that make forests critical for soil retention in high-energy limestone terrains.

KEYWORDS: Limestone Soil Erosion, Biogeomorphic Effects on Hydrology, Human Impacts, Fluviokarst Deforestation, Hillslope Hydrology

Linda Leann Martin

April 17, 2006

EFFECTS OF FOREST AND GRASS VEGETATION  
ON FLUVIOKARST HILLSLOPE HYDROLOGY,  
BOWMAN'S BEND, KENTUCKY

By

Linda Leann Martin

Dr. Jonathan D. Phillips  
Director of Dissertation

Dr. Anna Secor  
Director of Graduate Studies

April 17, 2006

## RULES FOR THE USE OF DISSERTATIONS

Unpublished dissertations submitted for the Doctor's degree and deposited in the University of Kentucky Library are as a rule open for inspection, but are to be used only with due regard to the rights of the authors. Bibliographical references may be noted, but quotations or summaries of parts may be published only with the permission of the author, and with the usual scholarly acknowledgments.

Extensive copying or publication of the dissertation in whole or in part also requires the consent of the Dean of the Graduate School of the University of Kentucky.

DISSERTATION

Linda Leann Martin

The Graduate School  
University of Kentucky

2006



EFFECTS OF FOREST AND GRASS VEGETATION  
ON FLUVIOKARST HILLSLOPE HYDROLOGY,  
BOWMAN'S BEND, KENTUCKY

---

DISSERTATION

---

A dissertation submitted in partial fulfillment of the  
requirements for the degree of Doctor of Science in the  
College of Arts and Sciences  
at the University of Kentucky

By  
Linda Leann Martin  
Lexington, Kentucky

Director: Dr. Jonathan D. Phillips, Professor of Geography  
Lexington, Kentucky

Copyright © Linda Leann Martin 2006

## ACKNOWLEDGMENTS

This dissertation was made possible by the scholastic and practical support supplied by the two principal members of my committee: my Dissertation Chair, Dr. Jonathan Phillips, and Dr. Alice Turkington, both physical geography professors in the Department of Geography at the University of Kentucky. They have both played invaluable roles as mentors, and I appreciate their willingness to help and their patience in offering advice. This work could not have been completed without them. I also wish to thank Dr. Daniel Marion, Dr. James Dinger, and Dr. Gary Shannon for agreeing to be on my committee, thereby placing themselves in the position of having to digest the reams of data that I have assembled for this project. Their forbearance and good-natured assistance have helped me through one of the roughest periods of my life. Along with my outside reader, Dr. David Moecher, I thank each and every one of you. In particular, I thank you, Dr. Phillips, for it was your unfortunate task to be forced to read the first versions, and the second, and the third, and you did it without complaint.

Funding for this study was provided by a Geologic Society of America Student Research Award in 2004, and by an Environmental Protection Agency Students To Achieve Results Fellowship for the years 2004-2005 and 2005-2006. Without this funding, I would not have been able to purchase the equipment used in this study, and I would not have been able to complete the hugely time-consuming task I set for myself. Having financial support allowed me to bury myself in this work for more than two years, and I only hope that I have produced results in some way worthy of that trust.

I also acknowledge the property access permission and information given to me so freely by employees of the Nature Conservancy, most particularly Dr. Julian Campbell, and by Vicki and Ken Brooks, owners of one of the most serenely beautiful landscapes in Kentucky. Ken and Vicki not only let me dig huge holes in their property and provided a permanent setting for my rain gauge, but also welcomed me into their home and were willing to share stories from their collected histories of Bowman's Bend. Thank you so much.

Not last, I thank those who have supported me personally. It's not easy being gone from the people you love. Thanks Kirk, and Nick, and Randy, and most of all Steve, who talked to me every night from far away.

# TABLE OF CONTENTS

|   |             |
|---|-------------|
| <b>ACKNOWLEDGMENTS</b> .....  | <b>III</b>  |
| <b>LIST OF TABLES</b> .....   | <b>VIII</b> |
| <b>LIST OF FIGURES</b> .....  | <b>IX</b>   |
| <b>CHAPTER 1 INTRODUCTION</b> .....                                   | <b>1</b>    |
| KARST LANDSCAPE SENSITIVITY .....                                     | 1           |
| LAND USE INFLUENCE ON KARST SOIL LOSS .....                           | 3           |
| STUDY OBJECTIVES .....  | 6           |
| METHODOLOGICAL APPROACH .....   | 6           |
| <b>CHAPTER 2 STUDY AREA</b> .....                                     | <b>8</b>    |
| LOCATION AND OVERVIEW .....   | 8           |
| LAND USE PATTERNS ON BOWMAN'S BEND .....                              | 12          |
| EROSION AND KARST FEATURES .....                                      | 19          |
| Karst Features .....  | 19          |
| Erosion Features.....   | 21          |
| <b>CHAPTER 3 THEORETICAL BACKGROUND</b> .....                         | <b>27</b>   |
| THE FLUVIOKARST LANDSCAPE.....  | 27          |
| Epikarst Development.....   | 28          |
| <i>Vegetation Effects</i> .....                                       | 29          |
| Regolith and Epikarst Interactions .....                              | 30          |
| HILLSLOPE HYDROLOGY .....   | 32          |
| Soil Properties.....  | 33          |
| Soil Anisotropy .....   | 34          |
| Water Movements on Slopes.....  | 35          |
| Preferential Flow .....   | 36          |
| Erosion Processes .....   | 37          |
| VEGETATION EFFECTS ON HYDROLOGY.....                                  | 39          |
| Evapotranspiration .....  | 39          |
| Water Infiltration and Movements .....                                | 41          |
| APPLICATION AND SUMMARY OF THEORETICAL CONCERNS.....                  | 45          |
| <b>CHAPTER 4 RESEARCH METHODS</b> .....                               | <b>48</b>   |
| SYSTEM DATA COLLECTION .....  | 48          |
| PHASE 1 RESEARCH – DETERMINING SOIL VARIABILITY .....                 | 49          |
| Particle Size Analysis of Sampled Profiles .....                      | 49          |
| <i>Particle Size Analysis Using Hydrometer Settling Tests</i> .....   | 51          |
| <i>Particle Density Determination</i> .....                           | 52          |
| <i>Problems and Corrections Applied During Texture Analysis</i> ..... | 53          |
| Soil Depth Measurements.....  | 58          |
| PHASE 2 RESEARCH – TESTING INFILTRATION RATES .....                   | 61          |
| Water Content Data Logging .....                                      | 61          |
| Infiltration Rate and Hydraulic Conductivity Determinations .....     | 62          |
| <i>Problems Associated With Infiltration Testing</i> .....            | 65          |
| Soil Profile Characterization.....                                    | 67          |

|   |           |
|---|-----------|
| <i>Bulk Density</i> .....   | 67        |
| <i>Porosity</i> .....   | 68        |
| <i>Tensiometer Measurement of Matric Potential</i> .....                        | 68        |
| Data Analysis .....   | 68        |
| <b>CHAPTER 5 THE LANDSCAPE SYSTEM ON BOWMAN'S BEND.....</b>                     | <b>71</b> |
| CLIMATE HISTORY AND RECENT EVENT-BASED EFFECTS .....                            | 71        |
| Climate History.....  | 72        |
| Local Climate Trends (1925-2005) .....  | 73        |
| Correlation of Tree Core Data with Climate Information .....                    | 77        |
| Event-Based Observations .....  | 79        |
| <i>May 2004</i> .....   | 80        |
| <i>September 18, 2004</i> .....   | 82        |
| <i>December 2, 2004</i> .....   | 83        |
| <i>February 5, 2005</i> .....   | 83        |
| Climate Summary .....   | 83        |
| GEOLOGICAL INFLUENCES .....   | 85        |
| Geologic Units.....   | 85        |
| Stratigraphy.....   | 88        |
| Structural Features .....   | 92        |
| Impermeable Layers .....  | 94        |
| Epikarst Development.....   | 97        |
| <i>Epikarst, Karren, and Conduit Interactions</i> .....                         | 97        |
| <i>Limestone Fragment Release</i> .....   | 101       |
| <i>Forest Gullies</i> .....   | 102       |
| Slope Profiles.....   | 105       |
| Geology Summary .....   | 108       |
| SOIL CHARACTERISTICS .....  | 108       |
| Parent Material.....  | 111       |
| <i>Residuum</i> .....   | 111       |
| <i>Alluvium</i> .....   | 114       |
| <i>Loess</i> .....  | 116       |
| Topographic Effects on Soil Development.....                                    | 117       |
| Soil Texture Relationships .....  | 119       |
| <i>Relationship of Bedrock Drainage to Particle Size Distribution</i> .....     | 119       |
| <i>Relationship of Texture to Source Materials and Surface Topography</i> ..... | 122       |
| Soil Series Mapping of Bowman's Bend .....                                      | 125       |
| Evidence of Water Movement.....   | 127       |
| <i>Gley</i> .....   | 127       |
| <i>Clay Films and Root Channels</i> .....                                       | 128       |
| <i>Discolorations Associated With Rock Surfaces</i> .....                       | 131       |
| Soils Summary.....  | 135       |
| BIOGEOMORPHIC EFFECTS .....   | 136       |
| Hillslope Stabilization .....   | 136       |
| Concentrated Sediment Movement along Tree Roots .....                           | 137       |
| Root Interaction With Bedrock .....   | 140       |
| <i>Grass Roots</i> .....  | 141       |
| <i>Tree Roots</i> .....   | 146       |
| <i>Bedrock Layer Breakdown by Tree Roots</i> .....                              | 150       |
| <i>Evidence for Historical Tree Root Action</i> .....                           | 156       |
| Macropores .....  | 161       |

|  |            |
|--|------------|
| Summary of Biogeomorphic Root Effects .....  | 162        |
| <b>CHAPTER 6 HILLSLOPE HYDROLOGY .....</b>   | <b>164</b> |
| INFILTRATION TEST RESULTS .....  | 164        |
| Factors Conducive to Infiltration .....  | 164        |
| General Infiltration Rate and Hydraulic Conductivity Data by Depth.....                | 167        |
| HYDROLOGIC DATA ANALYSIS .....   | 170        |
| Variables .....  | 170        |
| Augered Soil Sample Analysis.....  | 171        |
| Analysis of Infiltration Data .....  | 174        |
| a) <i>Distributions</i> .....  | 174        |
| b) <i>Variable Associations</i> .....  | 176        |
| c) <i>Clay vs.Organic Matter and Porosity</i> .....                                    | 181        |
| d) <i>Infiltration Comparisons by Vegetation Types</i> .....                           | 186        |
| Grass Surface Infiltration Test Results.....   | 190        |
| Soil Moisture .....  | 192        |
| <i>Observational Evidence for Preferential Tree Root Flow</i> .....                    | 192        |
| <i>Water Content Data Logging</i> .....  | 193        |
| Hillslope Hydrology Summary.....   | 210        |
| <b>CHAPTER 7 SUMMARY AND SYNTHESIS .....</b>   | <b>214</b> |
| SYSTEM CONNECTIONS .....   | 214        |
| Key System Variable Effects.....   | 214        |
| 1. <i>Climate – Establishing When Erosion Occurs</i> .....                             | 215        |
| 2. <i>Geology – Where Erosion is Likely to Occur</i> .....                             | 216        |
| 3. <i>Soils – How Vegetation Sets Up Pathways of Water Movement</i> .....              | 217        |
| 4. <i>Vegetation Influences – Why Current Patterns of Erosion Have Developed</i> ..... | 221        |
| Water Movement Pathways .....  | 223        |
| 1. <i>Soil Texture</i> .....   | 223        |
| 2. <i>Root Pathways</i> .....  | 225        |
| 3. <i>Gullies and Conduits</i> .....   | 226        |
| 4. <i>Rock Face Pathways</i> .....   | 227        |
| INFILTRATION PATTERNS .....  | 230        |
| Soil Wetting Differences.....  | 230        |
| Comparison of Forest and Grass Infiltration Patterns .....                             | 234        |
| Preferential Flow .....  | 235        |
| Development of Pathways over Time .....  | 236        |
| FUTURE CONSIDERATIONS.....   | 236        |
| Native Grass Influence and Future Management .....                                     | 237        |
| Importance of Rock Pathways .....  | 238        |
| Organic Influence on Surface Movements .....   | 238        |
| Surface Sediment Movement.....   | 239        |
| Preferential Flow .....  | 239        |
| CONCLUSIONS .....  | 240        |
| Implications for Soil Retention in Other Fluviokarst Regions .....                     | 243        |
| Broader Implications .....   | 245        |
| <b>APPENDIX 1 AERIAL PHOTOGRAPHS UTILIZED IN THIS STUDY .....</b>                      | <b>247</b> |
| <b>APPENDIX 2 DIGITAL DATA SETS UTILIZED IN THIS STUDY .....</b>                       | <b>251</b> |

|   |            |
|---|------------|
| <b>APPENDIX 3 SOIL PROFILE DESCRIPTIONS .....</b>                     | <b>253</b> |
| <b>APPENDIX 4 PARTICLE SIZE PERCENTAGES AND TEXTURE CLASSES .....</b> | <b>270</b> |
| <b>APPENDIX 5 DATA USED IN STATISTICAL ANALYSES .....</b>             | <b>281</b> |
| <b>REFERENCES.....</b>  | <b>287</b> |
| <b>VITA .....</b>   | <b>301</b> |

## LIST OF TABLES

|            |  |         |
|------------|--|---------|
| Table 4.1  | Particle Density and Organic Content Determinations for Infiltration Test Pits ..... | 54      |
| Table 4.2  | Comparisons between Estimated and Sieved Sand Weight Percentages .....               | 57      |
| Table 4.3  | Infiltration Test Variable Frequency .....   | 70      |
| Table 5.1  | pH Values for Infiltration Pits 1 and 2.....   | 112     |
| Table 5.2  | SSURGO Soil Series Properties .....  | 113     |
| Table 5.3  | Minimum and Maximum Infiltration Pit Soil Depths According to Elevations .....       | 118     |
| Table 6.1  | Mean Infiltration and Conductivity Values .....                                      | 168     |
| Table 6.2  | Comparison of Mean Forest and Grass Clay Percentages by Depths .....                 | 171     |
| Table 6.3  | Correlations for Total Forest Data Sets .....  | 179     |
| Table 6.4  | Correlations for Total Grass Data Sets .....   | 180     |
| Table 6.5  | Bivariate Linear Fit of Clay vs. Organics and Porosity by Depths.....                | 182     |
| Table 6.6  | Correlations of Organics According to Partitions .....                               | 185     |
| Table 6.7  | Probabilities of Differences between Forest and Grass Infiltration .....             | 189     |
| Table 6.8  | Soil Moisture Responses to Hurricane Katrina Events .....                            | 196-197 |
| Table 6.9  | Soil Moisture Responses to Storm Events.....   | 201-202 |
| Table 6.10 | Forest Water Content Measurements on January 17-18, 2006 .....                       | 206     |
| Table 6.11 | Forest Water Content Measurements on January 22-23, 2006 .....                       | 207     |
| Table 7.1  | Spatial and Temporal Factors Regulating Hillslope Hydrology .....                    | 241     |

## LIST OF FIGURES

|  |         |
|--|---------|
| Figure 2.1. Study area map.....  | 9       |
| Figure 2.2. Contour map of study area .....  | 10      |
| Figure 2.3. View north along the bend .....  | 11      |
| Figure 2.4. Aerial photos taken in 1937 (a) and 1990 (b) .....                       | 14      |
| Figure 2.5. Aerial photographs from 1960 (a) and 1966 (b).....                       | 15-16   |
| Figure 2.6. Large chinquapin oak .....   | 17      |
| Figure 2.7. Slopes are exposed to erosion following winter burns.....                | 18      |
| Figure 2.8. Large sink on the north end of the bend .....                            | 20      |
| Figure 2.9. Broad, shallow swale on the east side of the bend.....                   | 21      |
| Figure 2.10. Erosion and karst features on Bowman’s Bend, Kentucky. ....             | 22      |
| Figure 2.11. Root overhang above a moderate-sized gully .....                        | 23      |
| Figure 2.12. Prime areas for surface scour.....                                      | 24      |
| Figure 2.13. Soil pipes are associated with root overhangs at gully heads.....       | 25      |
| Figure 2.14. Seepage and pipe flow occurs below overhangs.....                       | 26      |
| Figure 2.15. Tree root exposed in gully base.....                                    | 26      |
| Figure 4.1. Locations of all slopes sampled during the project.....                  | 50      |
| Figure 4.2. Soil sampling sites.....   | 51      |
| Figure 4.3. Locations of soil depth measurement transects .....                      | 59      |
| Figure 4.4. Soil depth transect locations in the main study area .....               | 60      |
| Figure 4.5. Infiltration test pit and surface run sites .....                        | 63      |
| Figure 5.1. Dix Dam annual precipitation totals since 1925.....                      | 74      |
| Figure 5.2. Annual number of 24-hour precipitation events >1 inch (25.4 mm).....     | 75      |
| Figure 5.3. Annual number of 24-hour precipitation events > 2 inches (50.8 mm) ..... | 75      |
| Figure 5.4. Annual number of weekly precipitation events >4 inches (101.6 mm).....   | 76      |
| Figure 5.5. Mature trees positioned at the head of a gully.....                      | 77      |
| Figure 5.6. Double-headed gully.....   | 78      |
| Figure 5.7. Diagram of core #3 .....   | 79      |
| Figure 5.8. Small animal burrows function as exfiltration pathways.....              | 81      |
| Figure 5.9. Soil pipe opened through exfiltration pressure .....                     | 81      |
| Figure 5.10. Soil cover collapse pit opening .....                                   | 82      |
| Figure 5.11. Geology of Bowman’s Bend .....  | 86      |
| Figure 5.12. Alluvial sediments .....  | 87      |
| Figure 5.13. Geologic profiles .....   | 89-90   |
| Figure 5.14. Shallow linear depressions overlying epikarstal conduits.....           | 93      |
| Figure 5.15. Relict shaft below Hillslope A.....                                     | 96      |
| Figure 5.16. Downslope continuation of cutters.....                                  | 99      |
| Figure 5.17. Outcrops and swallets in the depression of a slope managed by fire..... | 100-101 |
| Figure 5.18. Rock fragment lines in soil depth transects on Hillslope J .....        | 102     |
| Figure 5.19. Forest gully .....  | 103     |
| Figure 5.20. Gully buried by soil under grass .....                                  | 104     |
| Figure 5.21. Hillslope A soil depth and ground surface profile.....                  | 106     |
| Figure 5.22. Water pools at the grassed base of Hillslope I .....                    | 107     |
| Figure 5.23. Soil series mapped on Bowman’s Bend .....                               | 109     |
| Figure 5.24. Main study area soil units .....  | 110     |
| Figure 5.25. Particle size distributions determined by layers for location B5.....   | 116     |
| Figure 5.26. Transects on Hillslope H.....   | 117     |
| Figure 5.27. Particle size distributions for soil sample site A7 .....               | 121     |
| Figure 5.28. Particle size percentages on Hillslope F.....                           | 123     |



|   |         |
|---|---------|
| Figure 5.29. Dark organic stains distinguish vertical grass root pathways.....                  | 129     |
| Figure 5.30. Large bands of discoloration underlie roots in pit 7. ....                         | 130     |
| Figure 5.31. Darker soil underlies a decayed root found at 85 cm .....                          | 131     |
| Figure 5.32. Dark gray soil film is revealed under a stone fragment in pit 5 .....              | 133     |
| Figure 5.33. Soil discoloration from contact with limestone in forest pit 5.....                | 133     |
| Figure 5.34. Soil surrounding a limestone fragment removed from pit 12 .....                    | 134     |
| Figure 5.35. Tree roots capture colluvial sediment on Hillslope F. ....                         | 138     |
| Figure 5.36. Exhumation of a large tree in a conduit on the north side of the bend .....        | 139     |
| Figure 5.37. Swallet opening at the base of a tree is connected to a soil pipe .....            | 140     |
| Figure 5.38. Fibrous root mat in soil removed from pit 13.....                                  | 142     |
| Figure 5.39. Fine roots emerge from beneath a tilted boulder in pit 10.....                     | 142     |
| Figure 5.40. Bedrock plates under grass display a roughened, subangular surface. ....           | 143     |
| Figure 5.41. Coarse roots emerge from openings in the rock bench walls in forest pit 8 .....    | 144     |
| Figure 5.42. Likely sequence of grass root mat exploitation of limestone bench walls.....       | 145     |
| Figure 5.43. A 2 cm root applies pressure along a fracture line at 75 cm in pit 5.....          | 146     |
| Figure 5.44. Root grooving caused by root entry into a fracture .....                           | 147     |
| Figure 5.45. Large scale root groove forms suggested by features of Tyrone outcrops.....        | 148     |
| Figure 5.46. Notch in a limestone plate fits tree root bend in pit 7 .....                      | 149     |
| Figure 5.47. Lifted limestone slab lies several meters uphill from pit 6.....                   | 150     |
| Figure 5.48. Exposure of bedrock along the grassed shoulder of the main study area. ....        | 151     |
| Figure 5.49. Transects matched for elevation on the main study area shoulder .....              | 152     |
| Figure 5.50. Decomposition of thin limestone layers by root action over time. ....              | 154     |
| Figure 5.51. Bedrock fracturing on the upper forest sideslope .....                             | 155     |
| Figure 5.52. A young tree establishes itself in a fracture in the bedrock near a large oak..... | 156     |
| Figure 5.53. Root forms at the epikarst surface .....   | 158     |
| Figure 5.54. Bedrock forms suggest possible root grooving .....                                 | 160     |
| Figure 5.55. Hole exposed at 75-80 cm in pit 11 .....   | 161     |
| Figure 6.1. Factors regulating infiltration.....  | 165     |
| Figure 6.2. Numerous macropore sources exist within soil.....                                   | 165     |
| Figure 6.3. Pit 14 infiltration tests at 55 cm .....  | 166     |
| Figure 6.4. Distributions of combined clay percentages .....                                    | 172     |
| Figure 6.5. Analysis of percent clay in soil above bedrock by drainage categories. ....         | 173     |
| Figure 6.6. Distributions of total forest and grass values by depths.....                       | 175-176 |
| Figure 6.7. Linear regression tests of clay vs. organics and porosity .....                     | 183     |
| Figure 6.8. Clay percent vs. organics. ....   | 184     |
| Figure 6.9. T-test (2-tailed) between-group differences for infiltration rates .....            | 187     |
| Figure 6.10. Example of soil depths determined under the area of the infiltrometer disk .....   | 190     |
| Figure 6.11. Comparison of surface K(-3) values by soil depth categories.....                   | 191     |
| Figure 6.12. Saturated soil layers found within an 8 m distance of a tree. ....                 | 193     |
| Figure 6.13. Soil water content changes during Hurricane Katrina storms.....                    | 195     |
| Figure 6.14. Early winter soil water content response to rainfall.....                          | 200     |
| Figure 6.15. Soil moisture changes December 24 through January 26.....                          | 204     |
| Figure 6.16. Flat grass mV readings at 125 cm on January 27 .....                               | 208     |
| Figure 7.1. Simplified cross-section of soil pit 13.....  | 219     |
| Figure 7.2. Simplified cross-section of epikarstal drainage under pit 12.....                   | 220     |
| Figure 7.3. Tree roots enter weakened zones in the epikarst.....                                | 222     |
| Figure 7.4. Forest water movements during dry, leaf-on conditions .....                         | 231     |
| Figure 7.5. Forest water movements during wet, leaf-off conditions .....                        | 232     |
| Figure 7.6. Main features of grass water movements.....   | 232     |

# CHAPTER 1

## INTRODUCTION

### KARST LANDSCAPE SENSITIVITY

This project examines the changes in hillslope hydrology created by the effects of long-term grass cover that appear to be responsible for erosion in a humid temperate fluviokarst landscape bordering the Kentucky River. In the Bowman's Bend area of Garrard County, Kentucky, the Kentucky River downcuts some 100 meters into the mature karst of the inner Bluegrass, truncating flat-lying limestone stratal layers that each support differing forms of epikarst, shaft, and sinkhole development. The river escarpment is edged by deciduous forest, but the inner bend area was cleared for crop and pasture in the early 1800's, forming a grassland/forest boundary at the bases of 8 to  $>16^\circ$  grassed slopes. Changes in hillslope soil water movements caused by both recent management and emergent long term grass cover effects appear to be operating concurrently at topographically and geologically sensitized locales along this grassland/forest boundary. Where the sod cover is lost at the edge of the forest in locations overlying convergent soil/bedrock interface flow, shallow incisions and exhumation of cutters are frequent. To develop an understanding of this emergent erosion pattern, this project works within an earth surface system framework in which overlapping lines of field and laboratory measurement are placed within a broader exploration of climatic, historical, and biogeographic variables pertinent to system evolution. In particular, focus has been placed on determining how the shift from forest to grass cover has sponsored the biogeomorphic changes in soil profile characteristics, infiltration rates, and bedrock penetration that may be causing recent erosion.

In sensitive landscapes, geomorphic response may occur where processes have low resistance to disturbance, operate very close to threshold boundaries, or are part of an inherently dynamically unstable system structure (Phillips, 1996, 2003, 2004; Harvey, 2001; Thomas, 2001; Burt, 2001). Investigations at Bowman's Bend indicate that all three conditions may operate in this fluviokarst landscape (Phillips, et al., 2004), so that small, incremental changes in soil properties induced by long-term grass cover may now be leading to subsurface water flow shifts within a landscape that is already susceptible to sediment movement. Because calcium is easily weathered from carbonate bedrocks by acid solution under normal humid climate conditions, karst landscapes that form in limestone/dolomite terrains develop water

movement pathways that focus groundwater into solutionally-opened joints and fissures (White, 2002). As karst landscapes mature, solutional pathways expand, transporting sediment through the dissolving bedrock networks and constructing sinkhole and shaft features visible from the surface (Sweeting, 1973; Smith, et al., 1976; Jennings, 1983; White and White, 1995). Because sediments erode through both surface runoff and subsurface entrainment processes, karst regions are particularly sensitive to the hydraulic effects of differing land uses and vegetation covers (Williams, 1993).

The initial movements of water into fractures are governed by vadose zone processes occurring in the regolith and epikarst, which is the fractured and partially decomposed bedrock surface directly underlying the soil in a karst terrain. Fluviokarst catchments, found where surface and subsurface pathways operate competitively, deliver most of their baseflow through dissolved bedrock pathways rather than through ephemeral surface streams, making these regions particularly sensitive to loss of infiltration capacity and shifts in sediment and flow regimes (Lastennet and Mudry, 1996; Ahmed and Carpenter, 2003). The amount and timing of meteoric water inputs into bedrock pathways are thus dependent on the series of factors such as soil composition, porosity, and permeability that control hillslope hydrologic conductivity (Petts and Amoros, 1996; Tindall et al., 1999).

Because distinct physical, chemical, and hydraulic soil profile characteristics develop over time under the influence of established plant communities (Birkeland, 1984), karst headwater features and the surface streams and aquifers they support are dependent on biologically influenced soil properties that evolve in concert with local hillslope topography, lithology, and land use history. Organic matter accumulation, physical and chemical soil properties, surface protection, support of soil fauna, and hydraulic patterns all realign within the climatic and topographic parameters of the system once a landscape is deforested. Channel incision and degradation in karst areas can be readily associated with human impact (Jacobson, 1995; Jacobson and Pugh, 1996), but little research has focused on the important relationships between particular vegetative covers and their abilities to maintain infiltration pathways in karst hillslopes. Research in this project seeks to expand this little understood area of knowledge through comparative study of soil and soil water movement characteristics as they have evolved over the past 200 years in the Bowman's Bend slopes.

The influence of different forms of vegetation on erosion are poorly understood in general (Thornes, 1985), and the mix of overlaying historical variables, plus the slow rate at which most regolith changes proceed (Trimble, 1990), make it difficult to determine direct geomorphic links between differing vegetation covers and soil stability in karst terrains. This

lack of specific information limits planning for land use management of limestone regions. It is felt that findings from this project will help to both inform sustainable management practices on inner Bluegrass slopes and to provide a broadened perspective for soil loss and management planning issues occurring in other karst landscapes. These findings should also widen our theoretical understanding of how complex variable interactions act together to generate threshold crossings within sensitive geomorphic terrains.

## **LAND USE INFLUENCE ON KARST SOIL LOSS**

Limestone and dolomite underlie some 12 percent of the earth's dry land area (Ford and Williams, 1989) and make up as much as 15% of the conterminous area of the United States (McKnight and Hess, 2002). Although some of these carbonate bedrocks exist in dry or arctic areas not conducive to solution, karst landscapes still cover between 7 and 10% of the earth's surface (Ford and Williams, 1989), making them important landscape terrains in terms of human occupancy.

That occupancy has not always had benign effects. A solid body of archeological research shows that karst pavements composed of broad areas of bare, fissured limestone now exist in regions of the world that once supported prehistoric agricultural communities (Bell and Limbrey, 1982). Although bare rock surfaces provide only limited sources of palaeoenvironmental evidence (Crabtree, 1982; Waton, 1982), strong cultural evidence for prior human occupation of what are now stone deserts is present in places as diverse as Yorkshire, Lebanon, Mallorca, and the Causses limestone plateaus of the Mediterranean (Drew, 1982). In the Burren of western Ireland, dwellings, stone walls, and burial mounds are built over remnants of mineral soils that disappeared from the surrounding rock plateau some three to four thousand years ago (Drew, 1982; Drew, 1983).

Although some researchers have credited karst pavement development to glacial planation (Williams, 1966; Trudgill, 1985), others have associated limestone soil loss to the effects of deforestation and subsequent agricultural practices (Bell and Limbrey, 1982; White, 1988; Williams, 1993; Gams, et al., 1993; Zseni, 2002). Processes of soil erosion that occur irrespective of bedrock type in association with runoff increases related to row-cropping are in general well understood (Trimble, 1988; Thornes, 1990; Boardman, 1993; Phillips, 1997a; Knox, 2001), and erosion in some limestone terrains can be directly associated with farming practices that expose bare soil surfaces, cause soil compaction, and concentrate surface flow on steep slopes. Dicken (1938) described the filling of western Kentucky sinkholes by more than 25 feet

of topsoil via sheet-wash and gully movement from surrounding fields cultivated sporadically since European settlement.

Even if direct effects of agricultural practices are deleted from the limestone soil loss equation, significant confusion still exists as to just what factors, and what properties of those factors, are most responsible for limestone erosion under differing vegetative covers. White (1988) states that “root systems from forest, brush, and grass cover retard soil loss into the solution cavities” (p 355), and claims that pavement karsts of semiarid regions around the Mediterranean were created by soil loss caused by overgrazing and subsequent loss of all types of vegetative cover. In the same passage he also ascribes development of Yucatan karst deserts to Mayan slash-and-burn farming that replaced jungle with crops and thus induced subsurface soil loss. Although White (1988) clearly associates limestone denudation to human land use changes, he lumps the influences of vegetative covers into a single category. However, simple vegetation shifts, such as from forest to long term grass cover, also change processes within karst regoliths. Some researchers have suggested that it is the act of deforestation, as opposed to effects of subsequent land use, that may be most responsible in some areas for limestone soil destabilization and loss (Ford and Drake, 1982; Drew, 1983, Williams, 1993; Daoxian, 1993).

Trudgill (1985) discusses pinnacle epikarst forms revealed in New Zealand pastures that are hidden by 10-20 cm of acid organic matter in native forests. Trudgill (1985) also suggests that mesolithic and iron age deforestation may have caused loss of thin organic soils in regions shown to support co-existing soil-free limestones and soil covered terrains of other bedrock types. Herak (1972, p. 75), in referring to the accumulative hydrogeologic and root stabilization effects of forest growth, stated that in the degraded Dinaric karst area of former Yugoslavia, “only forests can restore and increase soil productivity.”

These sometimes confused historical observations provide the impetus for this project. Historical information and aerial photographs provide a way to determine broad land use patterns for various portions of Bowman’s Bend. In particular, certain slopes have been found to have been maintained for pasture or hay production but have not been cultivated, permitting the effects of grass vegetation cover to be investigated separate from effects related to agriculture in this project. Observations on the bend since 2001 suggest that the evolving pattern of erosion reflects water movement patterns that are exacerbated by agricultural surface soil loss, but are basically controlled by grass community root systems and their effects on subsurface hydrology. Incision and gulying below grassed slopes is most frequently associated with sensitive spots at which shallow epikarstal conduits cross the grassland/forest boundary

line. At these points, subsurface flow aided by exfiltration appears to undermine gully head cuts. Exposures of large tree roots in eroded gullies suggest that the erosion patterns are active, but result from soil movements that may have had their earliest beginnings years ago. Field observation indicates that one or more regolith properties have shifted under the influence of long-term grass cover in areas of the Bend, leading to the downhill gulying.

This project involved developing sets of vadose zone data collected from slopes that were selected to be most representative of continuous pasture and deciduous hardwood forest growth on the eastern side of Bowman's Bend. Precipitation uptake, evaporative return, and groundwater recharge are handled much differently between forest and grass ecosystems (Jennings, 1985; Burch et al., 1987; Burt and Swank, 1992), but many system shifts related to permanent change in vegetative cover occur very slowly, creating properties leading to sediment movement that are only slowly emergent (Trimble, 1990). Some factors involved with vegetation change do emerge fairly quickly, however, when viewed on a historical time scale. Conversion of grassland to forest or the reverse may produce noticeable changes in soil properties in less than 100 years (Pettapiece, 1969). Pore volumes are generally higher in forest surface soils than in adjacent agricultural areas, and individual species are capable of establishing those volumes within 30 years (Challinor, 1968). Of particular significance to this study is the importance of plant roots in directing preferential flow and in controlling erosion, and the fact that differing species of plants develop characteristic root forms very quickly (Gyssels and Poessen, 2003).

The process of logging may itself have deleterious effects on soil loss (Phillips, 1997b), although such effects can be largely eliminated with good forestry practices (Reinhart, et al., 1963; Arthur et al., 1993). The methods employed in clearing the woods on Bowman's Bend are not precisely known, but evidence can be found for burning and the practice of rolling logs into channels in the downhill woods. A charcoal lump about 20 cm across was found within the soil at 40 cm depth on the bedrock surface in pit 13 opened during this project, and partially covered decomposing log piles can be found at the tops of several of the natural gullies existing in the escarpment forest. Any surface loss of soil that occurred during clearing would have likely depended on the time of clearing and the precipitation events that ensued prior to establishment of grass cover. These factors most likely varied with portions of the slopes as they were slowly cleared. Such initial soil loss can not be easily determined, and the focus of this project is on those processes that would have been set up immediately, but would only begin to create divergent properties within the system after a matter of decades.

## **STUDY OBJECTIVES**

The underlying hypotheses for this research are that (1) changes in soil horizon clay content and vertical and lateral subsurface water flux pathways have emerged in the former forest soils under either early row-cropping and later pasture use, or under long-term grassland cover, that are now responsible for soil erosion. The temporally lagged effects of these soil water pathway changes may have generated seepage increase at slope base collection points where the grass root mat is replaced by less cohesive forest ground cover. It is also hypothesized that (2) within this particular fluviokarst environment, tree roots enable penetration of fractured limestone and thin shale interbeds, and act as wicks that carry a significant volume of water deep into the limestone layers of the epikarst. After conversion to grassland, preferential root flow paths would be lost as decayed roots fill in with clay, resulting in a slowly evolving but inevitably significant rise in throughflow (sometimes referred to as interflow) concentration at the soil/bedrock interface.

Objectives of this study are to:

- 1) determine if grassland vegetation cover has caused soil profile changes that are influencing current hillslope hydrology, and
- 2) contrast and compare water flow paths within grassland and forest slopes and relate these pathways to both erosion occurrence and influencing factor variability in the landscape, and
- 3) determine whether preferential flow and bedrock penetration associated with tree roots constitute a significant variable in fluviokarst development.

The final aim of this project has been to enable more knowledgeable management of karst land areas by development of baseline data concerning the effect of differing vegetative covers on limestone soil loss.

## **METHODOLOGICAL APPROACH**

This project has been carried out based on the idea that some geomorphic questions can not be answered in isolation from other aspects of the controlling earth surface system (Phillips, 1992a). The development of any earth surface system, and most certainly a complex fluviokarst landscape, is regulated by the interaction of a large number of variables that have evolved co-dependently (Phillips, 1992b, 2001a). In geomorphic studies where a multiplicity of

variables is clearly evident, it is necessary to acknowledge that no one single cause may be responsible for changes, and that system development most likely lies in polygenesis and co-evolution related to multiple causality (Phillips, 1998, 2000, 2001b). This complexity of variables and interactions, tied as they are to site-specific historical and geographical contingencies, makes it necessary to reduce research to those components that most dominate system responses. If these dominant variable relationships are selected based on a detailed, overall knowledge of the system that acknowledges both global and local factors (Phillips, 2002), they can then provide an effective understanding of the principles guiding system behavior (Huggett, 1985; Phillips, 2001b).

A multi-faceted research approach has been used in this project to outline the broad array of variables present in the study area and to then reduce them to measurable major factors. An extensive field survey relating erosion to slope, lithology, topography, and land use was initially completed followed by interviews with local landowners and with Dr. Julian Campbell, Conservation Scientist with the Lexington, Kentucky Nature Conservancy office, which currently manages the escarpment forests. Information gained from interviews, aerial photographs, field observations, and tree cores was analyzed to determine land use patterns and to correlate physical landscape features with presence and timing of erosional features.

Once a composite picture of human impact on the Bend was derived, soil and water infiltration properties were measured during two phases of research. Work undertaken in phase 1 was geared toward defining the range of soil texture and depth variability present in selected slopes of the bend, and involved textural analysis of soil profiles sampled by auger as well as measurement of soil depth along probed transects. Information gained during phase 1 provided the means to select sites for phase 2 measurements of soil water content and infiltration rates. Two soil water content data logging stations were set up on neighboring forest and grass sites, with five dielectric probes set into pit walls at each station at increasing depths. In the final phase of field research, 14 pits were opened to bedrock so that constant-head infiltration rates could be measured at varying depths with a tension infiltrometer. Texture, bulk density, and organic content were determined for the differing pit layers during this process, and were used during multivariate analysis of the soil property relationships. Data gathered from these overlapping measures of soil and hydraulic properties could then be placed into context with the many surface and subsurface observations made during this study to generate an overarching description of system behavior.



## CHAPTER 2

### STUDY AREA

#### LOCATION AND OVERVIEW

The study area encompasses hillslopes that lie within and adjacent to the Sally Brown and Crutcher Nature Conservancy Preserves on Bowman's Bend, Garrard County, Kentucky (Figure 2.1). Bowman's Bend was formed during entrenchment of the Kentucky River, which flows northward along the bend's eastern side and then swings westward around the bend's northern tip. Over the past 1.5-2 million years, the river has incised into the flat-lying limestones of the inner Bluegrass plateau, creating 100-meter vertical limestone palisades (Andrews, 2004). Forests along the river's escarpment are protected by the Nature Conservancy because of their unique assemblages of rare species and unusual rocky habitats (Nature Conservancy, 2005). The three families who currently own the interior land of the bend have set up conservation easements with the Conservancy to aid in this protection. This study has incorporated data collected from within the Preserves along 1.5 km of the eastern and north sides of the bend, and from privately-owned grassed hillslopes overlying Crutcher Preserve along the bend's eastern side. The area from which most soil texture and infiltration data was collected for this project is indicated as the "main study area" in figure 2.2.

The gorge created by the Kentucky River is much more rugged and forested than the surrounding inner Bluegrass upland. The Bluegrass occupies the north central portion of the state and lies within the Interior Plateau ecoregion of the United States (Woods, et al., 2002). Centered within the Bluegrass, the inner Bluegrass has a weakly dissected, gently rolling topography that supports sinkholes, springs, and disappearing streams typical of fluvio karst environments. Larger streams may contain year-round flow, but first order streams are usually ephemeral. Along Bowman's Bend, high gradient, stepped bedrock channels that dissect the escarpment may carry spring flow for portions of their lengths, but otherwise remain dry most of the year. Elevations on Bowman's Bend range from <160 m (525 ft) on the river floodplains to >290 m (951 ft) on crests of the slopes above the escarpment (Figure 2.2). The view of Bowman's Bend shown in figure 2.3 was taken looking directly north along the upper escarpment of the bend's eastern side from a position at approximately 280 m elevation in the main study area. Slopes in this upper portion of the escarpment range between 8 and 16

degrees or more (16-29%), and steepen rapidly in the downhill forests and along the ephemeral stream dissections seen as forest covered terrains in figure 2.3.

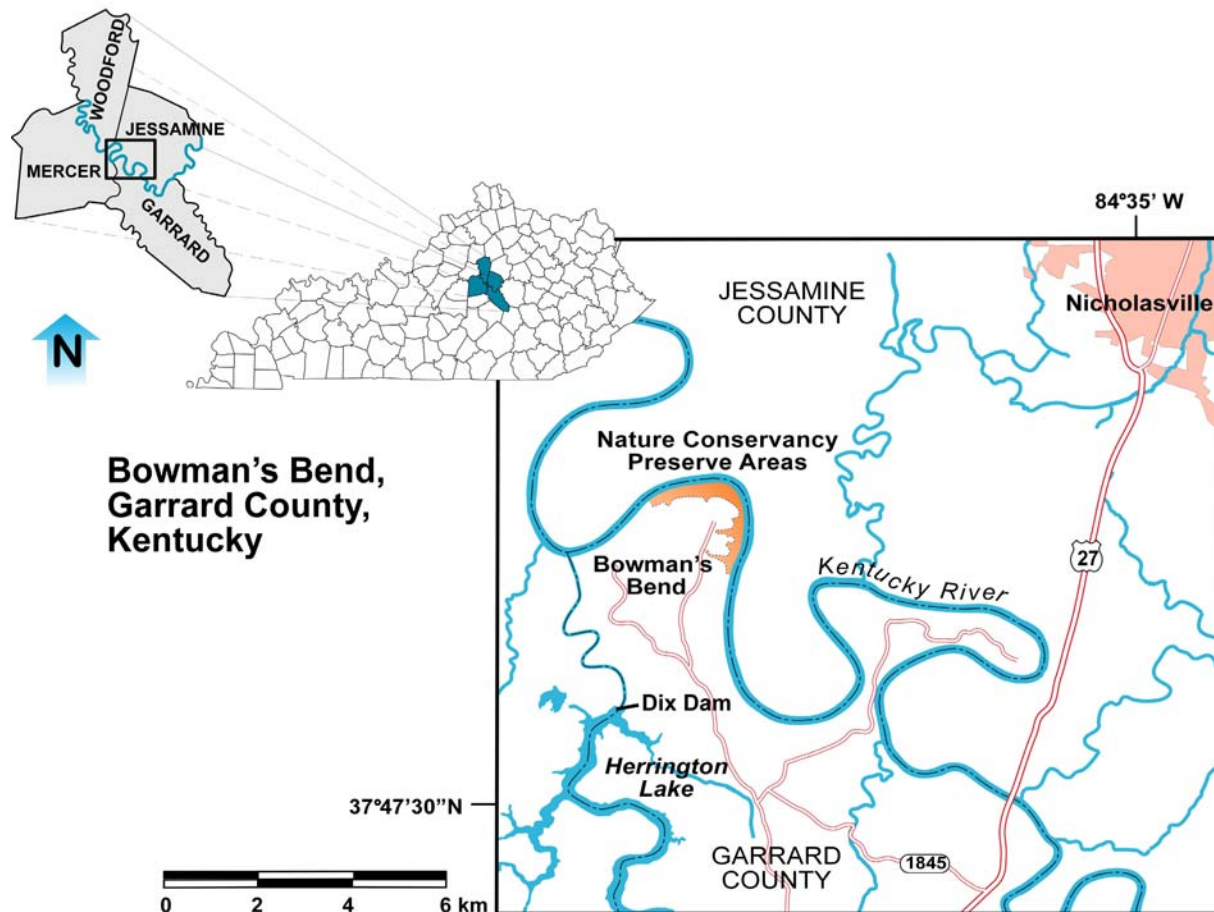


Figure 2.1. Study area on Bowman's Bend includes slopes next to and within the Sally Brown and Crutcher Nature Conservancy Preserves. The bend lies approximately 20 kilometers southwest of Lexington, Kentucky.

Inner Bluegrass geology consists of Middle Ordovician limestones and calcareous shales of the Lexington Limestones, which underlie the upland, and of the High Bridge Group, which is only exposed in the river's gorge (Woods, et al., 2002). A humid temperate climate coupled with absence of glaciation has produced fertile, often stony silt loam and silty clay loam Hapludalfs in upland areas of the bend that grade into flaggy Hapludolls in downhill forests (Soil Survey Staff, 2005). A mean annual temperature of 13.9 °C (57 °F), with annual maximum and minimum mean temperatures of 19.6 °C (67.3 °F) and 8.1 °C (46.6 °F), are recorded for the Dix Dam meteorological station located 4.8 km (3 mi) to the southeast of the study area (Midwest Regional Climate Center, 2005). Highest mean temperatures occur in July and August and lowest in January and February. Mean annual precipitation for the years 1971-2000 is 1161.5

mm (45.73 in), with monthly mean values ranging from 74.9 mm (2.95 in) in October to 118.9 mm (4.68 in) in May. Much of the precipitation received throughout Kentucky comes from frontal systems that pass west to east across the state or from convective storms that sometimes deliver “summer rains (that) are often torrential” (Dicken, 1938, p 15).

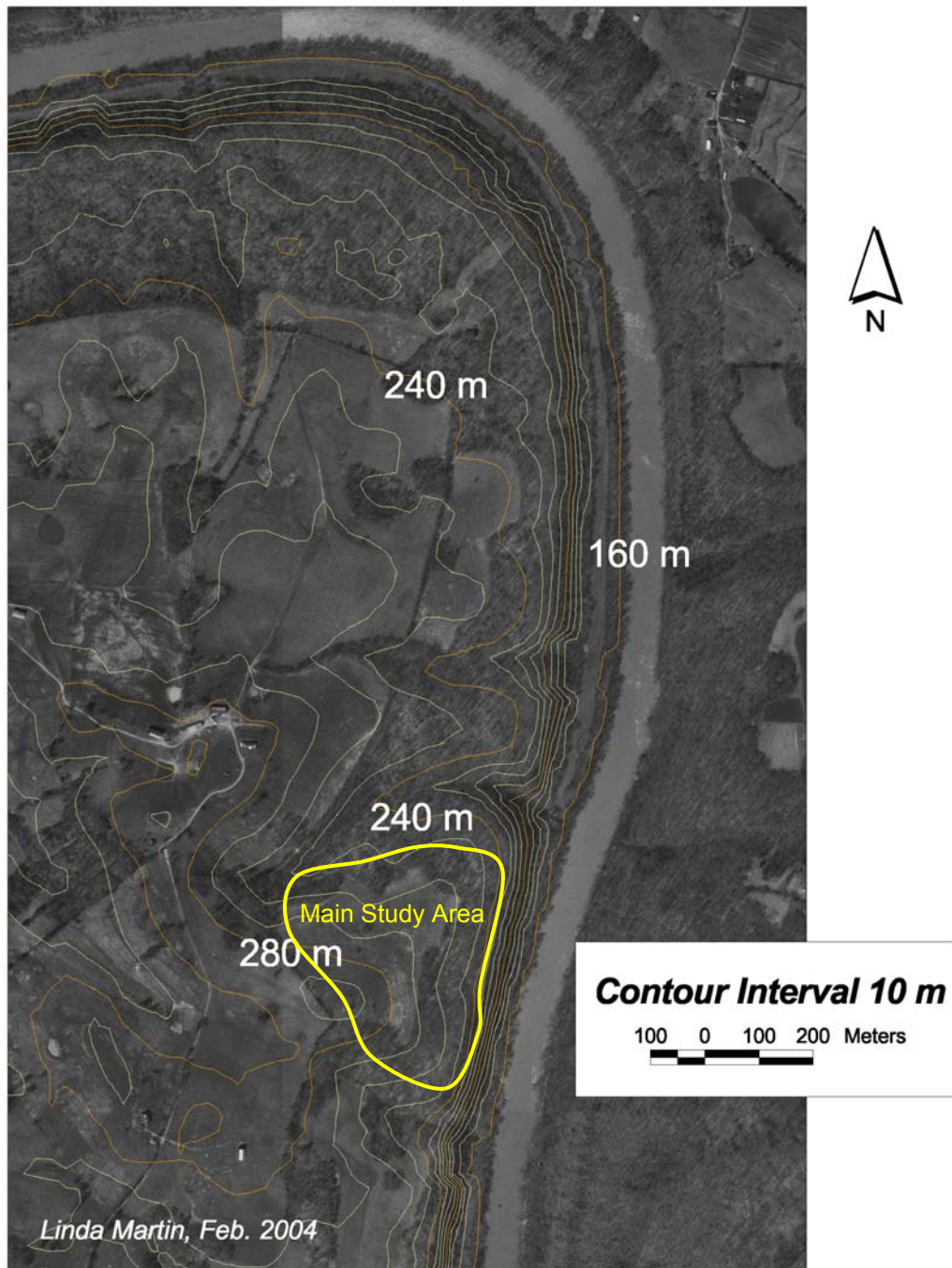


Figure 2.2 Contour map of study area, with digital elevation data overlaid on 1997 Wilmore (L40) DOQQ aerial images.



Figure 2.3. View north along the bend from the shoulder of Hillslope A in the main study area. Photo by author, November 2, 2005.

Hillslopes on the bend have a complex profile form, so that typically grassed convex-straight-concave slopes in the uplands overlie convex-vertically stepped slopes covered in forests along the escarpment. The upland convex-straight-concave portion is more extended in the north part of the bend than along the east side, and river gravel in soils indicates that the Kentucky River occupied this area prior to its incision of the plateau (Andrews, 2004). Slopes on all sides of the bend are dissected by both surface ephemeral stream channels and subsurface epikarstal conduits, which channel flow through the surface of the bedrock and create linear depressions on the overlying surface. Along the east side of the bend, areas between dissections created by surface channels form smoothly rounded noses perpendicular to the river. Side slopes of areas between dissections thus have aspects ranging from east to just west of due north or south. In the main study area, pits in which infiltration tests were taken in the forest had aspects of approximately 170 to 180°, whereas pits at matched grass elevations were directed to the east or northeast. The gradient of many slopes oriented to the east approaches the summer angle of solar inclination in the region, causing the sun to be almost directly overhead during the hottest portions of the year. However, relatively high

amounts of year round precipitation plus soil with high clay content ensure that in the great majority of years, enough moisture is retained in soils for vigorous plant growth on eastern slopes.

## LAND USE PATTERNS ON BOWMAN'S BEND

Land in the inner Bluegrass was converted from savannah and open oak-hickory forests to pasture and cropland use during European settlement. Woodlands currently cover only 1-10% of the uplands (Campbell, 1980), with the rest of the land used for agriculture, and increasingly, urban/suburban development (Woods, et al., 2002). The forested corridor of the Kentucky River contains the largest forests and the only remaining natural vegetation in the inner Bluegrass (Nature Conservancy, 2005). Blue ash (*Fraxinus quadrangulata*) and burr (*Quercus macrocarpa*) and chinquapin (*Q. muhlenbergii*) oaks dominate upland forest remnants, and are found on the plains along with black walnut (*Juglans nigra*), wild black cherry (*Prunus serotina*), hackberry (*Celtis occidentalis*), black locust (*Robinia pseudoacacia*), shellbark hickory (*Carya laciniosa*), sugar maple (*Acer saccharum*), and Kentucky coffeetree (*Gymnocladus dioica*) (Campbell, 1980; Woods, et al., 2002). River ravines, with their conditions of increased moisture, decreased temperature, and lower rates of disturbance, support somewhat different assemblages, with white ash (*F. Americana*) as well as Shumard (*Q. shumardii*), white (*Q. alba*), and northern red oaks (*Q. rubra*) common (Campbell, 1980). Where land is abandoned, eastern red cedar (*Juniperus virginiana*), Osage orange (*Maclura pomifera*), and locust (*Robinia pseudoacacia*) rapidly become established.

Land use patterns and tree composition on Bowman's Bend closely fit this generalized description. Bowman's Bend was first settled by Europeans in 1790, when a band of 30 Virginian families set up Bowman's Station across the Dix River on the western side of the bend (Brooks interview, 2005). George and Mary Bowman took possession of the portion of the bend that is now the study area, eventually passing ownership to their two sons, John and George, who both served in the Revolutionary War (Jessamine County, Kentucky River Task Force, 2005). To transport local products and to participate in the shipping that was centralized on the Kentucky River during that time period, John Bowman cut a road down the palisades at the bend's north end and set up a warehouse on the river floodplain. In 1818, George obtained a contract with the county and set up another warehouse and an inspection station for tobacco, hemp, and flour farther down the river near Elk Shoal (Jessamine County Kentucky River Task Force, 2005). In the decades following settlement, land clearing proceeded rapidly from west to east across the bend. By 1820, county records show that 4 km<sup>2</sup> (1000 acres) of the bend were

being operated as a plantation utilizing 29 slaves (Brooks interview, 2005). This number of workers remained constant throughout the Civil War period.

Most agricultural activity centered on hemp, tobacco, wheat, and livestock. Records through the 19<sup>th</sup> and 20<sup>th</sup> centuries show a continuation of this same mix of crops, although corn production became important after 1920 and hemp was discontinued after WWII (Brooks interview, 2005). The rich alluvial soils of the Kentucky River floodplains were used most continuously for row-cropping, followed by those portions of the gently sloping northern part of the bend where 1.5-1.8 m thick silt loams had developed in the palaeochannel floodplains. Row crops were rotated among the steeper, stonier slopes along the east side of the bend, and the least productive slopes were typically reserved for pasture or hay production.

Virtually all of the upland area of the bend was eventually cleared for row-cropping and pasture, with remnant forest patches left standing in ravines and around open karst features such as shafts and steep sinks. Although the remnants of forest found on the bend have been logged on multiple occasions, aerial photos indicate that most of these forest patches have been allowed to regenerate naturally in the same locations (Figures 2.4a and b). Demand for railroad ties was high between 1870 and 1910, and photos taken during this era show that the Kentucky River corridor was deforested. High Bridge, constructed in the late 1870's to permit rail crossing of the Kentucky River, lies near the confluence of the Dix River and the Kentucky River on the far western side of Bowman's Bend. Photographs taken during its construction show that the river's floodplain, now almost fully wooded, was cleared of trees at that time and that escarpment forests were much thinner than they are today (Hagee, 2000-2004). Aerial photos of Bowman's Bend going back to 1937 show periods of cutting and regrowth, with the last major cut occurring between 1960 and 1966 (Figures 2.5a and b).

Aerial photographs of the main study area indicate that the grassed areas seen in the 1960 photograph were cleared prior to 1937 and have remained open and under pasture use since then. Comparison of figures 5a and b, however, shows that two small sections presently included in the open area were not converted to pasture until the logging of the early 1960's. At that time, areas of approximately a hectare in size were deforested on the northeast and southwest corners of the slopes. The slopes supporting these sections are stony and typically have soils about 40 cm deep, with depth declining to 0 on portions of the hill shoulder. The 1966 aerial photograph suggests that Bowman's Bend was being intensively farmed at that time. Within the main study area, grass in the steepest areas of thinnest soils is shown to remain uncut, but the crest, the nose of the hill, and the 12 to >16° slopes facing north from the crest have been disturbed. These disturbed areas do not show the linear patterns associated

with row-cropping, and considered along with the poor quality of the soils, suggest that the white rectangular patterns visible on the photos are likely the result of summer haying. Records kept by land owners suggest that the slopes of the main study area have never been plowed (Brooks interview, 2005). Aerial photographs taken before and after 1966 show no other times during which the slopes of the main study area have been used for anything except pasture.

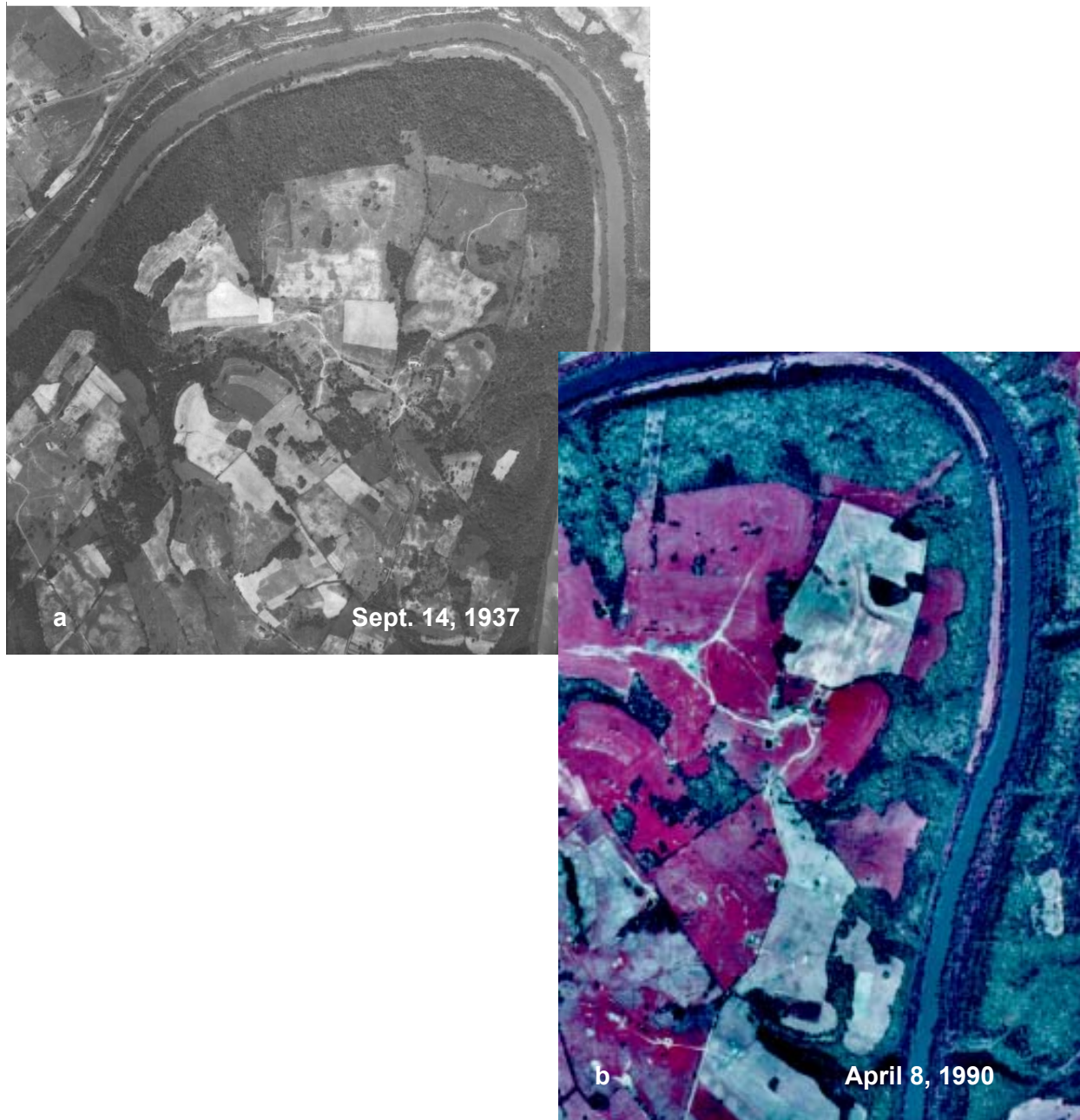


Figure 2.4. Aerial photos taken in 1937 (a) and 1990 (b) show the continuity of forest cover in the same general areas of Bowman's Bend along the escarpment and in areas dissected by streams.



Figure 2.5. Aerial photographs from 1960 (a) and 1966 (b) (next page) showing where patches of forest were removed in the main study area during this period of heavy logging.





Figure 2.5b. Main study area shows evidence of hay production in 1966.

Forests within preserve areas now largely consist of sapling to 60-year old second growth that is overshadowing and killing any eastern red cedar that gained a foothold immediately after logging in the 1960's. Large stumps in all stages of decomposition are ubiquitous in the woodlands, and in some locations isolated trees with diameters up to 1.15 m still exist, hinting at what the original forest must have looked like (Figure 2.6). The house constructed by John

Bowman in 1820 has been incorporated into a modern residence, and the dimensions of the original wood found in its doors, walls, and flooring indicate that the trees present at time of settlement were much larger, and were from a somewhat different species assemblage than is currently found on the escarpment. Poplar (*Liriodendron tulipifera*) supplies an easily-worked wood that was likely prized by settlers using hand tools, and boards of up to half a meter in width in the Bowman house indicate that this now rare species was once common. American chestnut (*Castanea dentate*) was also common and favored by early craftsmen. Selective logging was extensively practiced, in which undesirable species such as shag-bark hickory (*Carya ovata*) or specimens that were bent, diseased, or multi-trunked were left, or were perhaps burned. Records from neighboring farms suggest that the cuts which occurred in the 1960's were selective cuts for oak. The original forest most certainly contained much larger, more widely separated specimens in a species mix that differed in composition and percentage of shade intolerant trees from that found today.



Figure 2.6. Large chinquapin oak with a diameter at breast height of 1.15 m near the edge of the forest in the mid-shoulder region of Hillslope H (figure 4.1) in the main study area. Younger trees surround this isolated forest giant, which escaped logging in the early 1960's. The soil probe lying across its roots is 1.86 m long. Soil depths measured in a transect parallel with the contour at the tree base range from 0 to 54 cm, with a mean depth of 16.8 cm. Photo by author, March 15, 2005.

Under Nature Conservancy direction and assistance, privately-owned upland slopes in many parts of the bend have come under management as native-grass tracts since 2000. A stand of Indian grass (*Sorghastrum nutans*) has been established on the hillslope region just north of the main study area (Figure 3), and this grass, as well as little bluestem (*Andropogon scoparins*) and big bluestem (*Andropogon gerardi*) form monocultures in other fields that are harvested for seed each fall. These fields are burned each winter between January and March to eradicate tree sprouts and cool-season fescue grass (Figure 2.7). This process does not destroy the deeply-rooted native species, but it does expose bare slopes to wash during critical high-precipitation periods.



Figure 2.7. Slopes are exposed to erosion following winter burns. A folding measuring stick indicates scale. Photo by author, March 2005.

In the main study area, grassland management since 2001 has focused on a program of habitat replenishment implemented by the land owners under the guidelines of the U.S. Department of Agriculture's Wildlife Habitat Improvement Program (WHIP). In 2001, the bottom two-thirds of the main study area grassed slopes were planted with a mix of wildflowers and native grasses after spraying to kill fescue (*Festuca pratensis* and *Festuca arundinacea*). The top third, which includes all pit and surface infiltration test sites sampled for this project, was mowed and then planted with 3,000 native Kentucky tree bareroot seedlings. These trees, which include walnut, black locust, white and black oak, persimmon, silky dogwood, eastern redbud, and wild plum, are now typically 40 to 60 cm in height and are often hidden by thick fescue and herbaceous plant growth or by raspberry (*Rubus* spp.) thickets on parts of the sideslopes. Although fescue currently dominates the plant community in the upper hillslope area, many other plants are seasonally present. During fall of 2005, white snakeroot (*Eupatorium rugosum*), goldenrod (*Solidago* spp.), and Aster (*Aster* spp.) were heavily represented. Orchard grass (*Dactylis glomerata*), switch grass (*Panicum virgatum*), and foxtail (*Setaria glauca*) were found in localized clumps, and horse nettle (*Solanum carolinense*) and field garlic (*Allium vineale*) could be easily identified within the grass cover on pit sites. The young tree saplings present on the upper slopes did not have enough developed root growth to significantly influence slope hydrology during this project time period, and test sites were carefully selected away from any trees in spots retaining as much solid fescue cover as possible.

## **EROSION AND KARST FEATURES**

### **Karst Features**

Karst solution in the inner Bluegrass is typically limited by the multiple impervious layers of the Lexington Limestones to the top 30 meters of bedrock (Hamilton, 1946; Taylor, 1992). Observations of karst landforms on Bowman's Bend suggest that a shallow pattern of epikarst development is found in the upland areas underlain by the Lexington Limestones, but that deeper solutional features occur in the thicker, micritic limestones of the High Bridge Group. A study of karst features and fracture directions completed on Bowman's Bend in 2001 determined that most water in the upland moves laterally along relatively shallow epikarstal pathways to the escarpment edge, where it drops through High Bridge members behind the palisade walls to the river below (Phillips, et al., 2004). Over the extent of escarpment mapped for this project, two types of epikarst morphology can be distinguished that correlate with

shallow 1-3 m deep conduit flow mostly set up by the Lexington Limestones, and deeper vertical penetration to 15 m or more in the High Bridge Group.

The gradual slopes of the north end of the bend are underlain by High Bridge units, and in this area geology, palaeohistory, and fracture orientation have set up conditions for development of vertical and lateral conduit networks that interconnect below the epikarst within the bedrock itself. In this area, sinks 30-85 m across and from 3 to >15 m deep are numerous (Figure 2.8), and large, active swallets up to 3 m deep may exist within the large sinks. Deep vertical penetration in the High Bridge Group is best demonstrated by shafts, which typically occur as unroofed holes 3-4 m wide and 4-6 m deep that are solutionally opened along fracture intersections. In contrast, along the eastern edge of the escarpment where the Lexington Limestones underlie the upland slopes, sinks are either small (2-7 m in length) and often inactive or plugged, or are very shallow, forming broad, round swales less than a meter deep that may be difficult to distinguish under vegetation cover (Figure 2.9). Gullies and exhumed conduit channels are common in the east side of the bend along with scattered swallet openings 1-3 m deep that occur on the escarpment edge where conduits have been unroofed by sediment subsidence.



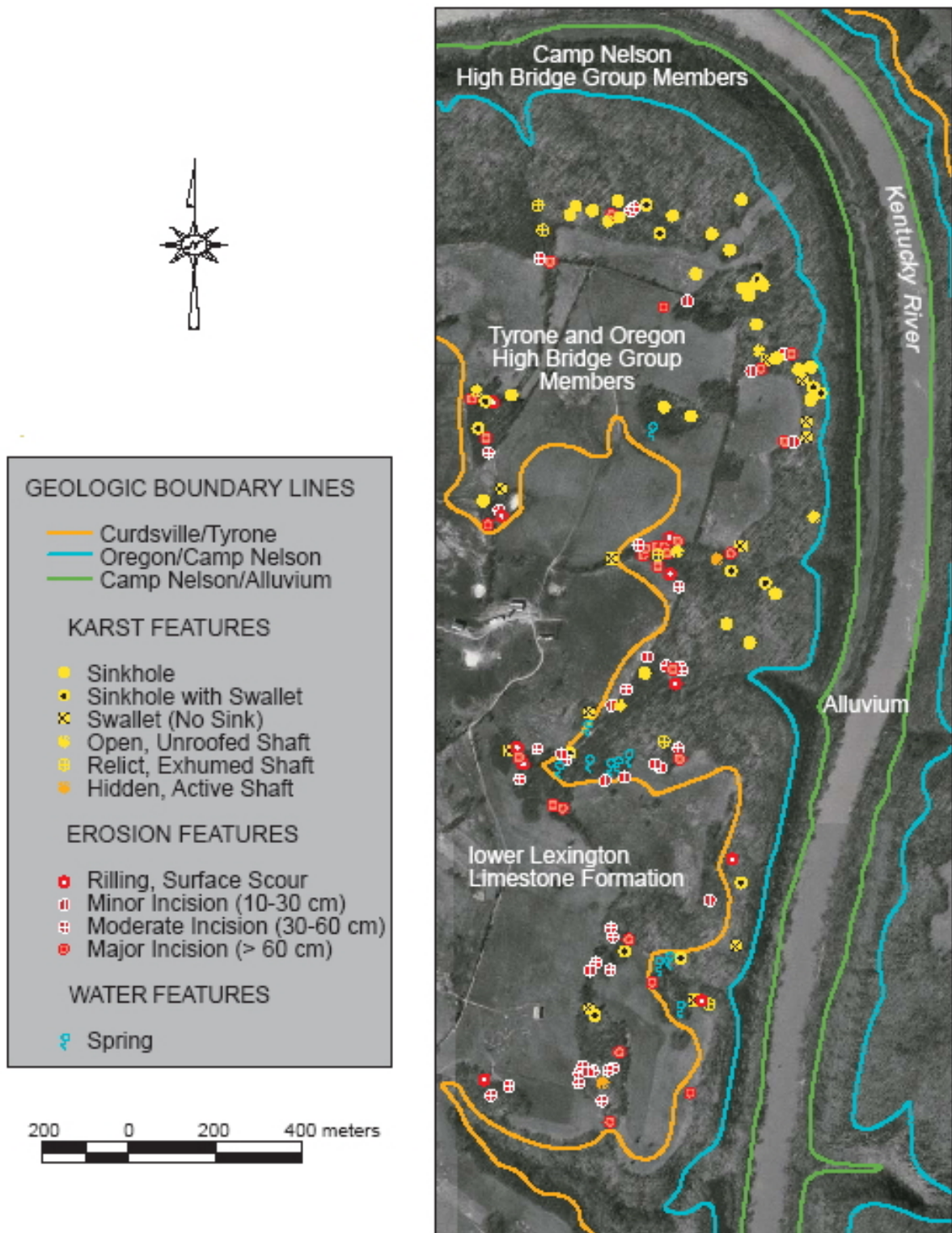
Figure 2.8. Large sink on the north end of the bend forms a section of the karst valley supporting the largest ephemeral stream. Although surface channels exist above and below the sink, all water moves through the subsurface in this section. Photo by author, November 2001.



Figure 2.9. Broad, shallow swale lies near the crest of the upland slopes on the east side of the bend. Although not connected to the swale by surface incision, a shallow channel has developed in the forest below this feature. A young tree has taken root in the center of the swale. Photo by author, May 20, 2004.

### **Erosion Features**

Observations during 2001 revealed a number of gullies and incisions that frequently began near or at the boundary lines between grass and forest. In fall of 2003, a pilot survey study was conducted to map erosion and karst features and correlate their occurrence with grass/forest boundaries. This survey covered a 1.5 km section of the east and north sides of Bowman's Bend (Figure 2.10). Erosion and karst features were measured and mapped by GPS during this survey, and their locations brought into a GIS system to match erosion incidence to geology and vegetation patterns. Shallow incisions were classified as those 5-30 cm in depth, moderate as those >30 but <60 cm, and major incisions as those deeper than 60 cm. Notations were made of soil loss as indicated by tree root exposure and of conduit exhumation as revealed by cutter, shaft, or fissured rock wall exhumations in incisions or gullies. Observations made during this survey, along with the overview gathered from the mapped data, were used to categorize the erosion features and to provide a framework for this project.



Map Compiled by: Linda Martin, April 2004

Geology Data Source: KGS, Harriidsburg 30x60 GQ, 2001  
 Aerial Photos: KGS, Wilmore DOQQ, 1990

Figure 2.10. Erosion and karst features on Bowman's Bend, Kentucky.

As demonstrated in figure 2.10, mapped scour and channel incision features of a large range of sizes do associate in most cases with grass/forest boundaries, and they occur on both Lexington Limestone and High Bridge units. Although they are found in all parts of the bend, their incidence is highest on the east side. From the pilot study it was also determined that 73% of the observed erosion features could be associated with water movement within or to some type of karst landform such as a sink, shaft, swale, or exhumed conduit or cutter. The deepest erosion features found on the bend are gully headcuts ranging from 0.3 m to 2.5 m in depth. These headcuts typically occur near or at the grass/forest boundary line in locations where pre-existing epikarstal conduits are exhumed where they pass from uphill grass slopes into the downhill forests (Figure 2.11).



Figure 2.11. Roots create an overhang above a moderate-sized gully at the forest/grass boundary at the bottom of the main study area area. A blue and white cooler is visible through the brush. Photo by author, October 7, 2004.

Those erosion features that do not seem to directly relate to karst landforms typically occur where compaction or changes in topography act to increase return flow at the sides and bases of grassed slopes. Scour features or incision may be found where flow descending one slope is captured at the base and concentrated at right angles to the slope (Figure 2.12a), where traffic along the edges of open areas compacts the surface, or where grass and forest



vegetation run side by side up a slope (Figure 2.12 b). In this later case, incision typically occurs just inside the grassed area at the hill base.

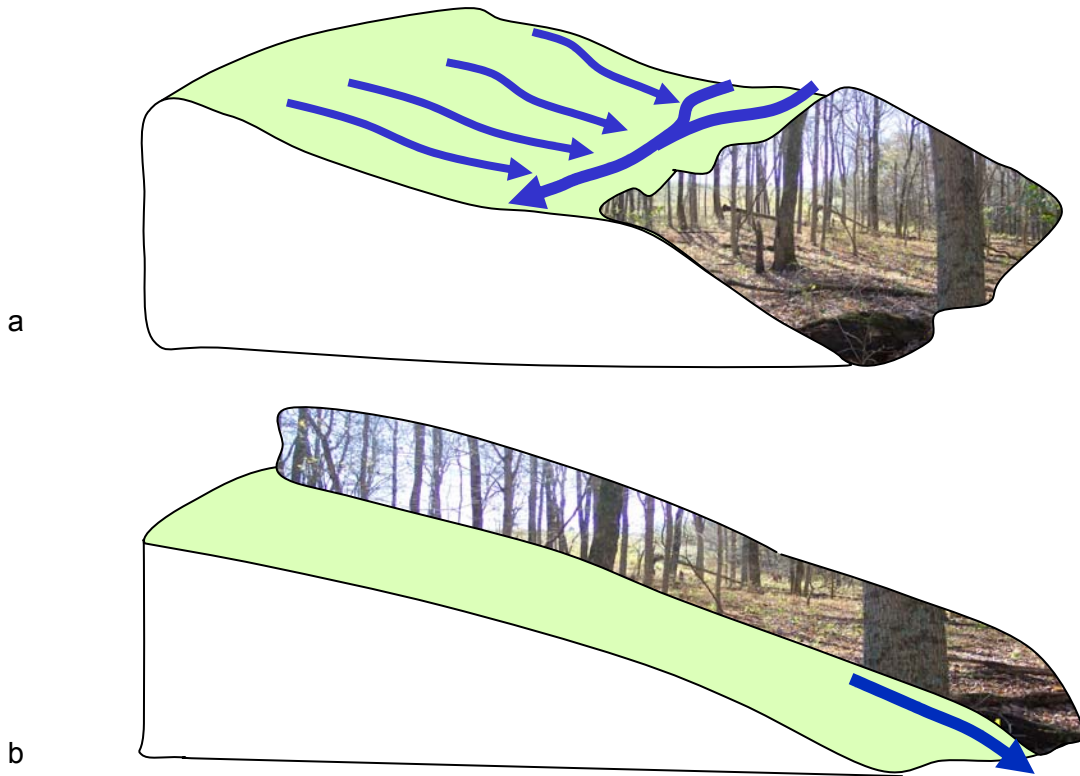


Figure 2.12. Prime areas for surface scour occur where (a) flow is captured at the toe of a grassed slope and directed laterally at the forest edge, or (b) at the bottoms of steep grass slopes that parallel vertically aligned forest patches. Green represents grass and photos indicate forests.

Root overhangs, soil pipes, and exfiltration processes observed during the pilot study indicated that much of the erosion relates to seepage and return flow at grassed slope bases (Figure 2.13). Because the depth at which subsurface pathways operate is a large determinant of their effect on surface erosion, soil depth and the depth of epikarstal conduit flow play a role in gully initiation. In the north area of the bend where soils and karst pathways are typically deeper, seepage flow was observed at only three locations at depths of 1.35, 0.95, and 0.9 m. Along the east side of the bend where sideslope soils are frequently <1 m in depth, emergence of seepage was observed from numerous knickpoint bases at about 60 cm (Figure 2.14).

The presence of large exposed roots in some gullies indicates that much of the erosion on Bowman's Bend has occurred relatively recently (Figure 2.15). This recent development of erosion, coupled with its widespread distribution across the bend and the high correlation between erosion features and subsurface flow features, suggests that some hydrologic process is occurring in the grassed slopes that is encouraging flow concentration at certain soil depths. This flow concentration is able to best express its erosive power where thin soil and pre-existing epikarstal pathways increase the likelihood of flow collection and sediment entrainment. Although headcuts and exhumed gullies are most often found in sensitive locations where pre-existing pathways cross the grass/forest boundary line, they are only the most obvious features of a widespread pattern of scour and incision.

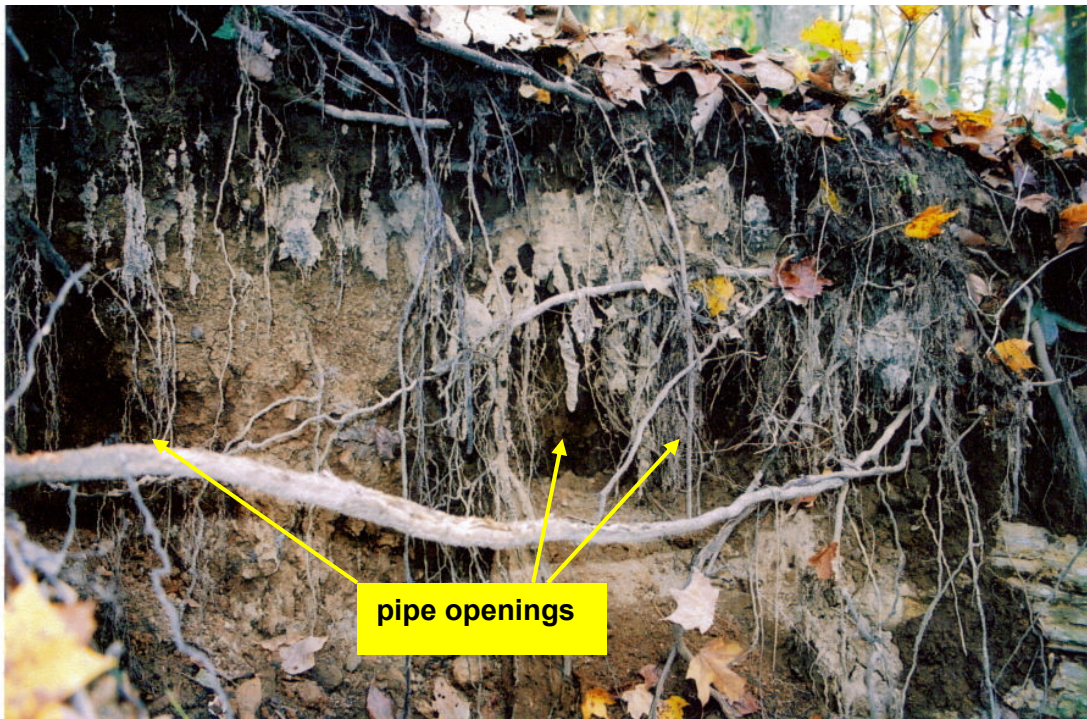


Figure 2.13. Soil pipes are associated with root overhangs at gully heads. Photo by author May 2003.



Figure 2.14. Seepage and pipe flow occurs below overhangs at approximately 60 cm depth. Photo by author, May 2003.



Figure 2.15. Tree root exposed in gully base. Photo by author, October 2003.

Copyright © Linda L. Martin 200

## CHAPTER 3

### THEORETICAL BACKGROUND

#### THE FLUVIOKARST LANDSCAPE

Carbonate bedrocks support the development of characteristic karst landscapes containing dolines (sinkholes), shafts, springs, and other features associated with the solutional opening of flow networks that penetrate the rock mass. During the solutional process, CO<sub>2</sub> is hydrated in the CO<sub>2</sub>-H<sub>2</sub>O-CaCO<sub>3</sub> system in a reaction regulated by its partial pressure. Carbonic acid is formed that is free to release Ca<sup>2+</sup> at the solution-rock interface, where calcium, bicarbonate, and carbon dioxide ions are subsequently removed in solution by diffusive mass transport (Kaufmann and Braun, 1999). General dissolution rates are dependent on the influence of climate acting on the stratigraphic, structural, and tectonic characteristics of the different forms of limestone, dolostone, or highly calcareous terrigenous rocks that commonly occur in a karstic area (LaMoreaux et. al., 1984). Because limestones typically have low primary permeability, the ability of dissolution to take place within the bedrock matrix is largely dependent on the secondary fracture content of the rock mass. The factors governing the presence of solute access points are very localized and resolve from sedimentary, diagenetic, and tectonic formative processes that regulate the joint, bedding plane, and fault lines that are solutionally attacked during weathering as well as the development of current topographic features that define recharge and discharge zones (LaMoreaux et al. 1984).

Focus in karst research is typically placed on the speleogenic processes that lead to development of the conduit and cave forms that create carbonate aquifers (Palmer, 1991; Klimchouk et al, 2000). The chemistry of the dissolutional processes that regulate conduit growth with aperture size and onset of turbulence is relatively well-understood and modeled (Dreybrodt, 1990, 1996; Groves and Howard, 1994a, b; Howard and Groves, 1995; Kaufmann and Braun, 1999, 2000; Gabrovsek and Dreybrodt, 2001), as are the structural factors that guide conduit development along zones of joint and bedding plane control (Deike, 1969; Williams, 1972; Palmer, 1991; Klimchouk and Ford, 2000a). Physical processes that guide the regolith raveling and subsidence that accompany solutional karst feature development have also been researched by a number of scientists (Jennings, 1983; White and White, 1995; Klimchouk and Ford, 2000b). Knowledge of these physical and chemical processes provides a foundation for karst landscape studies.

Surface landforms usually form from weathering occurring in stress release fractures in the upper part of the rock mass (Klimchouk, 2000). As diffuse infiltration works its way into a calcium-rich bedrock, it creates leached soils, and a sharp interface forms between the soil and bedrock so that a C-horizon of weathered material is frequently missing (White, 2002). Fractures along the rock interface will be differentially extended by acidified soil water, however, so that the rock surface of a mature karst becomes heavily indented by cutters. These deep crevices widen from the top downwards, creating a subcutaneous, or epikarst zone that can store significant amounts of water for long periods of time (Williams, 1983). Depressions are formed in the overlying regolith through subsidence and/or collapse. Once sinkholes form, they focus surface and subsurface recharge into major conduits (Jennings, 1985; Zambo and Ford, 1997; Palmer, 2002), causing karst aquifers to be influenced by the land features they create.

As a karst landscape matures, increasing amounts of precipitation are drained from the surface via conduits operating in the bedrock. Most of these landscapes in humid temperate regions support competing surface and subsurface pathways, with surface stream flow often restricted to major storm events. In these fluviokarst regions, such as that of the inner Bluegrass of Kentucky, precipitation is dispersed within the regolith and the upper surface of the bedrock to both surface channels and internally-draining conduits and sinks (White, 1988). Because of the simultaneous surface and subsurface routing of water and sediments within a fluviokarst landscape, processes leading to soil development, landform interactions, and aquifer quality are complex and interactive across a wide range of scales.

### **Epikarst Development**

The epikarst, or subcutaneous zone as it is called by some researchers, is defined as the fissured, diffusely karstified near-surface portion of the bedrock in a karst terrain (Jennings, 1985; Klimchouk, 2000). Both transmissivity and storage capacity of this 1 to 2 m deep zone is considerably higher than that of the underlying rock mass (Williams, 1983; Julian and Young, 1995; Perrin, et al., 2003). Fissures in the epikarst typically operate above the vadose, or unsaturated portion of a karst aquifer, forming a perched epikarstic aquifer that concentrates flow at its base into larger discrete fractures that then carry water into the phreatic zone of the limestone aquifer (Clemens, et al., 1999; Klimchouk, 2000). The epikarstic aquifer has a specific storage capability that may be exceeded during storm events, causing surface flow that temporarily activates ephemeral streams (Ford and Williams, 1989). Both vertical and lateral throughflow occurs in the epikarst as water moves along the potentiometric surface away from areas of high hydraulic potential. As water moves down gradient, cavities and conduits in the

epikarst form zones of low potential that draw in water from the surrounding rock (Ford and Williams, 1989).

In studies reported by Atkinson and Smith (1976), 60% of limestone erosion under soil cover takes place close to or at the surface of the bedrock. Under soil and vegetation, the surface of the epikarst will typically develop some form of karren, composed of “small scale dissolution pit, groove and channel forms at the surface and underground” (Ford and Williams, 1989). The forms and sizes taken by these features are largely dependent on lithologic and structural controls on hydrology. Karren forms take different appearances depending on whether they develop subaerially or beneath regolith, and the sharp edges of free karren created by direct rain contact differ from the rounded edges displayed by covered karren, or karren developed under soil cover (Sweeting, 1973; Bogli, 1980).

Cutters (called ‘grykes’ in Britain), are common karren forms created by linear solution along single joints that open to depths of from one to >10 m (White, 1988). Cutters and the related but smaller ‘kluftkarren’ (openings of less than a meter width) do not have well-developed internal drainage and are thus normally covered. They develop from vertical percolation or sometimes lateral water movement at the bedrock, and typically bottom out at impervious layers in Kentucky (White, 1988). Williams (1966) deduced that gryke development in Ireland was controlled by regolith thickness; glacial drift greater than 2 m in thickness prevented gryke development, but grykes deepened in concert with thinning of the drift cover and increasing exposure of the limestone to water acidified by plant activity. Solutional attack is always strongest in the epikarst along joints, bedding planes, and other structurally weak area, and rocks surrounding cutters will be left standing as pinnacles.

### *Vegetation Effects*

One recognized form of covered karren is deckenkarren, which includes solution forms created by roots (Sweeting, 1973). Deckenkarren are best recognized in humid tropical locations, and are found to be associated with permeable regolith conditions (Sweeting, 1973). Tree roots in certain locales have been directly associated with the development of pits created along joints in the top of the bedrock, rock grooving, and smooth, wavy surfaces full of holes along bedding planes and fracture surfaces (Sweeting, 1973). Root grooves, described as hemispherical grooves forming 2 x 3mm to 12 mm irregular networks on limestone joint faces, were first described by Wall and Wilford (1966), who related groove development to dissolution prompted by acid exudates from fine root hairs that penetrate into tight rock joints. Bull and Laverty (1982) reviewed several articles that cite the importance of root corrosional action in

carbonate rock solution, but admitted that information was scant. Taborosi (2002) speculated that roots are able to widen holes through both acidification of the rainwater flowing down the root and pressure exerted on the host rock. Some plants are known to produce pockets of acid soil around their roots through both root processes and litter accumulation that may affect weathering of the surrounding limestone (Trudgill, 1985). Etched micro-runnel have been observed on limestones exposed to stemflow at tree bases in the United Kingdom (Trudgill, 1985) and at even smaller scales, biokarst studies have shown a wide range of depositional and erosional influences played by organisms on karst development (Viles, 1984, 1988).

Because root activity, plant material decomposition, and plant-supported soil ecosystems all regulate soil development and transmissibility as well as organic acid and chelate content of soil waters, epikarst weathering is closely related to vegetative influences. Trudgill (1976b) states that limestone solution under soil cover will take place best where good drainage, vegetation capable of effecting cation exchange, and high levels of soil carbon dioxide exist. Under high moisture conditions, soil pores become filled by water and buildup of carbon dioxide partial pressure boosts the acidification of the water (Trudgill, 1976b). Drainage through organic horizons encourages water to pick up acids and chelating compounds, and leaching at the base of the profile provides the necessary mineral product removal (Trudgill, 1985). Root surfaces effect cation exchange by transferring hydrogen ions from the root surface to soil mineral particles, where calcium and magnesium are extracted for the plants use. Trudgill (1976b) states that cation exchange is a likely pathway for the formation of deckenkarren.

In comparison to pH values in permanent pasture soils, soil pH levels in paired forest soils were found to be two units lower to a depth of about 15 cm and to maintain pH levels about one unit lower through their entire depths (Ritter et al., 2003). Ritter et al. (2003) also found  $\text{Ca}^{2+}$  to be higher in pasture soils than in forest stands. It is thus possible that in karst landscapes, trees may exacerbate dissolution through increase in general soil acidity.

### **Regolith and Epikarst Interactions**

Research interest in soil, regolith, and epikarst hydraulic influences on karst aquifers has shown recent growth, prompted by engineering (Panno et al., 1994; Julian and Young, 1995; Ahmed and Carpenter, 2003) and environmental concerns (Zhu et al., 1997; Currens, 2002; Peterson et al., 2002; Plagnes and Bakalowicz, 2002). White (2002) recognizes a conceptual shift in thinking over the last two decades that acknowledges the importance of infiltration and recharge processes in karst areas. Flow conditions and antecedent recharge status in the infiltration zone may be as important as conduit structure in determining a

limestone aquifer's output, so that while constriction size normally controls fracture flow (Halihan et al., 1998), a large storm event may unclog an entire system and create new outlets (Lastennet and Mudry, 1997).

Because most drainage occurs through solution in subsurface pathways, particulates accumulate in a fluviokarst landscape to a degree dependent on the bedrock lithology, climate conditions, and topography (Atkinson and Smith, 1976). As limestone is attacked by solution, calcareous debris dissolves first, followed by microcrystalline cements, and dolomite particles (Gargarina, 1968). Finely dispersed iron hydroxides and clays are next removed, leaving silt and sand residues as accumulations. The finest silts and clays are leached in solution and suspension, and as they translocate, calcareous particles in lower soil layers act as precipitation foci. Thus tiny limestone fragments are replaced in subsoils with finely dispersed clay/iron particles (Gargarina, 1968). During this weathering process, dispersed brown clay/iron films and coatings flocculate and accumulate on unleached portions of rocks (Gargarina, 1968). This process occurs to the greatest rate in the illuvial portion of the soil profile, encouraging clay to build up in carbonate terrains.

Products of the karst weathering process must be removed from the system for solution to continue (Trudgill, 1976b). Where water cannot pass through underlying rock on the epikarst surface, dissolved calcium may remain at the soil profile base and impede further dissolution of the bedrock surface (Trudgill, 1976b). Zseni (2002) found that soil that is in direct contact with limestone has a higher pH than soils above it, suggesting that as soil aids weathering at the epikarst surface, the limestone in turn affects the soil and thus limits its own dissolution. Clay may also restrict vertical water movement, and in some circumstances clay may restrict downward penetration of water through soils highly charged with carbon dioxide, thereby preventing acidic water from reaching the bedrock base (Trudgill, 1985). At the slope scale, laterally moving water will tend to carry carbonate products downhill, so that diffuse uphill water flow is acidic, but converging downhill flows become increasingly alkaline and less able to cause the growth of karren (Trudgill, 1985).

In humid temperate regoliths developed on limestone, clay mantle soils and hydrological pathways evolve concurrently with the cutters and pinnacles of the epikarst surface. As argillic horizons develop over the abrupt soil/bedrock interface, runnels and soil arches formed under stress-consolidated soils often pipe flow through drains connecting cutter bases (Cooley, 2002), creating a highly transmissive flow region of integrated solution features at the bedrock interface (Julian and Young, 1995). Flow is predominantly lateral at this interface and within the upper



epikarst, since entry of water into the main aquifer is limited to vertical leakage paths that diminish with depth to a few major fissures (Klimchouk, 2000).

Research suggests that the hydrologic interrelationships that develop between regolith, epikarst, and main aquifer are very complex. Gunn (1981, 1983) carried out studies that show that water is transmitted to a karst aquifer through six different major pathways: overland flow, regolith throughflow, subcutaneous flow through the epikarst, shaft flow as films on shaft walls, vadose flow movement along enlarged joints through the rock mass, and vadose seepage through intergranular flow and/or percolation through tight joints. Overland flow and vadose seepage were deemed relatively insignificant, and shaft flow, rather than vadose flows, sent most water to aquifer cave systems. Shaft flows were supported by both epikarst and throughflow water, with somewhat more coming from subcutaneous movement. Both throughflow and subcutaneous delivery rates responded to storm events, and slower, more sustained flow developed in lower regolith horizons in comparison with the upper regolith. Conditions of water chemistry and quantity in the regolith affect subcutaneous flow, and thus solution processes and water conditions in the main aquifer.

Infiltration rates may be high in mid-latitude karst residuum soils (Jennings, 1985), particularly during storm pulses when flow enters macropores too large to be able to hold water by capillary action (Peterson et al., 2002). Often surface macropores, soil pipes, and sinkholes feed directly into the few vertical leakage paths through the epikarst that feed into the main aquifer (Ahmed and Carpenter, 2002). Macropores in the regolith, often operating along tree roots, are usually vertically oriented and may connect with runnels at the bedrock interface (Cooley, 2002). Because non-connected areas of the epikarst store water, the epikarst regulates base flow to the aquifer (Jennings, 1985; Klimchouk, 2000). During storm events, recharge creates quick flow along macropores that bypasses the soil matrix, rapidly moving stored epikarst water into conduit networks (Perrin et al., 2003). These vadose flows may be aggressive at points of concentrated fracture entry (Thrailkill and Robl, 1981; Palmer, 2002), aiding in enlargement of favored routes (Cooley, 2002). The amount, aggressiveness, and delivery of meteoric waters are directly mediated by the surface environment, which thus has a strong determining influence on karst aquifer development.

## **HILLSLOPE HYDROLOGY**

The distribution of hillslope water and sediment movements is dependent on a number of factors operating at a range of temporal and spatial scales (Post and Jones, 2001; Bond et al., 2002; Kishel and Gerla, 2002). Heterogenous soil composition, porosity, and permeability

characteristics generate water holding and movement capacities that are measurable as variations in hydraulic potential gradient and conductivity (Petts and Amoros, 1996; Tindall et al., 1999). Water content and soil matric pressure shift dynamically with antecedent moisture conditions and within individual storm events, causing hillslope water movements to be extremely complex (Navar et al., 1994; Clothier, 2002).

### **Soil Properties**

The transmission capabilities of a soil depend on the relative proportions and arrangements of pores and thus on the factors that influence soil porosity. Porosity, determined by size, shape, and arrangement of particles within and between soil peds, determines the capacity for water entry and drainage within the spaces of a soil material (Brady and Weil, 1996). Porosity is regulated by the soil's mineral constituents as derived from its parent material in combination with biological influences of root penetration and organic matter distribution, organic acid and binding agent additions, and bioturbation (Rowell, 1994). Soil particles assemble into defined structures under these combined physical and biological controls.

Soil structure, together with porosity, determines infiltration and throughflow patterns in a soil matrix because it sets up macrostructures that permit rapid drainage of water after heavy rainfall (Rowell, 1994). Macroporosity operates in spaces between aggregates that have openings of  $>0.5$  mm, whereas smaller pores, termed storage micropores, retain water available to plants between field capacity and wilting point values. Residual micropores of  $<0.2$  mm are associated with clay particles that tend to control the mechanical strength of the soil but to limit water to hygroscopic values (Rowell, 1994). Where macropore structure is at least  $0.1 \text{ cm}^3$  per  $\text{cm}^3$ , drainage is usually adequate, but soils supporting a higher proportion of the smaller micropores will have impeded drainage capabilities (Rowell, 1994). The presence of large amounts of clay in a soil layer is thus a marker for slowed water flux. As the micropores of dense soils become saturated, the soils swell and become impermeable to subsequent water penetration (Brady and Weil, 1996).

Organic materials incorporated into soil mediums typically promote high porosity and low particle density. Because pedogenesis usually incorporates organic matter in highest percentages in the upper mineral horizon, rainfall rates in areas where vegetation covers are thick are unlikely to be larger than the soil's infiltration capacity. Where high soil porosity and structural integrity are maintained, penetration of surface layers is diffuse, so that the presence of organic-rich horizons with crumb or granular aggregate structures suggests that vertical penetration is likely (Brady and Weil, 1996). As water enters the upper horizon, the matric

potential of the surface soils rises, and suction force is added to gravity in a vertically downward pull of water. Water will continue to be pulled downward at a rate dependent on the volume of the entering water and the impedance of any structures or characteristics in the profile that may lower the hydraulic conductivity.

### **Soil Anisotropy**

One effect of infiltration is to promote chemical responses in the material it passes through, setting up weathering and leaching processes that create accumulations of clays, salts, and amorphous complexes in lower soil levels (Birkeland, 1984). Illuviated clays coatings may bridge grains, coat peds, or create thin, discrete layers or lamellae that offer pedogenic evidence of basically vertical accumulation in a particular soil (Birkeland, 1984). Although water may penetrate deeply in a soil where aggregates are stable, illuviated clay particles may accumulate to the point where they restrict infiltration rates (Birkeland, 1984).

Soil anisotropy, defined as change in soil hydraulic conductivity with depth, is correlated with characteristic overland or throughflow pathways (Noguchi et al., 1999; Eisenbeer, 2001; Canton et al., 2002). Clay particles, because of their plate-like shapes, tend to pack tightly, forming aquicludes if present in soil layers in high enough amounts. Clays are well known to induce perching or lateral water movements in soils, and in limestone depressions where clay layers contact limestone surfaces, clay layers may focus erosion laterally along the limestone contact (Trudgill, 1985).

Lateral movements of water within a soil will respond to localized shifts in matric potential that override the general downward pull of gravity. Where saturated zones develop within soils, they tend to be thin, discontinuous, and perched above some lower flow system (Daniels and Hammer, 1992). These temporary zones usually relate to restrictive layers where changes in soil texture create a capillary barrier, and changes in soil texture within a soil profile may offer visual evidence that restrictive layers are present. Most often an impeding layer is related to an increase in clay content, but a coarse layer underlying a fine layer will also halt downward flow (Heilig et al., 2003). Discrete locations where flow has broken through impeding layers will be indicated by isolated zones of wetness in exposed soil profiles. Weiler and McDonnell (2004) report on studies in which impeding layers were mapped so that spatial patterns of transient water tables could be modeled.

Movements of illuviated particles also occur laterally on slopes, so that soils at slope bases can be expected to have stronger profile development with higher base content (Birkeland, 1984). When infiltration is high, water will accumulate above the low hydraulic

conductivity layer and eventually move along the hydraulic gradient (Daniels and Hammer, 1992). Subsurface flows conducted at boundaries between O and A, and between A and B horizons may carry fines downslope, contributing to catena development and thick argillic soils at slope bases. Soils at slope summits tend to be well drained and oxidized red, whereas high water tables in downslope areas might show up in mottling or gleying of soils (Birkeland, 1984).

### **Water Movements on Slopes**

Black-box type models are generally used to describe the downslope movement of water (Kendall et al., 2001). Vegetation transpires a large portion of the precipitation received by a catchment. Vegetation also intercepts a portion of the incoming precipitation, encouraging loss to evaporation, storage in leaf litter, or collection as throughfall or stemflow passing through leaves and down trunks of large plants (Petts and Amoros, 1996). As water contacts the soil surface, negative pore water pressures encourage infiltration, leading to throughflow, or subsurface flow, in the unsaturated zone and percolation downwards to the water table.

Major controls dominating recharge distribution and the likelihood of surface runoff in humid temperate regions are bedrock, climate, and soil, while vegetation and topography form secondary controls (Dunne, 1978). In temperate vegetated catchments, both overland and infiltration excess flow, or flow caused by higher intensity precipitation input than can be immediately absorbed, are usually uncommon. Most water is carried as throughflow, which passes downslope through both the soil matrix and through preferential pathways, which conduct water at a higher rate and volume than simple soil percolation. Throughflow may emerge again at the surface as saturation excess flow, which can take place where soil impermeability (Anderson and Burt, 1982; Burch et al., 1987), saturation of subsurface elements (Srinivasan et al., 2002), or a rise in water table height caused by flow convergence in topographic depressions pushes return flow back to the surface (Dunne and Black, 1970; Tsuboyama et al., 1994; Prosser et al., 1995; Burt, 2001). This later concept of water table rise in portions of slopes that collect soil water was established by Hewlett (1961), who introduced the idea that storm runoff sources are mostly controlled by subsurface water movements.

As various throughflow pathways are followed by vertical and lateral fluxes, overland flow is generated in variable source areas of saturation excess that change size and location within the slopes on both an hourly and seasonal basis (Hewlett and Hibbert, 1967; Thomas and Goudie, 2000). Under continuing rainfall, wedges of soil saturation grow in size in hillslope depressions, causing the size of areas contributing to overland flow to expand as well (Dunne,

1978; Petts and Amoros, 1996). Any rain falling on the saturated area will not be able to infiltrate, which adds quickflow to the seepage produced as overland flow by the wedge of saturation (Knapp, 1979). As water drains vertically from hillslope pores following the storm event, the water table in the wedge drops, and water movements drop to groundwater pathways (Petts and Amoros, 1996). In a fluviokarst landscape, saturation excess flow will generate overland flow when epikarst and regolith storage capacities, along with conduit drainage from the epikarst, are overwhelmed under high moisture conditions. Direct connections to the main limestone aquifer from points within the epikarst also assure that overland flow ceases quickly after rain events, causing streams to operate ephemerally.

Field studies have shown that hillslope water pathways are even more variable than first supposed. Certain basins may have rock areas or impermeable zones within the regolith that may provide a significant amount of the basin's stormflow as infiltration excess overland flow from a relatively small percentage of its surface area (Betson, 1964). Lateral throughflow in other locations may be instituted at the bedrock interface, through macropores, by high soil hydraulic conductivity areas, or through litter layers (Weiler and McDonnell, 2004). In any particular basin, infiltration, throughflow, and saturation excess flows operate dynamically with storm intensity, duration, and antecedent moisture conditions.

### **Preferential Flow**

Much of the dynamic nature of subsurface water movement resolves from utilization of preferential flow pathways, which are ubiquitous in natural soils and form disconnected open channels created in the soil by a number of often biologically influenced processes (Weiler and McDonnell, 2004). Preferential flow paths are classified by size into categories as micropores, mesopores, macropores, and soil pipes (Uchida et al., 2001). Mesopores, which generally drain at field capacity, are able to conduct infiltration that occurs during 90% of all rainstorms in some environments (Luxmoore et al., 1990). Macropore flow becomes increasingly significant with increased antecedent moisture and rainfall intensity (Jardine et al., 1990; Mizuyama et al., 1994; Sidle et al., 1994). Very large pipes are widespread in some semiarid or peaty environments (Jones, 1997; Guitierrez et al., 1997), but the "piping" effect commonly studied in humid environments involves macropore flow in structures from approximately 0.1 to 4 cm in diameter that do not necessarily develop from an outlet (Luxmoore et al., 1990; Bryan and Jones, 1997). Structures of this size can be visually observed and measured, and insides of soil pipes have been photographed (Terajima et al., 2000).

Uchida et al. (2001) distinguish 'topsoil pipes' sustained temporarily by high biological activity, from longer-lived 'lower soil pipes' that are sustained by soil properties of permeability, cohesion and hardness. Animal and earthworm burrows operate as topsoil pipes in grassland soils (Mitchell, 1988). Earthworms may create effective infiltration channels 1.35 to 1.8 m deep (Van Stiphout et al., 1987; Trimble, 1988), but exposed openings may seal under high intensity rains (Ela et al., 1992). Major macropores in forests develop from subsurface erosion around roots and rocks, from decayed or living root channels, from bedrock surface fractures, or from animal burrows (Sidle et al., 1995; Sidle et al., 2001).

Preferential flow through macropores may be activated, depending on soil properties and water content (Weiler and Nael, 2003), either when the soil reaches saturation (Embleton and Thornes, 1979), or when a high intensity storm exceeds infiltration capacity during unsaturated soil conditions (McIntosh et al., 1999). Sidle et al. (1994) measured macropore hillslope discharge contributions of 6.6-8% under dry antecedent conditions and up to 30% for the wettest conditions at one forested site. In another study, Sidle et al. (1995) found that in forested catchments in Japan, increase in soil moisture was not accompanied by an observable increased macropore component until halfway through the typhoon season. In this second study, forest macropores did not operate during storm events under dry antecedent conditions. Soil stores were recharged first, and as moisture content in the soil profile rose with subsequent rain events, macropores became able to deliver up to 25% of monitored subsurface flow during high intensity rain events. Although preferential flow often accompanies soil saturation, it has also been shown in some cases to bypass dry soil layers during very high intensity storms, saturating lower horizons and eventually supplying moisture to the dry soil layer through slower diffuse lateral flow. In both saturated and unsaturated conditions, preferential flow appears to operate as an overflow mechanism in hillslope regoliths (Trimble, 1988).

## **Erosion Processes**

Whereas homogeneous soil matrix flux rates can be estimated based on Darcy's law, preferential flow pathways tend to coalesce into hillslope networks that permit non-Darcian turbulent flow velocities capable of generating subsurface sediment discharge (Uchida et al., 1999). The macropore network self-organizes through three-dimensional expansion during wet conditions, connecting between buried organic matter pockets, areas of loose soil, areas of slowed water movement at organic-mineral horizon boundaries and locations of decayed roots or eroded cavities (Sidle et al., 2001). As the network grows with storm intensity, it extends upslope (Sidle et al., 1985; Tsuboyama et al., 1994). Even though these networks occupy only

a small percentage of the soil pore space, they may contribute important amounts of flow to storm hydrographs (Anderson and Burt, 1982; Wilson et al., 1990). Water in the pipeflow system does not normally sustain baseflow (Uchida et al., 2001), although high levels of both stormflow and baseflow may be carried where pipes directly feed into or out of bedrock fractures (Noguchi et al., 1999). Where hillslope lithology does not permit deep bedrock fissure entry, catchment storm hydrographs peak sharply from rapid soil water outflow (Onda et al., 2001), which may develop as lateral flow at the bedrock surface (Tani, 1997).

Hillslope sediments are carried as dissolved or suspended fractions according to the transport capabilities of the acting flow pathways, and sediment discharge can occur from both the surface and subsurface. Surface suspended particle movement occurs at flow-induced shear stress and soil resistance thresholds that determine erodibility (Ahnert, 1994; Montgomery and Dietrich, 1994; Kirkby, 1994; Bull and Kirkby, 1997; Canton et al., 2002). Identical erodibility factors control subsurface sediment movements, with further constraint created by upslope interconnections and pipe diameters of the macropore network (Mizuyama et al., 1994; Uchida et al., 1999; Uchida et al., 2001). Tergina et al. (2000) state that as pipe networks form and as sediment is removed, the pipes change the subsurface flow regime itself, thus adding a recursive element to further preferential flow development. In karst regions, subsurface soil transport and subsidence of the clay mantle are ubiquitous in the epikarst, where openings large enough to sustain fracture flow operate congruently between soil and rock (Cooley, 2002).

Sediment and water delivery are partly determined by a hillslope's soil properties and infiltration capacity (Wijdenes and Bryan, 2001). Slope influences the force exerted by surface flow, but actual erosion susceptibility is moderated by lithology and soil properties of texture, aggregate stability, shear strength, and infiltration capacity (Bull and Kirkby, 1997; Wijdenes and Bryan, 2000). While seepage, or water carried back to the surface by excess pore pressure, does not by itself increase erosion rates, it reduces the effective weight of soil particles and contributes to soil movement under surface flow (Owoputi and Stolte, 2001). Seepage caused by temporary saturation or perching at impermeable layers will create positive pore pressures that generate lift, lowering the soil's cohesive properties and destabilizing slopes (Sidle et al., 1985). Rockwell (2002) showed that erosion rates increase through soil shear strength loss even before the full soil depth is saturated and surface seepage is able to take place. Pipeflow increases the rapidity of downslope drainage and can thus rapidly drain the soil and eliminate perched conditions, but where the preferential flow system cannot handle the incoming rainfall, pore pressures may increase and contribute to localized instability (Uchida et al., 2001). Where

positive pore pressures operate concurrently with saturation excess and pipe flows, heightened hillslope sediment transport is likely to occur.

## **VEGETATION EFFECTS ON HYDROLOGY**

Erodibility is strongly influenced by vegetation, which lessens compaction and increases soil infiltration to a degree determined by plant community dynamics. Individual plants directly influence local soil properties (Zinke, 1962; Gersper and Holowaychuk, 1971; Birkeland, 1984). These effects are cumulative (Pettapiece, 1969), enabling mature grass and forest communities to build characteristic soil profiles that offer different advantages in maintaining landscapes under varying conditions (Trimble 1997). Differences in vegetation may affect distribution and storage of moisture, surface shear strength, soil stability, infiltration capacity, soil textural and structural properties, organic content, faunal and microorganism populations, and evapotranspiration, along with a number of other associated factors that all influence hydrology.

Properties of root thickness, extent, frequency, and orientation determine the different stabilization capabilities of forest and grass. Whereas deep intertwining tree roots stabilize slopes through the addition of soil shear strength (Sidle et al., 1985; Trimble, 1988), grass is more capable of protecting the soil from surface flows. Grassland stems and root mats are able to resist surface shear stresses as high as 1000-1800 dyn/cm<sup>2</sup>, preventing erosion even where saturation overland flow develops in spots of topographic convergence (Prosser et al., 1995; Gyssels and Poesen, 2003).

### **Evapotranspiration**

Approximately 70% on average of precipitation received by a temperate watershed is evaporated or transpired from soil and plant surfaces and is thus unavailable to streams or aquifer storage (Hewlett, 1982). This water use occurs through transpiration, which sends vapor back into the air through plant respiration processes, interception, in which water is evaporated from leaves before reaching the soil, and from soil, rock, and open water evaporation. Most of this evapotranspiration loss occurs in the periods between storm events, as moisture stored in the soil is used by vegetation or is evaporated from soil surfaces. Fujieda et al. (1997) found that most rainfall (59%) was stored in the forest soil, and that stormflow leaving his forest study basins accounted for only 11% of total rainfall. Evapotranspiration is influenced in different ways by varying types of vegetation, regolith, and bedrock conditions, and the effects may vary seasonally. Daily and hourly differences also occur, as trees are able to



influence lateral hillslope flowpaths through the daily pull of water out of the soil profile caused by transpiration (Bond et al., 2002).

The degree of precipitation lost before it reaches the ground is largely dependent on factors influencing the type of vegetation and degree of leaf cover, the size of the storm event, and the antecedent moisture held by the above-ground plant mass and litter (Hewlett, 1982). Development of canopy growth increases the likelihood of interception, and interception adds significantly to annual water yield loss in forests. However, the percentage of interception lost during single rain storms is dependent on the size of the rain events (Sidle et al., 1995). Approximately the same amount of interception occurs with each storm, so that with dry canopy coverage, almost all of a very small event may be intercepted. Interception is eliminated when foliage is already wet, and the percentage of precipitation lost through interception drops rapidly with high intensity or lingering storm events. Hewlett (1982) reports that interception loss in forests will also vary with age and type of forest stand, so that average loss among Southern Appalachian mature hardwoods was 12% of total annual precipitation input, whereas 60-year old white pine lost 26%. Seasonal leaf loss by hardwoods also diminishes interception loss during winter months.

Hewlett (1982) estimated that transpiration remained the same, at about 78% of total annual evapotranspiration, in both mature deciduous hardwoods and mature white pine in the Southern Appalachians. Hewlett (1982) also summarized experiments that found on average that a 10% reduction in deciduous hardwood cover would generate a 2.5 cm reduction in annual evapotranspiration. The actual percentage of annual precipitation that is lost to evapotranspiration is difficult to determine and varies greatly between watersheds.

High forest evapotranspiration rates limit baseflows (Sikka et al., 2003), and afforestation may decrease baseflow in some areas to the point where headwater streams may dry up (Burt, 1992). Increase in stream flow can be achieved by converting forest to open land (Reinhart et al., 1963; Sikka et al., 2003; Ziemer and Lisle, 1998). Sikka et al. (2003) report on studies that indicate a 16% drop in water yield following conversion from grassland to forest. Fujieda et al. (1997) report a 15% interception rate by forest cover in Brazilian subtropical forest, and a combined loss to the hydrological budget of 30% of rainfall to evapotranspiration. Evapotranspiration rates may overall be considerably higher in forests than grasslands, accounting for most changes in water yield with deforestation (Cheng et al., 2002; Holmes and Colville, 1970).

Although transpiration and interception loss from a forested area is typically higher than that under grass, evapotranspiration will vary seasonally in both, and in some cases actively

growing grass may have evapotranspiration rates that approach that of a growing forest. Most plants release a large amount of water to the atmosphere during rapid growth. If grass is planted in a cleared forest area and then fertilized, the water yield increase may drop to a level equaling that of the forest, showing that water requirements in rapidly growing grasses may be as high as those of forests (Burt and Swank, 1992). Despite the ability of plants to regulate water loss through their stomata, a dense grassland or wheat field may deliver 80% as much water to evapotranspiration as a body of water with an equal area (Rowell, 1994). Evapotranspiration losses in grasslands may thus be high during warm months when water is available for growth.

Because temperate forests have leaf cover only during growing seasons, evapotranspiration is only effectively influenced by deciduous forests during summer months (Post and Jones, 2001). Thus evapotranspiration losses in forest and grass humid temperate landscapes should be much the same during leaf-off months, but with the exception of heavy growth periods, should be substantially higher for forest than for grass during the rest of the year. At times of high growth, such as might occur after adequate spring rains in late May or June, grass evapotranspiration may be close to that of the forest.

### **Water Infiltration and Movements**

Temperate grasslands have the shallowest of all root systems, and the majority of their roots will be found in the top 30 cm of the soil (Robinson, et al., 2003). Grasslands thus incorporate a large amount of organic matter in their topsoils through both litterfall and root decay at shallow depth, creating A horizons that are rich in humus and dark colored (Birkeland, 1984). The large amounts of organic matter maintain high infiltration capacities in topsoil layers, and rainfall typically enters the soil in a diffusive fashion. Organic matter, along with some of the finer inorganic sediments, may be carried downwards with percolating vertical flows (Pettapiece, 1969). Earthworm burrows penetrate the organic layer and construct a macropore system that, depending on the grassland soil type, may transfer water vertically through unsaturated soil matrix to a deeper layer or to the bedrock (Weiler and Naef, 2003).

In contrast to the ability of grasslands to generate organic-rich A horizons, forests typically accumulate organic matter as litter in O horizons. The litter created by different tree species encourages different levels of surface soil porosity and permeability. In a study comparing decomposition rates of white oak, Norway spruce, white pine, and red pine litter, soils under oaks were found to have the lowest infiltration rates because the oak litter decomposed on the surface without being incorporated (Challinor, 1968). In other studies,

hardwood forest soils are reported to in general have higher infiltration capacity than conifer soils (Byrnes and Kardos, 1963), and all kinds of forest are reported to have a much higher overall infiltration rate than grasslands (Challinor, 1969; Heede, 1975; Trimble, 1988; Cheng et al., 2002). Surface permeability rates measured by Burch et al. (1987) were an order of magnitude higher for forest than for grassland.

Development of a top layer of humus protects the forest surface against surface sealing and aids in infiltration. Miyashita et al. (1994) estimated that maximum discharge from a studied forested catchment could reach 5% of incoming rainfall with a 15 cm humus layer but up to 60% without. Below the litter covering forest soils, A horizons are thin, and organic matter content decreases rapidly below the surface (Birkeland, 1984). Rapid mineralization of the litter reduces it to organic acids that tend to increase the acidity of the forest floors (Pettapiece, 1969), causing leaching to remove cations to a greater extent in forests than in grasslands (Birkeland, 1994). Leaching assisted by chelation processes moves colloids through the profile, sometimes resulting in bleached A horizons (Pettapiece, 1969). Because forests develop more interconnected macropore networks than grass, clay particles are translocated to deeper levels in forests than in grass, and clay contents of surface layers are thus higher in grasslands (Birkeland, 1994).

The clay layers that accumulate at shallow depths in grasslands may impede percolation (Burch et al., 1987). Impermeable layers in grasslands may develop perched zones of saturation in surface soil horizons (Bowden et al., 2001). Because of heavier clay buildup in upper soil horizons, grasslands tend to develop points of infiltration excess overland flow and saturation of near surface layers in localized spots. Macro and mesopore structures in the soil tend to organize with increasing soil moisture (Sidle et al., 1995), and fluxes across saturation boundaries may change abruptly. In grasslands, this results in sporadic water movement across the grassland surface in small areas of infiltration and saturation excess (Thornes, 1979; Srinivasan et al., 2002; Swiechowicz, 2002a,b). When water rises to the surface in small areas in cohesive soil grasslands, small amounts of loose sediment are transported short distances at all levels of shear stress, even though dense root matting prevents channel formation (Prosser and Soufi, 1998). Swiechowicz (2002a, b) found that sporadically distributed slope wash events moved most surface suspended material from the midslopes of studied Carpathian foothills, causing sediments to accumulate at hill bases. Particles carried downhill by dynamic movements are subject to sorting, so that depositional surface layers are significantly increased in silt content (Turnage et al., 1997).

The same buildup of clays that takes place in higher grass layers tends to slow water entry into deeper layers. In a hydrology study that compared paired forest/grassland watersheds, Burch et al. (1987) determined that grassland drainage continued for a longer time following storm events than drainage from forested basins, indicating slowed percolation into deeper grassland layers. Water was retained in higher soil layers in the grassland for a longer period of time than in the forest, so that response to new rain events from upper profile levels was immediate. In contrast, forest soils had deeper infiltration capacity and higher storage capabilities (Burch et al., 1987). Forest soils tend to recharge soil water content before delivering peak flows, whereas grasslands, through increased runoff, may generate high peak stormflows regardless of antecedent soil moisture conditions (Burch et al., 1987). In their study, Burch et al. (1987) measured high intensity storm peak discharge and runoff in forests that were three orders of magnitude lower than grassland rates.

Most water falling onto a wetted forest floor infiltrates into the soil (Tani, 1997) so that overland flow is not common in most undisturbed forests (Ziemer and Lisle, 1998). Forest soils typically have higher hydraulic conductivities than shrub or grasslands and generate lower runoff rates and peak stormflows (Heede, 1975; Burch et al., 1987; Fujieda et al., 1997; Cheng et al., 2002). The higher infiltration and conductivity capabilities of forest soils are largely created by root channels (Sklash et al., 1986). Forest root systems form macropore networks that rapidly transfer water vertically and laterally (Sidle et al., 1985), permitting deeper entry of water into forest soils than under grass. Macropores in forest soils may occupy up to 35% of the total soil volume and up to 50% of the upper half meter of the forest soil, and in areas where piping dominates, soil matrix properties become relatively unimportant in storm flow generation (Aubertin, 1971).

Smakhtin (2002) detected two zones of subsurface flow in forest soils: one associated with a loose upper soil layer, and a second subsurface drainage consisting of root channels parallel to the surface. Lateral water movements in forests may follow pathways along the organic material in the O horizon (Brown et al., 1997) and along the interconnected root network within the top 0.5 m of the soil (Burch et al., 1987). Other researchers have found that preferential flow along roots is important at deeper depths and has a vertical component of action. In forests, living roots may intersect both B horizons and bedrock and may associate with up to 70% of upper horizon and 55% of lower horizon macropores (Noguchi et al., 1999). Water may be conducted deeply along vertical preferential flowpaths by roots in forests, and where roots penetrate to the bedrock, ponding at the soil/bedrock interface may generate lateral flow that extends upward across an entire slope (Tani, 1997). The meso/macropore routes

noted by Wilson et al. (1990) acted at a depth of about a meter, showing that vertical and lateral components of root networks act to distribute water to all levels of the soil matrix.

Preferential flow pathways in forests act to quickly conduct high intensity precipitation along root networks from a source area that interconnects up the hillside as the storm proceeds (Sidle et al., 1985). Perching of water and lateral flow in the O horizon may also conduct a significant portion of stormflow in some forested basins (Brown et al., 1999). Conduction of flow either in the litter or as throughflow in the top 0.5 m of the soil prevents the generation of saturation excess flow, and the main source area for stream flow from many forested hillslopes is a dispersed movement of stored soil water into groundwater discharge (McGlynn et al., 2002). Impermeable bedrock structures or collection of water in hollows may permit saturation excess flow in some locations on forested hillslopes (Tsuboyama et al., 1994).

Burch et al. (1987) determined that preferential flow pathways responsible for rapid changes in water table levels in their forest catchment were not operative in the grassland catchment. Stormflow from upper grass layers is mainly supplied by direct subsurface movement from the soil matrix, rather than from preferential flow (Sidle et al., 1995). Under moderate moisture conditions, water exiting forested slope bases also typically does so through subsurface percolation that moves predominantly through the saturated soil matrix (Sidle et al., 1995). However, in some catchments, preferential flow through interacting mesopore and macropore nets may be the dominant mechanism in stormflow propagation (Wilson et al., 1990).

Determining the depth to which preferential flow will follow tree roots is not easily done, though as suggested by Willson et al. (1990), it operates to at least a meter below the surface. The majority of the tree roots lie above this depth, so that 77 to 89% of roots observed in West Virginian road cuts were found above 0.6 m (Kochenderfer, 1973). Although most tree roots are found in upper soil layers, deep tree roots are not uncommon (Robinson et al., 2003). Stone and Kalisz (1991) find that root length, as opposed to density, may be more important for tree survival where restrictive soil or substrate conditions exist, and a disproportionate amount of nutrients and water may come from deep-rooted systems (Jackson et al., 1999). Roots often clump where nutrients are available (Stout, 1956; Robinson, et al., 2003), and once past a barrier, deep roots may splay and proliferate (Stone and Kalisz, 1991). In his study of deep rooting in the Edwards limestone aquifer of Texas, Jackson et al. (1999) found 6 tree species that rooted from 5 to 10 meters deep and one species, the evergreen oak *Q. fusiformis*, that rooted up to 18 meters deep.

Stone and Kalisz (1991) state that extension of roots into fissured bedrock and solutionally opened limestone is common, but that a few larger dominants are likely to be most effective in utilizing deep root pathways. Of the species studied by Stout (1956), the characteristic rooting pattern developed by white oak was found to be the deepest, but among others, maple (*A. rubrum* and *A. saccharum*), walnut (*J. nigra*), and hickory (*Carya sp.*) are all capable of rooting 2 to >3 meters deep (Stone and Kalisz, 1991). In shallow soils on coarse surfaces, roots will tend to follow weaknesses in the substrate, often utilizing root channels left by prior growth (Stone and Kalisz, 1991). Stone and Kalisz (1991) also make the point that if species capable of extending roots into the substrate are replaced by pasture or cropland, the possibility for further substrate entry will be lost.

Flow diverts around the outsides of living roots, and when roots decay, the pathways expand and become more conductive (Noguchi et al., 1999). Challinor (1968) attributed the high rate of infiltration found in a white pine plot to high stand mortality within the prior 10-15 years, a length of time adequate for decomposition of roots and formation of water passages. Noguchi et al. (1999) found that as roots decay, loose vertical soil zones remain that can participate in preferential flow. Numbers of vertical channels created by root decay were estimated at more than 4,000 per acre (10,000/ha) by Gaiser (1952), and he felt that lateral decayed root pathways likely connected the vertical pathways. Soil-saprolite sequences in North Carolina contained clay-filled continuous pores to 2.5 m depths that consisted mostly of old root channels (Schoeneberger and Amoozegar, 1990). These studies indicate that root pathways have a finite life span, opening up as the root decays and eventually filling in and becoming inactive. The interaction between tree roots and the epikarst in the study area is not known, but in any landscape undergoing a change from forest to grassland, preferential pathways created by root decay will eventually be lost due to sediment infilling.

## **APPLICATION AND SUMMARY OF THEORETICAL CONCERNS**

A fluviokarst landscape is defined by the complexity and nature of the pathways that feed competing surface and subsurface outlets. These pathways are set up by the interacting solutional and pedogenic processes that simultaneously transform the epikarst and regolith. Vegetation influences the soil development and hydrologic dynamics of the epikarst/regolith interactions, so that different patterns of water and sediment storage and distribution are likely to manifest under different vegetation covers over time.

These variable patterns are likely to be revealed first in sensitive locations where hydraulic forces exceed the stabilizing capacities of soil cohesion and roots. In such locations,

erosion may either scour the surface or occur at a deeper level due to macropore flow. Because of resistance and shear strength capabilities associated with different types of vegetation, erosion may vary under different vegetation covers even if transport forces are equal. Whereas deep-rooted trees can anchor steep slopes, grass has a higher capacity than forest to offset surface shear stress because of root mat cohesion. Grass can remain non-incised under most runoff conditions, but it is susceptible to converging subsurface flow which promotes high pore pressures that create lift and soil destabilization from below.

The upland soils present when Bowman's Bend was settled were developed under deciduous forests, and as such likely had higher evapotranspiration, surface infiltration, preferential flow penetration, and soil storage than present day grassed slopes. Tree root systems create the majority of preferential flow pathways found in forest soils, and their deep vertical and lateral orientations ensure that base and peak flow from a forested watershed is largely subsurface. Tree root preferential pathways may provide viaducts for flow directly into bedrock fractures, and the thin limestone beds of the epikarst make it likely that this occurs in the study area.

Grassland soil profile development, because of lack of deep preferential flow pathways and the accompanying tendency to only translocate clay to shallow depths, tends to generate throughflow at shallower depths, creating more rapid storm response and higher peak discharges than forest. Increased sediment movement via sporadic saturation excess flows also takes place under grass, which thins upper slope soils and sends fines to slope bases where silts are preferentially retained.

These vegetation-influenced hydrologic tendencies in the study area are acting in soils formed within and overlying various karren and cutter forms created within bedrock layers with differing lithologic and structural properties. These karren forms have various degrees of connection to the solutional openings in the epikarst that provide storage capacity for the epikarst aquifer. The shallow translocation of clays under grass, or the deeper translocation of forests, may be taking place in karren pockets that retain colloidal particles, or in pathways dissolved along fractures and bedding planes that permit fines to be removed from the profile in solution or suspension. Thus epikarst forms affect soil profile development, while at the same time profile development determines how much and in what way precipitation input will be delivered to the epikarst surface.

In a mature grass soil, horizon clay content, profile development, and vertical and lateral subsurface water flux pathways would be considerably different from neighboring forest soils. In the study area, soil profile changes under grass have had only 200 years to develop, so that

variations in horizon characteristics between forest and grass may be hard to detect. It is likely, however, that the large difference in flow conductance patterns between forest and grass may have generated effects strong enough to affect sensitive slope locations. The current pattern of incision and conduit exhumation seen on Bowman's Bend may reflect a patchwork of sensitive landscape responses to shifts in hydraulic processes.

The shifts that may be occurring under grass in the study area are likely subtle, but may continue to gain in strength over time. Lack of deep preferential flow under grass may act to perch throughflow sufficient to increase lateral flow downslope and into epikarst conduit systems. As tree roots decay, the preferential pathways initially opened during their decomposition would become filled. Deep soil pipes and solutional pathways in the epikarst would become plugged, gradually encouraging more lateral flow in upper soil layers. Increased surface runoff under grass would tend to show up as thinner upper slope soils, and increased lateral movement would display as heightened water emergence at slope bases and in linear depressions overlying conduits.

Because of the ability of grass root mats to withstand shear stress, and the ability of tree roots to encourage rapid preferential flow, points of greatest sensitivity in the landscape at Bowman's Bend would be the places where increased lateral throughflow would create positive pore pressures at places where grass root mats no longer protect the surface, but tree roots became available for rapid subsurface flow: i.e. the grass/forest boundary line on Bowman's Bend. The review of data available on fluviokarst landscape formation, hillslope hydrology, and vegetation influence on hydrology suggests that it is quite possible that the erosion pattern on Bowman's Bend represents the first sign of a shift under grass to perched flow that may eventually denude portions of the slopes.



## **CHAPTER 4**

### **RESEARCH METHODS**

#### **SYSTEM DATA COLLECTION**

The research approaches chosen for this project were selected based on observations made during numerous visits to the study area under a wide range of weather and soil moisture conditions. Those observations, and the accompanying accumulation of background information through interviews, aerial photograph study (Appendix 1, Aerial Photographs), and analysis of topography, climate, geology, and soils data, are integral to this earth surface system project and form its framework. Based on this information, sampling sites for phase 1 soil texture and depth tests and phase 2 infiltration measurements were chosen from slopes that best represented characteristics of thin soil, high gradient, base erosion, and forest and grass cover that has been maintained continuously at matching elevations. Access permission to areas of the bend also played a role in site selection, particularly in regards to setup of soil water content data loggers. Because the data logging stations were long-term installations, their setup location is not within the main study area where grassed slopes are privately owned. Instead, the station sites lie within a few hundred meters of the main road at the west end of the Crutcher Preserve where neighboring forested and open toe slope locations are owned by the Nature Conservancy.

The pilot survey of erosion and karst features was made by traversing the bend, taking measurements of types, sizes, and depths of features along with site aspects, slopes, and descriptions, and then mapping locations with a Garmin® GPS receiver. Sinkholes, swallets, and shafts were mapped and measured for widths and depths, with records kept concerning their relative levels of visible activity based on signs of erosion and water movement. Some sinks and larger features were measured with a laser level, but most measurements of erosion features were taken by determining maximum depth and top extent with a tape measure. The laser level was used to determine slopes during the initial pilot survey, and a clinometer was used to measure slopes during infiltration testing in phase 2.

GPS locations of erosion and karst features mapped during this survey, and of all sites sampled later in the project, were layered in an Esri© ArcView 3.3 GIS system with 1997 digital ortho quarter quad (DOQQ) aerial photographic images, a 10 meter digital elevation raster/grid model (DEM), and digitally vectorized geology and soils data to allow analysis of feature

locations with respect to geology, soils, and topography (Appendix 2, Digital Data Sets). Interviews to collect historical settlement and land use information were conducted formally in 2003 and November of 2005 with the owners of the grassed slopes of the main study area, but informal contact with these individuals was continuous and helpful throughout the duration of the project. Contact with Nature Conservancy personnel also proved helpful in determining the goals and applications of the Conservancy's local management practices.

## **PHASE 1 RESEARCH – DETERMINING SOIL VARIABILITY**

### **Particle Size Analysis of Sampled Profiles**

Available soil survey data provides information that is too coarse in scale to answer the questions raised in this project. Using the SSURGO soil survey data (Soil Survey Staff, 2005) as a starting point, stratified random sampling of soil profiles to determine particle texture and soil depth was conducted for selected representative areas. Sites were selected based on vegetation type, lithology, and slope position in three different portions of the main study area (Hillslopes A, B, and F) and in the area eventually chosen for placement of water content data logging setups (Hillslope C) (Figure 4.1). The majority of samples were taken in the vicinity of a known epikarstal conduit on Hillslope A and included samples taken above, within, and at varying distances from the conduit location both within the uphill grassed portion of the slope and within the downhill forested area (Figure 4.2). Hillslope A grass sample sites were selected from the portion of the area bordering the conduit that was shown by aerial photographs to have been deforested since at least 1937. Sites sampled on other hillslopes were selected based on contrasting long-term forest/grass vegetation covers at matching elevations.

A total of 63 profiles were sampled by bucket auger, with samples taken at 0-10, 20-30, 40-50, and 60-70 cm depths, and at just above bedrock in each profile. Supplemental samples at 80-90 cm were sometimes taken in deep soils, and in shallow soils not all depths could be measured. Two to four hundred grams of material for each layer were bagged and brought back to the lab where they were air dried in trays for at least 48 hours. Large organics and gravel were hand sorted and set aside for weighing. The remaining material was then ground in a mortar, with care taken not to crush very small pebbles (Smith and Atkinson, 1975). Particles larger than 2 mm in diameter were sieved from the soil with an ASTM No. 10 (2 mm) brass sieve and added to the gravel taken from the sample. The total sample portion >2 mm was washed, dried, and weighed. Soil separates for the <2 mm portion were then determined through gravimetric lab techniques.

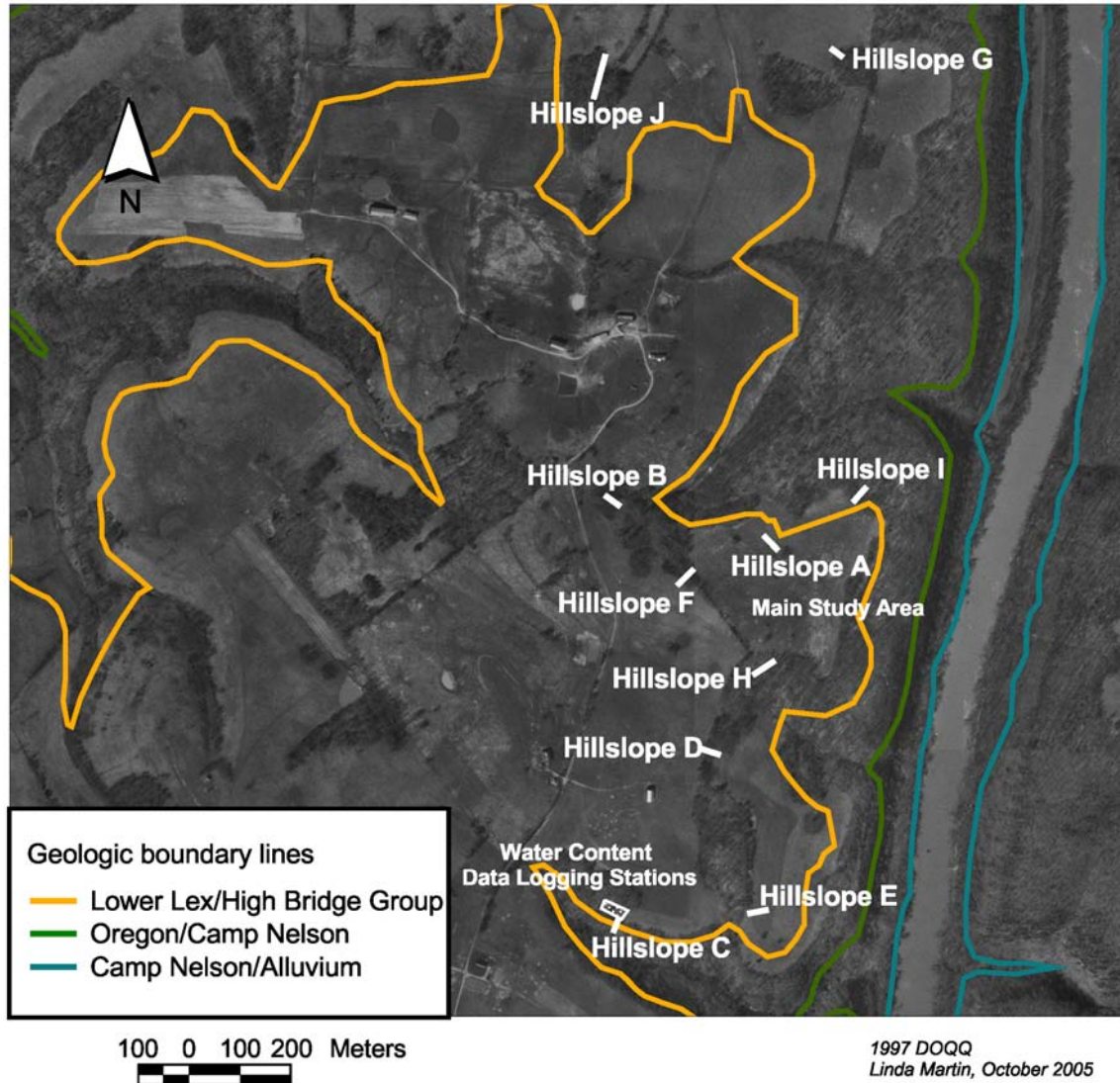


Figure 4.1. Locations of all slopes sampled during any part of the project. Soil samples were taken by auger from slopes A, B, C, and F.

The sample sizes taken for this project are within the weight ranges suggested for accurate statistical analysis for sand and smaller sized textural classes, but not for gravel portions and larger (Tan, 1994). Although the portion  $>2$  mm was washed and weighed, it represents only the stone percentage of the sample itself and may not be a representative percentage for the soil's horizon. Gravel portions were washed and weighed to help provide a determination of what types of gravel were represented as well as what proportion might be classed as very small and possibly small stones (McRae, 1988; Tan, 1994). Better estimates of stone percentages were obtained during phase 2 infiltration work when layers were assessed visually for stone content (McRae, 1988).

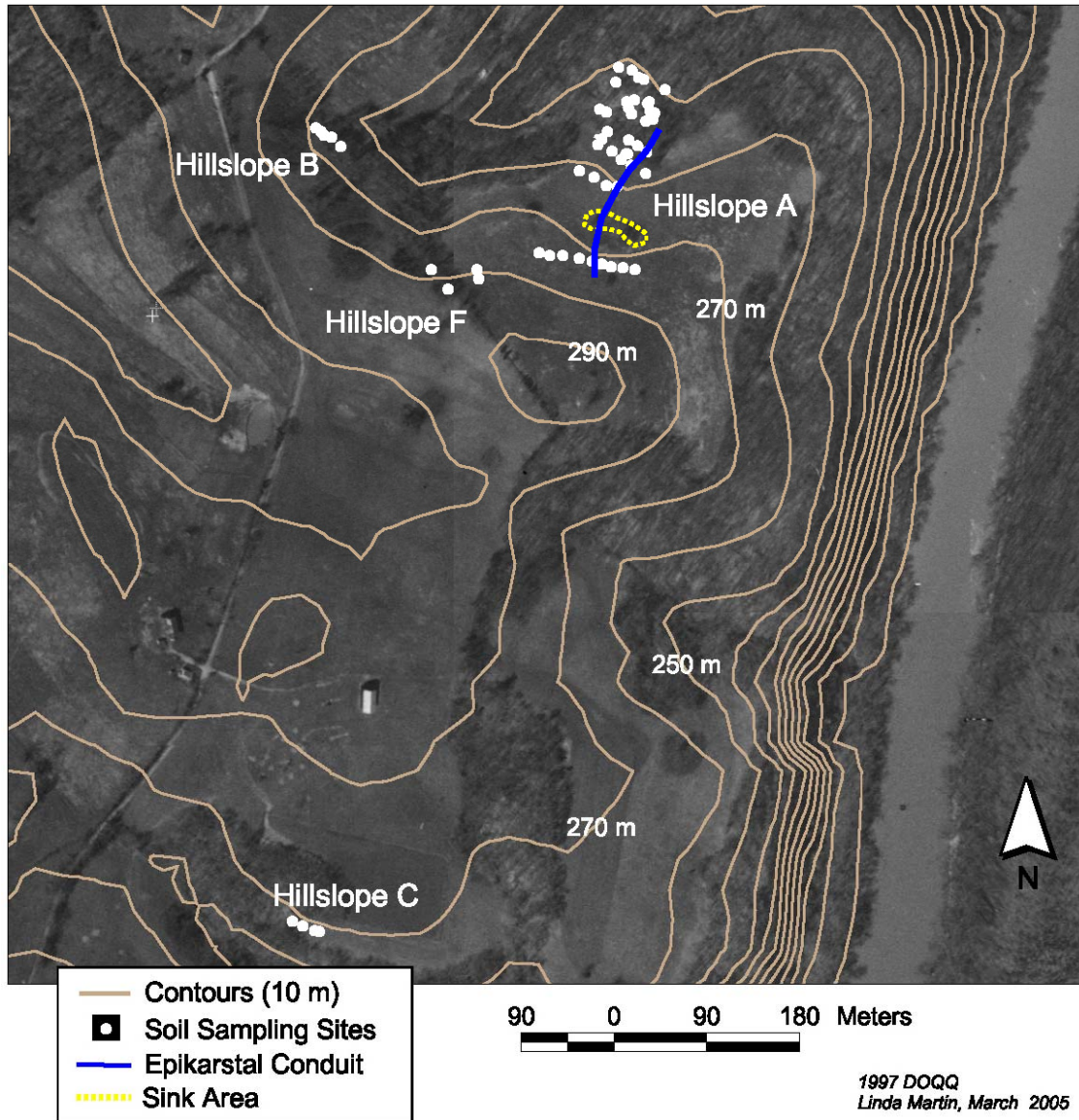


Figure 4.2. Soil sampling sites. Most samples were taken on Hillslope A in the vicinity of the epikarstal conduit shown in blue.

#### *Particle Size Analysis Using Hydrometer Settling Tests*

Mechanical analysis to determine the size distribution of individual particles in each soil sample was completed using the hydrometer method described by Gee and Bauder (1986). This method is based on the sedimentation principles of Stokes' Law, which relates settling rates of smooth, spherical particles to resistance offered by fluid of a known viscosity. The test employs both physical and chemical dispersion of soil samples in an aqueous solution, with hexametaphosphate (HMP) used as a dispersant. Corrections for density and viscosity are

made by measuring temperature and level of hydrometer flotation in a blank containing the same HMP solution as used in the sample tests for a specific test run. Nine to twelve samples were processed during each test run, and measurements were made with an ASTM 152H hydrometer calibrated for effective settling depth according to Kaddah (1974). Density and viscosity values for water at various temperatures were obtained from Spang (2004).

For each sample, 30 g of soil dispersed with 250 ml of deionized water and 100 ml of 50g/L (0.05g/mL) HMP solution were allowed to stand for 24 hours before being mixed for 5 minutes in a standard milkshake mixer (Day, 1965). Once samples were mixed, they were decanted into hydrometer settling cylinders and diluted by adding deionized water to the 1000 ml mark. Cylinders were each shaken vigorously for at least one minute, were turned end to end 3 or 4 times, and were set down at the beginning of a timing period. Hydrometer readings were taken at 30 seconds and at 1, 2, 3, 10, 15, 30, 60, 120, 240, 420, and 1440 minutes. Following test completion, the contents of each cylinder were washed through an ASTM No. 270 mesh (53  $\mu\text{m}$ ) sieve to separate sand contents from the silt and clay fractions. The sand portion was then oven dried and weighed to provide an independent comparison value to the sand percentage estimated by the hydrometer measurements.

Formulas provided by Gee and Bauder (1986) allowed calculation of the percentage of particles in suspension of less than a given particle size along with the logarithm of the effective particle diameter, given in micrometers. Percentage summation curves were created for each depth at each site using the particle sizes and percentages calculated for each measurement time. All curves for a given site were displayed on a single diagram to allow between-site comparisons. Total sand (2.0-0.05 mm), silt (0.05-0.002 mm) and clay (<0.002 mm) amounts for each layer were estimated directly from the percentage summation curves according to the USDA soil texture classification system.

#### *Particle Density Determination*

The sedimentation parameter from which mean particle size is calculated according to the Gee and Bauder (1986) methods is partially based on the difference between soil particle density and solution density. During phase 1 textural analysis, estimated values for particle density, or soil mass per unit volume, were used based on typical values recorded in the literature for mineral soils (Rowell, 1994; Brady and Weil, 1996; Tan, 1996). A particle density of 2.4 g/cm<sup>3</sup> was used for calculations for 0-10 cm, 2.5 g/cm<sup>3</sup> for 25 and 55 cm depths, and 2.6 and 2.65 g/cm<sup>3</sup> for 85 and 125 cm layers.

For phase 2 texture analysis, particle density was directly measured for samples taken from infiltration pit walls. At depths of <10, 25, 55, 85, and 125 cm, 3 to 4 approximately 50 g samples of soil taken from different wall locations were combined to form samples that were analyzed with the hydrometer procedure used in phase 1. Samples from the mixed and ground <2 mm portion for each depth were tested for particle density by the method described by Rowell (1994), in which weighed soil samples are placed in suspension and then boiled to release air. By bringing the water content to the full container mark following cooling, particle density can be calculated by subtracting the portion of the total mass that is made up by the mass of water dependent on its density at the measured temperature. Rowell (1994) calls for use of 250 ml beakers, but early tests results for this project were unreliable because of the poor accuracy involved in defining the 250 ml full mark. Volumetric flasks (100 ml) were substituted for the beakers (Tan, 1996), and results were consistent with known ranges for mineral soil particle densities (Table 4.1).

Particle densities determined by this method closely matched the estimated amounts that were used for texture analysis during phase 1 tests. Mean ( $\bar{X}$ ) and standard deviation ( $s$ ) values obtained for depths were respectively: 2.38, 0.064 for <10 cm, 2.52, 0.053 for 25 cm, 2.58, 0.057 for 55 cm, 2.59, 0.041 for 85 cm, and 2.61, 0.016 for 125 cm. Particle density tests were not duplicated in most cases due to the number of sample sites. Differences in particle density of  $\pm 0.1 \text{ g/cm}^3$  have been found to have a small effect on given size determinations in hydrometer tests (Gee and Bauder, 1986), indicating that the estimated particle densities used in the phase 1 texture analyses are suitably accurate.

#### *Problems and Corrections Applied During Texture Analysis*

Although the formulations relating settling velocity and particle diameters are based on solid physical premises, many sources of error may affect hydrometer test results. Unrealistic assumptions of spherical particle shape and independent particle action (Tindall, et al., 1999) lead to some unavoidable error during timed settling measurements, and Day (1965) discusses problems associated with sieving, in which particle shape and length of time spent shaking the sieve affect the percentage of particles falling through the openings. Even when care is taken to make sure that the HMP formulation is exact and that no soil or solution is lost during mixing and decantation, operator measurement error may cause significant hydrometer settling test errors. Some error may derive from reading difficulties, since the upper edges of the menisci seldom lie on the hydrometer g/L markings and the operator must judge what value is closest. The greatest chance of operator error related to reading difficulties occurs in the early testing

process at 30 and 60 seconds, when the solution retains a swirling motion from the shaking process, the hydrometer may not have stopped bobbing after insertion, and foam may obscure readings despite application of a couple drops of amyl alcohol. These early readings are used for sand calculations, making these measurements potentially less reliable than silt and clay values derived from later readings taken after cylinder contents have settled.

Table 4.1  
Particle Density and Organic Content Determinations for Infiltration Test Pits

| Pit | Soil Depth (cm) | Particle Density | Organic Matter (%) | Pit | Soil Depth (cm) | Particle Density | Organic Matter (%) |
|-----|-----------------|------------------|--------------------|-----|-----------------|------------------|--------------------|
| 1   | <10             | 2.43             | 8.03               | 8   | <10             | 2.35             | 20.86              |
|     | 25              | 2.48             | 5.12               |     | 25              | 2.51             | 11.96              |
|     | 55              | 2.52             | 3.67               |     | >30             | 2.50             | 9.73               |
|     | 85              | 2.57             | 3.51               | 9   | <10             | 2.39             | 15.74              |
|     | 125             | 2.62             | 5.03               |     | 10-25           | 2.57             | 8.03               |
| 2   | <10             | 2.44             | 7.16               | 25  | 2.60            | 6.69             |                    |
|     | 25              | 2.48             | 3.76               | 55  | 2.60            | 4.82             |                    |
|     | 55              | 2.52             | 3.21               | 85  | 2.60            | 3.90             |                    |
|     | 85              | 2.58             | 3.85               | 10  | <10             | 2.37             | 14.49              |
|     | 125             | 2.59             | 4.65               |     | 25              | 2.43             | 10.19              |
| 3   | <10             | 2.35             | 14.45              | 55  | 2.56            | 4.74             |                    |
|     | 25              | 2.50             | 4.27               | 11  | <10             | 2.35             | 13.51              |
|     | 55              | 2.54             | 3.91               |     | 25              | 2.52             | 6.21               |
|     | 85              | 2.60             | 4.53               |     | 55              | 2.56             | 5.97               |
|     | 125             | 2.63             | 5.67               |     | 85              | 2.66             | 6.04               |
| 4   | <10             | 2.41             | 9.04               | 12  | <10             | 2.46             | 9.35               |
|     | 25              | 2.52             | 3.38               |     | 25              | 2.52             | 5.11               |
|     | 55              | 2.55             | 4.00               |     | 55              | 2.57             | 5.92               |
|     | 85              | 2.57             | 4.69               |     | 75-80           | 2.58             | 6.11               |
|     | 125             | 2.61             | 5.84               |     | 110             | 2.60             | 5.58               |
| 5   | <10             | 2.32             | 16.04              | 13  | <10             | 2.43             | 11.15              |
|     | 25 (yellow)     | 2.51             | 5.55               |     | 8-22            | 2.52             | 6.97               |
|     | 25 (brown)      | 2.48             | 6.72               |     | 25              | 2.58             | 7.75               |
|     | 55              | 2.52             | 5.52               |     | 55              | 2.62             | 7.69               |
|     | 75              | 2.53             | 5.56               |     | 82              | 2.62             | 8.15               |
| 6   | <10             | 2.24             | 21.94              | 14  | <10             | 2.48             | 8.89               |
|     | 11-27           | 2.55             | 11.03              |     | 10-25           | 2.61             | 6.41               |
|     | 25              | 2.58             | 8.06               |     | 25-30           | 2.66             | 5.73               |
|     | 55              | 2.63             | 6.82               |     | 55              | 2.72             | 5.25               |
|     | 70              | 2.68             | 6.24               |     |                 |                  |                    |
| 7   | <10             | 2.35             | 20.32              |     |                 |                  |                    |
|     | 25              | 2.49             | 11.63              |     |                 |                  |                    |
|     | 40-45           | 2.61             | 8.35               |     |                 |                  |                    |

Although these sources of error can be significant, the largest problems associated with hydrometer settling test accuracy are caused by lack of complete dispersion of aggregates (Day, 1965; Green, 1978; Gee and Bauder, 1986). Problems with incomplete aggregate defloculation may arise if organic content of the soil is greater than 2% (McCarthy, 1997). Although removal of organics through heating with hydrogen peroxide is recommended for settling tests of samples containing large amounts of organic matter (Gee and Bauder, 1986; Tan, 1996), the decision was made to not remove organics for this project because of practical considerations of time and materials. Authors such as McRae (1988) suggest that typically between 3 and 8% organic matter is found in topsoil and from 1-2% in subsoil. Because typical subsoil organics percentages are acceptable for settling testing, and because subsoil measurements were felt to be most important to this study, the choice was made to forgo organic removal.

During phase 2, loss on ignition tests were run in which soil organic content was determined by heating 2 g of oven-dried soil from each layer sample in a muffle furnace to 550 °C for 6 hours and then determining the remaining soil mass (McCarthy, 1997; Cambridge Department of Geography, 2004). Loss on ignition test results can only give approximations that are dependent on the methods used, since loss related to dehydration of amorphous oxides and clay minerals may also occur during heating (McRae, 1988; Hein, et al., 2001). This may overestimate organics in clay soils by up to twice the actual amount (Rowell, 1994), as well as removing some portion of carbonates. Results from the loss on ignition tests for this study were very high, ranging from 3.21% to above 20% in topsoil layers (Table 4.1). These values suggest that it is highly likely that both clay and carbonate sand material loss occurred during testing. Test results are consistently at least twice as high as expected, and they likely reflect relative rather than absolute organic content. Nevertheless, all of the loss on ignition test results showed higher topsoil organic percentages than in lower depths. When particle size analysis sand estimates were compared with sand percentages determined by sieving, it was found that the estimated topsoil and upper layer sand percentages were usually considerably lower than sand percentages obtained from final sieved sand weights. In these upper layers, despite HMP soaking and vigorous mixing and shaking, small root pieces were able to float attached particles past the time when sand would normally fall out of suspension.

A second systematic problem with dispersion also became evident in association with the high amount of clay present in most lower horizons in the study area. In conditions opposite to that described above for organics, incomplete dispersion of clay aggregates caused a small portion of them to fall quickly, creating sand content estimates for subsoil layers that were



higher than amounts obtained through sieving. Although increasing amounts of physical action may aid in dispersion, the increase is not always recommended. Day (1965) indicates that more than 5 minutes of physical shaking may begin to cause soft rock and mineral fragments to disintegrate, which would have been particularly problematic for the relatively soft, decomposed limestone sand present in many samples.

After examining the early test results and determining the sources of dispersion error caused by high organic and clay content, the decision was made to continue running the tests in the same format, but to acknowledge the systematic deviations by using the sieved weights as baseline sand measurements. As shown in table 4.2, which compares estimated sand measurements with sieved sand weights for various samples taken from Hillslope A, hydrometer test estimates were farthest off in topsoil samples. The most common pattern of deviation is typified by sites 11 and 12 in table 4.2, where upper layers have estimated percentages that are lower than sieved weight percentages and lower horizons have higher estimated percentages. However, estimated sand percentages in most profiles clearly reflected actual sand weights in terms of relative amounts.

A method was devised to correct for both systematic dispersion deviations using the fact that test results reflected proportional relationships. Once texture was determined for each sample based on test estimates, the sand content estimate was compared to sieved sand weight. If the estimate fell more than 0.6 g higher or lower than the sieved weight, as determined by 2% of 30 g, the difference between the two measures was determined. This difference was then reapplied to the estimated silt and clay percentages according to their ratio, with a proportional amount added to each if the sand estimate was determined to be too high and a proportional amount subtracted if the sand estimate was too low. The formula used to recalibrate particle texture class percentages is as follows for clay:

$$\text{revised clay percentage } (c_r) = c_o - [c_o * (d / (100 - s))],$$

where  $c_o$  is the original estimated clay percentage,  $d$  is the difference between sieved sand percentage and estimated sand percentage, and  $s$  is the estimated sand percentage. A similar formula was used to revise silt percentages.

It was found that this recalibration shifted the sand/silt/clay compositions only slightly for the vast majority of the samples tested. For the particle size analyses run for the 14 infiltration pits, out of the 66 total samples, only 2 texture classifications were changed by recalibration. At site 1, results for 25 and 55 cm originally indicated a silt classification, but recalibration placed these layers into silt loam categories, which made test results consistent with sites 2, 3, and 4 sampled in the same slope position and soil type.

Table 4.2

Examples of Comparisons between Hydrometer Test Estimated Sand Percentages and Sieved Sand Weight Percentages

| Site | Depth (cm) | Test Estimate Sand Percentage | Sieved Sand Percentage | Sieved Sand – Sand Estimate |
|------|------------|-------------------------------|------------------------|-----------------------------|
| 4    | <10        | 7                             | 11.3                   | 4.3                         |
|      | 20-30      | 4                             | 9.2                    | 5.2                         |
|      | 40-50      | 19                            | 13.8                   | -5.2                        |
|      | 60-70      | 12                            | 8.1                    | -3.9                        |
|      | 110-114    | 11                            | 5.8                    | -5.2                        |
| 5    | <10        | 6                             | 11.0                   | 5.0                         |
|      | 20-30      | 6                             | 8.4                    | 2.4                         |
|      | 40-50      | 10                            | 8.1                    | -1.9                        |
|      | 60-70      | 16                            | 13.2                   | -2.8                        |
|      | 75-83      | 23                            | 17.6                   | -5.4                        |
| 6    | <10        | 6                             | 15.2                   | 9.2                         |
|      | 20-30      | 14                            | 11.1                   | -2.9                        |
|      | 40-47      | 17                            | 12.4                   | -4.6                        |
| 7    | <10        | 3                             | 8.6                    | 5.6                         |
|      | 20-30      | 13                            | 11.6                   | -1.4                        |
|      | 40-50      | 13                            | 11.0                   | -2.0                        |
|      | 60-70      | 13                            | 10.1                   | -2.9                        |
|      | 110-120    | 6                             | 4.3                    | -1.7                        |
| 8    | <10        | 3                             | 9.0                    | 6.0                         |
|      | 20-30      | 2                             | 7.9                    | 5.9                         |
|      | 40-50      | 9                             | 9.6                    | 0.6                         |
|      | 60-70      | 7                             | 9.1                    | 2.1                         |
|      | 110-117    | 2                             | 4.4                    | 2.4                         |
| 9    | <10        | 3                             | 9.1                    | 6.1                         |
|      | 20-30      | 10                            | 12.1                   | 2.1                         |
|      | 40-50      | 11                            | 10.6                   | -0.4                        |
|      | 60-70      | 12                            | 10.4                   | -1.6                        |
|      | 110-120    | 11                            | 8.5                    | -2.5                        |
| 10   | <10        | 10                            | 12.4                   | 2.4                         |
|      | 20-30      | 11                            | 15.8                   | 4.8                         |
|      | 40-50      | 17                            | 15.3                   | -1.7                        |
|      | 60-75      | 26                            | 24.0                   | -2.1                        |
| 11   | <10        | 12                            | 13.2                   | 1.2                         |
|      | 20-30      | 10                            | 12.2                   | 2.2                         |
|      | 40-50      | 11                            | 10.2                   | -0.8                        |
|      | 60-70      | 11                            | 9.2                    | -1.8                        |
|      | 70-80      | 15                            | 12.0                   | -3.0                        |
| 12   | <10        | 11                            | 15.6                   | 4.6                         |
|      | 20-30      | 8                             | 11.9                   | 3.9                         |
|      | 40-50      | 9                             | 9.2                    | 0.2                         |
|      | 60-70      | 13                            | 8.2                    | -4.8                        |
|      | 85-95      | 14                            | 9.1                    | -4.9                        |

As with possible error resulting from other aspects of the hydrometer tests, test results were surprisingly robust despite these systematic dispersion errors. Researchers familiar with settling tests warn that results are always relative to any method used and that “there is no ‘absolute’ size-distribution for a given sample” (Gee and Bauder, 1986, pp 389), so that the method used must be carefully reported along with results. All pretreatments carry the potential for altering or dissolving primary minerals (Green, 1978). It is even possible that “a less drastic chemical treatment and/or little mechanical dispersion may reflect the more ‘natural’ particle-size distribution of the soil” (Gee and Bauder, 1986, pp 390). The method used to analyze particle texture sizes for this study was employed consistently as reported here and should enable confident comparison of within-test results (Tindall, 1999). Because the texture classes as estimated tally well with SSURGO estimates for particle sizes given for soil series horizons mapped in the study area, a certain amount of confidence can also be extended to comparisons with out-of-study results.

### **Soil Depth Measurements**

Once it became apparent during phase 1 sampling that soils in many parts of the study area were shallower than expected, the decision was made to systematically measure soil depth by probing for bedrock. A total of 42 transects measuring soil depth parallel to the contour, and 4 measuring longitudinal slope profiles, were made by inserting metal probes into the soil at measured intervals (Figures 4.3 and 4.4). Using a standard 1 m tile probe and a 1.86 m probe specially made for this project, measurements were taken at 1 m intervals for parallel transects and at 2 or 5 m intervals for slope profiles, with surface profiles simultaneously measured by laser level for some transects. Although the ability to reach bedrock was frequently stymied by high stone or extremely high clay content, enough sites were measured along each transect to provide evidence for average soil depths. This method helped define current soil conditions at key slope locations, and it enabled general comparison between sites matched for equal elevation and contrasting vegetation cover. This method of investigating soil depths also provided a general means for studying stoneline, bedrock terrace, and bedrock surface variability.

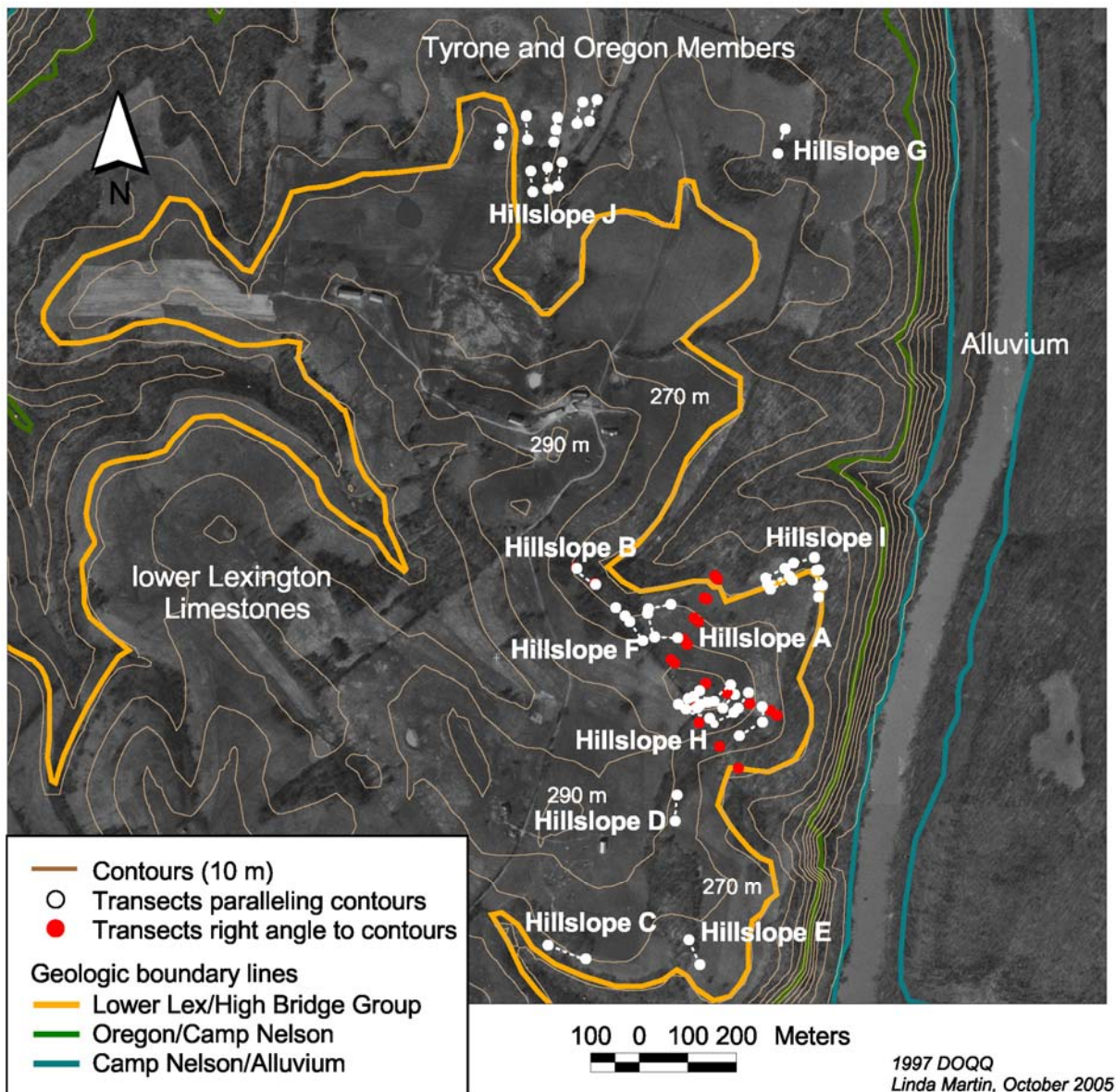


Figure 4.3. Locations of soil depth measurement transects.

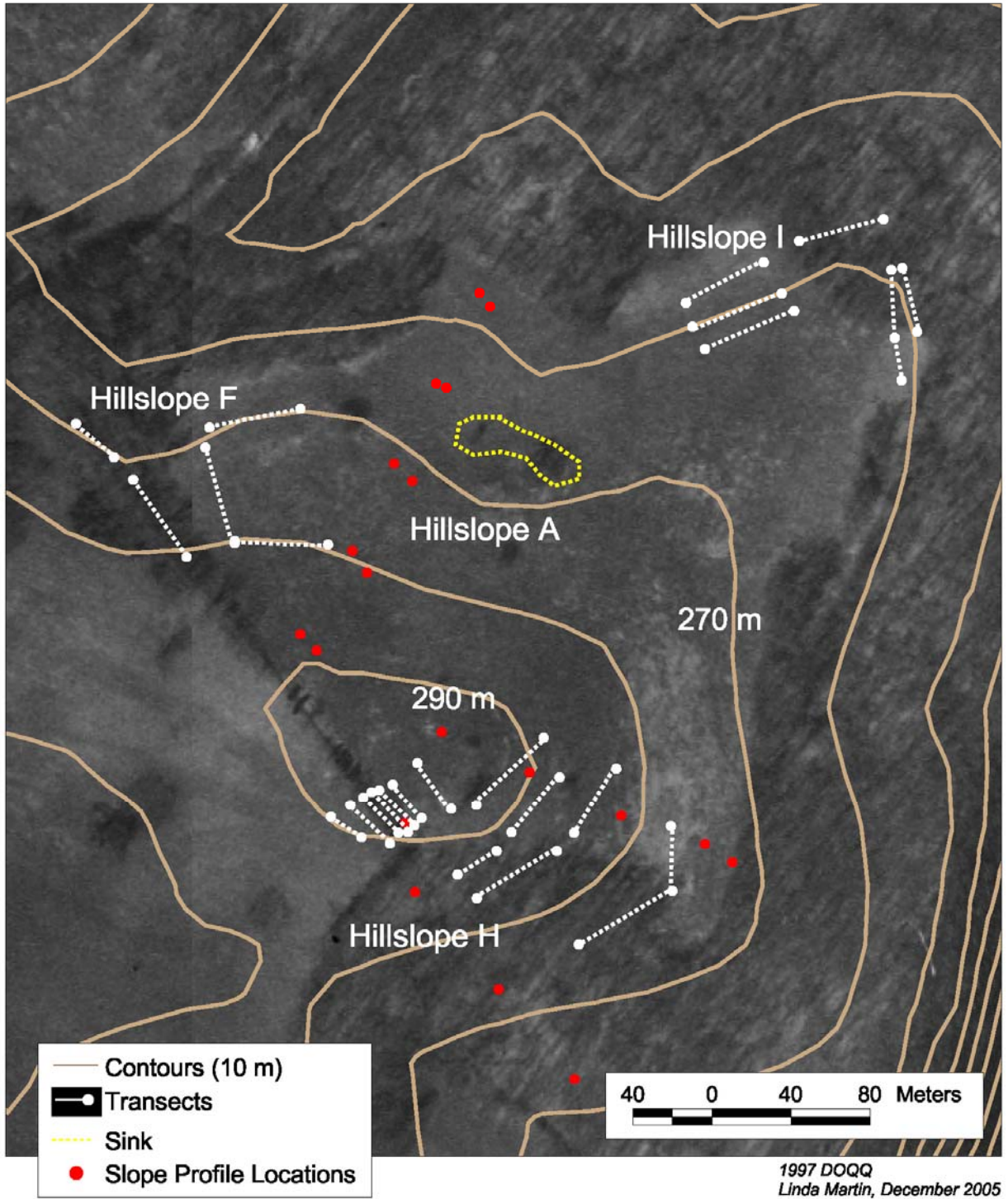


Figure 4.4. Soil depth transect locations in the main study area.

## PHASE 2 RESEARCH – TESTING INFILTRATION RATES

### Water Content Data Logging

Tree roots have been consistently found by researchers to support preferential flow pathways in the vadose zone (Burch et al., 1987; Noguchi et al., 1999; Sidle et al., 2001). To try to detect this preferential flow and the possible difference between percolation patterns in grass and forest, two soil water content data logging stations were set up in May 2005 in neighboring forest and grass locations on the southern end of Crutcher Preserve (Figure 4.1). Stations were set up at positions on Hillslope C where soil depth and type closely match soil characteristics found at the base of Hillslope H in the main study area, where infiltration tests were later run. At each station, five Decagon® ECH<sub>2</sub>O 20 cm dielectric capacitance probes were installed in pit walls at <10, 25, 55, 85, and 125 cm depths. Each probe was connected by cable to a Decagon® Em50 logger which was attached to a free-standing pole holding the unit above the ground. The loggers were programmed to send an electrical signal every 60 seconds to the buried probes, and return signals were averaged every 30 minutes and then stored in the data logger. Measurements were downloaded onto a laptop computer approximately once a month following installation.

The particular moisture probes used in these set ups measure the change in voltage registered in sensors embedded within the probes themselves (Decagon Devices, Inc., 2005). This ensures that accurate measurements of local changes in water content can be taken at a relatively low cost, since the system is not dependent on the measurement of transmission time along a buried cable that is utilized in time domain reflectometry (TDR) (Stephens, 1996). Electrical transmission is about 20 times higher in water than in air, so that water content in soil pressed up against the probe can be recorded as an increase in transmission rate.

After first setting up the data loggers, the moisture probes were checked to make sure they were functioning properly by inserting them in loose soil while the pits were dug. After it was determined that initial readings were essentially the same for all probes, they were inserted sideways into the pit walls by creating openings with a thin metal tool. All probes functioned after set up, but the 85 cm forest probe failed after the first rain. This failure, which necessitated the replacement of the probe in July, most likely resulted from a short caused by excessive bending during insertion, which was impeded by heavy gravel content at that depth.

Following an initial period of adjustment, the water content data logging stations worked without error. Each of the loggers recorded the original unprocessed transmission readings in millivolts, along with soil volumetric water content calculated using soil texture data for each

probe's installation depth. Soil texture data was obtained from hydrometer particle size testing, but consideration of later infiltration test results led to a fear that high amounts of gravel in some soil layers might distort the volumetric calculations. As a result, the decision was made to use only the unprocessed data to report or chart readings, since these best represent the immediate changes in transmission caused by the presence of water in the soil surrounding the probe as opposed to estimates of water volume in the surrounding cubic meter of material. All water content data presented in this report use unprocessed readings. Accuracy estimates given by the company (Decagon Devices, Inc., 2005), for a 10 millisecond volumetric water content reading with a  $0.002\text{m}^3/\text{m}^3$  (0.1%) resolution, are  $\pm 0.01\text{m}/\text{m}$  ( $\pm 1\%$ ) for soil-specific calibration and  $\pm 0.03\text{m}/\text{m}$  ( $\pm 3\%$ ) for non-calibrated readings.

At the same time that water content probe stations were set up, an Onset HOBO® data logging rain gauge was set up on a concrete cover in the lawn of the owners of the main study area grassed slopes. The rain gauge operates best when it is mounted on a masonry block and kept in an unobstructed level position, and this site provided an easy way to keep the instrument both secure and away from encroaching vegetation. The rain gauge was calibrated to tip at 0.01 inch increments following the manufacturer's suggested guidelines (Onset Computer Corporation, 2005). After field installation of the rain gauge, the number of tipping events was downloaded approximately once a month onto a laptop computer. This data was then compared to data from the water content logging stations.

### **Infiltration Rate and Hydraulic Conductivity Determinations**

Disc infiltrometers offer a good way to evaluate in situ vadose zone hydraulic properties (Hussen and Warrick, 1995). For this study, a Soil Measurement Systems® (SMS) tension infiltrometer was used to procure measurements of constant-head, unsaturated flow into soils at varying depths in 14 pits dug by hand on Hillslopes A, H, and C of the main study area. Surface infiltration tests were also run at 18 randomly selected locations on the grassed hill shoulder in the main study area (Figure 4.5). The two pits opened on Hillslope C were sited very close to the water content data logging stations to enable characterization of the soil and infiltration properties of the layers being data logged. Other pit locations were sited to enable comparison of forest and grass effects on soils at similar elevations. Pits were opened to bedrock where possible, and where stones and/or hard packed clay made digging impossible, every attempt was made to determine the depth to bedrock by opening a smaller portion of the pit and/or by using a soil probe. Large tree roots by themselves did not impede digging, but infiltration tests

could not be run where roots made it impossible to create a level surface. At each pit location, infiltration tests were run twice at <10, 25, 55, 85, and 125 cm depths where possible. Although water movement at depth can be more correctly defined as percolation, the term infiltration will be used in this project to indicate the rates of unsaturated flow detected below the infiltraometer disk at each depth.

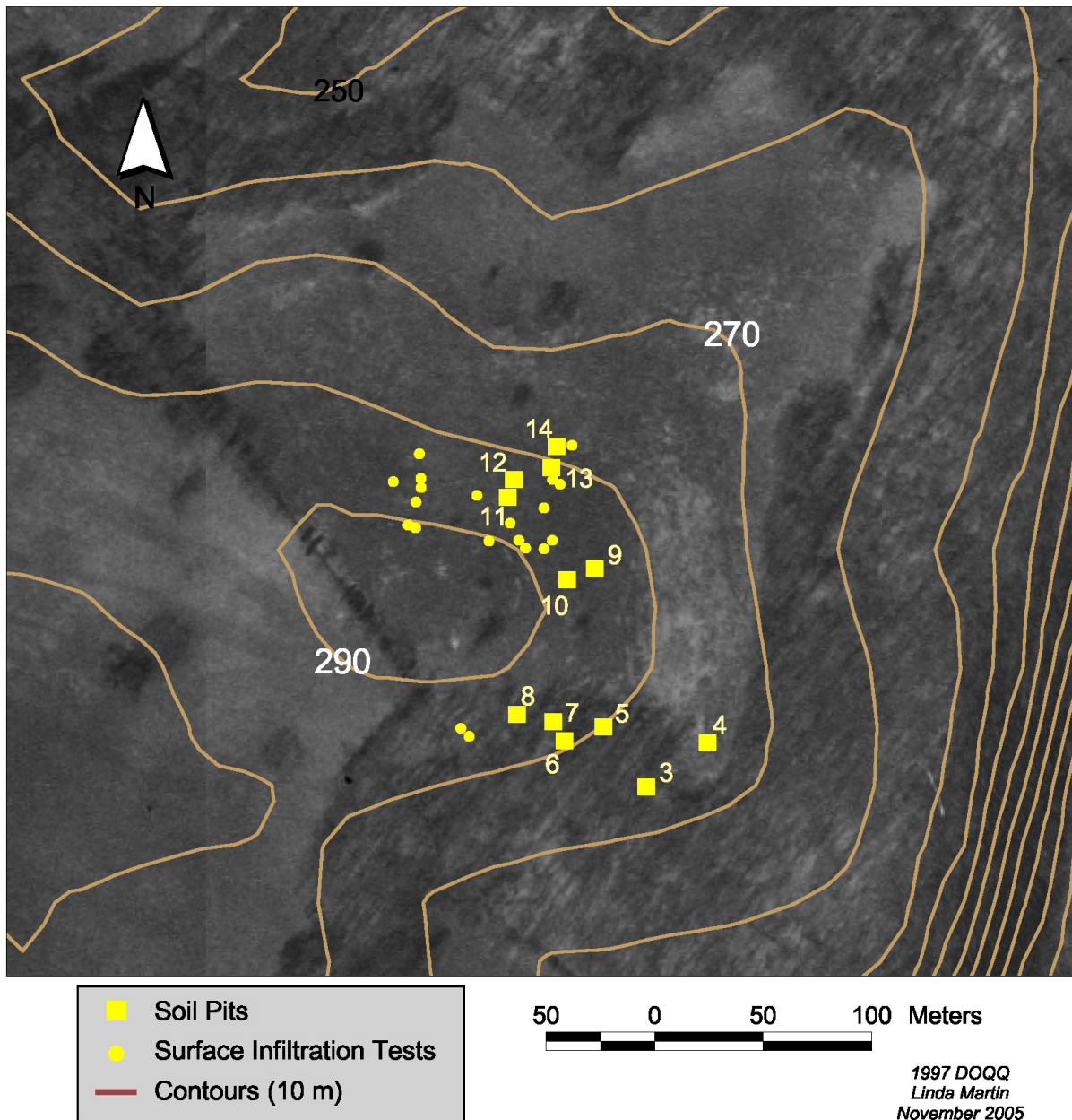


Figure 4.5. Infiltration test pit and surface run sites. Infiltration pits 1 and 2 on Hillslope C are not shown.



The tension infiltrometer was calibrated for correct pressure readings following the manufacturer's guidelines (Soil Measurement Systems, 2005). All tests were run with the infiltration disc separated from the water tower, which avoids problems related to disturbance of the tower by wind or change in pressure caused by the emptying water tower. This mode of operation necessitates that an area approximately 40 cm wide be leveled for each test so that the disc and tower can function side by side. Because all pits were dug on slopes, the uphill portions of the leveled areas were at slightly lower soil depths than the front. For surface tests, this typically meant that the uphill end of the leveled area was approximately 10 cm below the soil surface, resulting in tests being reported for <10 cm depths rather than as surface measurements. For lower layers, measurements of soil depth were taken from the tops of the walls at the sides of the pit rather than from the up or downhill walls.

For each test, the soil surface was prepared using a straight-edge trowel, a level, and scissors to cut off roots at the ground surface (Wyseure, et al., 2005). To prepare the surface for the disc, several mm of sand were placed over cheesecloth to prevent slaking and were leveled inside a 20 cm metal ring. Once the ring and excess sand were removed, the disc and water-filled tower were placed side by side so that the sand ring supported the disc and the tower base was level with the disc top. At each site, three infiltration tests were completed with tensions set at -15, -8, and -3. Readings were recorded manually at 1 minute intervals until a satisfactory steady-state rate was reached, which typically took 35 to 45 minutes. Where possible, two full test runs at these three tensions were completed at different spots at each depth. After completing tests at one depth, soil was removed to the next depth, where the process was repeated.

Infiltration rates for the various depths and tensions were entered into an Excel spreadsheet where unsaturated hydraulic conductivity values,  $K(h)$  cm hr<sup>-1</sup>, were calculated based on formulas which relate unconfined infiltration rates to the matric potential, or tension level set up for each test (Soil Measurement Systems, 2005). These formulas first use Wooding's (1968) algebraic approximations of steady-state unconfined infiltration rates from a circular source (Q):

$$Q = \pi r^2 * K(h) [1 + (4/(\pi r a))] , \quad (1)$$

where Q is the measured volume of water entering soil per unit time (cm<sup>3</sup>hr<sup>-1</sup>), r is the disk radius,  $K(h)$  is the hydraulic conductivity at a specific tension, and a is a parameter involving tension at the source (Hopmans, et al., 1999). Then, based on Gardner's (1958) assumption that unsaturated hydraulic conductivity relates to matric potential (given by h), a saturated

hydraulic conductivity value ( $K_{sat}$  cm hr<sup>-1</sup>) is substituted for  $K$  in equation 1. Gardner (1958) proposes that:

$$K(h) = K_{sat} e^{(ah)}. \quad (2)$$

By replacing  $K(h)$  in equation 1 with  $[K_{sat} e^{(ah)}]$  at two different tensions and solving the equations simultaneously, the parameter  $a$  for a specific test can be determined:

$$a = [\ln (Q(h_2)/Q(h_1))]/(h_2-h_1), \quad (3)$$

where  $h$  is tension at the water tower source,  $Q$  is the directly measured infiltration rate, and  $h_1$  is the least negative tension. Once  $a$  is determined, an estimate for  $K_{sat}$  at the measured tensions can be calculated through a reformatting of equation 1:

$$K_{sat} = Q(h) / \pi r^2 * e^{(ah)} * [1 + (4/(\pi r a))] \quad (4).$$

With  $a$  and  $K_{sat}$  known, unsaturated hydraulic conductivity ( $K(h)$ ) for any tension may be calculated through equation 2.

The parameter  $a$  is determined by knowing two differing tensions and their associated infiltrations rates. Because infiltration rates for three tensions were determined for each test run in this study,  $a$  values were calculated for both -15 to -8, and -8 to -3 tensions. The corresponding  $K_{sat}$  estimates have thus been determined for  $h_1 =$  both -8 and -3. Final estimates of  $K(h)$  for tensions of -15 are derived from  $a$  and  $K_{sat}$  values determined from the -15 and -8 tensions, whereas  $K(h)$  estimates for  $h =$  -8 and -3 are drawn from  $a$  and  $K_{sat}$  values derived for tensions of -8 and -3. Because the  $K(-3)$  near saturation hydraulic conductivity rates are those most likely to encourage transport (Hussen and Warrick, 1995), they are used most extensively in this project for comparative purposes.

### *Problems Associated With Infiltration Testing*

If care is taken that the instrument setup is correct, with both disc and tower accurately level, then most problems with infiltration testing are likely generated by site specific concerns and operator error. Large roots, high gravel content, and stones made leveling difficult in some sites, and in some cases impossible. At several sites, the combination of gravel and hard, dry clay made it necessary to wet the surface and let it sit overnight so that the site could be leveled the following day, taking care to see that only enough water was added to make the top surface malleable. Despite extremely dry conditions throughout summer and fall of 2005, open pits were rained on twice. Because the initial potential of the soil must be lower than the tension set on the infiltrometer so that water is not pulled back into the disc (Wyseure, et al., 2005), tests could not be completed at a tension of -15 on two occasions. Early pits were also not dug broad enough to permit the infiltrometer to be repositioned for second tests at deeper depths, and if

this project were to be repeated, consideration would be given to using the infiltrometer in the mode in which the tower is directly mounted on the disc so that less setup room would be required.

Readings are taken from the centimeter scale on the side of the water tower, and the lines representing each centimeter unit are precisely 1 mm apart. Because of heavy clay content at most tested depths, and because of hydrophobic conditions set up by dry topsoils, many -15 and sometimes -8 infiltration readings were extremely slow and necessitated readings at divisions of tenths of the centimeter unit marks. To get a reasonably accurate estimate of water drop rates in the tower, it was necessary to use an 8x magnifying glass and to develop a technique of consistently measuring the meniscus at the point where its base formed the thinnest line when viewed at eye level. The possibility of inaccuracy in estimating changes at a tenth of a millimeter necessitated that tests be run much longer than the minimal 16 minutes suggested by the instrument's manufacturer. Most tests were run for a minimum of 40 minutes so that a clear pattern could be detected that in many cases showed up in steady water loss rates spread out over three to five minutes rather than just one minute.

Most difficulty in obtaining constant water entry rates, however, arose from the anisotropic nature of the soil itself. Few soils were homogeneous enough to permit smooth water entry through the matrix alone, and in most locations water would enter the matrix at a steady rate for several minutes and then jump as matrix saturation built up to a high enough level to permit some macropore under the disk to operate briefly. Following this jump, detected as a sudden increase in the level of water drop in the tower, readings for the next minute or so were typically lower than normal as matrix pressure again built up. After a few more minutes of steady flow, another jump might occur, with a similar post-jump depression in rates. The timing of these "burps" was not necessarily even, making the task of obtaining steady-state rates difficult unless rates were determined based on longer spans of time. Wierenga (1995) discusses early or delayed breakthrough and tailing that has been found to occur in association with preferential flow, and these effects seem to match infiltration properties observed in this project.

Hussen and Warick (1995) suggest that some steady-state rates may not be obtained for well over an hour, but in this project, no tests were run for over an hour because of time considerations. On sites where measurements were extremely bumpy, rates were timed for 40 to 60 minutes until they settled to repetitious, if still slightly irregular patterns. That data was then entered into a spreadsheet where the final 20 minutes of the test measurements were averaged to obtain a test rate. These small irregularities are not believed to influence the test

results since the average after 40 to 60 minutes likely caught a measurement very close to the final converging steady state rate. Although some small error may be associated with this method, it was applied throughout so that results may be viewed as being internally consistent.

### **Soil Profile Characterization**

As pits were dug for infiltration testing, soil profiles were described for each site according to the methods given by McRae (1988) (see Appendix 3). Soil horizon depths, Munsell colors, structure, consistency, and texture as determined by hand feel were recorded along with comments on relative abundance, sizes, and types of mottles and coatings, stones, and roots. Samples were bagged from the same <10, 25, 55, 85, and 125 cm depths at which infiltration tests were run and were processed for particle size, particle density and organic content following methods previously described. Soil cores were also collected and were used to determine bulk density and porosity.

#### *Bulk Density*

Dry bulk density, or the dry mass per unit volume of the soil, was measured for different layers by taking almost undisturbed samples of known volume back to the lab for drying and weighing. Samples were collected by using an AMS® Soil Core Sampler which uses a steel hammer to drive a 2" x 2" coring device containing a liner into smooth vertical or lateral faces (McKeague, 1978) In the lab, soil removed from the liner was weighed, oven-dried at 110 °C for at least 48 hours, and then reweighed (Birkeland, 1984). Because the core liners have known dimensions, bulk density could be easily determined by dividing the oven-dried weight by the volume, determined as volume of core =  $\pi r^2 L = \pi * 1 \text{ in}^2 * 2 \text{ in} = 6.28 \text{ in}^3 = 102.96 \text{ cm}^3$  (Rowell, 1994).

Strict bulk density measurement of soils requires that no stones or gravel be present in samples. The Soil Conservation Service (1972) indicates that if cores contain no coarse fragments larger than 10 to 20 mm in diameter and are not extracted where large cracks are present, then they can be considered representative of horizon bulk density. Many soil layers in this project contained small gravel that could not be avoided, and the measurements obtained reflect general soil layer conditions rather than bulk density of just that portion of the soil that is less than 2 mm in size. Likewise, bulk density measurements reflect horizon characteristics at the location of specific infiltration tests rather than characterization of the horizon over the larger field area. Determination of large field area properties would necessitate an aggregated sampling approach (Rowell, 1994), and in the study area would likely not be able to capture the

heterogeneity of soils caused by the extreme variance in bedrock depths and epikarstal drainage pathways. Findings in this study do indicate that soil properties at profile depths typically remain within defined ranges across equal elevations. This, plus the fact that bulk densities at depths remain within ranges indicated for SSURGO mapped soil series (Soil Survey Staff, 2005), indicate that these site-specific measurements also provide a reasonable representation of general bulk densities across the slope.

### *Porosity*

The simplest method for determining porosity, or percentage of the soil volume occupied by voids, is by calculating the percentage of pore space from known values for dry bulk density and particle density such that (Tan, 1996):

$$\% \text{ pore space} = 100 \times (\text{particle density} - \text{bulk density}) / \text{particle density}.$$

Porosity was calculated for each depth sampled during phase 2 infiltration testing using bulk density and particle density measures obtained as described in previous sections.

### *Tensiometer Measurement of Matric Potential*

The matric potential, or soil water energy status, was measured as negative pressure or suction (Stephens, 1999; Tindall, et al., 1999) at each depth at which infiltration tests were conducted. Measurements were taken with a portable “Quickdraw” Soilmoisture tensiometer probe manufactured by Soilmoisture Equipment Corporation® that includes both a coring tool and a probe fitted with a ceramic base and a pressure meter. At depths tested for infiltration, the probe was inserted approximately 10 cm below the surface and was left until the pressure meter no longer registered change. Suction measurements were recorded along with pit data and were intended to help define relative depth of water penetration at sites following rain events, but dry weather conditions and loss of data at some sites limited the usefulness of this data. The ceramic base cup is susceptible to damage by rocks, plus insertion into heavy clay tends to “blow out” the probe by forming an airtight seal that raises air pressure in the probe beyond its tolerance limits. Replacement of the cup and recalibration of the tool was done in the lab, resulting in matric potential data loss for all depths tested subsequent to a cracked tip or incorrectly pressurized condition.

### **Data Analysis**

Qualitative data derived from survey and observation and quantitative data from soil tests are equally important information sources in this project. Because this project tackles soil loss and erosion from within an earth surface system perspective, quantitative information had

to be analyzed not only for its relationship to the immediate variables being measured, but for its meaning within the functions of the surrounding system as well. System connections built in small pieces from both qualitative and quantitative data have been used simultaneously in this project to build a coherent system picture, and analysis of both forms of data has occurred retroductively, in that spatial and temporal concurrence of observations suggested causal pathways for testing that in turn suggested different ways to view the system.

Statistical analysis of quantitative data was done using the Statistical Package for Social Sciences (SPSS©) software program, or JMP© 5.1 statistical software from SAS corporation. Data from the phase 1 particle size tests and the phase 2 infiltration tests were entered into different spreadsheets and analyzed separately. Infiltration rates, categorical stone content, clay content percentages, hydraulic conductivity, particle size classes, bulk density, porosity, organic content, and particle density values were entered as attributes in the phase 2 sheets, and all variables in both sheets were categorized for vegetation type and soil depth. Observations made during the testing process indicated that several different factors were responsible for infiltration rates, and during analysis, consideration was given to the importance of some of the measured attributes as actual or surrogate measures for these factors. In particular, relationships between clay content, root presence as reflected by organic content, porosity, and particle density were carefully explored for forest and grass categories.

Variables were first analyzed through exploratory tests to determine the distribution characteristics of the data. Where data were skewed, the data sets were transformed to logarithmic values to test log as well as non-transformed relationships. Determinations of normality and sample size (n) established what tests of relationship and correlation could be used (Burt and Barber, 1966). Although 80 records are available in the infiltration test pit data bank, not all depths are represented equally (Table 4.3). In particular, forest and grass comparison at 125 cm has no statistical significance since only four infiltration tests were run at this depth. The 18 surface tests completed on the grassed hill shoulder are not included in the infiltration test variable frequency count shown in table 4.3 because no additional attribute information was gathered for these sites beyond matric potential and depth to bedrock.

Variables were analyzed for significant relationships through linear regression and/or nonparametric Kruskal-Wallis tests that substitute for one-way parametric ANOVA of independent groups (Pagano, 1994). Variables were categorized by vegetation types and/or depths for most tests, and a significance level of 95% was accepted as indicating differences between groups. Capabilities of the statistical software permitted both parametric and nonparametric correlation testing at the same time, and parametric Pearson Correlation tests

were run simultaneously with Kendall's coefficient of rank correlation, which calculates the correlation of ranked variates (Sokal and Rohlf, 1997).

In the final stage of this study, information on significant variable relationships was used to reassess system properties observed and measured elsewhere in the project. In some cases, statistical evidence was able to bolster lines of interaction already noted during the study, and at other cases, significant relationships revealed system responses that had gone unnoticed. Final integration of the data involved merging the information to develop a final overview.

Table 4.3  
Infiltration Test Variable Frequency

| Vegetation Type | Total | < 10 cm | 25 cm | 55 cm | 85 cm | 125 cm |
|-----------------|-------|---------|-------|-------|-------|--------|
| Forest          | 33    | 10      | 9     | 7     | 5*    | 2      |
| Grass           | 47    | 10      | 15    | 13    | 7**   | 2      |
| Total           | 80    | 20      | 24    | 20    | 12    | 4      |

\* includes 2 measurements at 70 cm, which are categorized differently in the data

\*\* includes 2 measurements at 80 cm, which are included in the 85 cm data set

## **CHAPTER 5**

### **THE LANDSCAPE SYSTEM ON BOWMAN'S BEND**

Erosion occurs within a complex web of interacting variables that collectively govern processes at the hillslope scale. To establish what factors are active in erosion processes on Bowman's Bend, this chapter details the variables responsible for landscape evolution and ties those variables to their influences on hillslope hydrology. Information defining these variables is grouped into four general categories: climate and weather event effects, geologic and palaeoenvironmental influences, soil characteristics, and biogeomorphic influences. Each of these variables is explored through analysis of existing research information coupled to data derived through both observation and field measurement. Therefore, this chapter brings together a mixture of background information and results. In some cases, field observations by themselves provide a solid line of evidence for system tendencies, but in all cases, background information and observations provide a framework to which quantitative measurements can be related.

#### **CLIMATE HISTORY AND RECENT EVENT-BASED EFFECTS**

Regional landscape processes are regulated at a broad level by climate patterns. Within a regional climate regime, variations in event intensity, duration, and antecedent conditions act on the landscape to induce microscopic to megascopic geomorphic changes. Because regional climate regimes do shift over time, earth surface system study requires an understanding of climate variation that encompasses multiple scales, from historical generalities to current event-based specifics.

Current climate factors operate on landscapes that may have in part developed under regimes much different from that of the present. On Bowman's Bend, Holocene precipitation and temperature patterns, along with native American land use practices, set up the land cover conditions likely found by the earliest European settlers. More precise climate data for the study area are available for the years following 1925, when the first nearby meteorological station was established at Dix Dam. Analysis of precipitation data from Dix Dam allows a determination of the effects of possible recent changes in weather patterns as well as the relationship of a particularly large storm event to an erosion event identified through tree ring examination.



Meteorological data also provides the means for coupling rain events to smaller scale episodic geomorphic changes observed in the field during 2004 and 2005.

### **Climate History**

Little historical climate evidence is specifically available for Bowman's Bend, but research applicable to the wider region can be used to describe broad scale climate influences. Glacial ice at its maximum penetrated as far south as the Ohio River, approximately 120 km to the north, inducing cold, dry, and windy periglacial conditions during full-glacial Pleistocene periods (Watts, 1979) as well as changes in Kentucky River flow patterns (Teller and Goldthwait, 1991; Andrews, 2004) and possible interglacial loess deposition. Vegetation patterns shifted with glacial coverage, and pollen studies undertaken in Pennsylvania and West Virginia have revealed that stable grass-dominated tundra existed within 60 km of the ice sheet and that central Appalachian mountains supported sedge tundra (Watts, 1979). Forest tundra supporting spruce and jack pine existed at lower latitudes, and these species expanded northward with climate warming. In western Kentucky, Wilkins et al., (1991) determined that a closed spruce forest with jack pine subdominant existed in that area during the last full-glacial (from 20,400 to 16,800 B.P.). Because the Wisconsin ice sheet did not reach the Ohio River (Watts, 1979), and because the inner Bluegrass region of Kentucky would have experienced some ameliorative effects from prevailing westerly wind patterns, it is likely that some form of boreal taiga ecosystem existed in the study area during the last full-glacial. Taiga-like conditions with sparse conifer coverage developed at the end of the last full-glacial in western Kentucky (16,800 to 11,300 yr B.P.), followed by mesic deciduous forest growth between 10,000 and 7,300 yr B.P. (Wilkins, et al., 1991).

Temperature and, to some extent, precipitation increased in the central and southern Appalachians between 7,300 and 4,800 yr. B.P. (Delcourt et al., 1999). In the Dripping Springs Escarpment of western Kentucky, warming temperatures led to xeric oak-history forest development between 7,300 and 3,900 yr B.P. and to a mixed deciduous forest/prairie ecosystem after 3,900 yr B.P. (Wilkins et al., 1991). The first European settlers in the Bluegrass described a savanna terrain of canebreaks, grass and clover fields, and open woodlands (Campbell, 1980), but it is not clear that climate factors were solely responsible for the open nature of the pre-settlement vegetation. It is believed that fire played a large role in generating the savannah, but the relative effects of climate change, grazing and native human impact in controlling fire conditions have been a matter of speculation (Campbell, 1980; Wilkins et al., 1991).

Campbell (1980) notes that all areas of the Bluegrass are climatically capable of supporting forest growth. Pollen evidence from Jackson County in the Daniel Boone National Forest indicates that a cooling trend between 3,000 and 200 years ago brought increased precipitation, but that it was accompanied by a local pattern of recurring fire that did not exist prior to that time and was likely of human origin (Delcourt, et al., 1999). Fire-adapted oak, black walnut, chestnut, and pine became dominant on ridge areas as native peoples used fire to create openings for gardens, whereas ravines and steeper slopes retained forests composed of more fire-intolerant basswood, sugar maple, beech and hickory species (Delcourt, et al., 1999). The combination of climate and human impact variables likely produced a similar environment on Bowman's Bend, where cane, grass areas with open tree coverage, and forest patches probably occupied the central upland area, and mesic deciduous forest covered gorges and escarpment slopes in immediate pre-settlement times (Campbell, 1980).

### **Local Climate Trends (1925-2005)**

The nearest meteorological recording station to Bowman's Bend is about 4.8 km (3 miles) southwest at Dix Dam (COOP ID 152214), where data has been collected since 1925 (Figure 2.1). Most precipitation in Kentucky results from the passage of west-to-east moving frontal systems that generate rainfall over large regions, and it is thus possible to use the Dix Dam information to obtain a reasonable estimate of precipitation at Bowman's Bend. The Dix Dam station has existed in its current location since 1953 (37°48'N / 84°43'W; elevation 265.2 m (870 ft)), and a predecessor station, Burgin Dix Dam (COOP ID 151127) existed before then in the same general location but at a lower elevation (235.0 m (771 ft)).

For this study, Dix Dam climate data from the NOAA National Climatic Data Center (Daily Climatological Data, 1925-2005) was analyzed to determine monthly and annual precipitation totals, along with the number of events of size >1 in (25.4 mm)/24 hrs, >2 in (50.8 mm)/24 hrs, and >4 in (101.6 mm)/week. These are arbitrary cut-off levels selected based on their ability to generate field capacity conditions and on the nature of the data available. Lexington, Kentucky, 20 km to the northeast, has established 1.2 in/hr as designating a 1-year event and 1.98 in/hr and 4.37 in/24 hrs as 10-year cumulative rainfall events (L.-F.U.C.G., 2005).

Figure 5.1 shows annual total precipitation for 1925 to 2004. Average precipitation for this period is 1126 mm (44.3 in) and is shown in figure 5.1 as a dotted line. The 4 years between 1999 and 2003 constitute the longest stretch of below-average precipitation years in the Dix Dam record and contain the second and third lowest individual yearly totals. Elam

(1973) suggested that 11 and 22 year drought cycles may exist in Kentucky, and Campbell (1980) found inner Bluegrass evidence in the size distributions of mesic sugar maples for a 10.7 year growth disturbance pattern. If these cycles do represent normal climatic conditions since pre-settlement, then the current pattern is somewhat atypical.

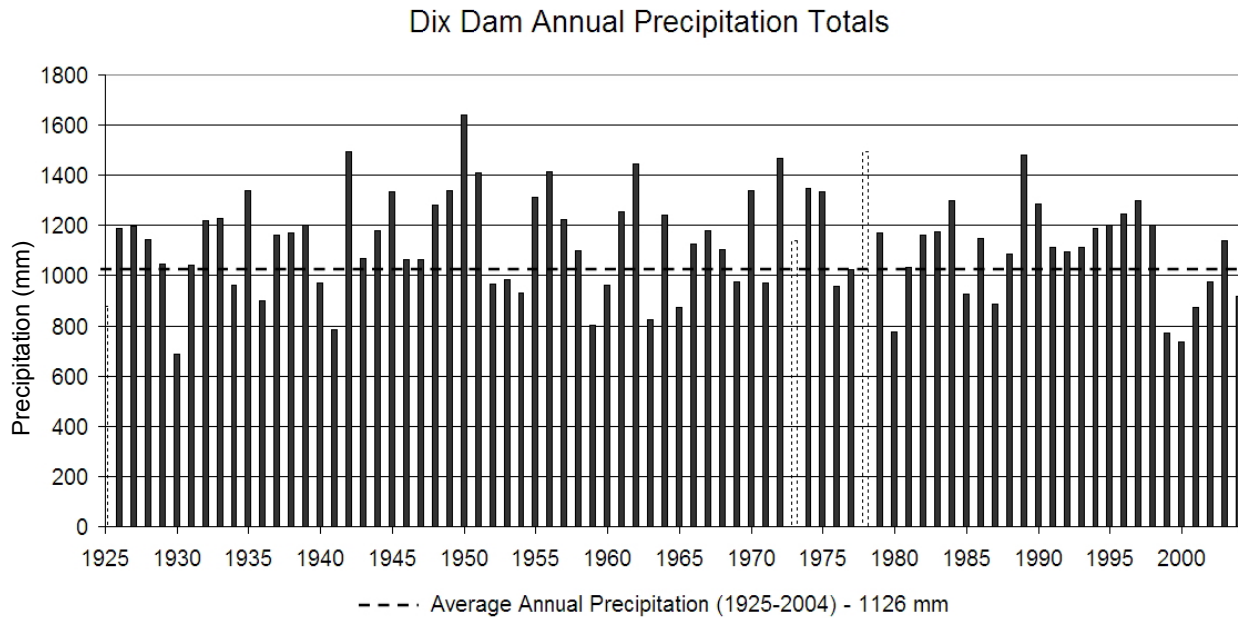


Figure 5.1. Dix Dam annual precipitation totals since 1925. Comparison of annual precipitation totals with the record average of 1126 mm suggests that a period of slightly below normal rainfall has occurred since 1999. This most recent span follows an 11-year period of above average rainfall, indicating that no clear change in precipitation is evidenced in the data. The years 1925, 1973, and 1978 are designated as inexact quantities because of incomplete records.

Figures 5.2-5.4 graph the number of events of the specified magnitudes recorded annually at Dix Dam. The mean number of events for each of these is 9.3, 1.7, and 0.94 respectively. The number of events  $>1$  in/24 hrs has remained at average or below since 1991, which constitutes the longest such stretch within this record. The data for average number of events  $>2$  in/24 hrs and  $>4$  in/week do not show any changes in recent years that are inconsistent with the rest of the Dix Dam record. Despite low total annual rainfalls, average or above average numbers of events were recorded for  $>2$  in/24 hrs between 2002 and 2004 and for  $>4$  in/week from 2001 to 2004.

### 24 Hour Precipitation Events > 1 in (25.4 mm)

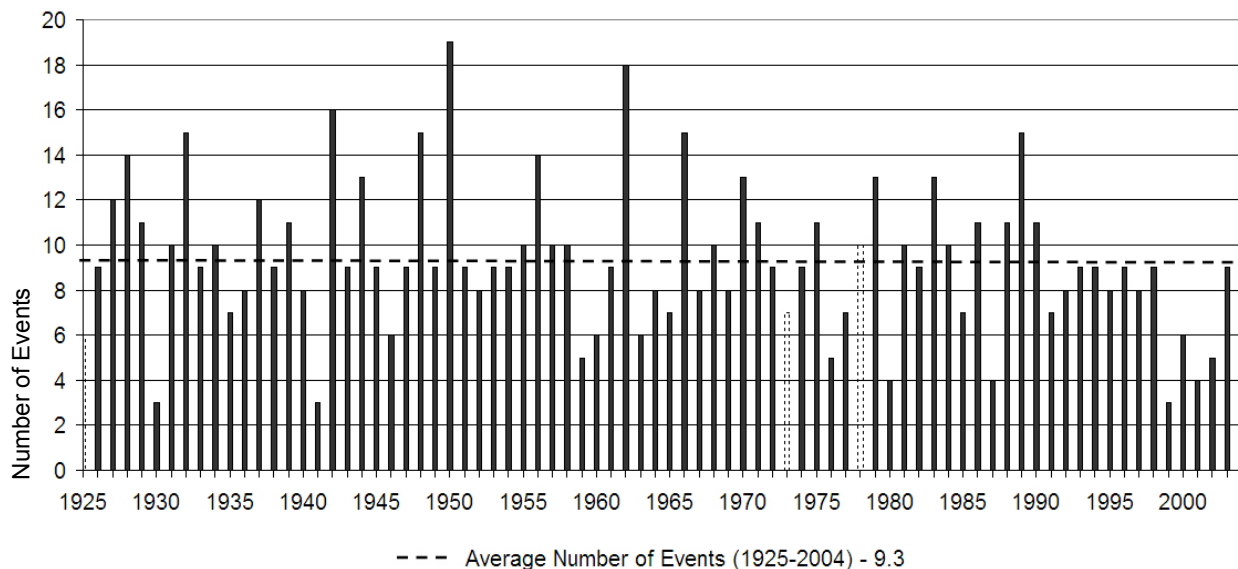


Figure 5.2. Annual number of 24-hour precipitation events >1 inch (25.4 mm). This record shows frequency to have been below average in the study area since 1991, which is the longest such stretch in the Dix Dam climatological data record. The years 1925, 1973, and 1978 are designated as inexact quantities because of incomplete records.

### 24 Hour Precipitation Events > 2 in. (50.8 mm)

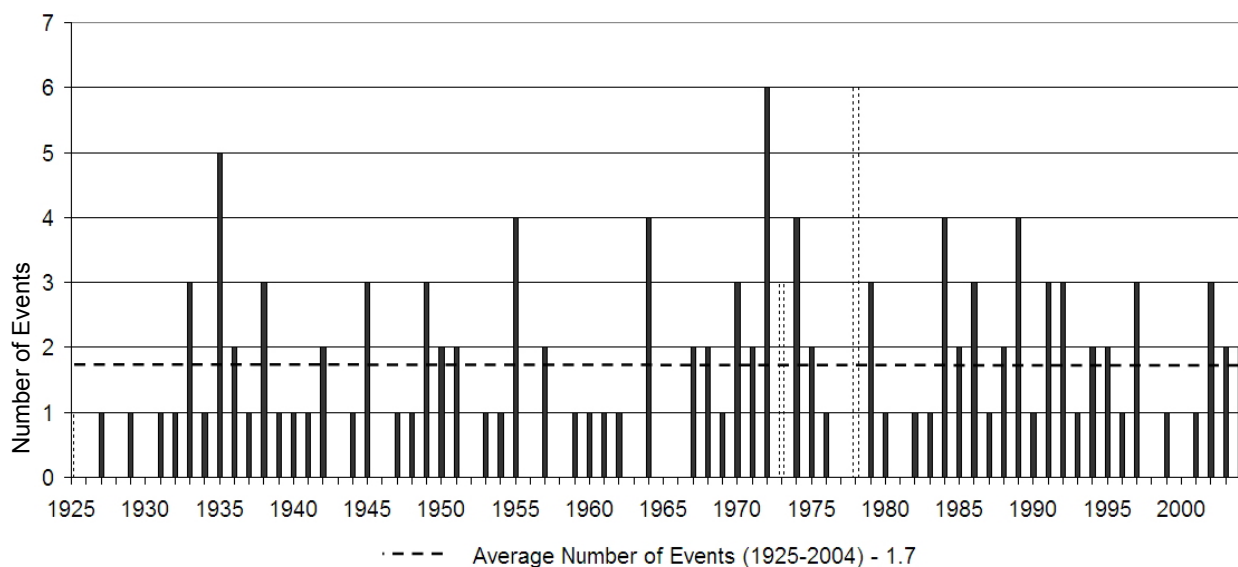


Figure 5.3. Annual number of 24-hour precipitation events > 2 inches (50.8 mm). As shown by the Dix Dam climatological record, there is no clear pattern of change within recent decades in the annual number of events delivering >2 in (50.8 mm) of precipitation within a 24 hour time period. The years 1925, 1973, and 1978 are designated as inexact quantities because of incomplete records.

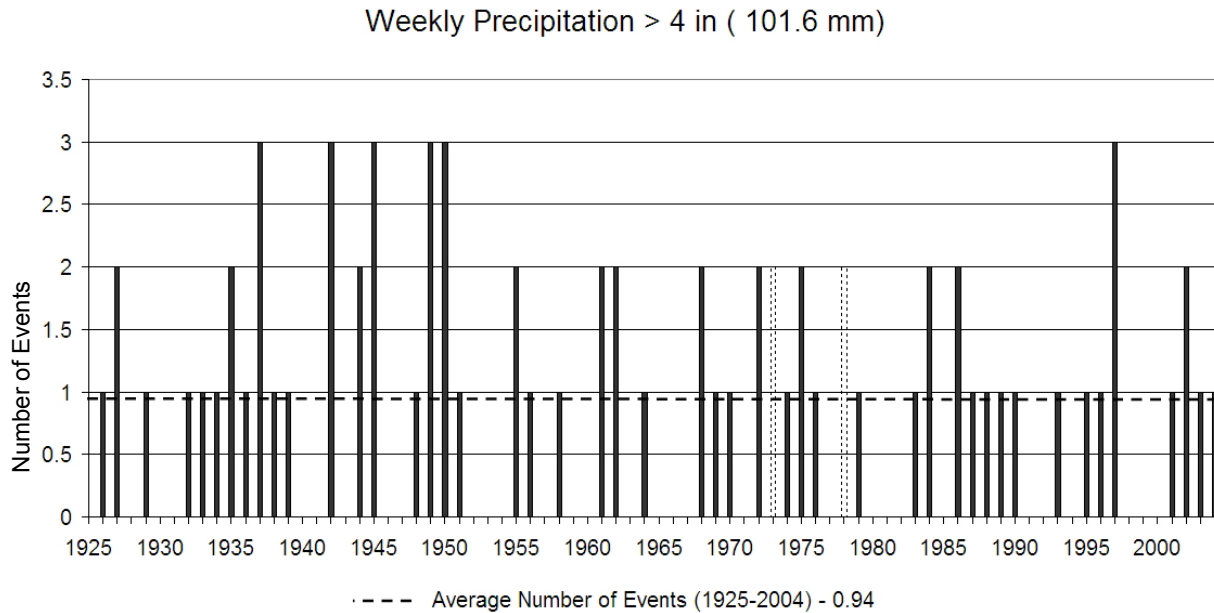


Figure 5.4. Annual number of weekly precipitation events >4 inches (101.6 mm). The number of events in recent decades appears to fall within a normal range for the Dix Dam climatological record. The years 1973, and 1978 are designated as inexact quantities because of incomplete records.

The length of this climate record precludes any consideration of long-term changes. However, the annual precipitation data and the event averages suggest that precipitation in the most recent years was more episodic than normal, with less total rainfall but with larger, more intense events. If the >1 in/24 hr event is viewed as a marker for lingering, low intensity, moderate-magnitude storm events, the number of these storm systems was apparently less than normal. Likewise, if the number of >2 in/24 hr events is seen as representing higher intensity storm systems, then these have not decreased despite a slightly lower annual average precipitation.

Matrix soil properties and conduit drainage in the study area set physical limits on subsurface water movement volumes that are more likely to be exceeded by short, high-magnitude storms than by lingering, low intensity events, even though equal precipitation amounts may be produced by both. Low antecedent moisture conditions will normally diminish any likelihood of erosion taking place since early precipitation will first replenish matrix and system storage, but high-intensity rainfall may exceed surface infiltration rates even under dry conditions (Stephens, 1996). In sum, analysis of Dix Dam data suggests that no distinct change in recent climate patterns has occurred that could account for erosion in the study area. A small tendency toward rain distribution in high-intensity events may have occurred over the past

decade, but the slight increase in erosion potential is not likely to have had much effect. Most certainly, if very current climate trends were to become long-term features of the area's system, episodic erosion occurrence would increase as well.

### **Correlation of Tree Core Data with Climate Information**

Tree ring analysis of two porous-ring ash trees growing at the head of an eroded gully about 400 m south of Hillslope A presents an opportunity to correlate climate data with episodic sediment removal and headward cutting at the grass/forest boundary line. These two trees, shown in Figure 5.5, are rooted in the upper bank of the gully and currently hold the head cut in place, causing the gully to take a double-headed form that brackets their position (Figure 5.6). The trunks of these trees form distinctive L-shapes, indicating that their headward positions have been undermined by soil creep.



Figure 5.5. Mature trees positioned at the head of a gully at the grass/forest boundary line are bent by soil creep. The trunk of the top tree shows twisting in addition to a sharp bend. Note orange bore handle and yellow field book for scale. Photo by author, June 2004.



Figure 5.6. Double-headed gully. The two bent trees shown in figure 5.5, plus a third tree seen on the left in this photo, anchor the soil at a gully head at the grass/forest boundary line. Photo by author, February 2004.

A total of 10 tree cores were taken in an attempt to accurately date the change in growth direction. A tree trunk that is bent from vertical will develop reaction wood to compensate for changes in stress, and hardwoods respond with distorted, thickened tension wood on their upper surfaces. The rings revealed that the upper tree twisted during its angled growth and that its center now consists of woody scar tissue. The lower tree, as suggested by the knob on the end of its bent base, most likely existed as a pole sapling when it was undermined. Ring counts are much higher in the bottom, right-angled trunk sections of the lower tree (27 rings) than in the upper section above the woody knob (21 rings), indicating that growth extended through a side branch after disturbance while the main stem died back.

Precise dating of such disturbed growth is difficult without cutting the trees down, but comparing samples allows some conclusions to be drawn. In all samples, a number of rings parallel with the current trunk surround inner rings that become progressively more diagonally slanted and end in a center oriented at right angles to the current stem growth. In the lower tree, core #3 taken from the side of the bottom trunk at 120 cm from the base displayed 27 rings, with the 20 outermost rings essentially parallel to the current trunk position, the next six

becoming progressively more slanted, and the 27<sup>th</sup> ring lying perpendicular to the first 20 rings (Figure 5.7). A second core taken at a slightly lower angle on the same tree duplicates this finding. Considering the difficulty in catching the exact center of the trunk because of the distorted growth, it seems likely that the main trunk underwent a displacement 27 years earlier that gradually stabilized over the following 7 to 8 years. The upper tree shows even more distortion in growth than the lower specimen, and cores from 100 and 160 cm above the base (as measured along the trunk top) respectively displayed 12 and 13 outer parallel rings and then 4 and 3 very slanted rings before reaching an area of brown, warped wood at the tree's center. The difference in ring numbers between the two trees suggests that the upper tree may have succumbed to soil creep a number of years after the lower one.

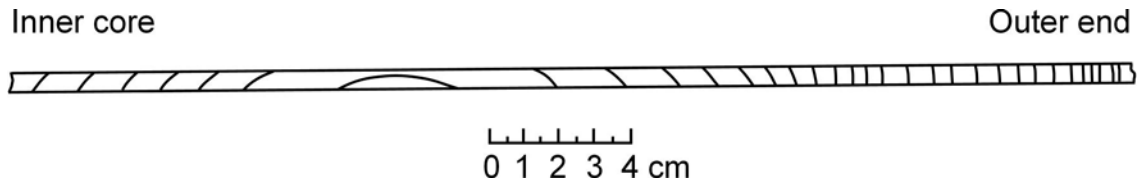


Figure 5.7. Diagram of core #3 from the lower tree, taken 120 cm above the tree base. Ring dimensions are as shown by the scale.

Dix Dam climate data shows precipitation to have been well above normal in 1978, 27 years before sampling, despite the fact that data for March is missing from the record. In 1978, 10 events >1 in/24 hrs and 6 events with > 2 in/24 hrs took place, and 2 weeks had over 4 inches of precipitation (see Figures 5.2-5.4). In particular, July 31 is recorded as having received 141 mm (5.55 in) of rain within 24 hours, which is the largest such 24-hour event recorded for Dix Dam between 1925 and 2004. The synchronous occurrence of this event with the bank undermining indicated by tree ring evidence suggests that infrequent, episodic large storm events are important in the study area in inducing major erosion occurrences. The subsequent development of the double-headed gully form around the stabilized trees indicates that lesser-magnitude events in the ensuing decades have had a significant but correspondingly more limited impact on erosion.

### Event-Based Observations

Locations of gully sites were surveyed beginning August 2003, resurveyed in May 2004, and were observed on multiple occasions subsequently. Many of these observations were



made within 24 to 48 hours of storm events, enabling association of particular forms of water movement or erosion to meteorological events and conditions.

### *May 2004*

On May 19, 2004, water was observed seeping from below overhangs at gully heads. Dix Dam climatological data record a 50.8 mm (2.0 in) rainfall on May 1 but only 15.2 mm (0.6 in) rainfall in the 7 days prior to May 19. Lexington daily climatological data, however, record 50.3 mm (1.98 in) for the preceding week, indicating that Bowman's Bend may have received somewhat more than 15.2 mm and that soil moisture conditions were likely to have been moderately high.

Erosion sites were visited again on May 31, following several days of heavy rains in which 93 mm (3.66 in) were recorded the preceding week at Dix Dam distributed as 1 day of 24 mm (0.95 in) and 4 days of >25.4 mm (>1 in) rainfall. This lingering moderate-intensity, moderately high-magnitude event, associated with plentiful antecedent moisture, produced a variety of visible water movement patterns. Scour lines appeared over the locations of drawdown areas between soil-covered pinnacles in the north end of the bend, surface water flow lines were indicated by downed grass in convergent grassed areas, and water pooled 2-10 cm in depth at the base of many grassed slopes.

Clear evidence for exfiltration was also observed. In one broad, shallow, forested sink on the east side of the bend, runnels below animal burrows approximately 3-4 cm in diameter provided evidence for return flow (Figure 5.8). Exfiltration within the sink was strong enough to knock small saplings over, and flow welled from cracks in the base of a 30-40 cm deep incision dissecting the area at the time of observation. At the top of one of the deepest gullies in the study area, a new soil pipe opening developed approximately 12 m uphill from the gully head. The opening occurred in the grass portion of the slope and had the size and shape of a groundhog burrow (Figure 5.9). The pipe extended directly backward into the hill for 57 cm, and it formed the top of a shallow, narrow, eroded channel that led downhill to the gully head across a distance that had not been incised prior to the storm. Subsequent investigation of this pipe opening showed that the channel partly filled in and revegetated during the summer.

Perching, exfiltration, and the opening of the soil pipe after the late May rains indicate the importance of subsurface lateral pathways, the likelihood of their activation under moderate moisture conditions, and the fact that these hydraulic pathways have capacity limits that are exceeded under increasing rainfall. Slope surface erosion observed on May 31 was minor and was related to shallow scour in areas of considerable water concentration, or to short runnels

developed by exfiltration. Grassed areas showing flow lines were not typically incised, indicating that surface runoff is not a major cause of erosion on Bowman's Bend under most circumstances.



Figure 5.8. Small animal burrows function as exfiltration pathways during large events, as evidenced by runnels below openings in a forested basin on May 31, 2004. Note field notebook for scale. Photo by author, May 2004.



Picture 5.9. A soil pipe opened through exfiltration pressure in the grass approximately 12 m above the head of a major gully following large rain events in May. A large animal burrow was most likely utilized for emergence. Photo by author, May 2004.

*September 18, 2004*

On September 18, 2004, a soil cover collapse sinkhole of the type described by White and White (1995) was observed just off the trail within a short distance of the road southwest of the preserve. This newly-opened feature was approximately 3 m deep with approximately the same internal diameter. The surface opening of the sink was less than a meter across (figure 5.10), and clumps of soil with attached vegetation were present on the sink bottom next to a hole that was absorbing a stream of water that emerged from the base of the sink's uphill wall. Soil loss had likely been occurring internally for some time in this location, but Dix Dam received 59 mm (2.34 in) of rainfall on September 17, indicating that this single large event may have caused high subsurface water movement and saturated conditions in the overlying soil that acted together to induce the final roof collapse. Because precipitation events of this size take place in the study area 1 to 3 times a year, mass subsurface soil loss related to eventual karst exhumation is likely activated at least this frequently.



Figure 5.10. Soil cover collapse pit opening revealed on September 18 following a single large rain event the preceding day. Photo by author, September 2004

*December 2, 2004*

On Hillslope B, grass vegetation vertically parallels the forest for a short distance before the slope drops abruptly into the top of an ephemeral stream course. A shallow gully has developed here along the edge of the forest within the grassed slope, and on December 2, saturated, liquefied soil was found at the bottom of an 82 cm profile augered in the grassed slope leading downhill to this gully. Dix Dam recorded 74 mm (2.92 in) of rainfall in November, which though below Kentucky's 96 mm (3.77 in.) average for November, provides adequate moisture retention during cooler weather. On November 30, Dix Dam received 13 mm (0.52 in) and on December 1 received 19 mm (0.74 in) of rain. In this case, the low-intensity rain, occurring with low-to-moderate antecedent moisture, was enough to cause water to concentrate in the soil in pathways running across the bedrock surface.

*February 5, 2005*

On February 5, soil depth measurements taken in a forest transect on Hillslope C revealed waterlogging in discrete, nonadjacent soil layers above the 160 to 170 cm bedrock depth. Probe measurements taken in a matching transect on the neighboring grass slope did not contain any saturated layers. Instead, portions of the grassed slope displayed signs of overland flow as indicated by flattened plants. Dix Dam data records only 21.8 mm (0.86 in) for the second half of January 2005 followed by 21 mm (0.81 in) spread out over the 4 days prior to February 5. Although the study area may have received somewhat higher rainfall, this field data still indicates that under moderate antecedent moisture and low evapotranspiration demands, low to moderate rains can saturate soil storage, causing water to follow characteristic surface and subsurface pathways.

### **Climate Summary**

Historical research suggests that this region of Kentucky was most likely covered by forest throughout the Pleistocene, either as sparse coniferous taiga during glacial periods or deciduous forest during interglacials. Since the last glacial episode, soils in the study area have developed under a climate regime that has experienced long-term swings between warmer/drier and cooler/wetter conditions, but has always been able to support deciduous tree growth. Beginning at least 3,000 years ago, however, fire became an important factor in the composition of regional plant communities. Fire, most likely spread by native peoples, created ecosystems in the inner Bluegrass that included savannas composed of cane and grass areas with thin tree coverage, and forest patches. In the study area, savannah may have occupied some of the

inner upland area, but escarpment slopes likely supported deciduous forest when the first settlers arrived.

Climatological data from Dix Dam shows that the longest stretch of below-average yearly precipitation totals on record occurred between 1999 and 2002. Although the total rainfall in 2003 was above the Dix Dam average, 2004 was again below average despite large storm events in May of that year. Along with this general slightly lower total rainfall in recent years, the number of events  $>1$  in/24 hrs has been at average or below since 1991, while the number of events  $>2$  in/24 hrs and  $>4$  in/week have been within historical records. No change in the climate pattern can be detected from the Dix Dam data that would point to a reason for increased erosion in the study area. However, a continuation of the current trend of precipitation distribution in larger events could cause more sediment movement over time.

Although large precipitation events tend to overwhelm the moisture storage capacities of the slopes, causing exfiltration, gullyng, and large scale soil removal, some erosion is also likely to occur in much smaller rainfall events. Even with low-to-moderate events, enough energy may be locally created to move small sized particles. Observations show that low amounts of rainfall under moderate antecedent moisture conditions cause subsurface water flux lines to operate in the slopes, creating downslope seepage in gully heads. Under moderate precipitation and moderate moisture conditions, preferential flow creates saturated patches in the forest soil, water collects in flow pathways on the bedrock surface, and surface water pools over impermeable Tyrone lithology at grassed slope bases. Many combinations of normally experienced degrees of soil moisture and storm intensity and length are capable of generating conditions under which flow may concentrate to the point of causing soil movement in the study area.

Loss of fines through forest surface and subsurface pathways probably occurs frequently, as is indicated by the abundance of thin-soiled vegetated gullies found on forested slopes. However, the scoured beds and exposed tree roots associated with eroded gullies indicate that current sediment removal greatly exceeds the normal loss of fines in forest pathways. Tree rings supply evidence that enhanced erosion of forest conduit systems occurred at least as far back as three decades ago. The existence of erosion prior to 2001, along with the average nature of high-intensity events since 2001, precludes climate change as a significant factor in explaining the current erosion pattern in forest gullies.

## **GEOLOGICAL INFLUENCES**

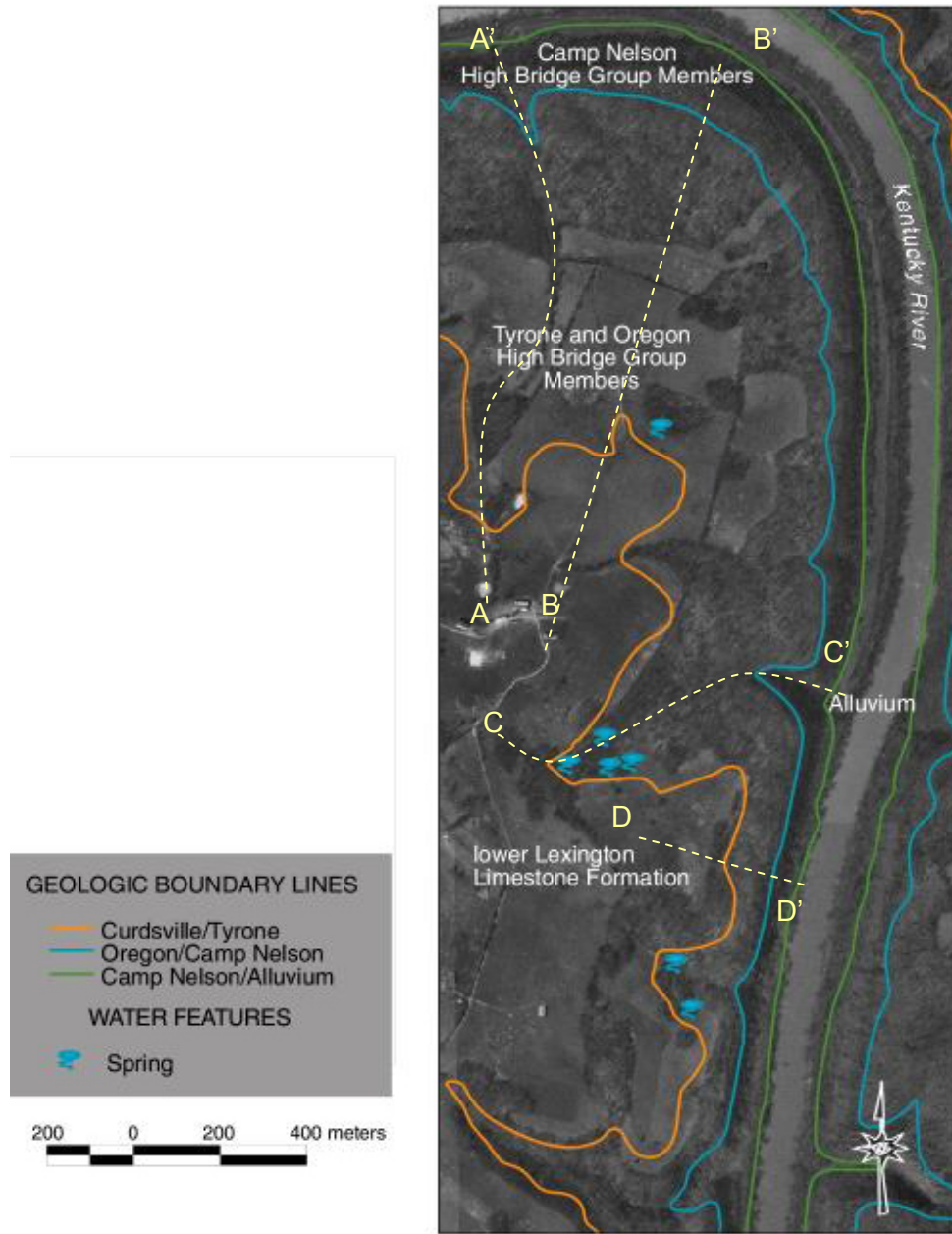
Geologic factors form the foundation for landscape development. On Bowman's Bend, the carbonate lithology supports the development of karst forms specific to the area's particular bedrock composition and structure. As solution opens the epikarst surface along weakened zones provided by bedding planes and fissures, insoluble materials in rock layers not only contribute minerals to the soil, but also guide pathways of solution and water movement as vertical flow is impeded or encouraged. Because water pathways through the regolith are controlled by soil texture properties largely determined by insoluble mineral constituents, and because regolith pathways operate in tandem with karren development in the epikarst, the nature of the decomposing bedrock must be considered in determining patterns of hillslope water movement. To relate geologic influences to other system processes, including differing vegetation effects, this subsection first describes the lithology of the bend and then outlines its relationship to water movements and epikarst development.

### **Geologic Units**

The bend is composed of flat-lying, mid-Ordovician limestones that outcrop within the river palisades as the oldest exposed rocks in Kentucky (Kuhnenn and Haney, 1986). Two sequences are represented: the High Bridge Group at lowest elevations, subdivided oldest to youngest into the Camp Nelson, the Oregon, and the Tyrone, and the lower Lexington Limestones, the later represented (oldest to youngest) by the Curdsville, Logana and Grier members. Figure 5.11 shows where these sequences have been mapped on the surface in the study area. As shown in figure 5.11, the central upland area of the bend is underlain by the lower Lexington Limestones, and exposure of the Tyrone and Oregon formations of the High Bridge Group is limited to narrow bands along the escarpment edge, the upper palisade walls, and upper portions of large tributaries (Carey and Stickney, 2001). The dense, micritic Camp Nelson limestones of the High Bridge Group form most of the palisade walls and extend below the river.

Bowman's Bend acted as the slip-off face some 1.5 to 2 million years ago for the river's currently entrenched position (Andrews, 2004), and the entire bend is edged by a fluvially-generated terrace that is seated in or above the Tyrone. Researchers have identified fluvial sediments on the north end of the bend (Andrews, 2004), suggesting that palaeochannel movement created the extended gradual terrace slope that comprises the bend's north end and exposes large sections of the Tyrone and Oregon. On the steeper slopes of the bend's eastern side, the terrace has not been associated with the palaeochannel and is confined to a much

narrower concave slope segment overlying the Tyrone. Although the terrace along the east side is obliterated by cross-cutting channels and slope erosion in some locations, terrace soil profiles examined during this project reveal the presence of fluvial sediments, suggesting that the remaining terrace portions represent the river's pathway during at least some portion of its palaeohistory (Figure 5.12).



Map Compiled by: Linda Martin, March 2005

Geology Data Source: KGS, Harribsburg 30x60 GQ, 2001  
Aerial Photos: KGS, Wilmore DOQQ, 1990

Figure 5.11. Geology of Bowman's Bend. The lower Lexington Limestones/High Bridge Group boundary is mapped at 260 m in the study area at the contact between the Curdsville and Tyrone members. Locations of geologic profiles (locations of figures 5.13a-d) are shown by dotted lines.

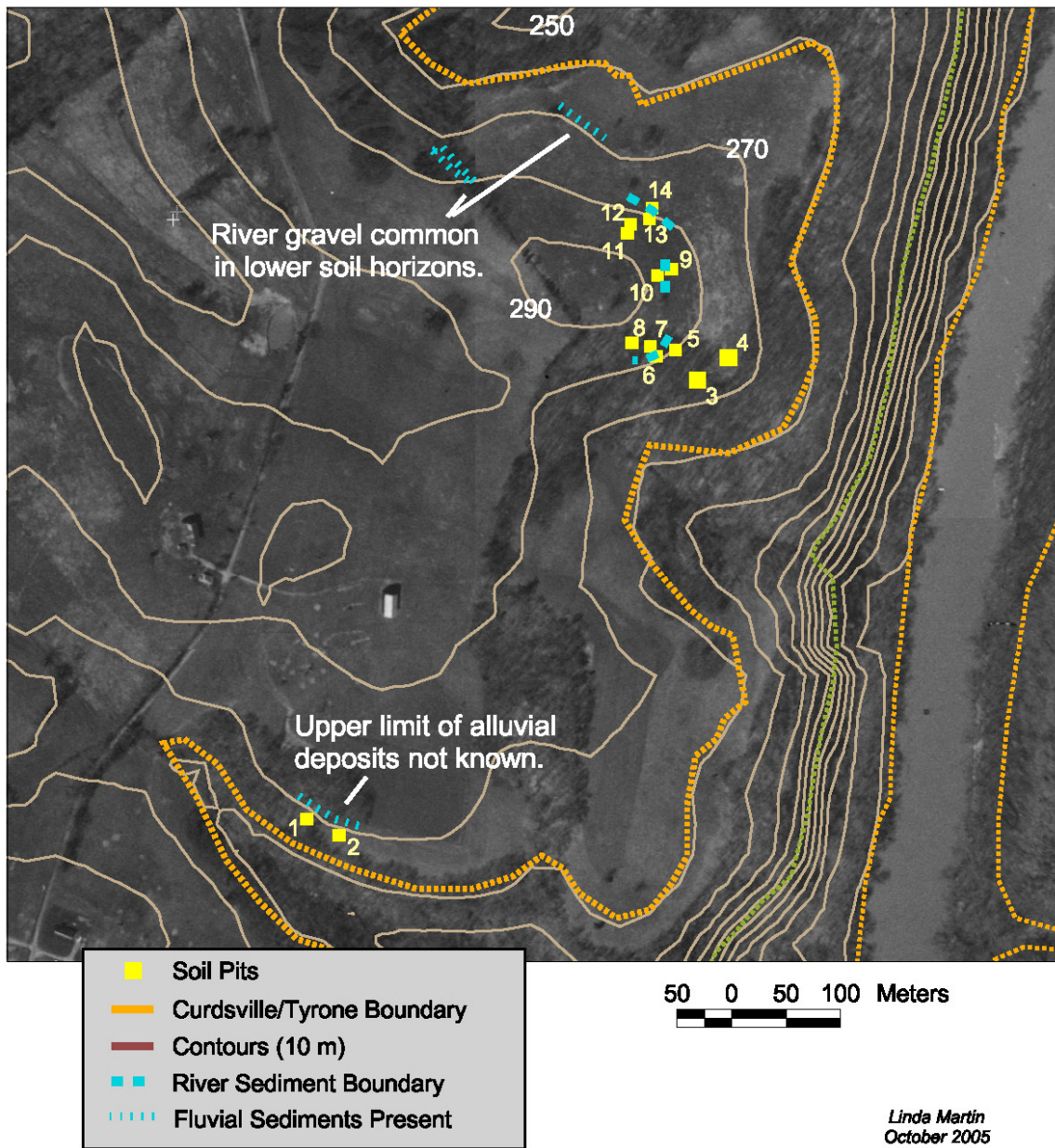


Figure 5.12. Alluvial sediments including geodes, chert, rounded gravels, and organic-rich clay deposits have been identified during this study in locations lying below the elevations marked with dotted blue lines. Where the upper elevation limits of these deposits are unknown, boundary lines are shown in smaller sizes.



The geological profiles in figures 5.13a-d demonstrate the differences in slope and topography between the north and east sides of the bend. Drawn from the 1:24,000 Wilmore Geologic Quadrangle (Cressman and Hrabar, 1970), these profiles compare relative elevations of geologic boundaries along both first-order streams and non-dissected slopes within the bend's elongated northern portion (A and B) and steeper eastern edge (C and D). Specific locations of these sites are shown in the map in figure 5.11. All of these profiles start at a 290 m elevation and include symbols indicating the approximate elevations of notable karst and erosion features found within 25 m of the profile transects.

Karst and fluvial features on the bend relate to particular stratigraphic, lithologic and structural properties of the bedrock, which also guided the tectonic pressure responses that led to the fracture systems that now direct the formation of the largest epikarst pathways. Hydraulic patterns have developed in study area soils in concert with localized bedrock decay, cutter and pinnacle growth, and emergence of epikarst drainage patterns, all of which relate to localized bedrock properties.

### **Stratigraphy**

Differences in depositional environments within and between the lower Lexington Limestones and the High Bridge Group have created localized stratigraphic characteristics that have a strong influence on soil and karst development. The formations of the High Bridge Group were laid in shallow epicontinental seas where sediment influx was limited to periodic volcanic ash deposition (Strafford, 1962), so that most of the group consists of fine-grained, tabular carbonate beds interrupted by thin zones of chert. An abrupt, disconformable boundary that often incorporates micritic Tyrone clasts occurs at the top of the Tyrone (Grossnickle, 1985), and it represents a change in the depositional environment to transgressive conditions (MacQuown, 1967). The shifting, unstable nature of this later depositional environment is represented in the thin limestone and shale beds of the Curdsville, Logana, and Grier members. Stratigraphic variations in thickness, mineral and insolubles content, porosity, permeability, and jointing define localized hydraulic, soil, and karst development tendencies and thus form the foundation of current slope evolution. In particular, this study's focus on changes in hydraulic properties of the soils and epikarst surface of slopes supported by the Grier, Logana, Curdsville, and Tyrone necessitates some investigation of the specific characteristics and solutional tendencies of these members.

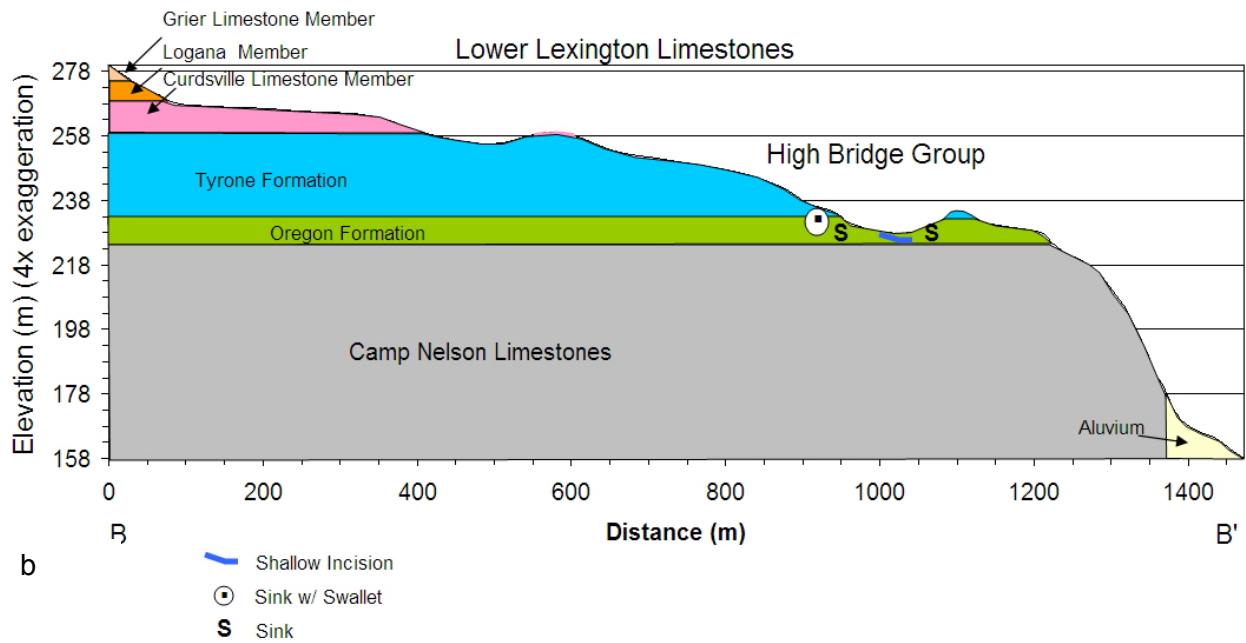
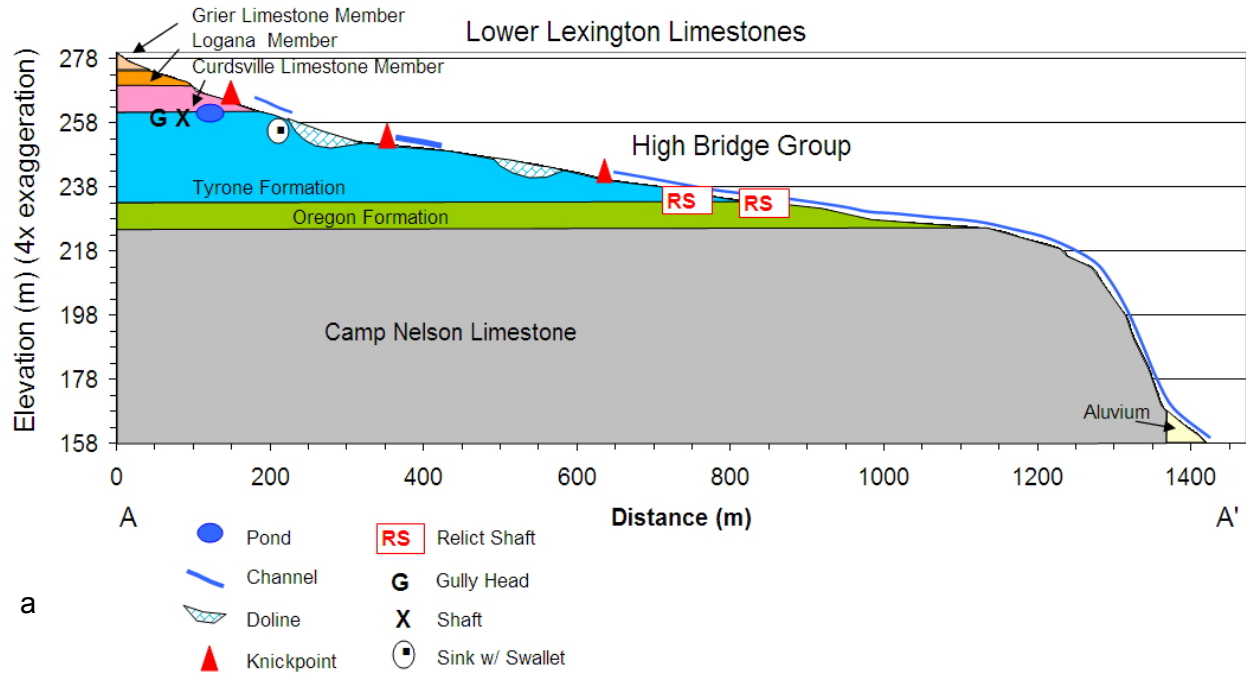
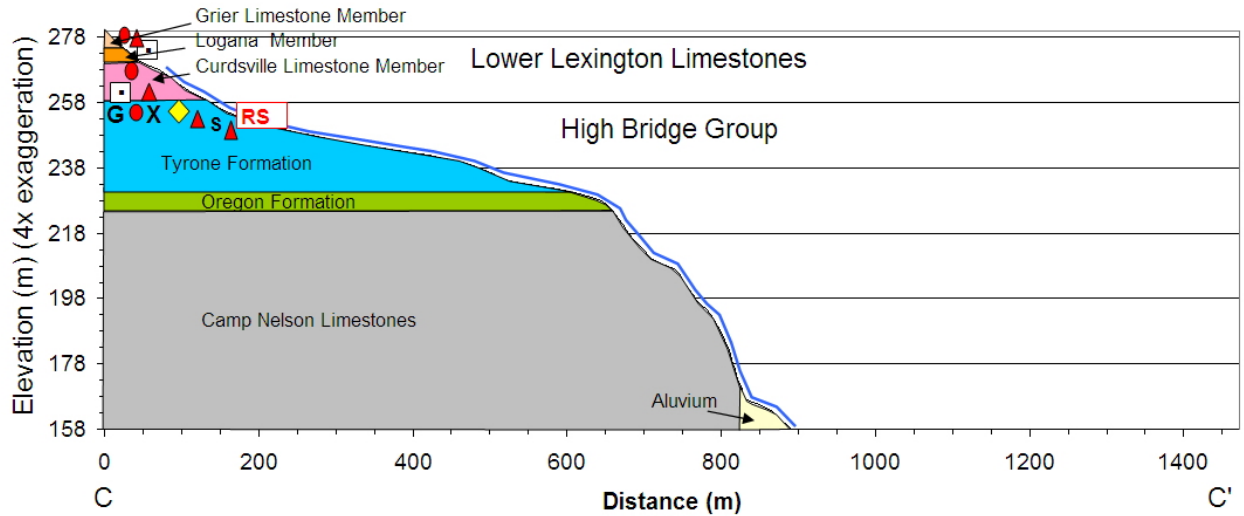
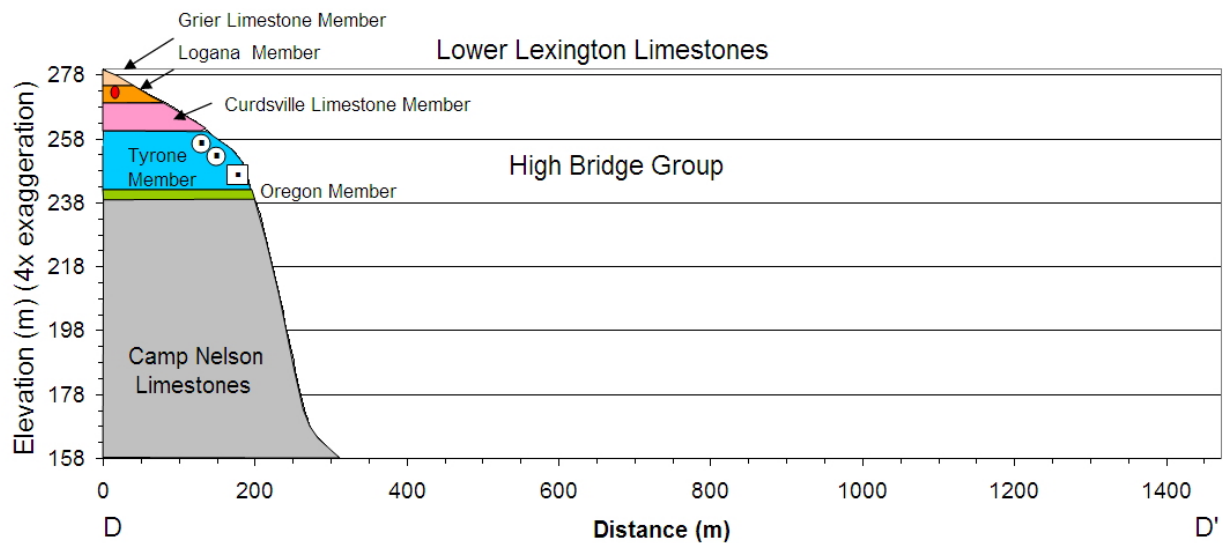


Figure 5.13 (a and b). Geologic profiles of the north end of the bend demonstrate the extended, gradual slope over the Tyrone. Figure 5.13a follows the main ephemeral stream, which passes through two dolines, or valleys created by solution loss. Figure 5.13b shows the area of highest elevation. Small to large sinks are frequent near the edge of the escarpment. Vertical exaggeration is 4x. See Figure 5.11 for profile locations.



- c
- Swallet
  - Shallow Incision
  - ▲ Knickpoint
  - RS Relict shaft
  - S Sink (small)
  - X Shaft (small)
  - ◇ Spring
  - Channel
  - G Gully Head



- d
- Shallow Incision
  - ⊙ Sink w/ Swallet
  - Swallet

Figure 5.13 (c and d). Slopes on the east side of Bowman's Bend are steeper than those found on the north end. Figure 5.13c shows an extended Tyrone exposure because it follows the largest ephemeral stream on the east side. The slope shown in figure 5.13d drops directly into the river. Vertical exaggeration is 4x. See Figure 5.11 for profile locations.

Both the Camp Nelson and Tyrone formations are primarily dense, thick-bedded micrograined limestones. The Tyrone, described as being semi-lithographic limestone 17-47 m (55-115 ft) thick (Grossnickle, 1985) is composed of clay-sized particles and displays conchoidal fracture (Strafford, 1962; Whaley, 1964). Fine, crystalline dolomite occurs as mottles and patches in the Camp Nelson and Tyrone, but comprises the main portion of the Oregon (Anderson and Barron, 1995). The Oregon (up to 20 m thick; Andrews, 2004) is composed primarily of dolostone interbedded with micritic limestone, but has a blocky, thick-bedded structure similar to that of the Camp Nelson formation (Kuhnhenh, 1986). Because of the thickness and fine-grain sizes of most beds, joints in the High Bridge Group may be continuous between layers (Hamilton, 1946), and the combination of deep jointing, massive, brittle bedding, fine grains, and probable unloading caused by the river's downcutting, promotes shaft development and water movement through vertical conduits that develop behind the palisade walls (Phillips, et al., 2004).

In contrast with the members of the High Bridge Group, the Lexington Limestones consist of a sequence of dominantly bioclastic, fossiliferous, shale-interbedded limestones that display complex stratigraphic relationships among repeating rock types (Black et al., 1965). The formation varies from 46 to 76 m in thickness (Strafford, 1962), and is identified as a unit mostly because it contains too many local facies changes to provide a consistent formation boundary at any point throughout its extent (Black et al., 1965). Black et al. (1965) define the Curdsville as a dominantly well-sorted bioclastic calcarenite found to be about 6 m (21 ft) thick in Jessamine County. The Curdsville is composed of planar beds greatly varying in thickness, residual content, and grain size. Grossnickle (1985) describes fining-up sequences in the Curdsville composed of calcilutite (carbonate mudstone) layers only a few millimeters thick, calcisiltite (siltstone) layers several millimeters to several centimeters thick, calcarenite (bioclastic sandstone) layers 3-15 cm thick, and calcirudite (coarse whole-fossil grain) beds 8-60 cm thick. Cross-bedding is present along with a few thin beds of shale or micrograined limestone, and chert is prominent in lower horizons (Black et al., 1965).

The Logana consists of micrograined silty argillaceous limestone interbedded in equal amounts with shale (Black et al., 1965). Limestone layers of the Logana are thin (3-5 cm), and isopachous mapping of the unit suggests that it is likely about 14.6 m (15 ft) deep in the study area (Grossnickle, 1985). The Logana forms a sharp contact with the thicker Grier (33-66 m thick), which is distinguished by the poorly sorted nature of the shale and limestone contained in its thin, irregular beds (Grossnickle, 1985). Limestone beds 1-30 cm thick in the Grier may be

rippled or cross-bedded and may contain chert, shale partings, or argillaceous nodular limestone on a local basis (Elvrum, 1994).

### **Structural Features**

The distribution of solutional activity is highly influenced by the size, spacing, and openness of joints, fractures, and bedding plane weaknesses (Deike, 1969; Gabrovsek, et.al., 2001). Bowman's Bend lies just west of the crest of the Cincinnati Arch, a northeast-southwest trending anticline which has its structural apex at the Jessamine Dome about 5 km northeast of the study area (Andrews, 2004). Although exposed layers in outcrops appear to be horizontal, the arch creates a regional dip to the west of about 6 to 10 meters/kilometer (Elvrum, 1994). Strafford (1962) analyzed jointing patterns of the inner Bluegrass in relation to major tectonic stresses and found that two main sets of joints likely developed as folding rotated an earlier position of the arch axis. The major joint set is expressed in the Wilmore geological quad as following a north-to-south trend that matches the orientation of the river on the bend's east side. The secondary joint set operates normal to the main set and appears to govern conduits and streams draining the eastern hillslopes.

Strafford (1962) found that vertical joints related to the major fracture set were closely spaced in the Tyrone formation but occurred with less frequency, more strike variation, and with a tendency toward more undulant joint planes in the Lexington Limestones. Joint swarms in association with this main fracture set are common, and long, straight joints may exist between the swarms (Strafford, 1962). Fracture swarms or shattered blocks appear to underlie the development of the numerous shafts found on the bend within the Tyrone lithology, as revealed by dissolution along vertical fractures that intersect at shaft locations. The largest first order stream draining the bend's north end (figure 5.13a) may have developed along a line of connected swarms, since it parallels the river's northeast trend and bisects a number of relict shaft features that display swarm jointing radiating from central points. Straight-line shafts opening along single fractures aligned with this major joint set occur in the High Bridge Group close to the escarpment edge or along large stream dissections where unloading has likely relieved pressure on the joint walls.

The secondary set, generally striking slightly north of due west and operating at right angles to the major set, was found by Stafford (1962) to be a much more irregular and variable regional joint pattern. In High Bridge Group exposures, juncture of this fracture pattern with the major joint set causes blocks to be orthogonally jointed. In contrast with the smooth, straight fractures associated with the major joint group, fractures in the second set are often curved and

rugged, although curving planes are less common in the Tyrone. Conduits draining the east side of the bend operate at right angles to the river and thus likely belong to this second joint set. The curvilinear nature of many of the conduits in the lower Lexington Limestones, as expressed in their overlying linear depressions, can be traced in aerial photographs (Figure 5.14).

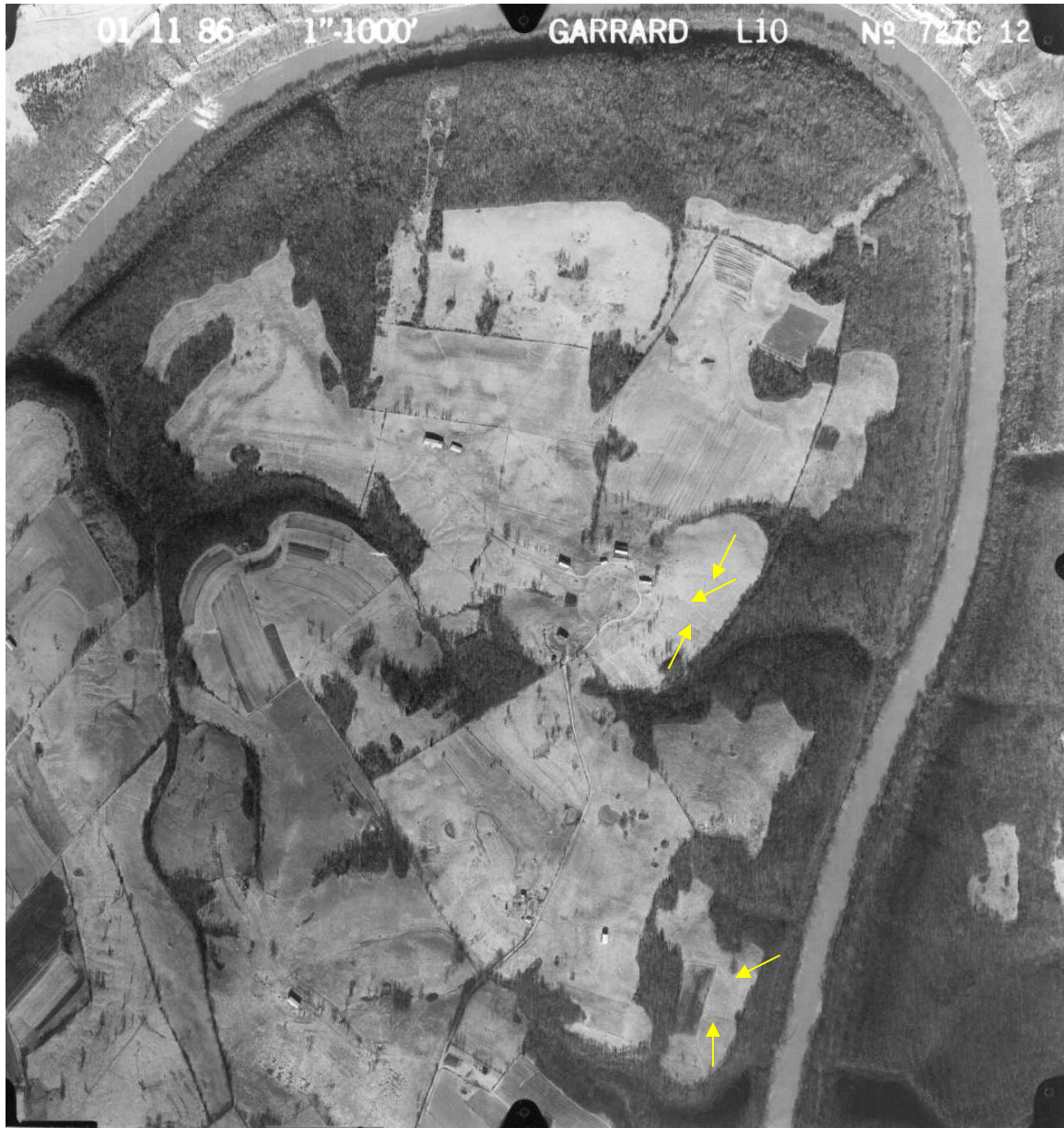


Figure 5.14. Shallow linear depressions overlying epikarstal conduits are visible in a 1986 aerial photo at 1:12,000 scale. As indicated by arrows, conduits on the east side of the bend orient with hydraulic gradient to the river and likely follow the minor fracture set for this region. Photo source; Kentucky Transportation Cabinet, Frankfort, Kentucky, January 11, 1986.

In some cases, the main and minor joint sets may dead end where they intersect (Strafford, 1962). In the main study area, sudden change in fracture direction caused by a switch between joint sets is likely demonstrated on Hillslope F (Figure 4.3), where a shallow, broad sink at the top of the forest patch is drained by a N45W flowing linear depression overlying the Grier and Logana formations. The depression abruptly switches to due north two-thirds of the way downhill as the conduit drops into the rock layers of the Curdsville and reappears as spring flow some meters below in the Tyrone. At the landscape scale on the east side of the bend, irregular shapes and orientations of concavities and upland hill noses are most often related to fractures in the horizontal layers that have curving courses oriented basically perpendicular to the river.

### **Impermeable Layers**

Impermeable layers in the Tyrone, Curdsville, Logana, and Grier may impede or encourage solution. Elvrum (1994) found that karst development in the Bluegrass was controlled more by shaley lithology and bed thickness than by fracture density. Resistant unfractured members composed of shale, limy shale, bentonite, or tabular-bedded micrograined limestone may act as localized aquicludes, impeding vertical water entry and delaying karst weathering (MacQuown, 1967). Karst dissolution tends to develop best where coarser-grained limestones provide some degree of porosity, so that where shale is present, fine silts and clays may confine water movement to coarser intervening limestone beds (MacQuown, 1967). Because shale impedes water percolation through the bedrock of the Lexington Limestones, deep karstification is precluded except along isolated very wide fractures.

Impermeable layers may even control fracturing to some degree, as shown by differences in joint directions between the Tyrone and Curdsville (MacQuown, 1967). In the Curdsville, MacQuown (1967) found that shale and bentonite layers more than a few centimeters thick are not cut by continuous joints. Nodular limestones in the Grier, however, permit joints to pass through multiple layers and thus encourage vertical flow as opposed to lateral flow along impeding layers (Elvrum, 1994). In general, local interruptions of jointing and downward flow in the Curdsville, Logana, and Grier, tend to create shallow epikarst solution that differs from the deep vertical solution present in the High Bridge Group.

Although the High Bridge Group has relatively few impervious layers in comparison to the Lexington Limestones, two major impervious layers in the upper part of the Tyrone restrict vertical water movement into the epikarst within the terrace found at the top of this unit. Because of this layer, and because the Curdsville and the underlying Tyrone units have such

contrasting compositions, the contact is often evident from field observation of slope contours. Impervious layers in the Tyrone likely held the original palaeochannel, as evidenced by fluvial sediments present on the terrace, but the coincidence of palaeochannel sediments and change in lithology now make it difficult to determine where the top of the Tyrone precisely lies. The elevation of the contact has been mapped by the Kentucky Geological Survey as largely coinciding with the 260 m contour line along Bowman's Bend.

The thick impervious layers at the top of the Tyrone are only two out of up to 18 metabentonite beds composed of altered volcanic ash found in this member and more than 43 metabentonite beds in sections measured from the Logana through the Camp Nelson (Conkin and Dasari, 1986). Metabentonite, also called k-bentonite (Huff, 1963) or simply bentonite, acts as an aquiclude if present in sufficient thickness, and bentonite layers in the upper 6 m of the Tyrone and the base and mid-to-upper portions of the Curdsville are sufficiently prominent to provide a base for local aquifer units (MacQuown, 1967). The Palaeozoic bentonites have devitrified, producing mixed-layer, illite-montmorillonite clays with swellable to non-swellable layer ratios of between 2:3 and 1:3 that are mixed with minor ash amounts (Huff, 1963). These clays are hard and blocky when fresh, but tend to slough and fill effective pore spaces when wet (MacQuown, 1967).

Many bentonite layers may be only a few millimeters thick, and the distribution of the two thicker layers is not consistent throughout the Bluegrass. Correlations by Huff (1963) show that the topmost "Mud Cave" layer is thickest (81 cm) at High Bridge but absent at Camp Nelson (with the study area lying about midway between). The "Mud Cave" may be located at a position either at or just below the contact between the Tyrone and the overlying Curdsville, but where it is present, it typically lies within the top 1.5 m of the Tyrone (Huff, 1963). Extended sloping terrace widths and observations of exposed conduit walls at the base of the main study area indicate that approximately 5 meters of rock may be present at the top of the Tyrone in this location, making it unlikely that the "Mud Cave" is locally continuously present. If the "Mud Cave" is present here, it may be thin enough to contribute insolubles but not thick enough to impede solution.

A second, thicker bentonite layer exists throughout the Bluegrass at approximately 5-6 m below the base of the Curdsville (Huff, 1963; MacQuown, 1967; Kuhnhein and Haney, 1986). This "Pencil Cave" bentonite layer supports numerous springs in the study area at approximately this distance below the Curdsville/Tyrone boundary (Figure 5.11). At the base of Hillslope A, a shallow (<2 m deep) epikarstal conduit breaches this bentonite layer and drains water from the shallow sink in the lower center of the slope into an exhumed relict shaft feature



in the forest. Figure 5.15 shows the exit location of the conduit in the uphill shaft wall, the top of which lies approximately 6 m below the top of the Tyrone. Bentonite, most likely belonging to the “Pencil Cave” layer, lies 40 cm below the surface in the soil directly above the shaft. The surface channel currently incising between the grass/forest boundary line and the shaft passes over the bentonite, causing it to decompose into soft, greenish-white gravel-sized pieces in the channel during flow periods. Where bentonite is found at the bottom of soil profile samples, it forms a stiff saprolite that can be penetrated with difficulty by auger for a short distance.



Figure 5.15. Relict shaft below Hillslope A, with widened vertical fracture through a Tyrone exposure in the uphill wall. The shallow eroded channel above the fracture passes over and within a 40-50 cm deep layer of bentonite. Current sediment movement processes are removing the soil lying to the left of the rock wall in the photo. This soil bank fills in the gap between the exposed rock wall shown here and a second exposed wall lying outside the photo range. Five such walls and intervening soil banks surround a central open area at this site. Photo by author, April 2005.

The nature of the bentonite impermeable layer is important to water movement at the base of the main study area, but the existence of erosion features both above and below the Tyrone boundary line in other areas of Bowman’s Bend show that it is not the sole factor involved in the current erosion process. Although impermeable layers in the Tyrone do limit epikarstal conduit development at this elevation, various other impermeable layers in the lower

Lexington Limestones also seem to prevent deep epikarstal flow. Soil depths measured in transects across various slopes indicate that numerous cutters may channel flow at the bedrock surface in the main study area. However, only three visible openings or depressions in addition to the conduit/sink system on Hillslope A can be positively related to deeper epikarst drainage. Some sideslopes do not have any well-developed conduits visible from the surface, creating overall conditions in which most flow should be diffusely distributed in the regolith or concentrated at the bedrock interface. Altogether, evidence indicates that epikarstal conduit development is strongly limited by the various impermeable layers of the lower Lexington Limestones and the upper Tyrone.

### **Epikarst Development**

The epikarst forms a zone of diffuse secondary permeability at the top of the bedrock that is defined not only by solutionally widened internal fissures, but by karren features that form a broken upper bedrock surface (White, 1988; Ford and Williams, 1989). Researchers define karst conduits as integrated systems of pipelike passages that operate within the limestone aquifer (White, 1988). In soil covered karst, most water enters the main bedrock conduit system through throughflow pathways in the regolith and/or subcutaneous flows in the epikarst. In contrast to rock-covered conduits, cutters are defined as operating at the surface of the epikarst. Cutters that incise single joints in the epikarst can concentrate flow at the epikarst surface and form important channels for delivery to deeper conduits (Cooley, 2001). However, pipes greater than 1 cm in diameter are capable of carrying turbulent flow (Smith et al., 1976), and conduits of this size and greater can operate within the epikarst in tandem with flows in soil-covered cutters and diffuse movements through smaller fissures. Whereas diffuse, cutter and conduit subcutaneous flows can all be categorically defined, the same hydrologic and chemical solution processes guide their development and make them difficult to separate in the higher slopes of the study area.

### *Epikarst, Karren, and Conduit Interactions*

Conduit development in the Bluegrass is favored in fractures that orient within 13 degrees of the strike of the potentiometric gradient (Taylor, 1992). Because of the number of impermeable layers in the Lexington Limestones, depths of solutional openings in the inner Bluegrass rarely exceed 25 to 30 meters (Hamilton, 1946; Taylor, 1992). Areas drained by conduit systems form groundwater basins that compose less than half of the total Bluegrass region, and subsurface flow in intervening interbasin areas remains only a few meters below

ground surface (Thraillkill, 1982, 1984). Bowman's Bend geomorphology seems to support the same approximate ratio of groundwater-to-interbasin development, as evidenced by the contrast of the area covered by slopes supporting sinks and other karst features to that occupied by convex slopes supporting no surface solutional features. Because hydraulic gradient is parallel to the secondary fracture set in the upland slopes, and because fractures of the secondary set are irregularly spaced and limited in depth, epikarst cutter and conduit networks on the east side of the bend appear to mostly drain single slopes with little movement of water under surface divides. Water movement under surface divides seems likely on the north side of the bend where deeper drainage connects large sinks in the Tyrone and Oregon formations.

Although deep karstification is usually precluded by the shale layers of the Lexington Limestones, shale layers often encourage solution by focusing water penetration. Cave development will initiate more easily along a limestone/shale contact than at bedding planes within the limestone (Klimchouk and Ford, 2000a). Because solution is encouraged along contacts, the many shales interlayers of the Lexington Limestones encourage solutional release of flagstones at the surface of the epikarst. In the main study area, edges of bedrock ledges and pit bases are typically composed of unconsolidated, stacked limestone plates separated by thin soil layers.

As solution proceeds in the epikarst along weakened zones and contacts, less resistant areas of the bedrock surface are removed. Soil depth measurements taken by probe show that the surface of the bedrock is typically pitted, with pinnacles that may stand half a meter or more above neighboring consolidated bedrock. Some pits relate to cutters opening along joints, but other pits appear to be isolated forms that may or may not be associated with drainage into deeper bedrock layers. Pits, cutters, and other karren forms appear to at least sometimes interconnect and funnel flow across sections of the slope bedrock.

Measurements from soil depth transects taken on Hillslope H, at the south corner of the main study area, demonstrate the irregular courses that pit and cutter interconnections may follow. Seven transects were taken paralleling a row of large trees along the fence line below the shoulder of the hill (Figure 5.16). These transects were intended to highlight the action of large tree roots on the bedrock surface, but they also serve to show cutter interconnections. Sited 26 m, 10 m, and 3 m both north and south of a central transect next to the trees, the stacked transects correspond to soil depth changes with elevation. As shown in the figure, an interconnected soil covered cutter enlarges downhill near the beginning of the transects, while a second cutter develops midslope near the transects' center.

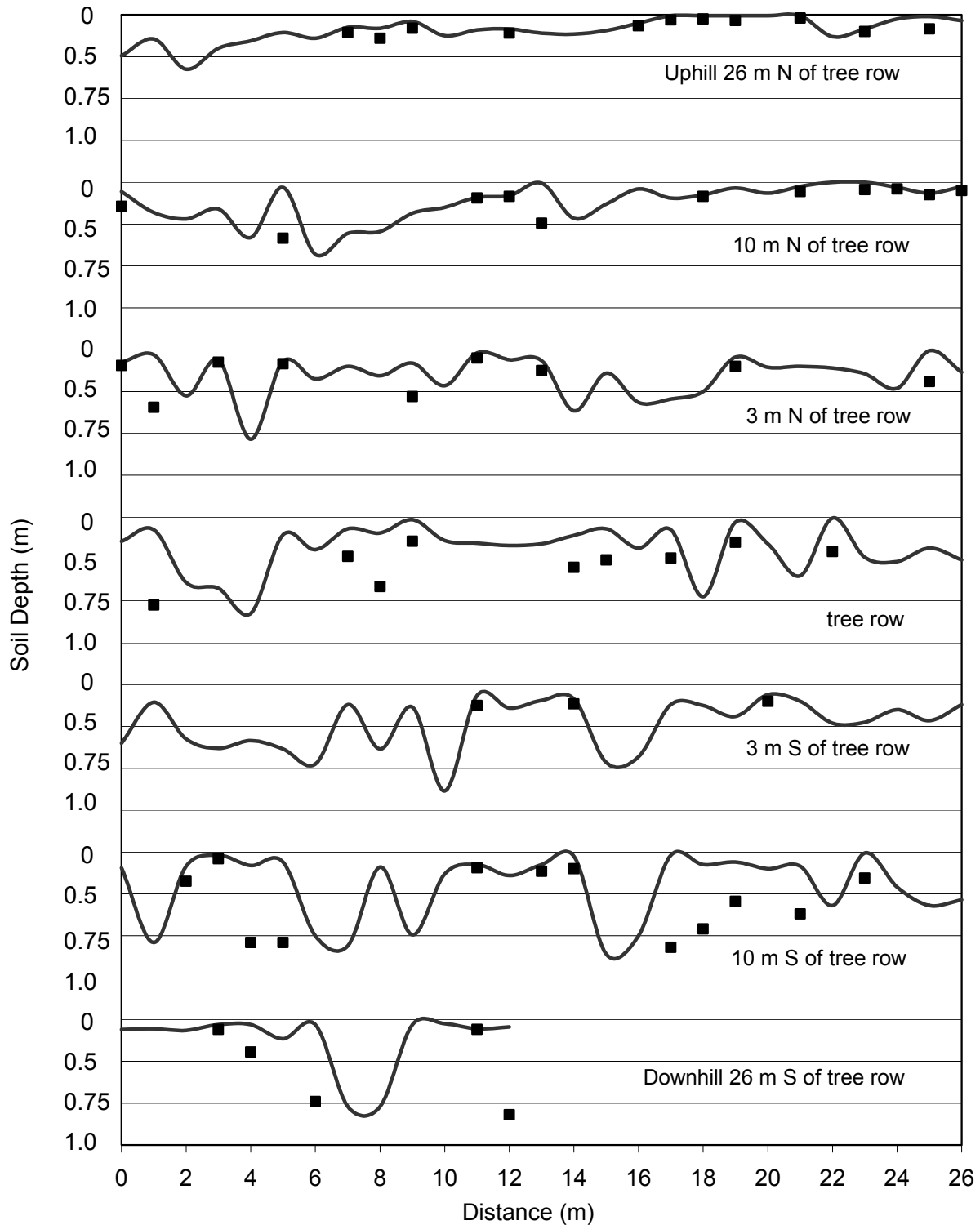


Figure 5.16. Downslope continuation of cutters is demonstrated by soil depths measured in parallel transects on the shoulder region of Hillslope H. Black squares indicate supplemental depth measurements taken where initial readings were less than approximately 15 cm deep, and indicate the presence of stones or fractures.

Observations of bedrock depths along linear depressions in the slopes indicate that the differences between cutters and conduits in the upland slopes may be fuzzy. Shallow fractures oriented with the hydraulic gradient permit vertical entry through only a few rock layers before water is forced to move across horizontal bedding planes. Above such a horizontal conduit, the rock appears to decompose into blocks as water is pulled down into the conduit along overlying fractures. Continued solution and sediment loss eventually creates a linear depression in the overlying slope, and pits, pinnacles, and cutters thus develop along the course of upland conduits. Soil depths measured in the thalweg of the linear depression draining the bottom of Hillslope A are very variable, ranging from zero to well over a meter in isolated spots. Observations of grassed slopes outside of the main study following winter burns reveal that bedrock exposure from surface erosion in linear depressions is typically short and discontinuous, ending in loss of flow through swallets (Figure 5.17).

At the same time, interconnected pits and shallow cutters with no underlying conduit systems are likely to aid in conduit development by concentrating flow at vertically weakened points in the bedrock. Mature cutter/epikarst conduit pathways that reach 2 m or more in depth as they cross the forest/grass boundary are most often roofed solely by clay mantles, even though rock clearly forms at least part of their cover higher on the slopes. This suggests that the combination of converging flow and dissolution may create the emergent soil-covered cutters through processes that integrate shallow conduit and interconnected cutter forms in the study area.



Figure 5.17(a). Outcrops and swallets in the depression of a slope managed by fire demonstrate the interruption of lateral flow by vertical penetration. In figure (a) the uphill slope is noneroded, with increasing surface flow collection just uphill from the outcrop.

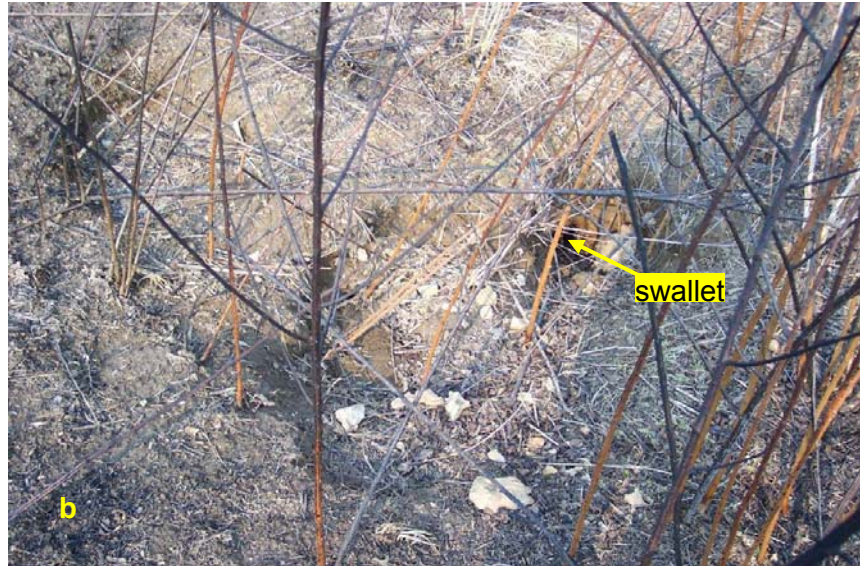


Figure 5.17(b). Directly below the outcrop show in figure 5.17a, water enters a swallet. Photos by author, February 2005.

#### *Limestone Fragment Release*

As the bedrock is decomposed along cutters and conduits, limestone fragments and coarse-grained insolubles are left at least temporarily as residuum. A similar process seems to operate across the hillslopes in general, in which solutational activity at the top of the bedrock bypasses less permeable rock layers and leaves remnant lines of limestone fragments in the regolith. Stone layers in transects that parallel slope contours, as indicated by noticeable accumulations of large fragments, typically remain consistent for an elevation but may differ from the depths of stone layers found immediately higher and lower on the slope, where rock layers have different compositions. Horizontal stone layer continuity is shown in figure 5.18, measured on Hillslope J on the north side of the bend. In this transect, which parallels the contours 20 m below the crest of the hill, most probe attempts hit stone fragments that appear to align in several layers above bedrock.

Tabular limestone pieces from channer (2-150 mm) to boulder (>600 mm) size were found in varying amounts in soil pits throughout the profiles. Whereas some of these pieces were continuous with intact limestone bedrock, many “floaters” in the soil matrix, disconnected from other stones. In some pits, these “floaters” were common in the A and AB or upper B horizons, but were absent or present in lesser amounts in lower horizons. The similarity of composition, thickness, and horizontal alignment between these free-floating rock slabs and stones at the edge of the inclined bedrock surface suggest that the floaters result from *in situ*

weathering and release rather than colluvial movement. Solution does not always attack the surface of the epikarst from the top down, and instead may bypass sections of the rock mass that are then incorporated into the regolith.

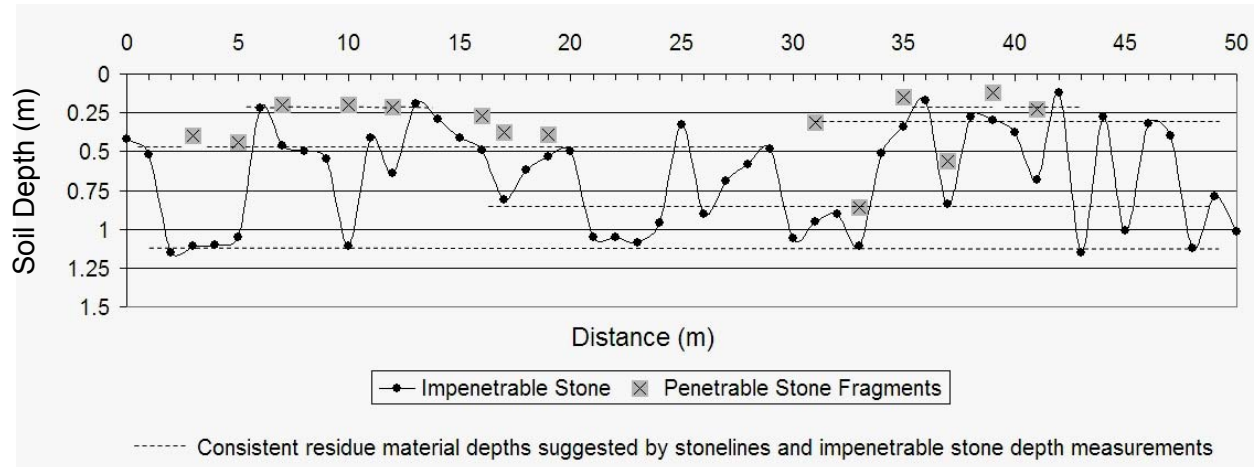


Figure 5.18. Rock fragment lines in soil depth transects on hillslope J are revealed in a transect taken 20 m below the crest of the hill. Readings at approximately 1.15 m depth likely represent bedrock. It can not be determined by probing if impenetrable stone readings above this level are associated with free-floating limestone flagstones or with pinnacle surfaces. Locations shown by “X” indicate spots where the probe hit multiple rock fragments that were not consolidated or large enough to stop deeper penetration.

### *Forest Gullies*

In the forest, interconnected cutters frequently appear as vegetated gullies 0.5 to >2 meters deep that display occasional bedrock steps and outcrops. Soils in these gullies are thin, (5 to 40 cm), but bedrock expanses are only open where erosion is currently active. Whereas karst underdrainage of some of these forest gullies is not obvious, conditions in other linear depressions point to the presence of subcutaneous pathways. In figure 5.19, a broad, shallow sink near the crest of an escarpment slope sits directly uphill from a vegetated gully. The outer rim of the sink rises above the gully head and is not connected to it, indicating, along with the gully’s non-scoured conditions, that flow from the sink follows a subsurface pathway that probably at least partly underlies the gully. Short parts of the forest gully systems likely carry surface flow at certain times, but the occurrence of gully surface flow is probably limited to high intensity storm events and was not observed during this study.



Figure 5.19. Forest gully. In the vicinity of Hillslope D (Figure 4.1), a broad, shallow sink on the crest of the hill (a) lies directly above the start point for an unscoured forest gully. (b) No channel connects the bowl to the gully, indicating that water passes under the gully through the epikarst. Backpack in (a) shows scale. Photos by author, February 2005.



Gullies associated with cutters may also be buried by soil where sediment delivery is sustained at a higher rate than transport. Erosion has exhumed soil mantled cutters in the forest near the grass/forest boundary line that are as much as 3 m deep in one location. Flat bedrock base expanses in these scoured gullies are typically unbroken by pinnacle forms, showing an advanced stage of solutional development. The current scour suggests that soil movements through the cutters has been at least partially transport-limited in the past. In contrast to the gullies seen in the forest, interconnected cutters found on grassed slopes are usually buried. In Figure 5.20, a 70 cm deep forest gully containing 45 cm of soil at its base exits the wooded patch and enters a grassed field, where the depression disappears as soil fill creates a level ground surface over the 117 cm deep cutter at its forest exit point. Any sediment that does move through this gully system is captured by the grass root mat, which consolidates the fine-grained materials and makes the channel invisible from the surface.



Figure 5.20. Gully buried by soil under grass. Vegetated open gully in a forest patch is buried by soil once it enters the grass field, demonstrating the ability of the grass root mat to capture and consolidate fines. Photo by author, February 2005.

Observation of conduit and cutter forms on Bowman's Bend indicates that the effect of vegetation on epikarstal geomorphology is likely highly significant. In a system in which small

scale cutter depressions at the bedrock surface may coalesce with neighboring cutters and interact with conduit development within the epikarst, vegetation plays a key role in mediating local water and sediment movements. Where cutters interconnect to channel flow at the top of the bedrock, grass roots are capable of holding soil. Under circumstances in which flow contained in deeper conduits induces drawdown between overlying fractures, grass again appears able to hold fines in all but the most concentrated vertical pathways. In the forest, the larger, deeper, and less surficially-coherent root systems are less able to trap surface fines when subcutaneous pathways are overwhelmed. Trees also likely root within subcutaneous pathways, making it likely that fine sediments are carried downward through preferential root flow. It would be expected that interconnected cutters or areas overlying conduits on steep forest slopes would eventually be opened if they lay in positions of concentrated local drainage, but that vegetation would become established between the infrequent events large enough to generate surface flow. This suggests that the current pattern of gully erosion at the grass/forest boundary, accompanied as it is by shallow incisions in sensitive grassed concavities, is an amplification of a pre-existing system of sediment deposition and movement.

Pinnacle and cutter development takes place on the bedrock surface of all geologic units on Bowman's Bend. The forest gullies described here exist on the slopes of both the Lexington Limestones and the upper Tyrone, indicating an overall similarity in solutional processes that operates despite large differences in rock composition. Not all cutters appear to be interconnected, and it is not clear if developed interconnected cutters have true subcutaneous drainage in the bedrock below them. True epikarstal drainage does occur within the bedrock of all geologic units, and the distinguishing factors between its development in the Lexington Limestones and the High Bridge Group seem to be those of depth and protected growth. Interconnected cutters, open forest gullies, and epikarstal conduits are thus a single related class of weathering features created on the steep escarpment slopes in response to a spectrum of vegetative, geologic, and topographic influences. Hydrologic changes on upland slopes may initiate somewhat different responses in these features, depending on local factors, but it should affect them all.

### **Slope Profiles**

Both pit observations and measurements of soil depth show that the wide compositional variation in the stratigraphy of the study area results in formation of bedrock benches that are typically poorly determined from the surface. These hidden benches are apparent in figure 5.21. Comparison of profile locations with topographic contours suggests that hidden benches

are present at numerous locations of resistant strata contained within all of the geologic units. Approximate elevations for the contacts were selected based on isopach map values given by Grossnickle (1985), which suggest that the Logana is about 4.6 m (15 ft) thick and that the Curdsville is about 6.1 m (20 ft) thick in this region of Bowman's Bend. These elevations were calculated on the profiles based on the mapped Tyrone upper boundary.

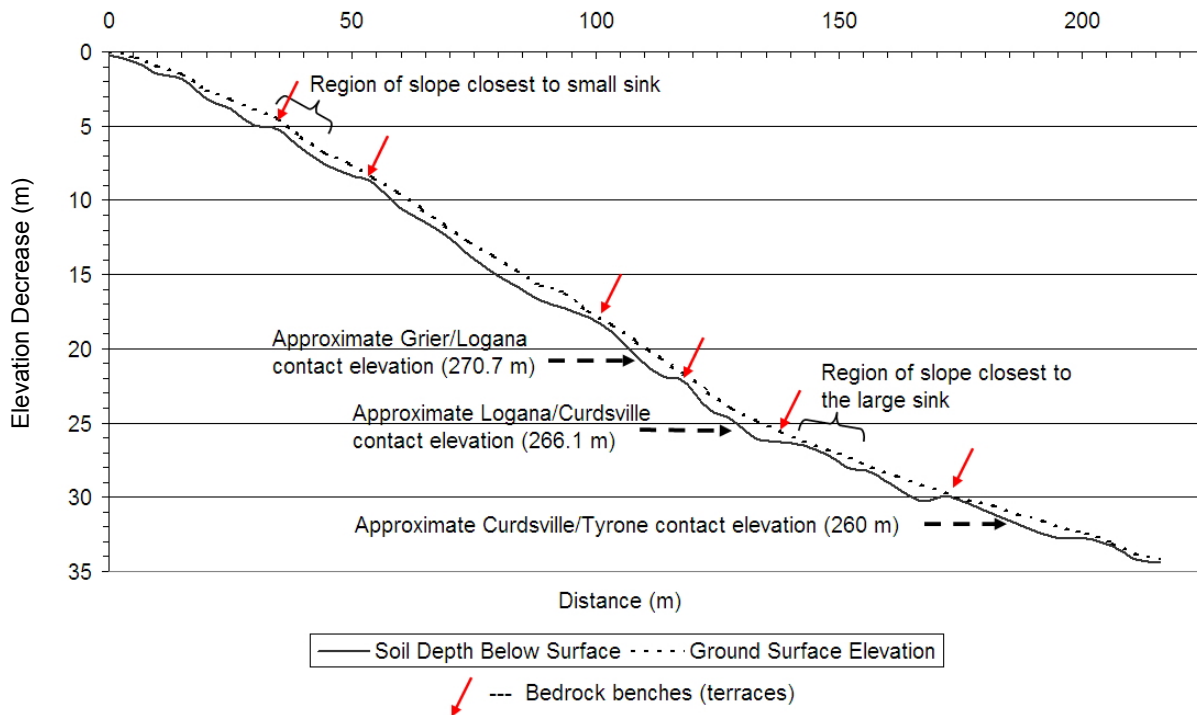


Figure 5.21. Hillslope A soil depth and ground surface profile shows the location of major soil-covered bedrock benches, as well as locations of soil loss related to epikarstal drainage. Measurements were taken at 5 m intervals by probe. Surface elevation was determined by laser level.

The most visible bench in the study area is the terrace created at the top of the Tyrone where the 'Pencil Cave' bentonite seals the underlying limestones, underlies alluvial sediments, and is likely the main factor responsible for the convex-concave profiles of the grassed portions of the slopes. Following large storm events, water pools along the lower end of this terrace at the base of many grassed slopes on the east side of Bowman's Bend (figure 5.22). Soil sampling by auger indicates that perching of slope drainage takes place where it is held above intact bentonite at the point where river sediments tend to pinch out downhill. Perching is greatly reduced or eliminated on grassed slopes where epikarst drainage exits, such as at the base of Hillslope A. Soil buildup in limestone terrains may be limited where constant

subsurface loss of sediments takes place through bedrock openings. Soil loss related to epikarstal sediment movement can be seen in the bench at the base of Hillslope A. Here the soils neighboring the conduit are greatly reduced in depth (<40 cm total soil depth in samples A17 and A18 at the base of Hillslope A) compared to those in other portions of the slope base (150 cm soil depth in pits 1-4). The locations of the two visible sinks on Hillslope A, and in particular the lower sink, correspond to areas of thinner soils. Because of the shallow epikarstal drainage on the upland slopes, percolation and return flow shift back and forth between the landscape compartments of regolith and near-surface bedrock. Where soil truncation is evident, consideration must be given to the sediment transport capabilities of both the regolith and the epikarst.



Figure 5.22. Water pools at the grassed base of Hillslope I following large precipitation events. Photo by author, April 2005.

## **Geology Summary**

Lithological and structural characteristics of the lower Lexington Limestones and the High Bridge Group control karst and soil development through soluble and impervious layer compositions, thicknesses, and fracture patterns. In both formations, two main sets of fractures operate, one paralleling the river and the other operating perpendicular to it. On the east side of the bend, the hydraulic gradient is oriented close to the secondary fracture orientation, but shallow, curving joints and multiple impervious layers limit upland karst development.

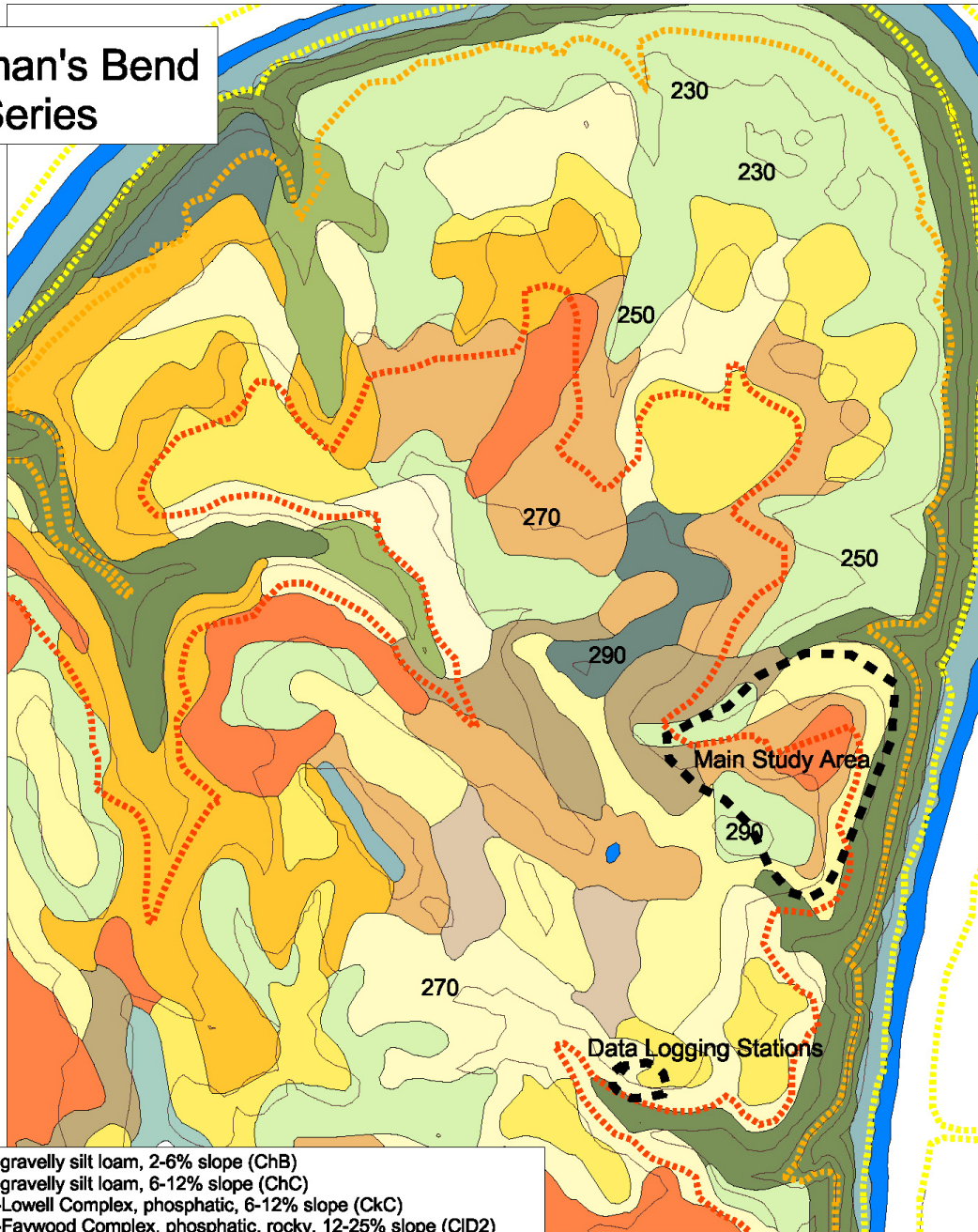
The largest effect of impervious layering occurs near the top of the Tyrone unit of the High Bridge Group where bentonite perches flow at the bases of some grassed slopes. In the upland slopes, impervious shale beds of the Lexington Limestones create an epikarst zone in which surface and subsurface pathways are highly interactive. As solution follows shallow fractures and weakened zones, karren forms develop that tend to concentrate drainage. Cutters may eventually interconnect, collecting flow that may drop into shallow epikarst conduits in the bedrock. As dissolution takes place at the edge of the epikarst, benches form in the hillslopes and resistant limestone pieces may be left floating in the regolith, disconnected from the main bedrock mass.

Where flow passes through conduits, the overlying rocks may be broken into blocks separated by pathways of vertical drawdown. Linear depressions overlying conduits are characterized by alternating near-surface rocks and pockets of relatively deep soil. The cutters that enter the forests at hillslope bases are typically mantled only by soil, and in the escarpment forests these take the form of thin-soiled, non-scoured gullies. Because the same processes govern interconnected cutters, forest gullies, and epikarstal conduits on the upland slopes, changes in slope hydraulics should have some effect on all of these landforms.

## **SOIL CHARACTERISTICS**

To determine what changes in hydrology may be related to changes in soil properties, it is important to understand both current and historical influences on soil development. The bend has a wide variation in soils ranging from deep floodplain alluvium to thin escarpment residuum (Figures 5.23 and 5.24). The down-cutting action of the river, coupled with karst solution, has also created a wide array of closed depressions, surface channels and subsurface pathways that dissect the landscape and cause topographic variation at a wide range of scales. Vegetation effects operate across these geologic, palaeohistorical, and topographic influences, so that not all locations respond in the same way to deforestation.

# Bowman's Bend Soil Series



|  |  |
|--|--|
|  | Chenault gravelly silt loam, 2-6% slope (ChB)                          |
|  | Chenault gravelly silt loam, 6-12% slope (ChC)                         |
|  | Chenault-Lowell Complex, phosphatic, 6-12% slope (CkC)                 |
|  | Chenault-Faywood Complex, phosphatic, rocky, 12-25% slope (CID2)       |
|  | Fairmount silty clay loam, very rocky, 6-12% slope (FaC2)              |
|  | Fairmount-Faywood-Rock outcrop Complex, 25-59% slope (FdF2)            |
|  | Faywood-Cynthiana Complex, very rocky, 12-25% slope (FeD2)             |
|  | Faywood-Fairmount Complex, phosphatic, rocky, 6-12% slope (FfC2)       |
|  | Faywood-Fairmount Complex, phosphatic, very rocky, 12-25% slope (FfD2) |
|  | Lowell silt loam, phosphatic, 6-12% slope, eroded (LsC2)               |
|  | Lowell-Faywood Complex, pphosphatic, rocky, 12-25% slope (LtD2)        |
|  | Nolin silt loam, frequently flooded (No)                               |
|  | Rock outcrop-Fairmount Complex, 50-120% slope (RoF)                    |
|  | Sandview silt loam, phosphatic, 2-6% slope (SdB)                       |
|  | Sandview silt loam, phosphatic, 6-12% slope (SdC)                      |
|  | Water (W)  |

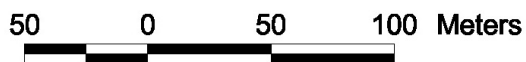
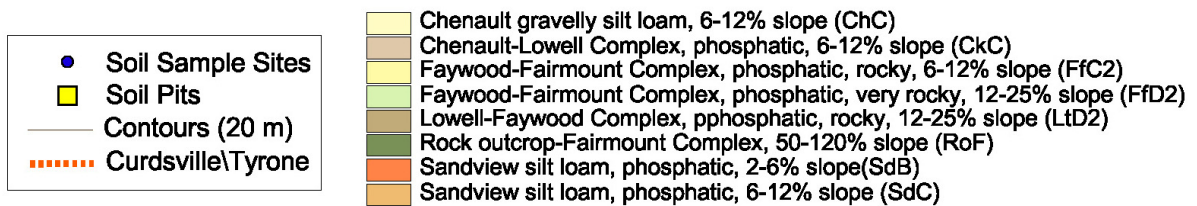
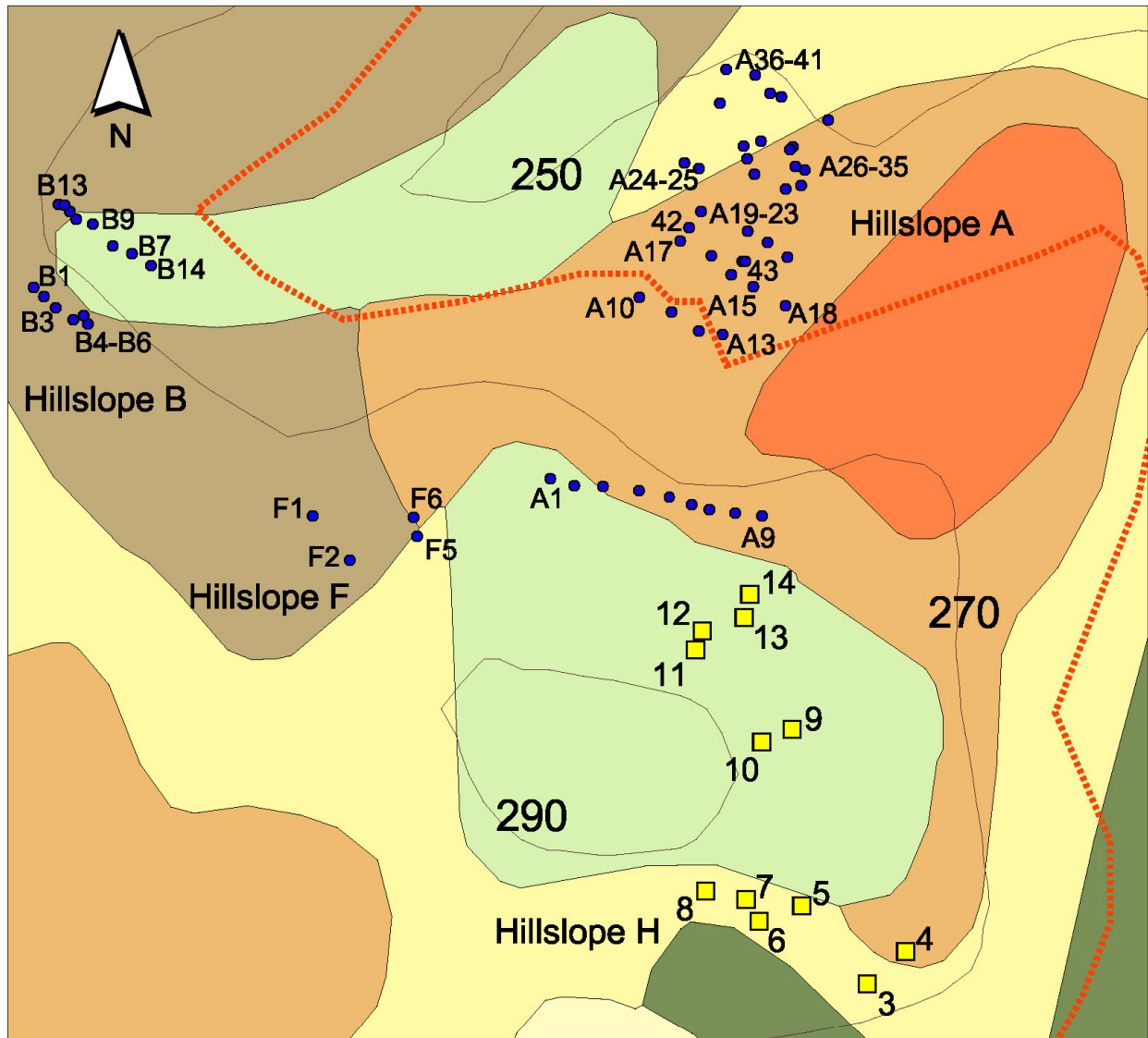
200 0 200 400 Meters



- Contours (20 m)
- Curdsville/Tyrone boundary line
- Curdsville\Tyrone
- Oregon\Camp Nelson
- Camp Nelson\Alluvium

*NRCS USDA SSURGO Data,  
Garrard and Lincoln Co., Ky. 2001*

Figure 5.23. Soil series mapped on Bowman's Bend.



SSURGO 2001 data for  
Garrard and Lincoln Co., Ky.

Figure 5.24. Main study area soil units, with locations of soil pits and soil sample sites overlain.

## Parent Material

Although the underlying bedrock is similar at any given elevation, soil parent material on the bend derives from three different sources: limestone residuum, alluvium, and aeolian deposits. Evidence from soil sampling and from soil survey maps indicates that residuum, alluvium, and loess are all important in soil composition and have become integrated through bioturbation, leaching, and colluvial processes.

### *Residuum*

In limestone terrains, carbonate solution of the bedrock releases insoluble impurities that form the mineral constituents of soils (Gagarina, 1968; Prawito, 1996). These mineral constituents are largely residual, as opposed to breakdown products, and mainly consist of silica and  $\text{Al}_2\text{O}_3$  and  $\text{Fe}_2\text{O}_3$  as clay minerals or hydrated oxides (White, 1988). Silica is preferentially leached from carbonate rock insoluble fractions and iron is dehydrated, leading to the development of deep red “terra rossa” soils in warm humid terrains (White, 1988). In areas of somewhat cooler soil temperatures, iron remains hydrated and silicas and clays are retained, resulting in soils with brown coloration. The great majority of soil layers identified in the study area had Munsell colors in the 10YR hue in chroma categories of browns, yellowish browns, or grayish browns, indicating retention of silicas and layer silicate minerals.

Soils in the study area also commonly contain a high number of tabular limestone fragments weathered *in situ* from adjacent bedrock ledges. These limestone flagstones or plates give most profiles a stony, or flaggy character and often form an unconsolidated stone layer directly above bedrock. Fragments in limestone soils have been found to offer a buffering effect by releasing calcium to percolating waters (Atkinson and Smith, 1976), so that bedrock solution rates may be lower where fragments occur. Depending on aggressiveness of the meteoric water and the solution potential contributed by soil carbon dioxide and organic acid content (Trudgill, 1976a), bedrock solution is likely to be influenced by the local presence of calcareous materials in the study area soils.

Soil series represented in the study area have pH values that may range from 4.5 to 8.4 in varying soil horizons (Official Soil Series Descriptions, 2005). Although pH was not tested systematically during this project, samples taken from pits 1 and 2 were measured for pH values using an Oakton Acorn® meter and a 1:1 mixture of air-dried soil and water. Results shown in table 5.1 indicate that in these sites at the slope base, which had little to no limestone in the profiles, pH remains well within the range at which solution may take place. Agreement between observed soil characteristics and most of the mapped SSURGO soil series



classifications (table 5.2) suggests that the soil reaction ranges described for the various series should apply in the study area. Thinner limestone residuum soils such as the Fairmount likely maintain neutral to alkaline pH, whereas deeper soils may tend to have acidic surface horizons that become increasingly neutralized in proximity to bedrock. In middle horizons, a range of reaction potentials are likely created dependent on local accumulations of limestone fragments in the soil. In all series, solution is likely to take place at all soil levels under some circumstances.

Table 5.1  
pH Values for Infiltration Pits 1 and 2

| Site         | Sample Depth (cm) | pH   |
|--------------|-------------------|------|
| #1<br>Forest | < 10              | 5.62 |
|              | 25                | 5.58 |
|              | 55                | 5.72 |
|              | 85                | 5.09 |
|              | 125               | 5.93 |
| #2<br>Grass  | < 10              | 5.37 |
|              | 25                | 5.08 |
|              | 55                | 4.97 |
|              | 85                | 5.26 |
|              | 125               | 5.49 |

The Curdsville, Logana, and Grier members of the lower Lexington Limestones contain varying amounts of impurities as shale partings or as clay mineral constituents of argillaceous limestones containing 50-90% carbonates (Elvrum, 1994). Soil profiles that develop on limestones rich in lenses or interbeds of shale have been found to provide enough mineral residue to create soil profiles that take on horizonation characteristics of their climate zone (Prawito, 1996). In the massive, largely pure limestone beds of the Tyrone formation, impurities are mostly found in the often very thin interbeds between layers, resulting in a smaller volume of residual material for soil development and limited horizon differentiation.

Table 5.2  
SSURGO Soil Series Properties

| Soil Name and Map Symbol | Depth (cm) | Clay pct | USDA Texture          | Fraggs pct 8-25cm | Moist bulk density | Organic matter pct | Soil reaction pH | Saturated hydr cond (cm/hr) |
|--------------------------|------------|----------|-----------------------|-------------------|--------------------|--------------------|------------------|-----------------------------|
| Sandview (SdB, SdC)      | 0-25       | 10-27    | SIL                   | 0                 | 1.30-1.40          | 1.0-4.0            | 4.5-6.0          | 1.523-5.080                 |
|                          | 25-97      | 18-40    | SICL, SIL             | 0                 | 1.30-1.45          | 0.5-1.5            | 4.5-7.3          | 0.504-1.523                 |
|                          | 97-188     | 40-65    | C, SIC                | 0-10              | 1.35-1.60          | 0.5-1.5            | 5.1-7.8          | 0.151-1.523                 |
| Chenault (Chc)           | 0-18       | 10-27    | GR-SIL                | 0-5               | 1.20-1.40          | 1.0-4.0            | 5.1-7.3          | 5.080-15.24                 |
|                          | 18-122     | 18-35    | CL, GR-SICL, SICL     | 0-5               | 1.20-1.50          | 0.3-0.8            | 5.1-7.3          | 1.523-5.080                 |
|                          | 122-147    | 40-55    | C, GR-C, GR-SIC, SIC  | 0                 | 1.30-1.60          | 0.0-0.8            | 5.6-7.3          | 0.504-1.44                  |
|                          | 147-152    | -        | UWB                   | -                 | -                  | -                  | -                | 0.00-0.151                  |
| Lowell (LtD2)            | 0-15       | 12-27    | SIL                   | 0                 | 1.20-1.40          | 1.0-4.0            | 4.5-6.5          | 1.523-5.080                 |
|                          | 15-107     | 35-60    | C, SIC, SICL          | 0                 | 1.30-1.60          | 0.0-0.8            | 4.5-6.5          | 0.508-5.080                 |
|                          | 107-132    | 40-60    | C, SIC                | 0-10              | 1.50-1.60          | 0.0-0.5            | 5.1-7.8          | 0.508-1.523                 |
|                          | 132-142    | -        | UWB                   | -                 | -                  | -                  | -                | 0.00-0.151                  |
| Fairmount (FfC2)         | 0-23       | 27-40    | SICL                  | 8-50              | 1.20-1.40          | 3.0-7.0            | 6.6-8.4          | 0.151-0.504                 |
|                          | 23-46      | 35-60    | FL-C, FL-SIC, FL-SICL | 8-50              | 1.40-1.60          | 1.0-3.0            | 6.6-8.4          | 0.151-0.504                 |
|                          | 46-56      | -        | UWB                   | -                 | -                  | -                  | -                | 0.00-0.151                  |
| Faywood (FfC2 )          | 0-15       | 27-40    | SICL                  | 0-15              | 1.30-1.40          | 1.0-4.0            | 5.1-7.8          | 0.151-0.504                 |
|                          | 15-76      | 35-60    | C, SIC, SICL          | 0-15              | 1.35-1.45          | 0.00-0.5           | 5.1-7.8          | 0.151-0.504                 |
|                          | 76-86      | -        | UWB                   | -                 | -                  | -                  | -                | 0.00-0.151                  |

USDA Texture code: C – clay; CL – clay loam; SIL – silt loam; SICL – silty clay loam; SIC – silty clay; GR – gravelly; FL – flaggy; UWB – unweathered bedrock. From NRCS USDA SSURGO Soil Survey Data for Garrard and Lincoln Counties, Kentucky, 2001.

Most of the interbeds in the Tyrone and many of those found in the members of the lower Lexington Limestones are composed of metabentonite (Conkin and Dasari, 1986). During the process of clay formation from bentonite ash devitrification, silica is released to surrounding limestone layers, so that silica replaces calcium carbonate volume for volume in zones above and below bentonites (Huff, 1963). Silica content grades out by about 6 cm on either side of the larger bentonite beds, with a somewhat greater content in the underlying limestones than those above (Huff, 1963). Clay and silica grains released from pyroclastic intercalated clayey shale and chert layers of the upper Tyrone and lower Lexington Limestone members thus form important residuum materials.

Compositional variation of limestone layers and interbeds has a direct influence on soil depth and development. Because the layers of limestone found on the bend vary greatly in thickness and composition, different residues are released at varying elevations on the slopes. Differences in residuum source material release are reflected in the demarcation of some of the soil units mapped on Bowman's Bend, where series such as the Faywood and Lowell are associated with shale interbeds and the Fairmount is more specifically related to interbedding of calcareous shales (Official Soil Series Descriptions, 2005). These and other soil series mapped on the bend also reflect the catenary mixing of minerals at different landscape positions caused by water and sediment movement (Prawito, 1996). Soil evolution proceeds within materials moved laterally downslope by surface wash, throughflow, and along the basal weathering surface (Johnson, 1994). Thus, although limestone residuum soil units may develop under the preponderant influence of one type of bedrock, all soil units are likely to be composed of a mixture of minerals from varying bedrock source layers.

### *Alluvium*

Because the Kentucky River historically occupied the upland area of the bend, alluvial deposits have been retained in the terrace rimming the escarpment and now form an important component of some soil units. Properties of soil sampled in the main study area indicate an alluvial origin for at least part of the material on the terrace occupied by the hill base. This interpretation is based on the presence in all lower and mid-slope soil samples of rounded pebbles, subrounded chert, and geodes that clearly did not derive from the underlying bedrock. These fluvial gravels are associated with heavy clays that contain prominent very fine to medium black concretions.

Clearest evidence of alluvial parent material source came from soil pits 3 and 4, cut into the terrace foot at the south end of the main study area. In pit 3 in the forest, rounded pebbles,

coarse chert pieces and geode cobbles 100 to 250 mm long formed distinct layers at 60 to 65 and 90 to 96 cm that were separated by gravelly clay. Similar rounded gravel/geode layers were found at 58 and 80 cm depths in pit 4, where clear coarsening upwards patterns were found between stone layers. Fine, rounded fluvial pebbles were commonly found in small numbers in soil samples taken in upper horizons of all pits. However, higher elevation pits did not have the subsoil layers of yellowish, heavy clay intermixed with varying amounts of larger fluvial gravel that were found on Hillslope C and in pits 3 to 6 in the forest and in pits 9 and 14 in the grass. The spatial distribution of these gravelly clays, which disappears upslope abruptly at approximately 283 m elevation, their occurrence in subsoils that cross a range of underlying lithologies, and their strong association with fluvially-rounded gravel and geodes, suggest an alluvial source for the material.

The original alluvium has been modified through deposition of colluvium and mixing and translocation of layer materials. This creates abrupt boundaries between mixed-material surface horizons and alluvial subsoils in sampled soil profiles and pits from lower regions of the slopes. In pit 5 in the forest, the AB horizon has a dip identical to that of a similarly-shaped cutter uncovered in the bedrock directly below the solum (see Appendix 3, Infiltration Pit 5). The dip places an organically-enriched AB silty clay loam soil side-by-side at 25 cm with a yellowish brown clay containing alluvial pebbles. The abrupt occurrence of yellow clay at the irregular boundary at 25 cm suggests that vertical flow impedance at the epikarst surface throughout most of the pit has slowed the pedogenic development of the subsoil, allowing characteristics of the original alluvium to be retained.

In a similar manner, augered soil samples suggest that clay materials derived from alluvium may be retained in epikarstal pockets or in discrete deposits in areas lying below the elevation of the terrace created by historical river flow at the top of the Tyrone. These clays may have subsided into pockets as dissolution attacked the bedrock following the river's drop along the slip-off face of the escarpment. On Hillslope B, an abrupt increase in clay content is found in lower horizons in some of the deeper soil samples (Figure 5.25). At sites B1, B5, B6, B13, and B14, the sharp rise in clay percentage is accompanied by the presence of a dense yellow soil (10YR, values 6 or 7 and chromas 4 to 8) at 45 to 75 cm depth that forms a distinct boundary with the darker 10YR soils above it. Similar abrupt increases in clay are found in some soils from Tyrone locations sited well below the "Pencil Cave" bentonite layer, where a residual source for such clay-rich material is unlikely.

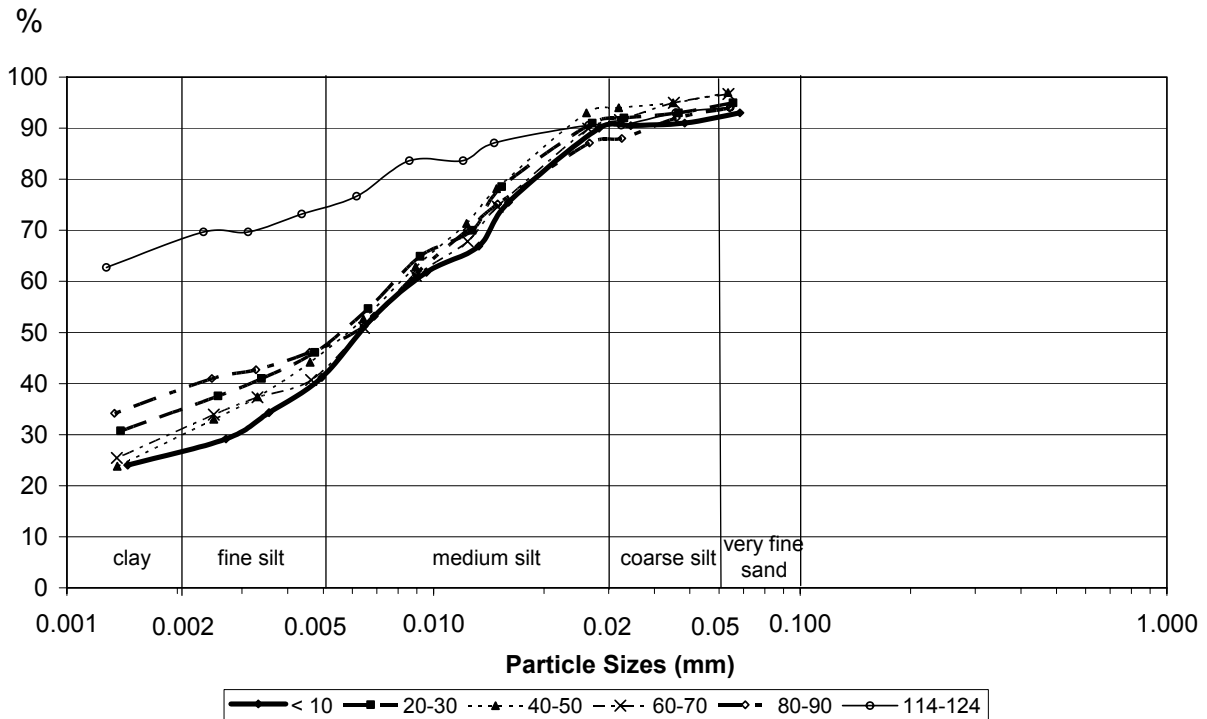


Figure 5.25. Particle size distributions determined by layers for location B5. Note the large increase in clay content at the 114-124 cm layer at the bedrock surface.

### Loess

The surface textures of all soils on the bend are silt loams or silty clay loams. Particle size analysis shows that the thin soils overlying the Tyrone typically retain a silty texture to bedrock, whereas all lower Lexington Limestone pedons, except those found in association with drainage pathways, have argillic subsoil horizons (Appendix 4, Particle Size Percentages and Texture Classes). An important source of parent material for the silts found in these soils may be loess.

Incorporation of a loess mantle is noted for some geographical settings for the Lowell series, which has a type location a few kilometers from the study area in Jessamine County (Official Soil Series Descriptions, 2005). Because loess deposition thickness decreased with distance from its presumed glacial drift source, loess in soils beyond approximately 150 km east of the Ohio River is likely to be too thoroughly mixed with residuum to make it possible to distinguish parent material origins (Barnhisel et al., 1971). This mixing of loess into pre-existing soils makes it impossible to determine how much of the silt and clay was originally delivered as

dust, but the high silt content of some sites in the study area suggest that it may have been considerable.

### Topographic Effects on Soil Development

In the main study area, topography plays a key role by promoting water movement that thins soils via erosion at the shoulders of the hill and moves sediments through surface and subsurface pathways downslope to thicker deposits on the terraced slope foot. Soils on the summit, or crest, of the hill are deeper than those on the shoulder, as would be expected in hilly terrains where water flux and gravity provide the energy for most sediment translocations (Ruhe and Walker, 1968; Walker and Ruhe, 1968; Conacher and Dalrymple, 1977). Hillslope H forest and grass transects clearly show that soil depths in general increase from the thin soils on the shoulders to deeper soils at the hillslope base (Figure 5.26).

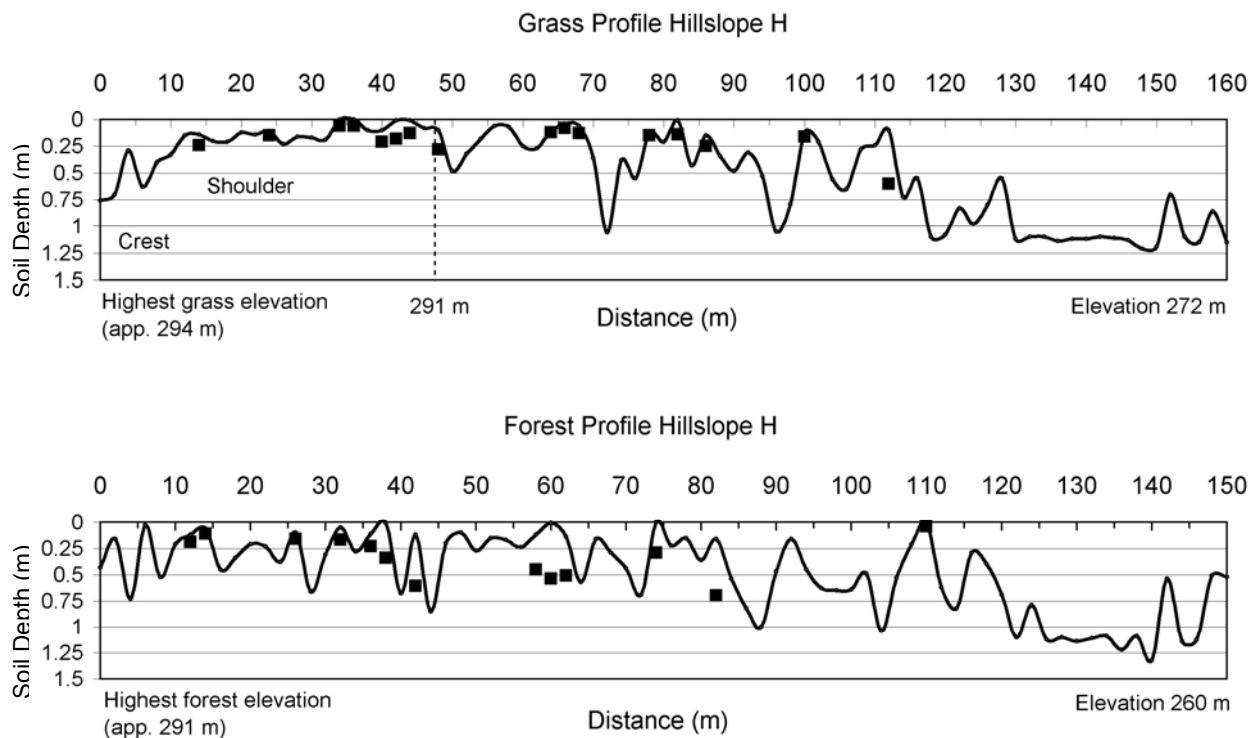


Figure 5.26. Profile transects on Hillslope H demonstrate the gradual increase in soil depth with drop in elevation. Measurements were taken at 2 meter intervals, and black squares indicate depths of supplemental readings.

The location of alluvial terraces below higher limestone slopes has encouraged pedogenesis within materials developed from limestone residuum overlaid and mixed with the alluvium, and the Chenault soil series found on the bend typifies this source pattern (Official Soil Series Descriptions, 2005). The lateral merger of residuum and alluvium between upland hill crests and downhill terrace locations is inverted at the outer edges of the terrace where the downslope gradient becomes increasingly steeper. Here the alluvial deposits pinch out as they merge with the thin High Bridge Group residua.

Soil development is simultaneously affected by karren development at the epikarst surface. Comparison of pit elevation to soil depth as determined by the irregular karren forms found in pits shows that depth does not increase consistently with decreasing elevation (Table 5.3). Within the broad scale hydrologic processes mediated by slope topography, pedogenesis is closely regulated by site specific conditions caused by karren development related to specific bedrock layer characteristics. This localized interplay between epikarst development, lithology, and topography is best shown by soil depths on Hillslope A, where an epikarst conduit crosses the Curdsville/Tyrone boundary beneath alluvial sediments. Soil depths are actually greatest at midslope and decrease across the foot of the slope because of soil loss into the conduit. Downslope within the forest, soil depth decreases farther because of the lack of insoluble minerals supplied by the Tyrone residuum source. At the same time, rock benches, pits, pinnacles, and impermeable layers within the bedrock surface throughout this extent of the slope create localized soil depths that may be at variance with the overall soil depth trends.

Table 5.3  
Minimum and Maximum Infiltration Pit Soil Depths According to Elevations

| Approximate Elevation (m) | Hillslope H |                 | Hillslope A |                 |
|---------------------------|-------------|-----------------|-------------|-----------------|
|                           | Pit #       | Soil Depth (cm) | Pit #       | Soil Depth (cm) |
| 288                       |             |                 | 10          | >80             |
| 287                       |             |                 | 11          | 55-110          |
| 286                       | 8           | 35-60           | 12          | 45->160         |
| 284                       | 7           | 15-50           | 13          | 40-82           |
| 283                       |             |                 | 9           | >135            |
| 281                       | 6           | 68-68           | 14          | 50-85           |
| 290                       | 5           | 45-80           |             |                 |
| 273                       | 3           | 133-145         |             |                 |
| 273                       | 4           | 90-138          |             |                 |

Any attempt to define a topographically-determined soil development pattern for the bend is complicated by several factors. First, covariations in lithology, elevation, and slope cause minerals of differing compositions and amounts to be transported varying distances from their original site of release. Alluvial deposits also confound attempts to identify toposequences, as does the fact that pre-existing sinks and karst features may have alluvial or aeolian sedimentary fills. Further complexity is added by the ongoing sediment loss to subsurface conduits. As a result of these factors, soil depths and horizon thicknesses and properties may have a wide range of variation even within a single lithologic unit.

### **Soil Texture Relationships**

Different soil textures will set up conditions for varying water pathways. In the study area, clay-rich soils tend to restrict vertical water movement, whereas layers containing gravel and sand may encourage movement in various directions. The clayey soil texture of the bend is also influenced by the epikarst topography, since fines are selectively removed from soils when water movement is high. To distinguish vegetation effects from water pathways set up by soil texture and bedrock topography, particle size patterns were compared to lithology, epikarst development, and parent material. Summaries of the most important patterns are given here.

#### *Relationship of Bedrock Drainage to Particle Size Distribution*

Clay content in the soils of the study area may rise to 70% or more in deeper layers or above bedrock in any kind of parent material (Appendix 4, Particle Size Percentages and Texture Classes). Seventy-six percent of sampled profiles showed a steady increase in clay content with depth, while another four percent showed no change in clay content between soil directly above bedrock and the overlying soil layer. The remaining 20% of sites displayed a decrease in clay content in the soil layer directly above bedrock as compared to the clay content of the layer overlying it. Comparisons of topographic forms on the bedrock surface to particle size distributions indicate that soil clay content, especially of the layer above bedrock, can be associated to local bedrock surface drainage conditions.

Clay distribution in lower horizons appears to rise highest where vertical water movement is locally impeded at the profile base, so that pits with highest base level clay contents were found where the bedrock, even if pitted or fractured, appeared laterally consolidated. This retention of residual fines and capture of clay from illuviation also evolves within the complex of other pedogenic factors operating in the landscape, as can be seen by examining pits 11 through 14, which were opened to bedrock.



Whereas pits 13 and 14 are underlain by consolidated limestone layers, both 11 and 12 contained solutionally rounded holes in their bases. In pit 13, clay content increased steadily to 79% at its 82 cm base. In pit 11, clay content remained constant at 67-68% between 55 and 110 cm at the base of the hole. In contrast, the hole in pit 12 was measured to >160 cm without determining bedrock contact, and clay percentages here decreased from 59% at 80 cm to 52% at 110 cm. Vertical particle size distributions within these three locations suggest that clay translocation is highly responsive to local epikarst drainage conditions.

In pit 14, a drop in clay percentage above bedrock occurred despite apparently consolidated bedrock. This pit has an alluvium source material as evidenced by rounded gravels present in its subsoils. A large increase in sand content from 11 to 22% between 25 and 55 cm, which is well above the 85 cm pit depth, suggests that sandy material may have an overriding influence on texture proportions. Bedrock drainage thus mediates vertical particle distributions within the texture properties determined by parent materials.

Soil samples from the mid-slope region of Hillslope A (A1 through A9) also demonstrate the effect of epikarst drainage on soil texture. In this area, several faint linear depressions with localized soil depths of 0 to >100 cm feed downhill into a large sink. Soils in these sites all increase in clay content with depth, but where the bedrock topography indicates that flow is likely to converge at the bedrock surface, clay content of the layer directly above the bedrock is lower than that of the overlying layers (Appendix 4, Particle Size Percentages). A correlation between epikarst surface drainage and either increase or decrease in clay content in the soil layer above bedrock can be made at eight of these nine sample sites. Bluish gray (Gley 2 5/1-6/1) soil was observed at the base of the A7 profile, lying closest to the main slope conduit, indicating frequent saturation. At A7, clay content also dropped from 71% at 60-67 cm depth to 65% at 120 cm (Figure 5.27). Together, the clay percentages and gley conditions suggest that epikarst topography encourages water collection at this site that periodically flushes the base of the profile during storm events.

Similar vertical particle distributions were found in samples taken in the linear depression leading from the large sink on Hillslope A. Sample A13 occupied a 118 cm deep soil-filled hole at the conduit center in which clay content at 60-70 cm was 30.5% but decreased above bedrock to 28.4%. This slight clay content decrease contrasts with the increase in clay content to bedrock seen at the shallower sites (A10 to A12) located on the slope perpendicular to A13. Clay percentages from samples taken in shallow conduit locations did not increase with depth, showing that clay does not concentrate in flow paths.

Most clay percentages in surface layers on Hillslope A were between 19 and 22%, and where shallow soil depths indicate that flow may be diverted laterally, as on channel banks, within linear depressions, or on high-energy surface slopes, clay content tends to remain in this range down to bedrock. Fines can even be preferentially removed from bentonite saprolite located in flow paths, as is shown by decrease in clay within the lowest soil layers at A30, which was sited in a cutter pathway. Movement of fines in general accompanies thinner soil profile development, so that clay buildup with depth typically accompanies soil depth increase. Thus the irregular nature of fractures, karren, and impeding layers in the bedrock become significant in soil formative processes as they capture or encourage removal of fine particles.

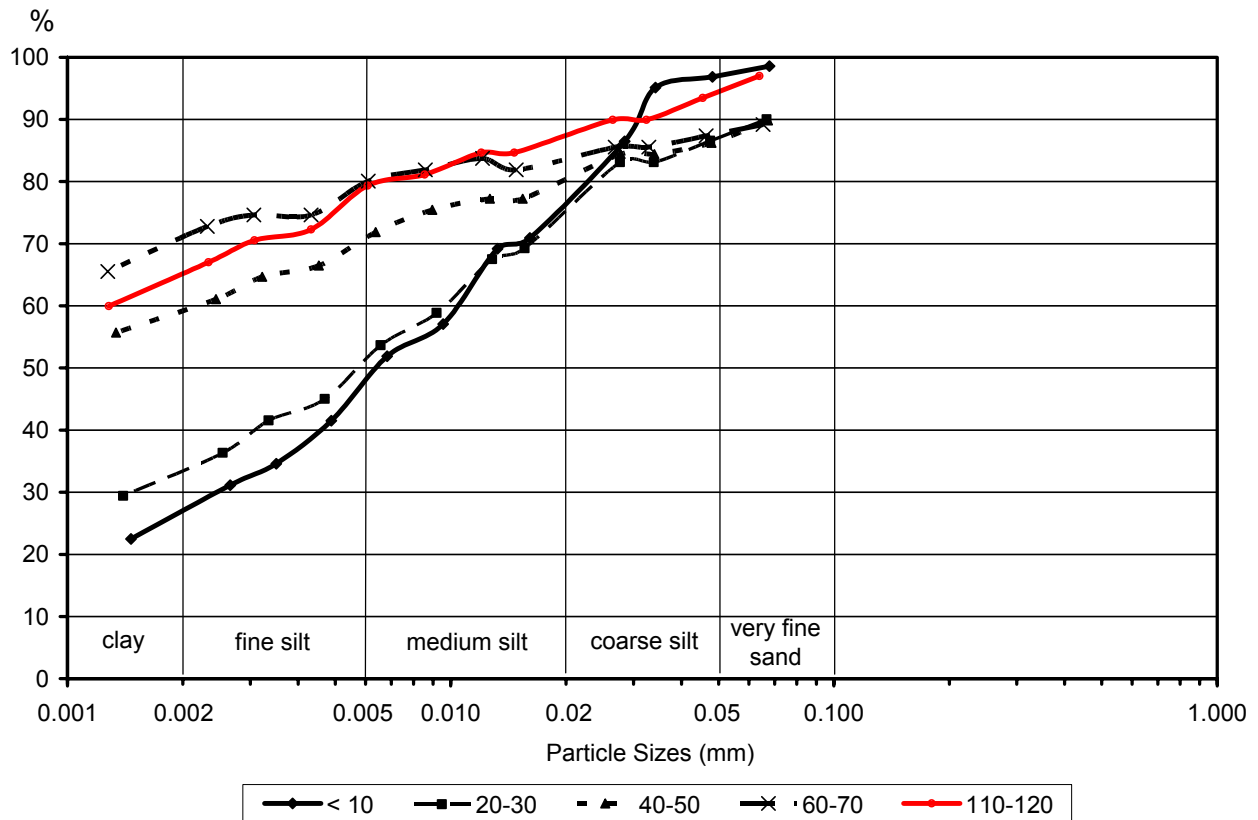


Figure 5.27. Particle size distributions for soil sample site A7, showing a clay percentage in soil above bedrock at 110-120 cm that is lower than the clay percent found at 60-70 cm depth.

### *Relationship of Texture to Source Materials and Surface Topography*

Because area soils have such high clay content, gravel or sand in significant amounts may open certain layers to vertical or lateral flow. Development of texture-contrast (coarse textures overlying finer layers) soils is characterized by polygenesis and multiple causality (Phillips, 2001b). In the main study area, the texture contrast may have several causes that operate simultaneously: 1) inherited differences related to aeolian or alluvial deposits 2) clay illuviation, 3) mixing with residuum weathered at the bedrock surface, 4) biomechanical processes, and 5) colluvial movement. Some of these factors can be associated with specific locations in the study area, allowing primary textural influences on matrix water movement to be identified.

Sand percentages at particular depths could be clearly related to source materials in some areas, as is best shown by soils overlying the Tyrone. Deeper soil samples at sites A30, A31, A33 and A21 were extracted from the extremely firm, greenish-gray saprolite formed in the 'Pencil Cave' metabentonite. At these four sites, sand content in the surface horizons ranged from 13 to >21% but fell to 3 to 6% in the saprolite horizons as clay content rose to between 72 and 84% (Appendix 4). Sites in the forest overlying the Tyrone but located uphill from sites which produced bentonite samples had sand contents from their residuum/alluvium sources that ranged from 10 to over 20% in all layers. In sites downhill from the area in which bentonite was found, sand in all layers remained below 11%. In the uphill forest locations closest to the grassed slopes, alluvium likely provides high sand amounts, but *in situ* weathering of limestones containing high amounts of chert from bentonite silica replacement may also release silica grains. This mixture of parent materials prevents any correlation of source to particle size in these locations. However, a better relationship of sand percentage to source is set up downhill, where low sand content would be expected from the low insoluble content of Tyrone bedrock not associated with bentonite. Between these two areas of the forest, vertical flow impedance is clearly created by the high clay content of the bentonite. Because of the lateral continuance of the bentonite layer under the terrace, vertical flow at the base of the grassed slope is most certainly impeded by the bentonite as well.

Most sites associated solely with lower Lexington residua (and possibly loess) showed a typical increase in clay content with depth. Although sand content remained low, lower Lexington sites displayed a particular pattern in which sand percentages at the surface and just above bedrock remained slightly higher than mid-profile percentages. The persistence of this profile pattern in sites over the Grier (pits 8 and 11 to 13, and Hillslope F samples F2, F5, and F6) can be seen by comparing particle sizes for sites F2 and F5, which were taken from forest

and grass locations matched for elevation (Figure 5.28). Part of the increase in sand content directly above bedrock may derive more from decomposing limestone fragments or limestone particles scraped off the bedrock surface during augering and incorporated into the samples, than with actual change in insoluble content at the epikarst surface. In many sites, decomposing flagstones form a BC layer typically 2 to 5 cm thick above the bedrock, which also likely contributes sand as well as gravel content.

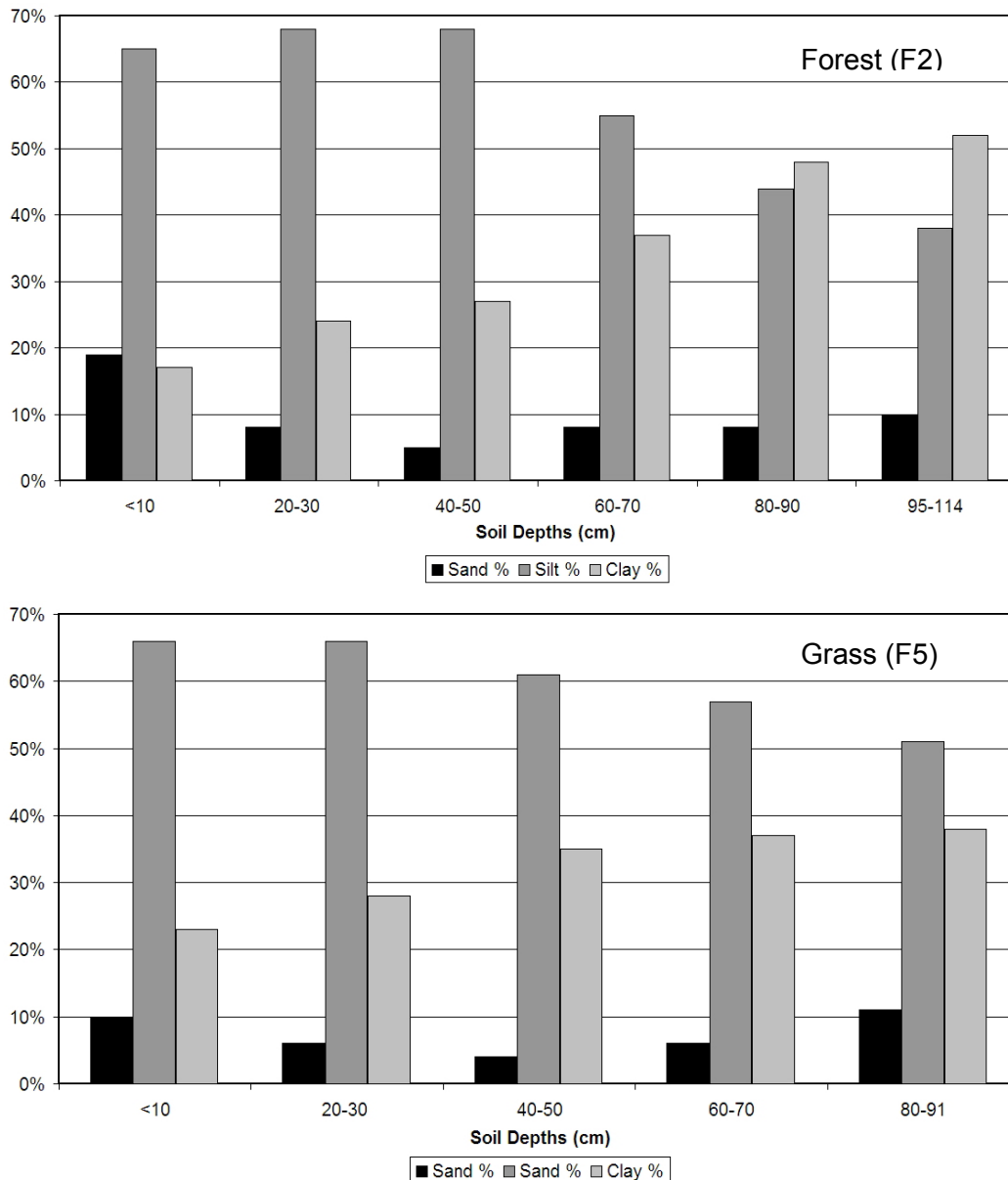


Figure 5.28. Particle size percentages on Hillslope F. Similar trends of lower sand percentages in mid-profile horizons are shown by forest (F2) and grass (F5) sites overlying the Grier member.

As a whole, the combination of Grier residuum and loess produces low sand, high clay content soils on the shoulders and crests of the study area slopes. Lower Lexington Limestones soils are very flaggy, and although water movement may be affected by high stone content, no textural differences exist in soil layers on the shoulder and mid-slopes that would deflect flow or stop percolation through the soil matrix. However, the high clay content of deeper soil layers is certainly likely to slow vertical penetration and perhaps encourage lateral flow above the most clay-rich layers. Where water reaches profile bases, gravel content in BC layers is likely to encourage movement at the bedrock surface.

In the mid and lower segments of the main study area slope where subsoil layers are associated with alluvium, sand contents range from 10 to 21%, and may go as high as 31% (see Appendix 4, Infiltration Test pit 9). However, samples taken from pits 1 through 6 and sites A1 through A9 on Hillslope A reveal that sand content just above bedrock in alluvial materials may decrease from levels found in overlying layers, in some cases to 7% or less (pits 3 to 6). High sand and gravel content may foster vertical water movement, whereas the related increase in clay above bedrock at these sites may restrict percolation, encouraging water to move laterally. This makes a consideration of alluvial deposit patterns important.

Sites where sand content is lowest just above bedrock in alluvial material are clustered at the same elevation on Hillslopes H and A in the main study area. Layers of geodes mixed with rounded pebbles and subangular chert create stonelines in pits 1 to 4. In pit 4, coarsening-upwards sequences were identified in gravelly clay layers between stonelines. These stone distributions preclude biomechanical construction because of their depths beginning at 50 to 55 cm below the ground surface, their stratigraphic layering, and their multiple inclusions of single layers of large (100 to 250 mm geodes) sandwiched between graded alluvial gravel sequences. In addition, the lack of decomposing limestone fragments in lowest horizons and above bedrock suggests that residuum input from dissolution at the bedrock is minimal. However, subsoil horizons in these locations do show considerable evidence for clay translocation, as displayed in clay films on peds (see Appendix 3, Soil Profile Descriptions). This makes it likely that the above-bedrock texture contrast, in which a low sand-content clay layer underlies sandy/gravelly clays, largely results from illuviation acting on deposits that were originally lower in sand or gravel content in comparison to higher soil layers. Regardless of source, the existence of sandy/gravelly soils over high clay content layers implies that vertical drainage should percolate freely between 50 and >100 cm depth, but be directed laterally at approximately 125 cm in the downhill main study area soils.

Farther up the slope, where alluvium is found in the subsoils of pits 5, 6, 9, and 14, sand percentages above bedrock are more variably distributed. This suggests that colluvial transport, clay production from within the soil profiles, and biomechanical mixing have likely played important roles in texture development of soils. Site specific influences thus make a large difference in the development of soil horizon properties in the study area, and seem to do so particularly where soils are shallower.

Overall, general patterns of water movement on the upland slopes of the main study area can be deduced from particle texture data. On shoulders and upper mid-slopes, low sand content and lack of contrasting soil layers should encourage slow vertical percolation of soil water that may be impeded by clay concentration at depth. Under high-intensity events, and particularly where soil moisture is already high, moisture is likely to be deflected sideways downslope if it is not pulled into solutional pathways. Once laterally moving water in the soil matrix reaches the downhill alluvium deposits, low sand-high clay content soils underlying sandy/gravelly layers are likely to encourage more lateral movement, creating prime conditions for saturation excess flow at the bottom of the main terrace.

### **Soil Series Mapping of Bowman's Bend**

Soil survey data provides a means of extrapolating sample data to the larger study area by identifying regions of common soil characteristics. Figures 5.23 and 5.24 show the distribution of mapped soil units for the entire bend and for the main study area. SSURGO mapping units each represent from 1 to 3 different soil types (Penn State Cooperative Extension, 2005), and many of the units mapped on the bend are complexes that contain two or more soils that cannot be separated within the limits of the mapping scale. Where single soil series are reported for a unit, they are consociations where 75% of the map unit is within the taxon range (Soil Survey Staff, 2005). Comparison of the characteristics of these mapped soil units to sampled profiles shows a reasonable approximation to site conditions.

The soils of Bowman's Bend are moist Alfisols displaying minimum horizon development (Soil Survey Staff, 2005). Within the upland, soil series attributes are largely a function of the near-escarpment topography and parent material, and because forests have typically been left in steep or dissected locations, mapped soil series to some degree coincide with current vegetation cover. Soils in the high-energy portions of the upland are typically well-drained and less than 1.5 m in depth, except where depressions have retained deposits. Dependent on parent material, many of the soil series display high concentrations of rounded gravel and/or tabular limestones. The large variance in soil depths and limestone fragment percentages

indicates that soil solutional aggressiveness is widely variable and may range from slightly alkaline to strongly acid in different layers (Soil Survey Staff, 2005).

The flattest, 2-6% slope portions of the bend are topped by the Chenault gravelly silt loam and the Sandview silt loam consociations, classed respectively as fine-loamy, and fine-silty, mixed, mesic Typic Hapludalfs. The official series description for Sandview, which appears as the dark orange section of the main study area in figure 5.24, shows it to be the deeper unit, at >152 cm (>60 in) as opposed to between 102 and 152 cm (40 and 60 in) for the Chenault (Table 5.2). However, the Chenault is described as being formed in old alluvium over limestone, whereas the Sandview does not have an alluvial source. Because alluvial sediments composed the subsoils of the main study area base, a Chenault gravelly silt loam series description appears to be a much better fit for the slope base than the Sandview. Interestingly, Chenault soils as described permit higher saturated hydraulic conductivity ranges (up to 5.08 cm/hr) in mid-profile layers and are a better match for the large  $K(-3)$  measurements (4.38 and 4.13 cm/hr) recorded for 85 cm in pit 4 than the moderate (up to 1.523 cm/hr)  $K_{sat}$  rates found in Sandview mid-profile layers (Table 5.2).

Various complexes of Faywood, Lowell, and Fairmount series comprise other soils sampled during this project. Sources for these three clay-rich series are residua of limestones interbedded with shales, although a loess mantle may be incorporated into some Lowell soils. All have highly variable soil depths that reflect the irregularity of the epikarst surface, and because of bench and karren development on the slopes, the three series intermix to a higher degree than indicated by mapping. The clayey, mixed, mesic Lithic Hapludoll Fairmount soils are shallowest, with depth to bedrock ranging from 25 to 51 cm. Steeper areas, as in the shoulder regions of the main study area, support shallow Fairmount soils distinguished by their high content of large limestone fragments and common association with rock outcrops. Lowell and Faywood soils are deeper. Lowell soils have more horizon development, lithochromatic (“rock-colored”) mottling, and will develop a distinctively colored BC horizon in comparison with the Faywood, in which BC horizons, if present, have color and texture the same as the overlying material. Such differences in BC horizons were detected in pits, where development of soils fitting these descriptions related to the bedrock composition and bench and karren forms particular to pit sites.

Sampling shows that mapped soil boundaries do not match current vegetation patterns in some areas, and that transition zones may be broad. Alluvial materials extend farther uphill than indicated by mapping, and series boundaries do not reflect the similarity of forest and grass soils found at the base of the Hillslope H. The transition of complexes on Hillslope B is also

broader and less related to current vegetation cover than indicated. However, difficulties in mapping heterogeneous soils are well acknowledged in soil studies, and although Chenault series descriptions appear to offer a better characterization of the central main study area soils than the Sandview, other mapped units seem to adequately correspond to field and test observations. The heterogeneous nature of slope conditions is usually well reflected by the range of properties attributed to the described soil complexes. Soil units as mapped provide a good baseline data source for broad scale profile characteristics in the main study area, suggesting that infiltration and texture test results can be considered as applicable across the general areas of these soil units.

### **Evidence of Water Movement**

Areas of soil profiles that retain high levels of moisture for long periods or that form portions of persistent preferential water movement pathways, will usually develop characteristic discolorations caused by organic or clay build-ups and/or redox concentrations (Brady and Weil, 1996). These discolorations, along with the mottling that occurs when alternating periods of oxidation and reduction affect mineral groups in a soil, are strong indicators of water flow patterns that affect particular areas of the soil profile. While mottling and grayish soil colors may in some cases be inherited from parent materials or represent historical weathering conditions (McRae, 1988), their occurrence within specific sites and the ability to compare numerous sites makes their use as drainage markers fairly reliable. In this project, soil discolorations, when taken in context with other soil horizon properties, offer a framework for evaluating the factors behind the infiltration rates found in varying pit layers.

#### *Gley*

Gleying, or grayish-blue soil discoloration (indicated by Munsell chroma <3) caused by anaerobic reduction of minerals constantly saturated by water, appears to be relatively rare in this study area and restricted to small-scale sites where flow at the soil/bedrock interface is centrally collected over impervious bedrock layers. Such sites are likely to occur only where shallow epikarst development concentrates water most of the year but does not encourage flow strong enough to move large portions of the clay, which would create the soil arches described by Cooley (2002). Gleying was found in only 2 locations in this project: at sample site A7 next to the conduit above the large sink area on Hillslope A, where heavy, wet, gray-blue soil was pulled up by auger from just above the bedrock, and at site F5, where thin gray-blue lines passed through the base of the profile. Relatively deep soil depths plus consistent low clay



content or drop in clay content above bedrock suggest that these sites both occupy locations that collect flow at the epikarst surface.

### *Clay Films and Root Channels*

Although gley is not common in the study area, discolorations associated with root zones and root channels were found in all pits. Root penetration adds organic material, acids, root exudates, and clay/organic matter binding agents to soil (Tindall et al., 1999), affecting porosity and giving upper soil layers a characteristic dark color. Root action and processes related to microbial decomposition together create soil structure, which in turn regulates percolation, so that ped faces become pathways for movement of water carrying clay and organic colloids (Rowell, 1994). Clay films on ped surfaces are commonly interpreted as indicating clay particle translation (Birkeland, 1984), and they are typically distinguishable from the surrounding matrix because of their darker coloration. Because of the scope of this project, no attempt was made to determine mineral origins of any of the discolorations identified in study area soils, and their presence or lack thereof are used as simple indicators for likely colloidal migration.

In both forest and grass soils, most boundaries between A and AB, or A and B horizons could be described as wavy and related to the varying depths of root networks. Below the topsoil, the amount and depth of discoloration associated with water movement along roots differed between forest and grass sites because of differences in root size, abundance, orientation, and depth of growth.

Grass topsoils contained such thick root growth that the top 10 cm of the soil consisted of a solid mat of roots so thoroughly interwoven that extraction of the roots from the aggregate mineral component was impossible. This mat contained the majority of grass roots, however, and below 30 cm, the vertical networks that contained fine roots decreased proportionate to depth. In B and Bt horizons, very fine roots entered pores in many peds, but the majority of grass roots typically occupied vertical macropores surrounding ped faces. Dark organic and clay films were thus commonly distributed in grass mid-profile horizons along channels where root networks descended into the soil matrix (Figure 5.29).

Dark clay/organic films decreased in depth in correspondence with decrease in root numbers. In grass pit 2, for example, films were found where fine roots remained common. Grass roots entered all peds at 55 cm, but were scarce by 110 cm and occurred only occasionally at 125 cm, so that below a meter, evidence for root channel clay translocation was limited. Although brown (10YR 4/2) films were common on ped faces at the 125 cm depth in pit 2, they did not associate with the vertical networks of root channels seen higher in the profile. In

grass pit 4, no grass roots were found at the 138 cm bedrock depth, and although pale brown (10YR 6/3) mottles at this depth indicated possible illuviation, these discolorations were also not associated with roots. Thus, although deepest grass pit layers hold signs of illuviated materials, fine particles are not likely carried directly to those layers by grass roots.



Figure 5.29. Dark organic stains distinguish vertical grass root pathways in pit 10. Photo by author, August 26, 2005.

Forest topsoils, although rich in organics, contained common fine roots distributed unevenly in discrete root systems that could be traced to individual vines, shrubs, or herbaceous plants. Topsoil roots supported coatings in pores and along aggregate faces that had very dark gray (10YR 3/1) to very dark grayish brown (10YR 3/2) coloration. Roots up to 2 cm in diameter also occurred in topsoil layers, but most large roots were found below 10 cm, where stains of the same colors as found in the topsoil were associated with soil directly surrounding individual roots of all sizes.

Dark discolorations also associated with root channels in forest subsoil horizons. Whereas discolorations surrounded the channeled networks of grass roots found along peds, root channel discolorations in B and Bt forest horizons were always found in the soil immediately surrounding individual roots. Because medium to very coarse tree roots typically followed lateral as well as vertical orientations, forest discoloration distributions related to root channels in lower horizons were not only more localized than those seen under grass cover, but less vertically oriented. The amount of discoloration surrounding individual tree roots was also a function of root size, so that larger, older roots overlay more extensive discolorations. Figure 5.30 provides an excellent example of soil discoloration under two large lateral roots (7 and 9 cm in diameter) that emerge from and enter bedding planes in pit 7.



Figure 5.30. Large bands of discoloration underlie 9 and 7 cm roots revealed by removal of decomposed limestone fragments in pit 7. All soil surrounding the roots except for soil immediately underneath has been removed. Photo by author, August 12, 2005.

Pit observations showed that colorations associated with tree roots extended down to the bedrock level. As examples, in forest pit 3, tree roots 6 and 14 mm in diameter entered the bedrock at 145 cm, and dark stains were found along root channels at this depth. In forest pit 1, roots up to 5 mm in diameter were still common at 125 cm in accompaniment with 10YR 3/2 stains, and roots continued to the 135-145 cm bedrock depth. Decayed tree roots also

supported organic discoloration in the surrounding soil, indicating that decaying roots form pathways for water movement. In grass pit 12, two decayed tree roots (largest of which was 2.3 cm across) at 50 cm and a third at 85 cm (2 cm diameter) were found to have a distinct very dark grayish brown (10YR 3/2) tone that differed from the surrounding dark yellowish brown (10YR 4/4) soil for the distance of up to a centimeter underneath each root (Figure 5.31).

Although grass roots were common in the soils surrounding the decayed roots found in pit 12, grass roots did not reach bedrock in the deepest pits. Tree roots were not only able to reach bedrock at these depths, but were able to enter it. Distributions of root films thus indicate that the major differences between tree root systems lie in their abilities to orient flow directions and to convey water to deeper depths.



Figure 5.31. Darker soil underlies a decayed root found at 85 cm in the wall of pit 12. Photo by author, September 6, 2005.

#### *Discolorations Associated With Rock Surfaces*

Discolorations related to individual rocks and bedrock surfaces indicate that stones are highly involved in hydrologic movements in the thin soils of the slopes. As carbonate rock debris is leached, brown films and coatings form in leaching zones surrounding and entering pores of the rocks as clay and iron materials from the surrounding soil are flocculated by carbonate

minerals (Gagarina, 1968). The highest degree of calcareous replacement by solutionally dispersed clay-iron material takes place in the illuvial horizon (Gagarina, 1968). Along with increase in translocated minerals with depth, increased conditions of continuous high moisture are likely to promote both decomposition and flocculation.

Discolorations in pits were often associated with rocks. In some locations the entire soil layer directly above the soil/bedrock interface was deeply stained. In pits 5, 6, and 14, grayish brown or brown 10YR 5/2 or 10YR 5/3 layers 1 to 2 cm thick were found above the depth at which limestone plates became too consolidated and embedded to be removed. These layers contrasted with overlying yellowish brown (10YR 4/6) or brownish yellow (10YR 6/6) soils, and contained decomposing, unconsolidated limestone plates within discolored BC horizons. In pit 14, the discoloration was 5 to 30 cm thick and extended from a clear, smooth boundary 2 cm above the fragment layer downwards to the solid irregular epikarst surface (see Appendix 3, Infiltration Test Pit 14). In pits 5 and 6, the discolorations in the thin BC horizons were thinner and more closely related to the individual stones themselves. The similarity of elevation between pits 5, 6, and 14 (figure 5.24) suggests that they may all overlie a common bedrock layer. Clay content increase to bedrock in pits 5 and 6 indicates that the bedrock layer tends to hold water, and it likely has a composition such that dissolution along contact lines with saturated soil releases minerals that cause the particular dark coloration.

Discolorations were also associated in some subsoils with individual decomposing limestone fragments, as shown in figure 5.32. In some deeper locations, very dark gray or dark brown discolorations 5 to 6 mm thick followed the irregular topography of the stone surfaces directly adjacent to the tops and bottoms of the plates. This staining of surrounding soil is shown in figure 5.33 in a clod removed from between weathered limestone plates found at approximately 60 cm depth in pit 5.

At depths at which staining surrounding individual rocks became obvious, soils were generally high in clay content. In forest pits 5 and 6, where fine roots were not found in discolored clods, sticky clay constituted >70 % of subsoil horizons, but did not cling to stones as they were lifted. This suggests that a separation is maintained between the soil and rock surfaces. The mechanism for this separation is unknown, but it may involve some physical process of soil drying and/or removal of fines along the rock surface through preferential flow.

Where free-floating limestone fragments in upper horizons were disconnected from the underlying rock mass, they typically did not display surrounding soil discoloration (Figure 5.34). Lack of staining surrounding upper horizon stones suggests that water does not remain in

contact with rocks at this depth long enough to initiate the full process of decomposition and flocculation.



Figure 5.32. Dark gray soil film is revealed under a stone fragment in pit 5. Photo by author, July 2005.



Figure 5.33. Soil discoloration from contact with limestone plates at the bottom of forest pit 5. Photo by author, July 22, 2005.



Figure 5.34. Soil surrounding a limestone fragment removed from the upper B horizon in pit 12 displays no discoloration. Photo by author, September 5, 2005.

Stains surrounding stones in pit subsoils indicate that conditions are conducive to leaching, and that those pits likely support high water content conditions for significant periods of time. Soils in most pits became somewhat darker at their profile bases, but pits that displayed prominent discolorations of their BC horizons clearly indicated some degree of water retention above bedrock. The retention of clay and iron products in distinct zones in stained soils lying between closely layered stones also indicates that minerals involved in the discoloration process are not being mobilized once they are produced. Discolorations are locally mediated, and vary in some cases within the small area exposed by a single pit. Stains associated with stones and bedrock also likely reflect bedrock composition, so that in pit 13, bedrock decomposition appeared to be associated with the very many distinct medium grayish brown (10YR 5/2) mottles that surrounded limestone fragments. Bedrock composition thus likely functions in conjunction with hydraulic conditions in the production of stone-related

discolorations, but the occurrence of the stains appears to be a marker for clay and water retention in slope profiles.

### **Soils Summary**

Soils of the upland region of the bend are thin, high in clay content, and likely to contain either alluvial gravel and stones or limestone flagstones. Profile development at individual sites in mid and upper slope regions is largely determined by the immediate topography of the epikarst, as is reflected in the mapped Fairmount, Faywood, and Lowell soil complexes. Mixing of residua, alluvium, and loess occurs through bioturbation, surface wash, throughflow, and flow at the bedrock surface or within the epikarst. Water pathways develop in profiles according to textures created by the actions of these mixing processes on the properties of the original parent material deposits.

Residual soils in the upper elevations are typically flaggy and increase in clay content to 70% or more with depth. This degree of clay content tends to slow vertical water percolation, but decomposing rocks and slight increase in sand content in BC horizons may provide avenues for water movement at the bedrock surface. In all locations, clay content in soil layers above bedrock will be lower than clay content of overlying layers where drainage moves across the bedrock surface. In contrast, downhill alluvial soils are high in gravel and sand, but have lower sand content in the soil directly overlying the bedrock. This is likely to encourage lateral movement at approximately 125 cm depth, which should carry water across the main terrace to where alluvium pinches out.

Soil markers of water movement show that vegetation creates characteristic water pathways that operate concurrently with epikarst influence. Root channels in grass, as shown by organic/clay discolorations on ped faces in subsoil horizons, operate vertically in networks that drop along ped faces. Grass roots also decrease significantly in number below 30 cm, and few to no grass roots were found at bedrock in the deepest pits at the hill base. In contrast, discolorations along tree roots indicate that root-regulated flow pathways in the forest are discrete, may have lateral or vertical orientation, enter bedding planes and fractures, and extended to bedrock in the deepest pits. This overlay of different modes and depths of water entry into subsoils as regulated by vegetation should be detectable in hydrologic tests.



## **BIOGEOMORPHIC EFFECTS**

The effects of vegetation on processes such as on evapotranspiration, infiltration, water retention, sediment movement and capture, or biogeochemical activity are fairly well understood. Likewise, a great deal of information is available on their influence on slope stability, tree throw, root distribution, depth of root penetration, and root ability to deteriorate minerals through introduction of mycorrhizae and organic acids (Jones, 1998; Sterflinger, 2000; Landeweert et al., 2001; Egerton-Warbuton et al., 2003). However, little work has attempted to show the cumulative effects of grass and forest as geomorphic agents. Most current information elucidates the function of a single process related to species or vegetation communities. Where processes have been studied over broader areas, most research has focused on a single effect, as for example, runoff chemistry (Likens et al., 1967; Moulton and Berner, 1999) or pedology (Ritter, et al., 2003; Phillips and Marion, 2004). Only a few studies, such as the global consideration of belowground vegetation effects on soil nutrients, fauna, and water distribution by Jackson et al. (2000), consider multiple variables.

To create a broad scale picture of vegetation effects on geomorphology for this project, this section compares forest and grass root system effects in the study area within the background context provided by these many other researchers. Most of this information derives from field observations, which show that vegetation has differing effects on hillslope stability, sediment release, and movements of water into the epikarst. Tree root action is particularly emphasized, since it plays a very active role in focusing solution of the limestone surface. Some water movement also takes place along pathways created by soil fauna, and their role in study area hydrology is briefly discussed.

### **Hillslope Stabilization**

In the study area, upland grass soils are protected by dense topsoil root mats. The ability of the root mat to capture and retain fine sediments, and thus hide connected cutters operating on the slopes, was described earlier (Figure 5.20). Grass roots appear to protect steep slopes from surface erosion except under conditions of concentrated shear. Even in these locations, such as above the conduit at the base of Hillslope A, grass may grow in soil only a few centimeters thick.

Because of grass protection, surface erosion in the study area is limited to sensitive locations. Winter burning of the native grasses, as discussed in chapter 2, does provide pathways for surface sediment movement during large storm events that occur before spring growth is renewed. In the main study area, surface erosion on grassed slopes appears limited

to localized spots above the conduit on Hillslope A, and to patchy bands at the bases of slopes such as Hillslope I, where water perches under saturated conditions (Figure 5.22). Seepage creates positive pore pressures that lift soil particles, lower cohesion, and aid in surface soil movement (Sidle et al., 1985; Owoputi and Stolte, 2001; Rockwell, 2002), and the underlying impermeable bentonite layer most likely causes exfiltration that has sufficient force at this elevation to reduce root mat coherency by unlocking fine particles from soil aggregates.

Loss of root mat coherency also occurs where grass growth is limited, as it is under the shading that takes place at the forest edge. Gully head erosion at the forest/grass boundary takes place concurrent with loss of grass root mat protection. Similar loss of protection occurs in locations where the forest/grass boundary orients upslope perpendicular to the contour. Incision in these cases takes place along the edge of the forest near the base of the slope, often within a band of weeds growing between the forest and grass. As grass is replaced by shade tolerant plants with more discrete root systems, soil stability in the advent of surface wash or saturation excess seepage is weakened.

Tree roots can contribute to hillslope stability by anchoring soils. In the study area, trees appear to stabilize channel or gully banks, such as in the placement described earlier for the two bent trees cored for this project (Figures 5.5 and 5.6). Trees also stabilize outer rims of karst features, and hold soils where slope increases sharply (Figure 5.35). Tree root anchoring certainly plays a role in maintaining lush forest growth along the outcrop terraces that drop into the river from the escarpment. In these rocky, inhospitable locations, as in the main study area, trees appear to be able to stabilize their growth through root penetration of bedrock layers and fractures.

### **Concentrated Sediment Movement along Tree Roots**

Whereas stains along the extent of tree roots indicate that water movement along root preferential pathways is likely, evidence for sediment movement through this process is inconclusive in study data. Clay content typically rises rapidly with depth in the study area and may reach 75% or more above bedrock, but comparisons of horizon clay percentages, as examined in detail in Chapter 6, show no statistically significant differences at equal depths between forest and grass. If changes in sediment movement are occurring because of loss of tree root preferential flow under grass, they are not currently detectable as soil layer differences in particle sizes.

Large erosional features do offer some evidence of tree root influence on sediment movement. Where flow at the epikarst surface is collected and drawn at a high rate into

subsurface pathways, it is not unusual to find swallets that have opened in conjunction with trees rooted into the draining fissures. Trees can become easily established above a soil filled cutter, and in some cases, such as in figure 5.36, may be exhumed simply because they occupy an eroding conduit. More commonly, however, swallets open within forested areas in places where trees occupy sloping banks bordering surface channels. If a large tree happens to overlie a cutter oriented perpendicular to the channel, swallets may form near the tree base or along its larger main roots. In these locations, the effect of the tree roots on the original cutter development is not known, but the removal of soil in the vicinity of large roots can be readily observed.



Figure 5.35. Tree roots capture colluvial sediment on a steep slope on Hillslope F. Soil on the uphill side is more than 25 cm higher than that on the downhill side. Note field book for scale. Photo by author, March 6, 2005.

Swallets that occur over High Bridge limestone conduits usually originate from the inner roof soil loss and eventual soil cover collapse that occur in cutters developed on the bedrock surface (Cooley, 2002). Most of these High Bridge swallets are associated with tree bases, however, suggesting that soil cover collapse can occur in this environment most effectively where preferential flow funneled from above operates coincident with internal soil loss from the

roof. The importance of preferential flow in moving sediments is suggested by the site shown in figure 5.37. At this location, a swallet opens near a tree just to the side of a gully headcut. The swallet opens into a soil pipe that exits under the main root overhang at the gully head at approximately 30-40 cm depth. Flow from the uphill grassed slope converges in this particular location where the forest begins at the edge of the relatively flat lower end of the main terrace.



Figure 5.36. Exhumation of a large tree established within a conduit on the north side of the bend. Photo by author, November 2003.

Soil pipes will develop in relatively noncohesive materials subjected to subsurface flows with a high hydraulic gradient (Shirmohammadi, et al., 1991), and have been found to operate between sinkhole bases and bedrock fracture openings in karst areas (Ahmed and Carpenter, 2003). In this case, the depth of the pipe and its geomorphic position suggest that the soil pipe is maintained by episodic saturation of relatively light soils above more clay-rich material, with subsequent soil loss within a defined conduit. The placement of the swallet and pipe are of chief interest here, and indicate that whereas tree roots may not be the primary cause of

subsurface soil loss in circumstances where perched water seeks an exit path, they likely promote it and possibly guide the channels along which such soil loss can most easily take place. Root orientation likely plays a role in this process, with piping taking place where roots orient with the potentiometric gradient. Within a saturated soil mass, tree roots seem to provide pathways of least resistance to both surface and belowground sediment movements.



Figure 5.37. Swallet opening at the base of a tree is connected to a soil pipe, shown by the end of the folding measuring stick. The pole marks the swallet location. The soil pipe emerges below the tree root mat at a gully head. Photo by author, June 2004.

### **Root Interaction With Bedrock**

Within the upland slopes, grass and forest root systems interact with the epikarst surface in completely different ways. Contrasts in root orientation and distribution between forest and grass create different solution enhancement capabilities and thus different effects on karren development. Grass roots decrease in number with depth, but where they contact limestone benches, they will coat the sides of the rocks and likely increase solution across the entire surface. In contrast, tree roots create root grooving along discrete entry points in the bedrock. Tree root entry will lead to breakdown of the highest limestone layers, and observations indicate that trees develop an increasing impact on the epikarst as they age. Evidence supplied by

current tree root growth and by features likely created by historical root action indicates that the ability of tree roots to penetrate the epikarst plays a critical role in hillslope hydrology.

### *Grass Roots*

Because soil depths on the shoulder and upper sideslope of Hillslope A were within the potential >1 m rooting depth of the grass vegetation, vertical grass root networks were able to surround and interact with the limestone plates present either as “floaters” in upper horizons or forming the benches in the epikarst. The number of roots in the soil matrix decreased with depth in all grass pits, but where root networks were able to contact rocks to depths of over a meter, fibrous mats of very fine to fine roots typically covered the tops, and sometimes the bottoms, of stones and boulders (Figure 5.38). The abundance of roots found in mats surrounding stones was greatest between 40 and 85 cm, increasing from little to none on surface rocks and decreasing in abundance below 1 m depth. In grass pits, fine root numbers typically decreased with depth to 10-25 per 100 cm<sup>2</sup> (common) in the matrices of Bt horizons, but rose to 25-200 or more per 100 cm<sup>2</sup> (many) within the mats surrounding the limestone plates of the BC horizon. In figure 5.39, the localized association of these fibrous mats with rock surfaces can be seen in pit 10, where tilted limestone boulders in the B horizon were coated top and bottom with fine roots in a layer that was typically about 5 mm thick.

Horizontal limestone plates in upper grass horizons did not usually display root coatings, and smaller plates in particular were less prone to support them. Where root coatings were present on horizontal stones in upper horizons, the stones were usually the outer, decomposing edges of the bedrock benches at the uphill sides of the pits. Thin soil layers (<2 cm) were typically found where high-residue bedrock layers had decomposed between the edges of limestone plates protruding from bench walls. Grass roots in these situations commonly coated the top and bottom of the soil where it pressed against the over and underlying stone surfaces. Grass roots thus coated those stones that were most likely to have some degree of continuous vertical or lateral contact with other rocks, or that were separated from other stones by thin soil layers developed between stones that had decomposed *in situ*. Isolated rocks supported fewer roots.

Discolorations associated with the thin root mats surrounding limestone plates were highly variable in distribution and thickness, and in most cases consisted of a thin, dark film localized around the roots. In figure 5.39, soil surrounding the roots protruding below the tilted stone demonstrates the very thin nature of this discoloration.



Figure 5.38. Soil removed from the bedrock surface in pit 13 reveals the fibrous root mat along with small decomposed limestone fragments that coat limestone slabs. Photo by author, September 14, 2005.



Figure 5.39. Fine roots emerge from beneath a tilted boulder in pit 10 (upper right corner). Roots have been scraped off the top of the stone. Photo by author, August 26, 2005.

Although the extent of grass root penetration into the rock surface was not determined for this study, roots were apparently only able to access the top few millimeters of rock surfaces and could be easily removed by scraping. Grass root mats likely play a role in increasing solutional activity on the outsides of the stones they cover because of the coincidence of increased water movement in root channels and high organic matter content, with its resultant higher CO<sub>2</sub> production in the immediate surrounding soil (Trudgill, 1976b, 1985). Evidence from pit bases and bench walls indicates that the solutional effect of grass roots may be subtle, operating with a dispersed overall action on the rock surface. Stones in grass terrace walls and at the bedrock show a characteristic micro-roughened surface texture, although the stones themselves are subrounded. The process of rounding is shown to be progressive, in that if stones are fractured but not weathered along the fracture, then edges are sharp when loose stones are removed (Figure 5.40). Upper horizon floaters in both forest and grass typically displayed the characteristic rough-surfaced subrounding associated with weathering. In pits 7 and 8 in the forest, however, decomposing plates removed from holes within the bedrock had sharp edges, suggesting that rock decay in the forest pits may be less activated by dispersed solutional attack along rock surfaces than in grass pits (Figure 5.41).



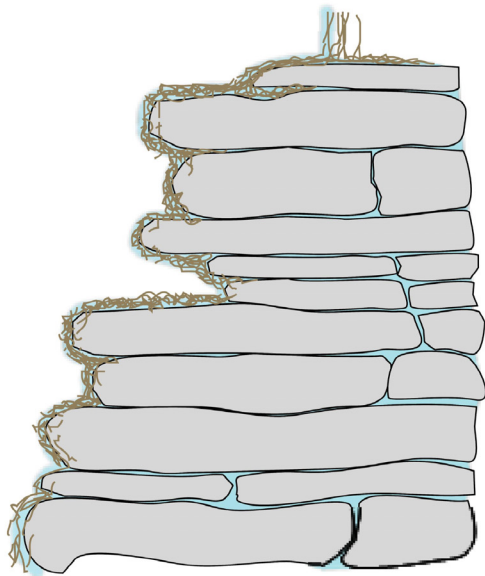
Figure 5.40. Bedrock plates under grass display a roughened, subangular surface in pit 13. Stones are rounded where weathering has attacked corners. Red arrow shows the location of a sharp edge where a tight-fitting plate was removed along an unweathered fracture. Photo by author, September 14, 2005.





Figure 5.41. Coarse roots emerge from numerous bedding plane and fracture openings in the rock bench walls in forest pit 8. Sharp limestone plate edges define the sides of the hole in the bedrock. Photo by author, August 14, 2005.

Fine grass root mats penetrate only a few centimeters or less between consolidated stones that are not separated by weathering. Where roots are present, however, increase in solution along the protruding edges of rocks in the limestone bench walls would tend to round protruding rocks and expedite their weathering separation from the rest of the rock mass as grass roots slowly penetrated ever deeper at the outer edges of decomposing layers. This possible top-down sequence is illustrated in figure 5.42, which shows the placement of floaters, bench wall rocks, and grass mats as observed. The positioning of root mats along the rock bench faces, and their lack of matting around all but the largest floaters, suggest that some physical and/or hydrologic property of the connected bench faces encourages the mat development.



a) Grass root mats form on the outside wall of a soil covered limestone bench. Roots decrease below a meter in depth, and can only penetrate between limestone plates where decomposition has provided openings.

b) Grass roots aid in the dispersed solutional attack of the surface of the limestone. As plates are decomposed, roots exploit enlarged openings. As upper level plates are separated from the main rock mass, fewer roots occupy the soil separating the disconnected rocks.



c) With continued decomposition, "floaters" disconnected from the main limestone mass do not support grass root mats.

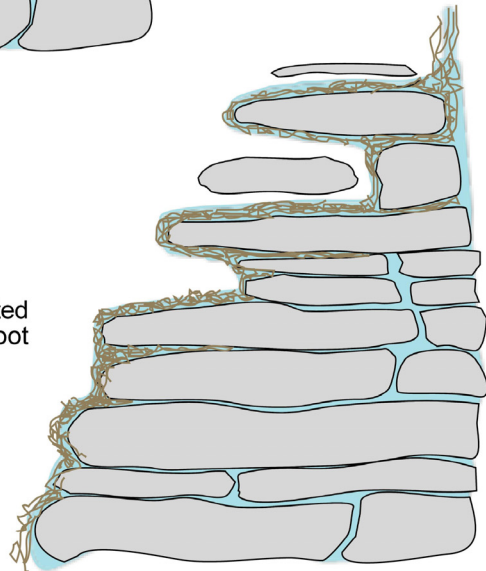


Figure 5.42. Likely sequence of grass root mat exploitation of decomposing limestone bench walls, as suggested by field observations.

### *Tree Roots*

In contrast with grass root mat concentrations, root mats in association with rock surfaces were seldom found in the forest, and where present consisted of small, patchy distributions of much less abundant, somewhat coarser root nets. However, in forest pits, individual medium to very coarse roots were observed to enter and exit from fractures and bedding planes in otherwise consolidated stone layers (Figure 5.41). Tree roots also entered fractures between bedrock plates in all forest pits (Figure 5.43). Tree roots thus act at numerous discrete points of entry between rocks, in contrast to the diffuse rock surface action taken by grass roots.



Figure 5.43. A 2 cm root applies pressure along a fracture line at 75 cm in pit 5 as it grows. Grayish brown soil discoloration associated with relatively smooth bedrock stones is shown in the soil filling the fractures. Photo by author, July 22, 2005.

Root grooving was observed in the bend in multiple locations. Figure 5.44 shows a tree root exposed in an exhumed cutter overlying the Tyrone. Here, root entry along a fracture line over time caused the surrounding rock to dissolve in a circular form. Occasional larger, but

inexplicable shapes in the flat-lying beds of exposed outcrops also suggest root action. In figure 5.45a, a large hemispherical groove is dissolved along the plane between non-fractured bedrock layers in a Tyrone outcrop. This channel narrows and disappears within less than two meters, and is associated with a rounded rock face at the front of the channel that is at variance with the flat planes found in the rest of the outcrop. In figure 5.45b, the source of the hemispherical groove and rounded rock face is suggested by studying the roots embedded between bedding planes at the base of a live tree.



Figure 5.44. Root grooving caused by root entry into a fracture is exposed in an eroded gully. Note glasses for scale. Photo by author, January, 2006.

Several different but overlapping mechanisms may cause root grooving. Roots hairs provide acidic exudates (Wall and Wilford, 1966; Spyridakis et al., 1967) that extract calcium and magnesium for biomass storage from surrounding rocks (Hinsinger, 2001). Roots also support mycorrhizal and microbial populations that generate organic acids and chelates (Stone and Comerford, 1994; Smith et al., 2003). As precipitation follows root pathways during high

moisture conditions, acidified water penetrates the bedrock zone surrounding the root, causing pressure and rock fragmentation (Taborosi, 2000). Because solutional processes in limestone are sensitive to acidic water concentration, all of these mechanisms promote carbonate rock root grooving.



Figure 5.45. Large scale root groove forms suggested by features of Tyrone outcrops. (a) Channel approximately 2 m long narrows to a point as it extends at a slight downward inclination into the rock mass. The soil probe is seated at bedrock next to a smoothly curved rock face at the channel opening, suggesting that a tree once occupied this location. (b) Tree roots utilize Tyrone bedding plane and fracture weaknesses to gain support. Probe is 1 m long.

The concurrence of observed solutional features with root placement suggests that the primary effect roots have on rocks in the study area is created by introduction of acidified water and resultant concentrated dissolution along lines of root penetration. Stains around tree roots as observed in infiltration pits suggest that water utilizes root pathways, and that water is able to follow those pathways into bedrock fissures. Solutional removal of limestone is shown in figure 5.46, which shows a notch in a limestone plate overlying the bend in a 9 cm tree root uncovered in pit 7. This limestone plate is likely a remnant fragment of a larger slab that impeded the root, shown without the rock in figure 5.30, and forced it to grow downwards. Preferential water movement and pressure from the root probably hollowed the notch as the root increased in size.



Figure 5.46. Notch in a limestone plate fits tree root bend in pit 7. The root is 9 cm in diameter and pressed firmly against the notch when it was uncovered. Photo by author, August 12, 2005.

### *Bedrock Layer Breakdown by Tree Roots*

Lifting of rock plates near trees is ubiquitous on the upper sideslope and shoulder surfaces of the forest. Trees typically construct mounds at their trunk bases where roots push soil material upwards, but this same action in the shallow soils of the study area can raise slabs up to several meters long above the surface (Figure 5.47). The same lifting of individual plates does not take place on the grass slope, and where outcrops are exposed in grass areas of the bend, they are not lifted, but rather uncovered by thinning and loss of their soil covers. Non-fractured rock expanses have been exposed along the shoulder area of the grass main study area (figure 5.48), and although soils are extremely shallow at equivalent forest elevations, fractures, thin soil accumulations, and vegetation break the forest bedrock surface.



Figure 5.47. Lifted limestone slab lies several meters uphill from pit 6. The stump of the large tree which picked up the slab is shown in the upper right. Photo by author, July 24, 2005.

The more broken nature of the bedrock on the forest portion of the shoulder of the hill is shown by figure 5.49, which compares the soil depths of two transects measured parallel to the contours in sites matched for elevation in forest and grass locations. Depth was measured at one meter intervals, and where the probe hit rock at <15 cm, supplemental measurements were taken in a circle with a 10-15 cm radius from the site to determine if the probe had hit a loose

rock, or to see if any fractures were present containing deeper soil. As shown by the transects, soils on this grass portion of the shoulder were not only shallower, but typically covered a smoother bedrock surface than in the forest.



Figure 5.48. Exposure of bedrock along the grassed shoulder of the main study area. Photo by author, March 15, 2005.

The sinkers that develop from lateral roots of many tree species, including the oaks, are quite capable of exploiting joints, fractures, or solution holes in seemingly impervious regolith and bedrock conditions. (Stone and Kalisz, 1991). Often such penetrating roots expand in size and number once the restricting physical feature is passed, and longer roots, though few in number, may provide a significant amount of a plant's nutrient and moisture needs (Jackson et al., 1999). In limestone bedrock, root branching is constrained by joint and bedding plane patterns, but in slopes composed of thin-bedded sediments at shallow to moderate depths, "upslope laterals" may develop that grow obliquely or horizontally into weathered bedding planes and joints (Stone and Kalisz, 1991). Observations in the study indicate that lateral tree roots follow this pattern of upslope lateral development in both the Tyrone and Lexington



Limestones. The thinness of the Lower Lexington beds also seems to provide added opportunity for roots to drop between rock layers so that they occupy multiple bedding planes.

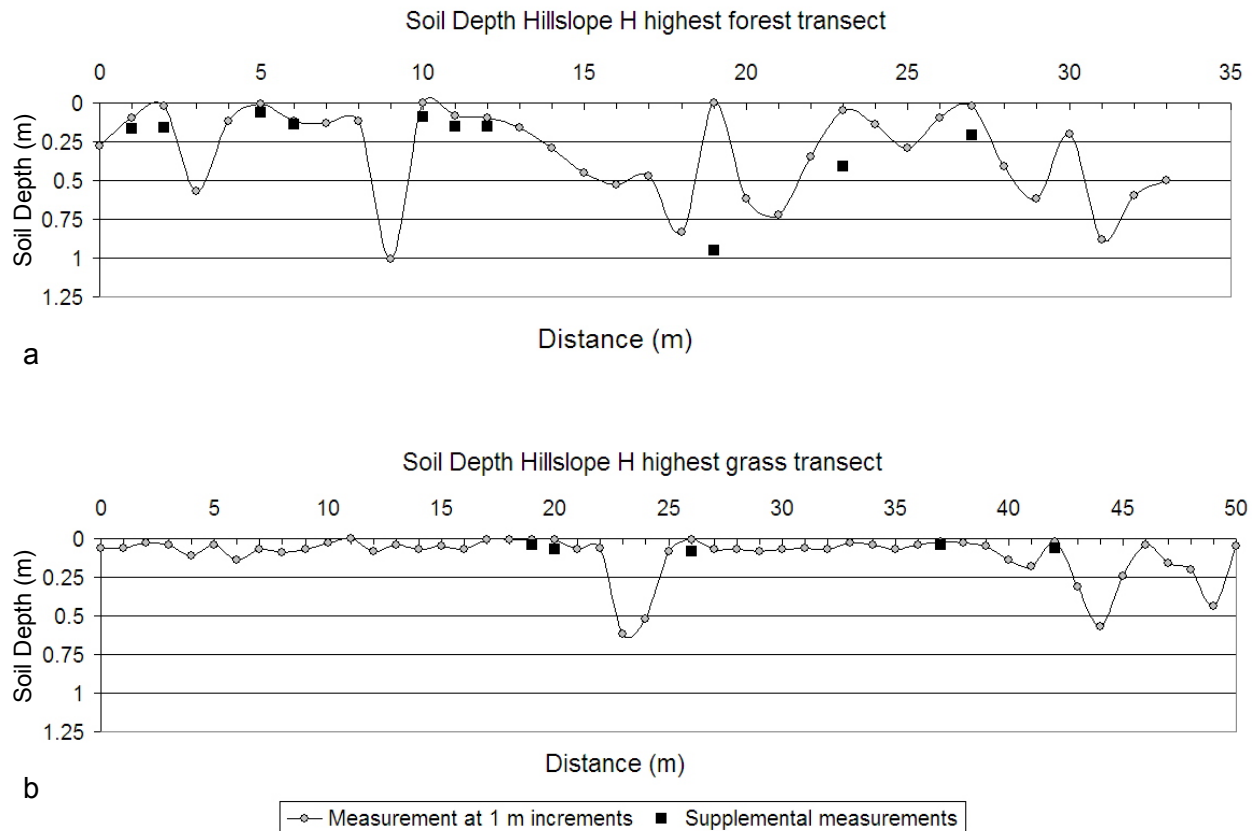


Figure 5.49. Transects matched for elevation on the main study area shoulder. (a) Forest and (b) grass transects show the higher number of fractures and cutters found in the forest. Supplemental measurements are the deepest depths found within a twenty centimeter circle surrounding original measurements that were less than 15 cm in depth.

Solutional weakening of limestone permits a root to expand, so that it continuously presses against the groove walls in an expanding sphere of solutional influence. Whereas thick limestone beds have too much tensile strength to be broken by this pressure, observations indicate that in the portion of the study area underlain by the Lexington Limestones, the occurrence of thin limestone beds with shale partings and interbeds may allow for pressure-related fragmentation of decomposing rock plates at the top of the epikarst. The high number of broken and lifted limestone plates at the surface, plus the very thin nature of the soil cover in the forest shoulder, suggest that the lifting work done by roots at the surface most likely occurs to some degree below the soil in the uppermost bedrock layers as well. This mechanical breakdown occurs as solutional processes expedited by tree roots weaken the already thin

limestone layers. The likelihood of this fragmentation probably increases slowly over time in conjunction with rock decomposition and root size increase.

In pit 7, the 7 and 9 cm roots shown exposed in figures 5.30 and 5.47 could be associated through their size, orientation, and composition to a very large 1.15 m DBH chinquapin oak located 7 m uphill from the pit site (Figure 5.50a). A solid horizontal rock slab occupied the north half of pit 7 but was broken into numerous small to very large decomposing plates in the Bt horizon that surrounded the two large roots. The decomposing plates removed from this the pit are shown in figure 5.50b. The solid nature of the limestone slab in the north half of pit 7 contrasted sharply with the fragmentation of the pieces weathered *in situ* from around the tree roots, making it unlikely that this degree of fragmentation existed before root growth. This suggests that root pressure pushing up on the decomposing slab helped to expedite its breakdown. Although roots penetrated bedrock fractures in other forest pits, most roots were small (<3 cm in diameter) in association with the second growth age of trees and did not provide evidence for the possible strength of root action on bedrock. The rock breakage uncovered in pit 7, however, suggests that this action can be significant in those concentrated areas where tree roots penetrate fractures and bedding planes and grow to a large size near the surface.

The possible distribution of this root action effect on the surrounding bedrock is shown by a forest soil depth transect that was measured beginning at the base of the large chinquapin oak described above (Figure 5.51). The bedrock within approximately 17 m of the tree is split by fissures, and the tree itself is nested within a pit that is deep relative to the surrounding soil conditions. An oak sapling was found rooted in one of the bedrock fissures, suggesting that the root action of older trees may actually help younger plants become established by providing the means to accomplish deep rooting more easily in very shallow-soiled environments (Figure 5.52).

Soil depth transects from lower portions of Hillslope H indicate that tree root effects on rock decomposition likely becomes less important with increase in soil depth. The larger, main roots of the observed species appeared to be laterally oriented within mid to upper profile depths, with vertical sinkers angling downwards along their extents. Although tree roots tapped into bedrock in even the deepest pits measured in this project, diameters of tree roots decreased with depth below 100 cm, so that only small roots were witnessed entering bedrock below 125 cm. Although root action at the bedrock likely increases with root size as a tree ages, because most roots tend to remain above 1.5 m, their ability to dissolve bedrock is likely limited in frequency and size of effect by deeper soils.



Figure 5.50. Decomposition of thin limestone layers by root action over time. (a) Large roots found in pit 7 are connected to the Chinquapin oak located 7 m uphill. (b) Decomposing limestone plates, shown by arrow, were removed from surface layers and from around two large roots that have exploited weakened zones in the bedrock, encouraged their dissolution, and expedited breakdown of the rock slab into pieces. Photos by author, August 12, 2005.

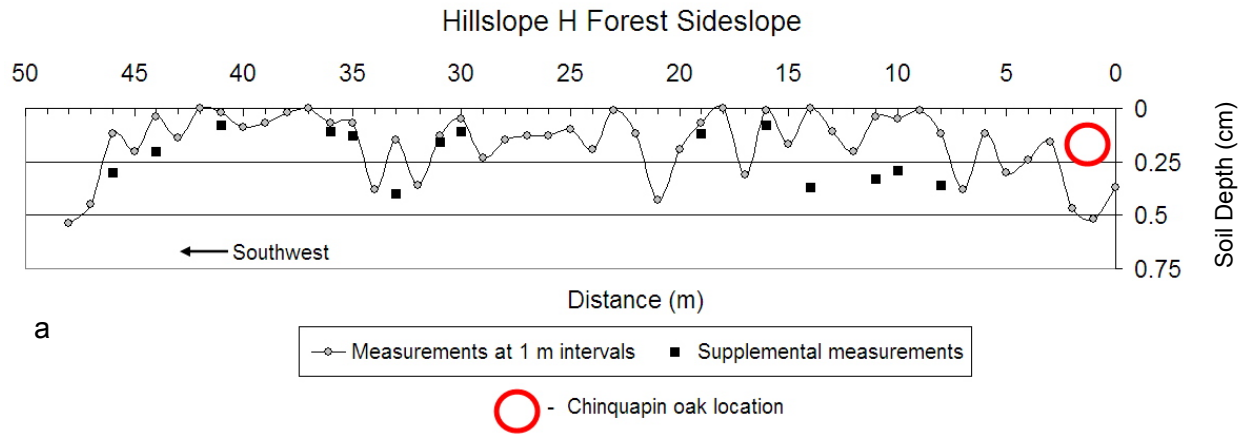


Figure 5.51. Bedrock fracturing on the upper forest sideslope. (a) Soil depth transect starting at the base of a 1.15 m DBH oak shows fractures within 17 m of the tree as well as a deeper area associated with the tree base. (b) Transect start point at tree base. Photo by author, March 21, 2005.

Introduction of preferential flow and increased weathering in fractures likely occurs in deeper sites, however, to the limit of rooting depth. This would still set up conditions that could generate eventual differences between forest and grass, but would likely do so at a slower rate than in areas of thinner soils. Because of the relatively young ages of most trees, the degree of decrease in root action relative to soil depth increase can not be determined by this project.



Figure 5.52. A young tree establishes itself in a fracture in the bedrock near a large oak. Photo by author, March 21, 2005.

#### *Evidence for Historical Tree Root Action*

##### *a) Hillslope H*

As suggested in the preceding section, the introduction of acidic water and the accompanying limestone decomposition and potential rock breakdown induced by growing tree roots likely play a large role in the break-up of near-surface rocks in shallow-soiled regions of the main study area. Geomorphic evidence from the grassed main study area also indicates

that the resultant bedrock forms are retained in the epikarstal surface, and may become an important factor in the evolution of subsequent epikarst pathways.

A second chinquapin oak the same size as the one uphill from pit 7 stands as an isolated single specimen near the summit of the grass slope. For either of these oak giants to gain their current age and size, they would have had to have developed root systems proportional to their aboveground biomass (Casper et al., 2003). Such root growth in their current locations seems outwardly remarkable, considering the shallow, often <20 cm soil depth of the hill's shoulder and upper sideslope, and indicates that the trees likely exploit the epikarst for support. The form of a ragged, up to half a meter deep incision cut into the epikarst of the upper sideslope of the grassed hill approximately 30 m below and southeast of the second oak suggests that it may have been created by a tree the size of the one on the hill crest at some time in the past (Figure 5.53).

It is likely that large lateral tree roots in this environment may follow near surface bedding planes and orthogonal joints in the bedrock, leaving channel forms in the epikarst surface as their roots decay. In figure 5.53a, the incision is shown located below a small depression in the slope. The incision makes a fairly sharp bend to the left, as seen at the base of the probe in 5.53b, and has a large limestone flagstone wedged vertically into the head of its upper opening, shown in 5.53c. Lateral growth of a large root is suggested by the channel pattern, which follows a joint perpendicular to the gradient for a portion of its extent, and the ability of root growth to supply a natural mechanism for sideways wedging of a large stone. The incision currently seems to funnel flow from the surrounding local slope area, and dark, organic fines have accumulated in spots on the highly irregular base of its bed.

Larger trees similar to the isolated giant found at the top of the hill very probably existed on this portion of the slope prior to deforestation in the early 1960's. It is likely that the gradual decay of those trees, possibly cut during much earlier logging events, have left remnant forms in the bedrock. Such forms should take the shape of depressions associated with the tree's actual trunk location, which would likely cause a pitting of the bedrock surface (Sweeting, 1973), as well as channels partially covered by decomposing limestone flagstones broken by root action in bedrock layers at the top of the epikarst. Soil depth transects taken in this region of Hillslope H show the existence of shallow pits distributed at random, but not in close proximity. A few of them now act as drawdown centers for water movement on the slope, such as occurs in the channel described for figure 5.53.



Figure 5.53. Root forms at the epikarst surface. (a) An up to half a meter deep channel is cut into the surface rocks of the grass sideslope below a small depression (indicated by an arrow). (b) Grass and overlying plates have been removed to expose the channel. Probe is 1 m long. (c) A large plate is wedged vertically at the channel head, with its position shown in (b) by dotted lines. Photos by author, March 15, 2005.

It seems likely that as the lateral root described for figure 5.53 decayed, the channel remaining in the epikarst surface was incorporated into the surface hydrology, with subsequent increased solution along the weakened zone. In this case, a pre-existing fracture pathway was exploited by root action, which in turn increased the existing drawdown, so that flow from an expanding region of the slope is now being drawn into a small sink-like area downslope from the channel. Soil is being moved in this process, localized downhill solution has likely been increased, and the likelihood of development of continuous downhill cutters and eventual gully development is advanced. This example shows the tight biogeomorphic interrelationship between roots, rocks, and water pathways that occurs in this steep, thin-soiled karst environment, and suggests the potential importance that tree roots might take in landscape formative processes.

*b) Possible Root Evidence From Pit Bases*

If tree roots affect bedrock solution, evidence of tree root action should be visible in rock forms found in those parts of the main study area that have been deforested for 200 years. Stump burning was practiced as the slopes were cleared. A lump of blackened charcoal was found on the bedrock surface at approximately 40 cm depth in the north end of pit 13 (Figure 5.54a). This pit also revealed bedrock forms that were suggestive of solution along a root, rather than simple fissure weathering. Many decomposing limestone plates were found above the bedrock layer in pit 13, and their removal revealed a level, 10 cm diameter channel filled with soil and small rock fragments at 55 cm depth that ran along the length of the pit for over a meter before splitting into two smaller segments approximately half a meter from the pit end. Figure 5.54b, taken at the level of the bedrock, shows the circular nature of the channel and the unusual sharp-edged character of the surrounding rocks.

Simple solutional weathering within a conduit seems unlikely to explain the geomorphic occurrence of this circular channel, since fluid pressure high enough to create a circular form could not have developed at this height on the hill in a level spot perpendicular to the gradient. Although inconclusive, the circular channel shape at the base of pit 13 could be interpreted as resulting from the weathering action of a large tree root, with rounding of confining rock walls taking place as the root increased in size.

Similar rounded channel features were found in pit 14, but at a much smaller scale that would make it difficult to differentiate them from non-root related solutional activity. However, a different bedrock form found in pits 11 and 12 also brings into question the possibility of root action. Both of these grass pits had large, rounded holes in their bases (see Appendix 3,



Infiltration pits 11 and 12). The hole in pit 11 in particular shows overhanging walls reminiscent of those seen in the circular channel in pit 13 (Figure 5.55).



Figure 5.54. Bedrock forms suggest possible root grooving. (a) Level, 10 cm wide channel indicated by arrow at bedrock base in pit 13. Box shows location where charcoal was found. (b) Circular channel walls, with unusually sharp edges. Photos by author, September 14, 2005.

These holes can no doubt be explained by many types of solutional weathering, but their occurrence in two close, randomly selected sites just below the hill shoulder limits many of those choices. Rock forms in pits 11 and 12 indicate that flow collection at the epikarst surface does not occur in these sites, and the likelihood of the holes being remnant portions of palaeoconduits is limited by lack of surrounding channel evidence in the hillslope or the pits themselves. The bedrock base at 110 cm in the hole in pit 11 additionally indicates lack of large-scale concentrated throughflow. In addition, the overhangs in pit 11 suggest that they may have been induced with pressure exerted upwards from within the hole. As with the channel in pit 13, the holes in pit 11 and 12 offer suggestive but inconclusive hints at a broad scale, highly potent weathering effect played by tree root action in this shallow-soiled limestone terrain.



Figure 5.55. Hole exposed at 75-80 cm in pit 11 has rounded overhanging walls. A rock base was found in the hole at 110 cm, but the end lateral lengths of the hole were not determined. Photo by author, September 4, 2005.

### **Macropores**

Macropores were common in both forest and grass topsoils and down to 25 cm or more, but very large pores that had at least some degree of continuity at depth were chiefly related to

earthworm movements. However, during the extremely dry conditions during which most pits were dug, earthworms remained tightly curled into clay-sealed cysts in lower horizons because of their need to conserve moisture. Thus worm tunnel openings were not apparent in the forest topsoils, or could not be distinguished from cracks caused by desiccation along ped faces and next to shrinking roots. Worms were observed down to 125 cm, however, and the presence of wormholes in grass surface soils after the August rains indicates that worms likely provide a means for vertical preferential flow activation in both grass and forest soils. In the thinner soils, this flow activation should definitely reach bedrock.

### **Summary of Biogeomorphic Root Effects**

Differences in the roles played by grass and forest rooting systems derive from differences in size, orientation, and distribution. Fine grass roots drop vertically from the surface, mostly passing along the outsides of peds in B horizons. In contrast, coarser tree roots direct preferential flow both laterally and vertically. Whereas tree roots enter bedding planes and fractures in the bedrock, grass roots are limited to rock surfaces and places where weathering has introduced soil between close-lying limestone plates. Grass roots fully exploit the decomposing conditions of the epikarst surface, however, and form root mats that coat the tops and bottoms of weathered slabs and protruding stones. Root mats develop best in mid-horizons between 45 and 85 cm depths, but can extend to >100 cm, disappearing with depth only where constrained by the particular root depth capabilities of the grass species. Tree roots have a deeper rooting capability than the fescue grass found in the study area, and although the majority of tree roots were found above 1 m, were found entering bedrock in all pits.

Observations indicate that removal of sediments in saturated environments can take place best where tree roots provide subsurface pathways oriented with the flow direction. However, the chief effect tree roots have in shallow soils is the solution that takes place along root pathways in accompaniment with introduction of potentially acidic preferential flow. Growing roots widen circular dissolution pathways in confining bedding plane and fracture walls, and where soil is shallow, the coupled effects of dissolution and increasing root pressure may fragment thin rock layers at the top of the epikarst.

The ability of tree roots to break down rock along root pathways increases with tree age and increase in root size, and it appears to be most geomorphically important in the thin-soiled regions of the study area's shoulders and upper sideslopes. In these portions of the slope, tree roots lift limestone plates above the surface and maintain a slow, discretely distributed, but inexorable attack on the epikarst surface. The fractures and pockets made by one generation of

trees are eventually exploited by succeeding generations to establish their own root systems. On the grassed slope where tree roots no longer maintain this attack, the rock surface is relatively smooth and non-fractured.

## **CHAPTER 6**

### **HILLSLOPE HYDROLOGY**

Having defined the earth surface systems responsible for landscape evolution on Bowman's Bend, this chapter discusses water movement within those systems. The varied natures of the soils and supporting bedrock in the study area create conditions that cut across vegetation differences, sometimes providing overarching influences that obscure vegetation effects. In addition, grass soils still largely retain textural properties developed under forest. Thus, although current vegetation influences on water movement are different, evidence for why those patterns should exist is not so obvious. Statistical analysis of infiltration and soil property measurements shows that factors may have subtle interactions that in some cases tend to move forest and grass systems toward similar patterns of water movements. To best understand the role played by vegetation, results from infiltration tests and water content data logging are first analyzed, and then combined into an overall picture.

#### **INFILTRATION TEST RESULTS**

##### **Factors Conducive to Infiltration**

Over the course of the project, it became clear that at least five different variables acted together to regulate infiltration: 1) soil texture as determined by proportions of soil particle sizes, 2) soil structure, degree of particle aggregation, and porosity, 3) presence, orientation, length, size, and type of roots, 4) presence of open macropores, created by earthworms, desiccated roots, or cracks between peds, and 5) distance from and connection to the rock surface, as either gravel and free stones and/or the semi-consolidated limestone terrace walls or bedrock base (Figures 6.1 and 6.2). In addition, hydrophobic tendencies were noted in many very dry topsoils. These tendencies, which made it difficult to moisten samples for color determination or for field tests of texture by hand, were particularly noticeable in the forest pits 5 through 8 (Figure 4.5), but also occurred in dry grass surface layers that resisted wetting. This resistance to wetting, recognized by researchers elsewhere and attributed to fungi and organic aggregate coatings (Trimble, 1988; Dekker, 1998; Mitchell, 1998), may have helped create surface infiltration rates that were often lower than rates determined for deeper soil layers.

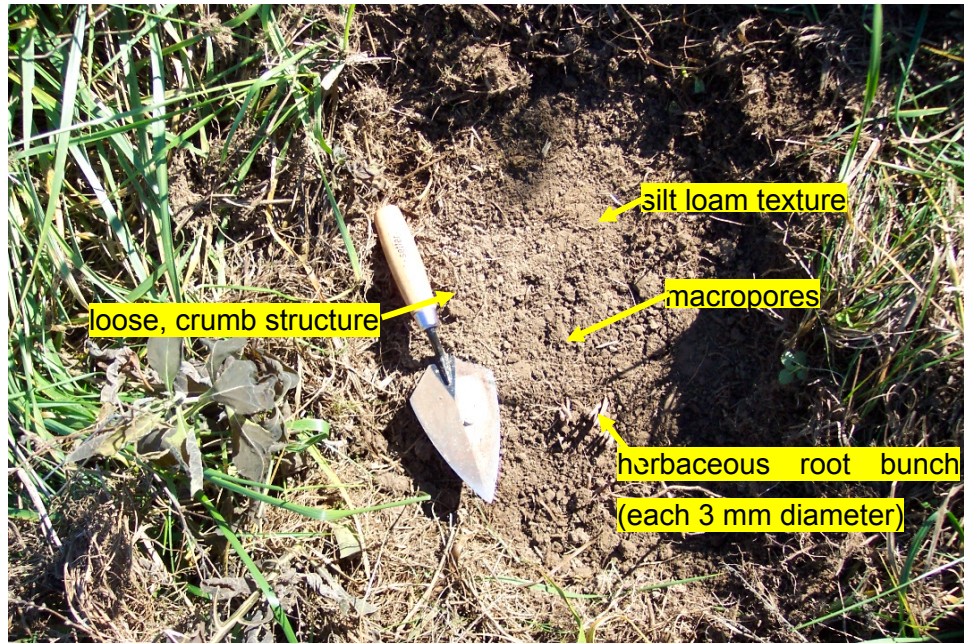


Figure 6.1. Factors regulating infiltration. Shown here on a surface site at <10 cm depth are 1) soil texture, 2) soil structure, 3) presence, orientation, length, size, and type of roots, and 4) presence of open macropores. Photo by author, November 2005.

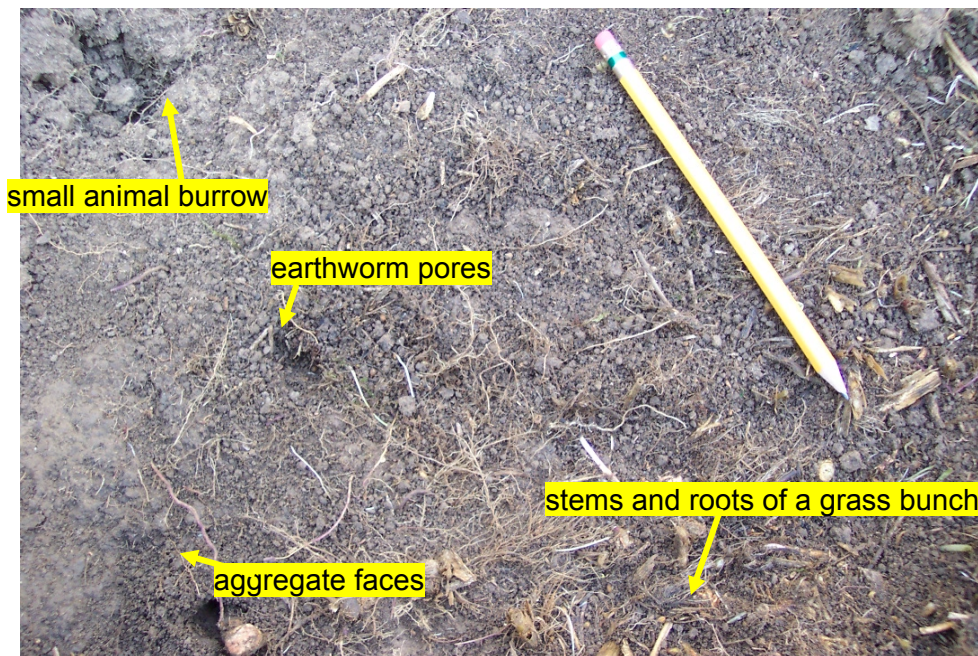


Figure 6.2. Numerous macropore sources exist within soil uncovered during a surface infiltration test at <10 cm depth inside a small sink on the upper sideslope of Hillslope A. Lower bases of grass stems are exposed here, and the fine root systems that splay downwards directly below this level create only small mesopores. Soil was 46-49 cm deep under the infiltrometer disk, and a  $K(-3)$  value of  $2.53 \text{ cm hr}^{-1}$  was generated by the sizes and depths of penetration of the combined factors. Photo by author, November 2005.

Infiltration rates were most often not dominated by a single influencing variable. Instead, the combination of factors acting together at a single site determined not only the final steady state rates, but also the time it took to achieve a steady rate as well as the degree of variation between measurements during the test period. Because of the integration of variable actions, similar final steady state rates often resulted from quite different combinations of factors. The hydraulic conductivity  $K(-3)$  values generated by light soil texture, crumb structure, and numerous roots and macropores at <10 cm at the site shown in Figure 6.2 almost equaled the  $K(-3)$  values generated for the blocky, dense clay soil at 55 cm depth in Figure 6.3 that had few fine roots and macropores, but lay just 15 cm above fractured bedrock.



Figure 6.3. Pit 14 infiltration tests at 55 cm were taken less than 15 cm above bedrock in soil found to be 60% clay with few to common fine roots between the disk and the root mat on the rock face. Near-saturation  $K(-3)$  calculated for this spot was  $2.48 \text{ cm hr}^{-1}$ , which almost equals the conductivity calculated for the deep-soiled, much more organic and pore rich sink location shown in Figure 6.2. Photo by author, July 2005.

Because texture, structure, and rock presence were often the same across forest and grass divisions, differences in infiltration rates related to vegetation tended to be blurred. In addition, vegetation-related differences were controlled by volume and perhaps orientation of roots that lay directly under the infiltrometer disk location. Because tests had to be run on level surfaces, coarse potential tree root preferential flow pathways were not typically measured, and it is possible that this lack may bias forest measurements. All of the above factors are reflected in the statistical analysis of the infiltration data, which finds only moderate differences between forest and grass infiltration and conductivity values at equal depths, but discernible differences in associations of variables that regulate conductivity.

### **General Infiltration Rate and Hydraulic Conductivity Data by Depth**

Mean values for steady state infiltration rate measurements and unsaturated hydraulic conductivity calculations were determined for categories set up according to depth and vegetation type (Table 6.1). This data set does not include the <10 cm measurements collected for the special grass surface tests. For the reasons discussed above, individual test values varied greatly between sites and often between tests in the same pit location.

Mean values for < 10 cm were highly variable. If all measurements at this depth are considered, little difference is shown between forest and grass, though forest rates are somewhat larger at higher tensions, with differences disappearing at near saturation. However, the <10 cm grass rates are strongly influenced by the large values obtained during a single test, run #2 in pit 4, where conductivity was determined to be  $13.46 \text{ cm hr}^{-1}$  at  $K(-3)$ . Elimination of pits 1 through 4 from the data shows that on the sideslopes, forest conductivity at <10 cm at a tension of -3 is more than two and a half times that of grass (Table 6.1). Data from this sideslope data set suggests that infiltration is higher at the surface (<10 cm) under forest than grass, and that the difference manifests best at near saturation conditions.

At 25 cm, examination of all pit measurements shows that overall infiltration and conductivity values are higher in forest than grass. These results stem largely from three forest sites: pit 1, where infiltration at a tension of -3 was recorded at 8.0 cm/min, and pits 7 and 8, in which the -3 infiltration rates at 25 cm depth were 5.0 and 6.7 cm/min respectively. In contrast to these high infiltration rates, the first 25 cm test run in forest pit 5 was taken in that portion of the pit underlain by dense yellow clay and few roots, and  $K(-3)$  for that test was only 0.81 cm/hr. This points out the huge variation created by the site specific factors that influence infiltration: in pits 1, 7, and 8, tests were made over soil that supported medium to coarse tree roots and/or nearby fractured rocks (Figures 4.2).



Table 6.1

Mean Infiltration Rates and Hydraulic Conductivity (K) Values for Depth and Vegetation Type Categories

(Infiltration rates and unsaturated K estimates are given for tensions of -15, -8, and -3)

| Depth (cm)          | Forest                             |      |      |                             |       |       | Grass                              |      |      |                            |       |       |
|---------------------|------------------------------------|------|------|-----------------------------|-------|-------|------------------------------------|------|------|----------------------------|-------|-------|
|                     | Infil Rates (cm <sup>3</sup> /min) |      |      | K(h) (cm hr <sup>-1</sup> ) |       |       | Infil Rates (cm <sup>3</sup> /min) |      |      | K(h) (cm h <sup>-1</sup> ) |       |       |
|                     | -15                                | -8   | -3   | K(-15)                      | K(-8) | K(-3) | -15                                | -8   | -3   | K(-15)                     | K(-8) | K(-3) |
| < 10 (all pits)     | 0.43                               | 0.67 | 1.58 | 0.26                        | 0.8   | 2.86  | 0.30                               | 0.55 | 1.59 | 0.34                       | 0.95  | 2.94  |
| <10 (pits 1-4 only) | 0.90                               | 1.03 | 1.33 | 0.32                        | 0.71  | 1.05  | 0.53                               | 1.00 | 3.00 | 0.64                       | 1.70  | 5.59  |
| < 10 (pits 5-14)    | 0.26                               | 0.51 | 1.6  | 0.24                        | 0.84  | 4.70  | 0.19                               | 0.36 | 0.99 | 0.21                       | 0.63  | 1.81  |
| 25 (all pits)       | 0.67                               | 1.26 | 3.51 | 0.5                         | 2     | 6.35  | 0.38                               | 0.79 | 2.26 | 0.49                       | 1.43  | 4.17  |
| 25 (pits 1-4 only)  | 1.53                               | 2.27 | 4.50 | 0.75                        | 3.17  | 6.80  | 0.70                               | 1.17 | 2.47 | 0.73                       | 1.87  | 3.96  |
| 25 (pits 5-14)      | 0.23                               | 0.75 | 3.01 | 0.38                        | 1.41  | 6.12  | 0.3                                | 0.7  | 2.21 | 0.43                       | 1.32  | 4.23  |
| 55 (all pits)       | 0.74                               | 1.6  | 2.73 | 0.98                        | 1.88  | 3.57  | 0.46                               | 0.91 | 2.25 | 0.48                       | 1.48  | 3.88  |
| 85                  | 0.39                               | 0.95 | 2.13 | 0.56                        | 1.5   | 3.50  | 0.39                               | 0.91 | 2.07 | 0.56                       | 1.48  | 3.45  |
| 125                 | 0.11                               | 0.25 | 1    | 0.15                        | 0.5   | 2.05  | 0.1                                | 0.16 | 0.45 | 0.09                       | 0.28  | 0.82  |

Despite the large  $K(-3)$  values determined for pits 7 and 8, infiltration rates at higher tensions of -15 and -8 for these pits are low, and are similar to those rates generated under grass at these tensions. If just the data for sideslope pits (pits 5 through 14) at 25 cm depth is examined, differences in infiltration rates at -15 and -8 are negligible between forest and grass, but grow larger with increasing saturation, so that conductivity at  $K(-3)$  is half again as high as that under grass. Data obtained at 25 cm for grass showed a consistent range of measurements, and little change in grass mean values occurred by eliminating pits 1 thru 4 from the data. This suggests that the values in Table 6.1 are fairly good estimates of general grass infiltration and conductivity at the 25 cm depth. The overall results of infiltration tests for the 25 cm level indicate that tree roots increase flow over that promoted by grass roots. On the upper mid-slopes, where soils are thin and roots are in close contact with rock faces, higher infiltration capacity in forest than grass also seems to only occur under near saturation conditions.

Infiltration rates and conductivity values at 55 cm are very similar between forest and grass both with and without incorporation of data from pits 1 to 4. Grass  $K(-3)$  values are slightly higher, but this may be partly attributed to measurements from Pit 9, which had 25-40% small to medium rounded pebbles between 40 and 60 cm depth. As noticed in alluvium pits in the hill base, infiltration increases where gravelly clay layers are present. At grass pit 9, infiltration at 55 cm at a tension of -3 was 3.58 cm/min, giving a conductivity estimate of 6.81 cm  $hr^{-1}$  for that site. The high rates obtained at grass pit 9, plus the fact that lower mid-slope forest pits contained heavy alluvial clays without large stone proportions at 55 cm, suggest that the data may not correctly represent the full range of difference between forest and grass infiltration rates at this depth. In addition, if infiltration rates for all pits combined at 55 cm are examined, they can be seen to be slightly higher than all of the infiltration rates for grass. Because conductivity is calculated based on the differences between infiltration rates rather than just the rates, higher infiltration rates may sometimes generate lower conductivity values.

Ranges of infiltration and conductivity values at 85 cm were relatively high and consistent. Data in Appendix 5, Data Used in Statistical Analyses, show that infiltration rates for many lower depths in pits 1 through 4 actually increase over rates for higher soil layers, so that 55 or 85 cm measurements may be higher than <10 or 25 cm measurements. These elevated measurements appear to reflect gravel content in the 2 to 60 mm range in these clayey layers. Increased infiltration at 85 cm in comparison with overlying soil layers is best represented by pit 4, where  $K(-3)$  values of 4.38 and 4.13 cm  $hr^{-1}$  contrast with values of 1.44 and 1.86 cm  $hr^{-1}$  at 55 cm depth. Similar elevated measurements at deeper depths occur in forest pit 6 and grass pit 12, but in both of these cases, readings were obtained from soil just above bedrock. In pit

12, this layer was comprised of decomposing limestone channers and flagstones. Because of the coincidence of gravelly conditions at 85 cm in pits 1 through 4 with the stony BC horizon conditions found at this depth range on sideslopes, no difference can be detected between forest and grass estimates at this depth category.

At 125 cm, forest rates were clearly higher than grass rates at near saturation tensions. In the four sites tested, and forest tests had  $-3$  infiltration rates and  $K(-3)$  values more than double that measured under grass. Although this is strongly suggestive of much higher grass impedance, particularly since these results were consistent across the two different hillslopes where pits were sited, only 4 tests were run at 125 cm and do not provide a large enough sample for statistical evaluation. The drop in conductivity between 85 cm and 125 cm does offer evidence for impeded entry into the lowest soil layers, and suggests that under high input, flow will be directed laterally across the lowest soil layers at the slope base.

In summary, infiltration rates at  $<10$  cm are lower than underlying layers, and highest infiltration rates occur at 25 cm. Upper soil layers tend to have higher infiltration rates under forest than grass at all tensions, but chiefly manifest this higher rate in thin sideslope soils at only near saturation conditions. Little difference is found between forest and grass rates at 55 and 85 cm, but site specific influences may override or blur the possible range of forest capabilities. Infiltration rates at 125 cm are definitely higher under forest than grass, but significance is limited by low sample number. These findings, along with possible variables responsible for their development, are explored further through statistical analysis.

## **HYDROLOGIC DATA ANALYSIS**

### **Variables**

A number of both direct and surrogate measurements were analyzed to find evidence for influences on water movements. Infiltration and conductivity values were set up according to soil depth and vegetation type, along with measured values for soil layer clay content, organic content, bulk density, particle density, and porosity (Appendix 5, Data Used in Statistical Analysis). Clay content was selected because of the known association of clay with flow impedance. Soil layer organic content was accepted as a measurement likely to represent humus and fine roots, though not coarse tree roots, and bulk density and particle density were considered to partially represent soil texture and structure. Although porosity is a composite measure calculated based on bulk density and particle density, bulk density, particle density, and organics values were all determined through independent tests. For augered soil samples,

layer clay content was also compared according to depth, vegetation, geology, and association with drainage conditions created by surface and bedrock topography.

### Augered Soil Sample Analysis

Soil depth differed significantly between the two broad geological categories of Tyrone and Lexington Limestone soils, with the Tyrone being much shallower. However, most statistical analysis of augered soil sample data focused on clay content and its distribution in the main study area. Statistical analysis of the data from Hillsopes A, B, C, and F (Figure 4.3) showed that clay percentages do not differ significantly between forest and grass at any depth. This finding was duplicated when infiltration pit data was added, as is shown in the nonparametric Kruskal-Wallis ranking test scores in table 6.2 that compare all forest and clay percentages measured at equal depths. However, distributions of clay percentages at all depths show a great deal of variation, as is demonstrated in figure 6.4 for clay percentages at <10 and 25 cm. This variation reflects the wide range of site specific topographic and parent material influences responsible for soil texture. This suggests that broad-scale comparisons of forest and grass soil textures by depth may not provide a sufficiently sensitive means for distinguishing biogeomorphic influences on soil properties from other environmental factors.

Table 6.2  
Comparison of Mean Forest and Grass Clay Percentages by Depths  
Wilcoxon/Kruskal-Wallis Test Scores

(Probabilities determined for 1-way tests, with Chi-Square approximations.

| Depth (cm) | Forest Count | Grass Count | Chi Square | Prob >ChiSq |
|------------|--------------|-------------|------------|-------------|
| 10         | 40           | 38          | 0.1226     | 0.7263      |
| 20-30      | 38           | 39          | 1.2918     | 0.2557      |
| 40-50      | 24           | 25          | 0.0256     | 0.8728      |
| 60-70      | 21           | 30          | 1.4093     | 0.2352      |
| 80-95      | 11           | 19          | 0.0375     | 0.8464      |
| >100       | 9            | 8           | 1.1217     | 0.2895      |

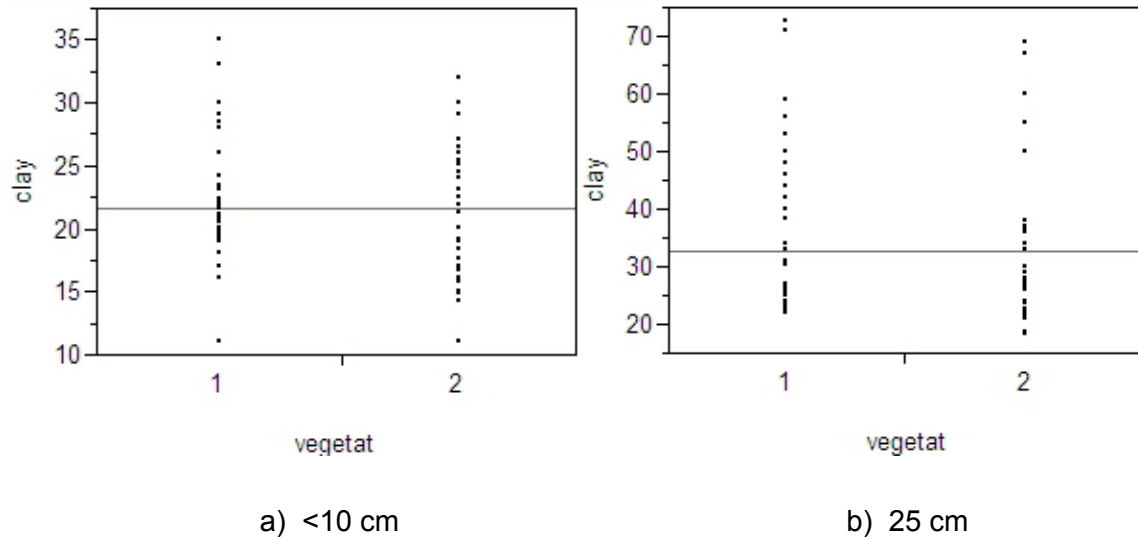


Figure 6.4. Distributions of combined clay percentages of augered soil samples and infiltration pit samples at (a) < 10 cm (surface) and (b) 25 cm. Black lines indicate total combined group means. 1 = forest, 2 = grass.

Statistical analysis of augered soil samples did show that soil layer clay percentages could be characterized by two major correlations: with soil depth, and with site association to drainage conditions. To characterize drainage conditions, each site was placed into one of five broad categories determined from a combination of surface and bedrock topography considerations: 1) freely draining, with no restrictive features, 2) pocket, as in a bench base or a karren pit measured by probing, 3) within a visible surface linear depression or channel, 4) overlying bentonite visible in auger samples, and 5) unknown.

Analysis suggests that depth and drainage conditions work together to help create the clay content found in study area soil layers. Linear regression determined that clay percentage is related to soil depth at greater than 99% significance ( $R^2 = .408$ ), but that the coefficient of determination increases to  $R^2 = .643$  when only sites labeled as “pockets” are included. At pocket sites, clay percentages tend to increase continuously to bedrock.

If the clay percentage of only the soil samples extracted from directly above bedrock is considered, clay is also significantly related to the drainage classes as described above at the 99% level (Figure 6.5). The clay percentage-to-drainage class relationship varied at other depths, with significant relationships found at 20-30 and 40-50 cm, but not at <10, 60-70, or 80-90 cm. The significant relationships at 20-30 and 40-50 cm reflect the fact that banks, hill knobs, and soils within or above water pathways will be shallower than soils in other locations, causing horizons with relatively low clay percentages to develop at those depths. At 65 and 85 cm, even if deep soil overlies free drainage at the bedrock surface, clay content will be

undistinguishable between drainage classes because of increase with depth, and will only reflect a decrease in clay content directly above the bedrock where water movement takes place. So whereas clay content is most strongly related to soil depth, its distribution is moderated by drainage, which in turn partially governs soil depth globally.

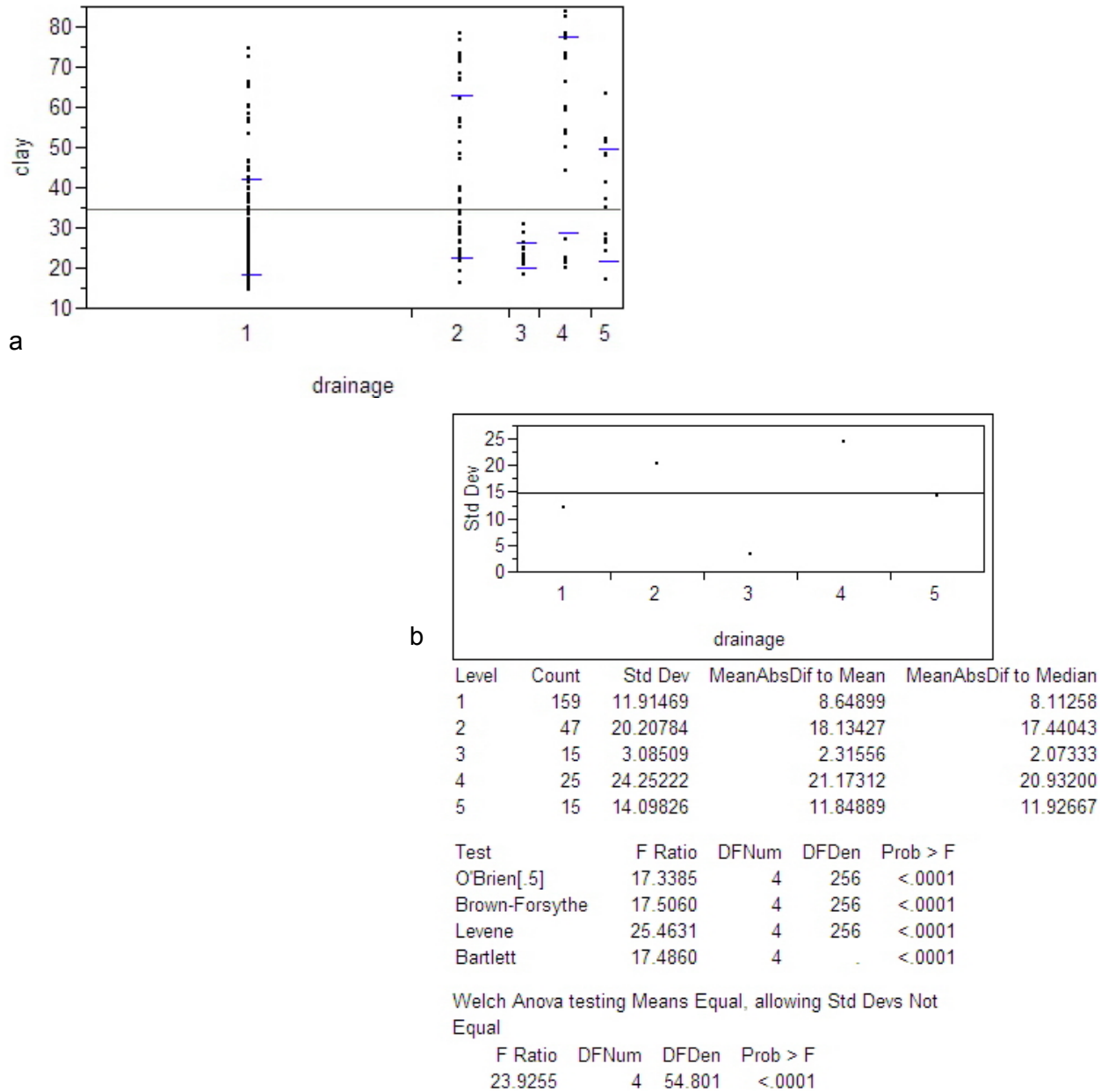


Figure 6.5. Analysis of percent clay in soil above bedrock by drainage categories (oneway). (a) Clay is given as percent. Drainage refers to categorical classifications: 1 = freely draining, 2 = pocket, 3 = within a visible linear depression, 4 = betonite, 5 = unknown. Black horizontal lines indicate total combined groups means. Blue bars are standard deviation lines. (b) With unequal variance shown by Levene and Brown-Forsythe tests, Welch anova testing is used to show unequal means for drainage categories.

The determination of a significant relationship between clay and drainage, particularly as it occurs directly above bedrock, offers a way to assess the drainage capacity of hillslope sites. In the thin, dense clay soils of the study area, particles are likely to be lost from profile bases where drainage is rapid either through the epikarst or along its surface. A decrease of clay in the layer above bedrock may result. Soil layer clay content thus provides one line of evidence for determining general water movement pathways in the slopes.

## **Analysis of Infiltration Data**

### *a) Distributions*

Distributions for all samples for each surrogate variable were explored to determine their shape before using the data for statistical analysis. Clay was found to be log-normally distributed through use of best fit procedures, which compared data distributions to algorithms that defined median and mean values for various distribution types. Skew in the clay percentage data was positive, with mean value equaling 36.3% and median value equalling 29%. Clay percents for only the infiltration pit data presented a somewhat bi-modal shape around a sample mean of 45%. Particle density, bulk density, and porosity totals were all normal in distribution, although bulk density was negatively skewed. Total sample sets for organics were log-normally distributed with positive skew opposite to that of bulk density. Infiltration and conductivity data had log-normal distributions at infiltration rates for -8 and -3, and  $K(-8)$ , and exponential distributions for infiltration at -15 and  $K(-15)$  and  $K(-3)$ . These infiltration distributions all centered on smaller values with positive skew and large value outliers. Transforming organics and infiltration data to log base 10 helped normalize the data, but weakened relationships to other variables, such as clay content. This suggests correlation between the variables, and indicates that the data was best handled nonparametrically.

Comparisons between forest and grass were run across total sample sets, but most analysis involved looking at samples contrasted by depth categories. Many of these smaller sets were not normally distributed and often did not have equal variances. At some depths, skewed infiltration and conductivity results responded to similarly distributed soil properties represented by various surrogate measurements, so that comparative data set variances were often similar, despite the data distributions. Both nonparametric and parametric tests were run, along with regression testing of various potential best-fit lines. Thus consideration was given to distributions on a test-by-test basis, so that parametric tests were used where possible, but

conservative nonparametric results were accepted as best supporting most data comparisons. Figure 6.6 shows distributions at varying depths for forest and grass values of clay percentages, bulk density, porosity, particle density, and organics. Dots represent individual data points, and the clustering and spread of the smaller data sets can be clearly seen by examining individual sets.

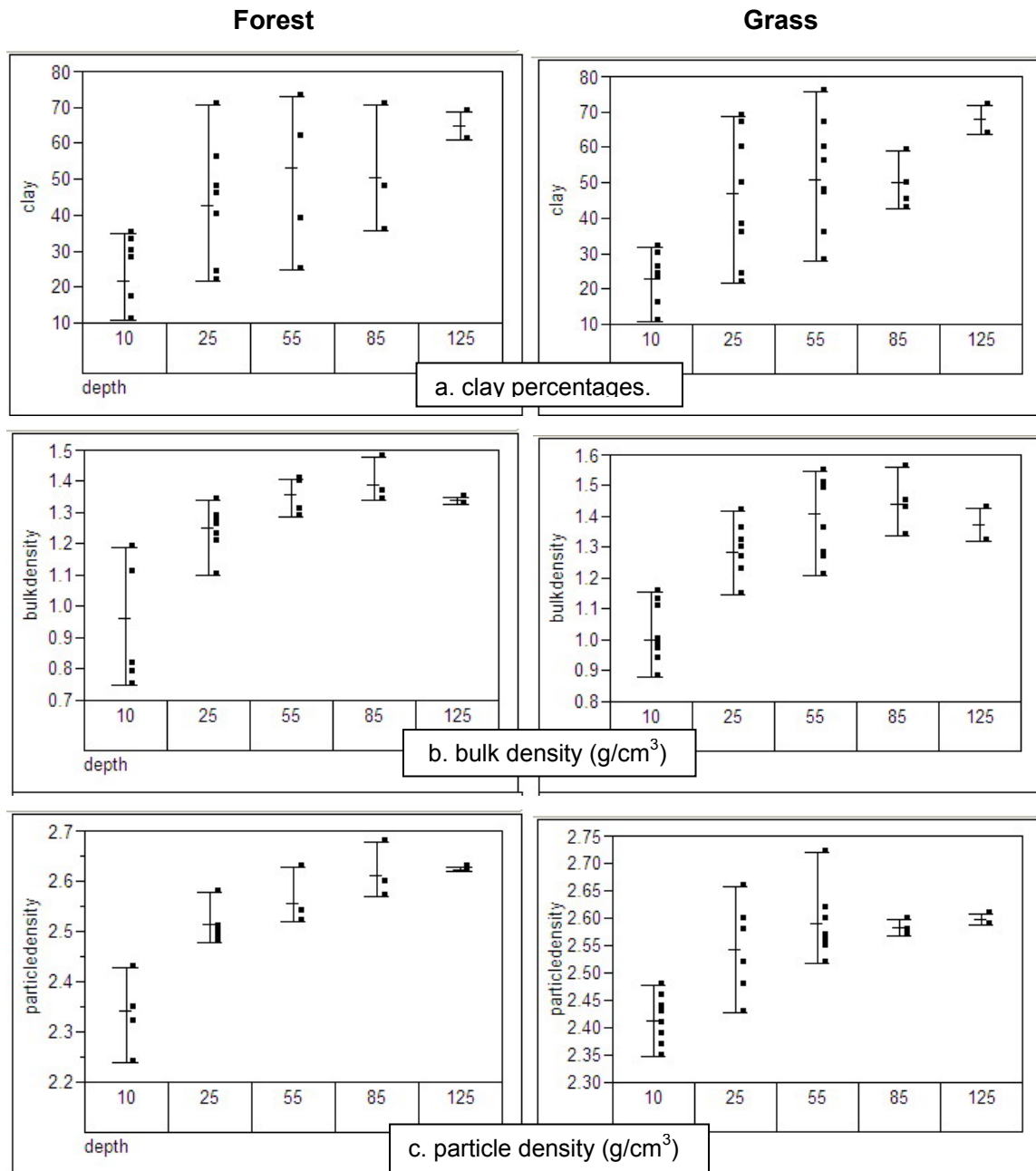


Figure 6.6. Distributions of total forest and grass values by depths. Mean and range are shown by lines. Dots represent data values. Note differences in scales between some forest and grass variables. (a) clay percentages, (b) bulk density, (c) particle density.



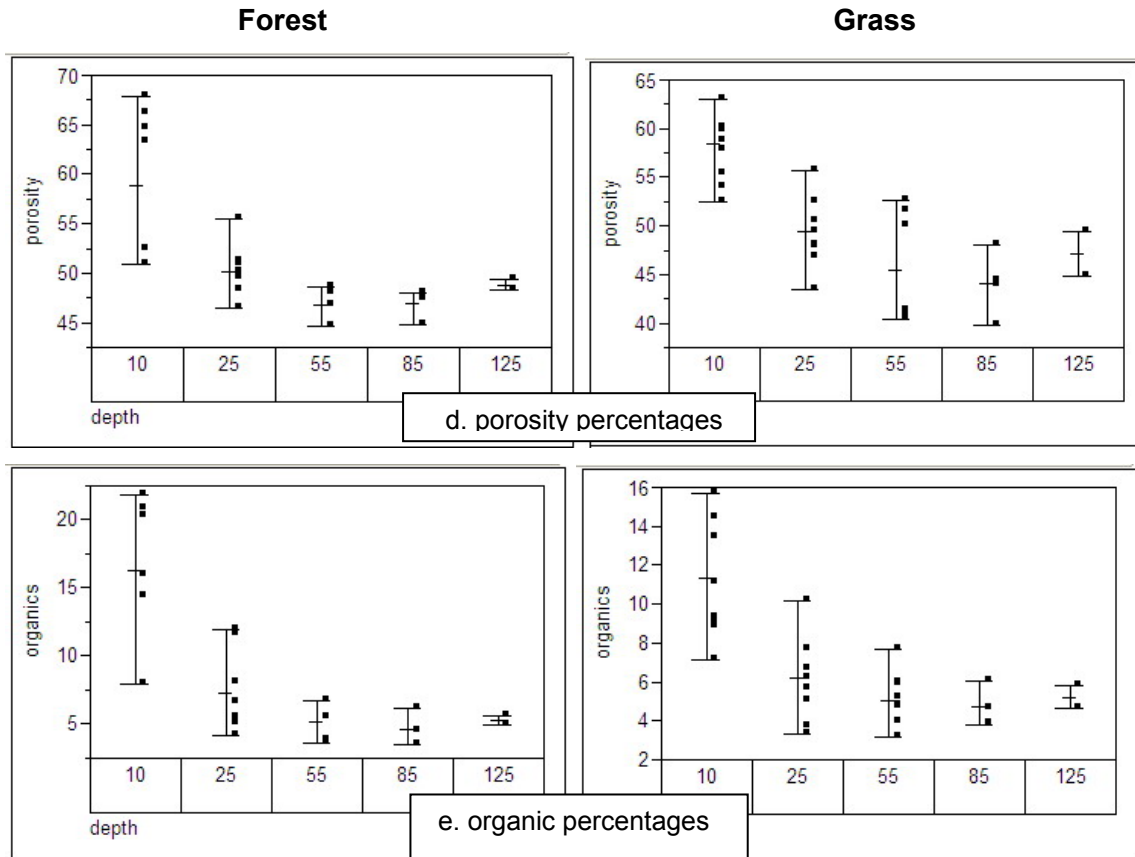


Figure 6.6. (continued). (d) porosity, and (e) organic percentages.

*b) Variable Associations*

When data do not conform to bivariate normal distribution, the degree to which two variables measured on a single subject are related may be determined by nonparametric tests that rank the data and calculate coefficients of that ranking (Sokal and Rohlf, 1997). The commonly used Pearson product-moment correlation coefficient calculates covariance based on bivariate normal frequency distribution, making it sensitive to outliers, unequal variances, and nonlinearity. For this project, Spearman’s rho ( $r_s$ ), a test that uses the Pearson correlation formula on ranked data, as opposed to the actual data, was used. Spearman’s rho eliminates many concerns with data distribution, yet like the Pearson coefficient yields a test value between 1 and -1, with 1 representing a perfect positive relationship, 0 representing no relationship, and -1 representing a complete inverse association (Sokal and Rohlf, 1997).

Surrogate variables and infiltration and conductivity rates were compared and contrasted to determine associations. In tables 6.3 and 6.4, Spearman’s rho and relationship probabilities

are given for the total data sets for both forest and grass. Correlations significant at the 95% level are shown in yellow and those at 90% level in green.  $\text{Prob}>|\text{Rho}|$  is calculated based on degrees of freedom and represents the probability that there is correlation between variables. The “Plot” shown on the right side of the tables visually demonstrates the direction of relationships as well as their relative sizes.

The independent tests show consistent relationships among clay content, bulk density, and organic content (Tables 6.3 and 6.4). Significance levels of test results between paired surrogate measurements were much the same between total forest and grass data sets. Clay corresponds significantly to bulk density and to a high degree of significance to particle density in both sets, but not to organics. Organics correlate significantly to bulk density, porosity, and particle density. The only major difference between forest and grass surrogate measure relationships appears in the relationship of porosity to clay, which is significant in the forest ( $P = 0.0059$ ), but not significant under grass ( $P = 0.2738$ ). Since porosity is a composite measure that strongly correlates with organics ( $P = <.0001$ ), the lack of significant correlation between grass porosity and clay content indicates that porosity is more randomized in relation to clay under grass than under forest because of the more dispersed distribution of grass root systems. Overall, as would be expected, where clay increases, particle density increases and causes bulk density to increase as well.

Subtle influences of surrogate variables on infiltration and conductivity can also be seen on tables 6.3 and 6.4 by considering correlation probabilities in combination with trends. Of the variables examined, clay and organics have the most pronounced influence on infiltration as determined by significance. Both are negative influences, in that increases in clay and organic matter both bring about decreased infiltration. The correlation of clay to infiltration in both forest and grass decreases as tension decreases from -15 to -3, showing that infiltration at saturation is little dependent on clay content. Organics at near saturation are also uncorrelated to infiltration, but in contrast to clay, organics had highest negative correlations with tensions of -8 in both forest and grass. The negative correlation between organics and infiltration may at least partly reflect the repellent tendencies created by organics in soils. Under the very dry conditions present when most pits were opened, hydrophobic topsoil tendencies were noted as discussed earlier, and this likely impeded water entry at higher tensions.

Bulk density is not statistically correlated to infiltration in either forest or grass, but it does display a consistent positive trend in its relationship to higher infiltration rates. This contrasts with the negative trends to infiltration created by clay and organics. This positive relationship trend between bulk density and infiltration is largest at an infiltration tension of -8. The positive

direction of the bulk density influence, which is opposite to the negative influence of organics, may reflect a tendency for water to move through the soil more easily where a moderate amount of clay is present to offset organic repellancy. Particle density is not significantly correlated to infiltration and has no discernable trends. Trends of porosity correlations to infiltration are all weakly negative and not statistically significant at 95% in either forest or grass, although correlations of porosity to infiltration at -8 and -3 both correlated negatively at the 90% level under grass.

The trends and significant correlations between surrogate measurements and infiltration rates suggest that rates are largely determined by the interactive influences of clay, organic matter, and bulk density. Both clay and organics strongly correlate with bulk density, but do so in opposite directions, with clay content positively related to bulk density and organic content negatively related to bulk density. Thus the influences of clay and organics tend to nullify each other, despite their common overall negative influence on infiltration.

The importance of the relationships between clay, organics and bulk density lies in the fact that organics at high tensions may offer enough resistance so that dry soils that have a slightly elevated bulk density, i.e. higher clay content, may promote greater infiltration than soils with lower clay content. The main effect of negative organic influence on infiltration is likely seen in topsoil layers, where grass organic matter is concentrated in root mats that may delay infiltration until near-saturation is reached. In deeper grass soil layers, increase in porosity and thus reduction of bulk density and decrease in clay impedance, is likely to provide an overall boost to infiltration. As interconnected grass root channels support preferential flow, infiltration is increased even though organics remain high in subsoil samples. Because larger roots were not included in organics samples under forest, infiltration and porosity under forest are not statistically correlated. Under grass, these are correlated at higher tensions at the 90% level.

Examination of this data thus suggests that differences between forest and grass infiltration, organics, and clay responses are established by differences in their rooting systems. In addition, the lack of correlation between porosity and clay under grass, as compared with the significant negative relationship between porosity and clay under forest, suggests that infiltration under grass is less limited by clay impedance than forest infiltration may be. Grass root networks are able to increase porosity and thus infiltration across the range of clay values found in the study area soils.

Table 6.3

Correlations for Total Forest Data Sets (N=30)

(yellow indicates statistical significance at 95 % confidence level, green at 90%)

| Variable         | by Variable      | Spearman Rho | Prob> Rho | Plot of Spearman Rho Value |
|------------------|------------------|--------------|-----------|----------------------------|
| clay             | infil15          | -0.5394      | 0.0021    |                            |
| clay             | infil8           | -0.3865      | 0.0349    |                            |
| clay             | infil3           | -0.1568      | 0.4080    |                            |
| clay             | K15              | -0.1223      | 0.5272    |                            |
| clay             | K8               | -0.0645      | 0.7348    |                            |
| clay             | K3               | 0.1231       | 0.5169    |                            |
| bulk density     | infil15          | 0.0725       | 0.7034    |                            |
| bulk density     | infil8           | 0.1425       | 0.4524    |                            |
| bulk density     | infil3           | 0.0216       | 0.9099    |                            |
| bulk density     | K15              | 0.2715       | 0.1542    |                            |
| bulk density     | K8               | 0.2457       | 0.1906    |                            |
| bulk density     | K3               | 0.0682       | 0.7201    |                            |
| bulk density     | clay             | 0.5511       | 0.0016    |                            |
| porosity         | infil15          | -0.0932      | 0.6244    |                            |
| porosity         | infil8           | -0.1512      | 0.4251    |                            |
| porosity         | infil3           | -0.0388      | 0.8388    |                            |
| porosity         | K15              | -0.2177      | 0.2566    |                            |
| porosity         | K8               | -0.2450      | 0.1918    |                            |
| porosity         | K3               | -0.0581      | 0.7602    |                            |
| porosity         | clay             | -0.4907      | 0.0059    |                            |
| particle density | infil15          | -0.0374      | 0.8443    |                            |
| particle density | infil8           | 0.0517       | 0.7862    |                            |
| particle density | infil3           | -0.0475      | 0.8032    |                            |
| particle density | K15              | 0.2226       | 0.2457    |                            |
| particle density | K8               | 0.2085       | 0.2689    |                            |
| particle density | K3               | 0.0535       | 0.7789    |                            |
| particle density | clay             | 0.6930       | <.0001    |                            |
| organics         | infil15          | -0.3312      | 0.0738    |                            |
| organics         | infil8           | -0.3748      | 0.0413    |                            |
| organics         | infil3           | -0.1849      | 0.3281    |                            |
| organics         | K15              | -0.2510      | 0.1891    |                            |
| organics         | K8               | -0.4170      | 0.0219    |                            |
| organics         | K3               | -0.1216      | 0.5220    |                            |
| organics         | clay             | -0.1693      | 0.3711    |                            |
| organics         | bulk density     | -0.7031      | <.0001    |                            |
| organics         | porosity         | 0.7488       | <.0001    |                            |
| organics         | particle density | -0.5520      | 0.0016    |                            |

-1-----0-----+1

Infiltration rates at tensions (cm<sup>3</sup>/min): infil(-15), infil(-8), infil(-3)

Hydraulic conductivity at tensions (cm hr<sup>-1</sup>): K (-15), K(-8), K(-3)

Table 6.4

Correlations for Total Grass Data Sets (N=47)

(yellow indicates statistical significance at 95 % confidence level, green at 90%)

| Variable         | by Variable      | Spearman Rho | Prob> Rho | Plot of Spearman Rho Value |
|------------------|------------------|--------------|-----------|----------------------------|
| clay             | infil15          | -0.5394      | 0.0021    |                            |
| clay             | infil8           | -0.3865      | 0.0349    |                            |
| clay             | infil3           | -0.1568      | 0.4080    |                            |
| clay             | K15              | -0.1223      | 0.5272    |                            |
| clay             | K8               | -0.0645      | 0.7348    |                            |
| clay             | K3               | 0.1231       | 0.5169    |                            |
| bulk density     | infil15          | 0.0725       | 0.7034    |                            |
| bulk density     | infil8           | 0.1425       | 0.4524    |                            |
| bulk density     | infil3           | 0.0216       | 0.9099    |                            |
| bulk density     | K15              | 0.2715       | 0.1542    |                            |
| bulk density     | K8               | 0.2457       | 0.1906    |                            |
| bulk density     | K3               | 0.0682       | 0.7201    |                            |
| bulk density     | clay             | 0.5511       | 0.0016    |                            |
| porosity         | infil15          | -0.0932      | 0.6244    |                            |
| porosity         | infil8           | -0.1512      | 0.4251    |                            |
| porosity         | infil3           | -0.0388      | 0.8388    |                            |
| porosity         | K15              | -0.2177      | 0.2566    |                            |
| porosity         | K8               | -0.2450      | 0.1918    |                            |
| porosity         | K3               | -0.0581      | 0.7602    |                            |
| porosity         | clay             | -0.4907      | 0.0059    |                            |
| particle density | infil15          | -0.0374      | 0.8443    |                            |
| particle density | infil8           | 0.0517       | 0.7862    |                            |
| particle density | infil3           | -0.0475      | 0.8032    |                            |
| particle density | K15              | 0.2226       | 0.2457    |                            |
| particle density | K8               | 0.2085       | 0.2689    |                            |
| particle density | K3               | 0.0535       | 0.7789    |                            |
| particle density | clay             | 0.6930       | <.0001    |                            |
| organics         | infil15          | -0.3312      | 0.0738    |                            |
| organics         | infil8           | -0.3748      | 0.0413    |                            |
| organics         | infil3           | -0.1849      | 0.3281    |                            |
| organics         | K15              | -0.2510      | 0.1891    |                            |
| organics         | K8               | -0.4170      | 0.0219    |                            |
| organics         | K3               | -0.1216      | 0.5220    |                            |
| organics         | clay             | -0.1693      | 0.3711    |                            |
| organics         | bulk density     | -0.7031      | <.0001    |                            |
| organics         | porosity         | 0.7488       | <.0001    |                            |
| organics         | particle density | -0.5520      | 0.0016    |                            |

-1-----0-----+1

Infiltration rates at tensions (cm<sup>3</sup>/min): infil(-15), infil(-8), infil(-3)

Hydraulic conductivity at tensions (cm hr<sup>-1</sup>): K (-15), K(-8), K(-3)

### *c) Clay vs. Organic Matter and Porosity*

When grouped separately, neither forest nor grass data showed significant relationships between clay and organics, as already shown in Tables 6.3 and 6.4. However, separation of clay vs. organics data by depth and vegetation categories indicates that these variables have different relationships to each other at varying depths under forest and grass.

In table 6.5, probability results and relationship directions from linear bivariate analysis, which tests changes between two continuous variables, are shown for clay and organics, and for clay and porosity. This analysis eliminated any repeated data points for surrogate measures. Significant positive relationships between clay and organics are found in topsoil (<10 cm) samples in both grass (95% level) and forest (90% level). Relationships between clay and organics are not significant under either type of vegetation at 25 cm, but the relationships again become significant below this depth. At depths of 55 to 85 cm, clay content under grass has a significant positive linear relationship to organics (Figure 6.7), whereas a significant linear relationship between clay and organics only occurs at depths of 85 cm under forest. At the same time, grass is associated with positive linear relationships between clay and porosity at all depths, while forest clay vs. porosity relationships at most subsoil depths are negative. At 55 cm, clay and porosity under grass are significantly related at the 95% level (Figure 6.7).

If the assumption is made that forest and grass soils had the same original texture, this data can be used to suggest that some evidence exists for clay movement in the grass profiles that differs from that occurring under forest. Assuming equal vertical translocation of organics and clay under both vegetation types, then clay and organics should be positively related. This occurs under both forest and grass, although the relationship is particularly high at 55 cm under grass. However, increase in porosity is likely to counteract an increase in clay content from colloidal transport, so that a negative relationship between porosity and clay would be expected at deeper profile depths. The fact that clay vs organics or porosity at 55 cm are positively related under grass and that a similar correlation is not found under forest, plus the fact that clay and organics at 85 cm are positively related under grass and negatively related under forest, suggest that grass roots facilitate clay accumulation at mid-profile levels. Whereas clay and organics may be translocated by both forest and grass root systems, a widespread, dispersed entry of clay may occur within grass root networks, so that clay increases even though porosity as a whole is higher.

In both forest and grass data sets, data sets were least related at 25 cm. At the 25 cm level, the relationship between clay, organics, and porosity is likely obscured by local site conditions and factors such as bioturbation.

Table 6.5

Bivariate Linear Fit of Clay vs. Organics and Porosity by Depths  
(yellow indicates statistical significance at 95 % confidence level, green at 90%)

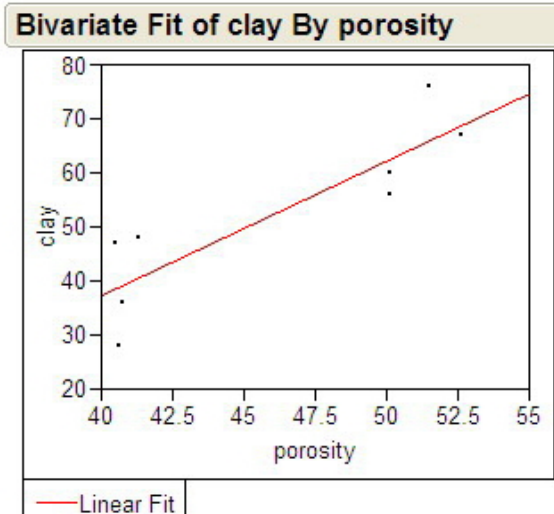
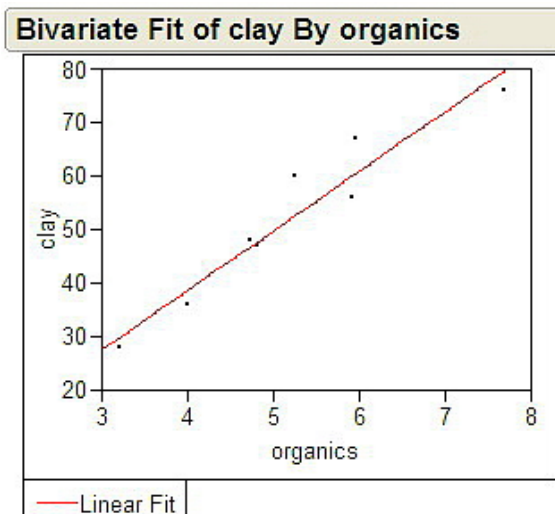
## Clay vs. Porosity

| Depth (cm) | Forest  |           |   | Grass   |           |   |
|------------|---------|-----------|---|---------|-----------|---|
|            | Prob >F | Direction | N | Prob >F | Direction | N |
| <10        | 0.0030  | +         | 6 | 0.4009  | +         | 8 |
| 25         | 0.8819  | -         | 7 | 0.2971  | +         | 8 |
| 55         | 0.6901  | +         | 4 | 0.0043  | +         | 8 |
| 85         | 0.0940  | -         | 3 | 0.1891  | +         | 4 |

## Clay vs. Organics

| Depth (cm) | Forest  |           |   | Grass   |           |   |
|------------|---------|-----------|---|---------|-----------|---|
|            | Prob >F | Direction | N | Prob >F | Direction | N |
| <10        | 0.0722  | +         | 6 | 0.0460  | +         | 8 |
| 25         | 0.3379  | +         | 7 | 0.2874  | +         | 8 |
| 55         | 0.1795  | +         | 4 | 0.0002  | +         | 8 |
| 85         | 0.0220  | +         | 3 | 0.0052  | +         | 4 |

When divided into forest and grass categories without division by depth, plots of clay vs. organics revealed clustering into two distinct groups in both vegetation types. This was most obvious in grass data, as shown in figure 6.8. Partitioning of the clay/organics data, based on splits in organics values that created the largest differences in group means, determined that the grass data were best divided into groups in which organics were  $\leq 8.89$  and organics were  $> 8.89$ . Further exploration of the data provides evidence for correlations between organics and soil properties set up by different vegetation within these partitions (Table 6.6).



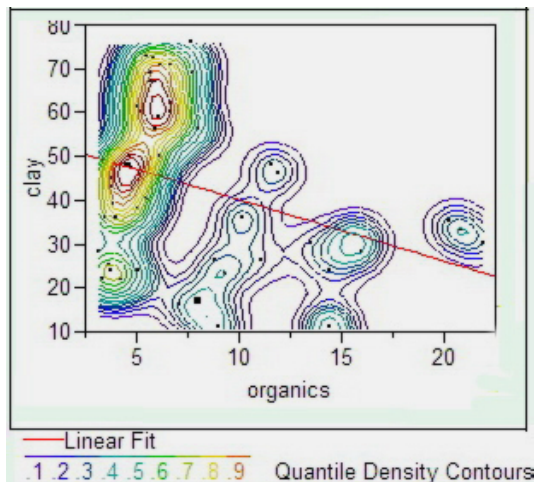
|  |    |          |         |         |
|--|----|----------|---------|---------|
| Linear Fit: clay = -5.554744 +<br>11.116297 organics |    |          |         |         |
| Summary of Fit                                       |    |          |         |         |
| RSquare  |    | 0.92106  |         |         |
| RSquare Adjusted                                     |    | 0.90790  |         |         |
| Root Mean Square Error                               |    | 4.80300  |         |         |
| Mean of Response                                     |    | 52.25    |         |         |
| Observations   |    | 8        |         |         |
| Analysis of Variance                                 |    |          |         |         |
| Source   | DF | Sum Squ  | Mn Squ  | F Ratio |
| Model  | 1  | 1615.086 | 1615.09 | 70.0115 |
| Error  | 6  | 138.4132 | 23.07   | Prob >F |
| C. Total   | 7  | 1753.500 |         | 0.0002  |

|  |    |          |         |         |
|--|----|----------|---------|---------|
| Linear Fit: clay = -62.22967 +<br>2.4895679 porosity |    |          |         |         |
| Summary of Fit                                       |    |          |         |         |
| RSquare  |    | 0.76776  |         |         |
| RSquare Adjusted                                     |    | 0.72905  |         |         |
| Root Mean Square Error                               |    | 8.23848  |         |         |
| Mean of Response                                     |    | 52.25    |         |         |
| Observations   |    | 8        |         |         |
| Analysis of Variance                                 |    |          |         |         |
| Source   | DF | Sum Squ  | Mn Squ  | F Ratio |
| Model  | 1  | 1346.265 | 1346.26 | 19.8352 |
| Error  | 6  | 407.235  | 67.87   | Prob >F |
| C. Total   | 7  | 1753.500 |         | 0.0043  |

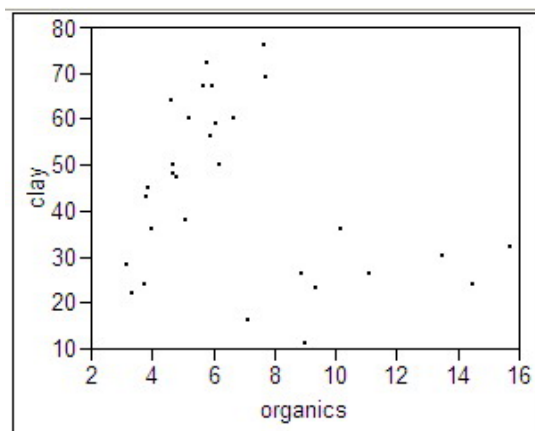
Figure 6.7. Linear regression tests of clay vs. organics and porosity for 55 cm grass data.

Samples in the organics  $\leq 8.89$  group come from deeper, clay-rich depths. At these deeper levels, organics are significantly correlated to clay in both forest and grass, but correlations to other variables are otherwise opposite between vegetation types. In the forest data, bulk density and particle density are positively correlated to a significant degree, but no correlation exists between organics and bulk density, particle density, or porosity. In contrast, under grass, bulk density is not correlated to particle density, but organics are highly correlated to both porosity and bulk density, though not to particle density.

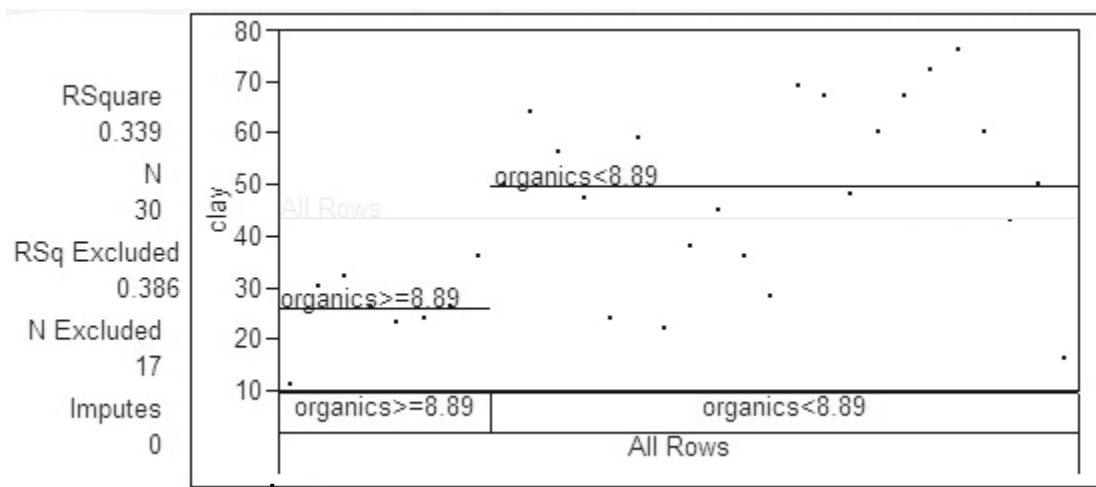




a



b



c

|          |          |
|----------|----------|
| All Rows |          |
| Count    | 30       |
| Mean     | 43.5     |
| Std Dev  | 18.44797 |

|                  |           |
|------------------|-----------|
| organics >= 8.89 |           |
| Count            | 8         |
| Mean             | 26        |
| Std Dev          | 7.4642003 |

|                 |           |
|-----------------|-----------|
| organics < 8.89 |           |
| Count           | 22        |
| Mean            | 49.863636 |
| Std Dev         | 17.097188 |

Figure 6.8. Clay percent vs. organics. (a) Bivariate nonparametric density diagram of the relationship between clay and organics values, with a bivariate fit probability of 0.0321 (N = 52;  $R^2 = 0.089$ ). (b) Clay vs. organics distribution for grass values only, showing clustering of measurements into two groups. (c) Partitioning of grass clay vs. organics data shows that the largest break as determined by group means of clay percentages occurs at organics  $\geq 8.89$ .

Table 6.6  
Correlations of Organics According to Partitions  
(yellow indicates statistical significance at 95 % confidence level, green at 90%)

| Subsoil Partition - Organics ≤ 8.89 Forest (N=15) |                  |              |           | Plot            |
|---|------------------|--------------|-----------|-----------------|
| Variable  | by Variable      | Spearman Rho | Prob> Rho | -1-----0-----+1 |
| particle density                                  | bulk density     | 0.7955       | 0.0004    |                 |
| organics  | bulk density     | -0.1950      | 0.4862    |                 |
| organics  | porosity         | 0.2681       | 0.3340    |                 |
| organics  | particle density | 0.0466       | 0.8691    |                 |
| organics  | clay             | 0.4597       | 0.0360    |                 |

| Subsoil Partition - Organics ≤ 8.89 Grass (N = 23) |                  |              |           | Plot           |
|--|------------------|--------------|-----------|----------------|
| Variable   | by Variable      | Spearman Rho | Prob> Rho | 1-----0-----+1 |
| particle density                                   | bulk density     | 0.2109       | 0.3340    |                |
| organics   | bulk density     | -0.6449      | 0.0009    |                |
| organics   | porosity         | 0.6838       | 0.0003    |                |
| organics   | particle density | 0.1073       | 0.6261    |                |
| organics   | clay             | 0.5624       | 0.0003    |                |

| Topsoil Partition - Organics > 8.89 Forest (N = 7) |                  |              |           | Plot           |
|--|------------------|--------------|-----------|----------------|
| Variable   | by Variable      | Spearman Rho | Prob> Rho | 1-----0-----+1 |
| particle density                                   | bulk density     | 0.5049       | 0.2478    |                |
| organics   | bulk density     | -0.7027      | 0.0782    |                |
| organics   | porosity         | 0.6429       | 0.1194    |                |
| organics   | particle density | -0.7783      | 0.0393    |                |
| organics   | clay             | -0.1724      | 0.657     |                |

| Topsoil Partition - Organics > 8.89 Grass (N = 7) |                  |              |           | Plot           |
|---|------------------|--------------|-----------|----------------|
| Variable  | By Variable      | Spearman Rho | Prob> Rho | 1-----0-----+1 |
| particle density                                  | bulk density     | 0.6847       | 0.0897    |                |
| organics  | bulk density     | -0.6071      | 0.1482    |                |
| organics  | porosity         | 0.5714       | 0.1802    |                |
| organics  | particle density | -0.6307      | 0.1289    |                |
| organics  | clay             | 0.5309       | 0.1144    |                |

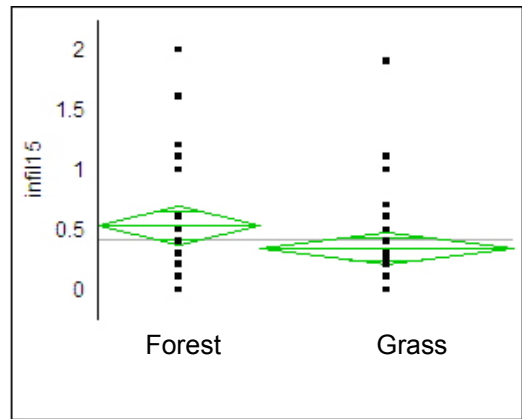
As discussed in the previous subsection, this data indicates that grass roots act diffusely to lower bulk density. This data also follows the findings discussed earlier in this subsection, in that significant positive clay vs. organics grass correlations, coupled with lack of correlation of organic matter to porosity under forest but positive significant correlation under grass, indicate that clay content in deeper soil layers corresponds to root growth under grass. This data suggests that grass roots are active in encouraging clay accumulation at deeper profile depths.

Organics at >8.89 all occurred in the highest soil horizons where overall clay content was low. Grass and forest correlation magnitudes and directions become very similar in these highest soil layers, except for the clay to organics relationship, which is negative in the forest and positive in the grass. The significant negative correlation of organics to forest topsoil particle density likely stems from humus, which in the forest may be high enough to replace a proportion of the soil mineral content. In the grass topsoil, the root mat to some extent traps clay particles and binds them into aggregates, so that a nonsignificant positive trend develops between organics and clay. Although high organic content should somewhat limit infiltration into both forest and grass topsoils, the differing distribution of organic matter as humus and roots, along with site dependent clay content, should govern their comparative infiltration capacities.

#### *d) Infiltration Comparisons by Vegetation Types*

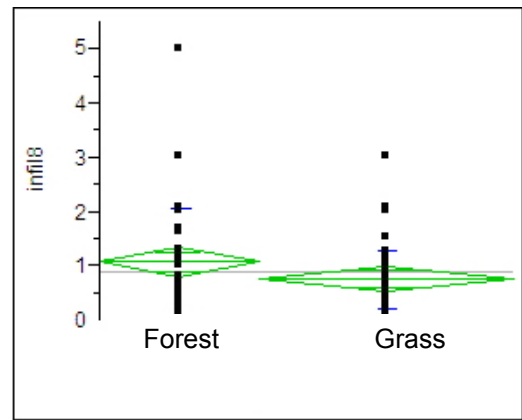
Infiltration rates at tensions of -15, -8 and -3 for all combined forest and grass measurements were compared through independent groups t-tests assuming unequal variances. Graphs of group means and confidence limits for each vegetation type (forest N=30, grass N = 46), along with t-test statistics, are shown in figure 6.9. One-tailed test results show that there is a statistical difference at the 95% level between forest and grass at a tension of -15 (Prob >t = 0.0489), a significant one-tailed group difference at the 90% level (0.0518) at a tension of -8, and no statistical difference between groups at a tension of -3. Group means become increasingly similar as tensions decrease toward saturation, and in all total group comparisons forest means are higher than grass means, suggesting at least a trend toward increased infiltration capacity in forest over grass that decreases at near saturation conditions. This trend of significant differences at high tensions (-15), but not at near saturation (-3), appears opposite from the trend observed during comparison of forest and grass mean infiltration values for higher soil layers in sideslope locations (Table 6.1). A tendency towards higher infiltration under forest than grass under near saturation as opposed to higher (-15 ) tension is seen in the mean values at <10 and 25 cm depths. Thus, the lumped data sets may hide different factors responsible for infiltration at varying depths.

| Infiltration (-15) Forest and Grass Differences<br>(forest N = 30, grass N = 46) |          |           |          |
|--|----------|-----------|----------|
| Difference   | 0.19442  | t Ratio   | 1.693325 |
| Std Err Dif  | 0.11482  | DF        | 41.61454 |
| Upper CL Dif   | 0.42619  | Prob >  t | 0.0979   |
| Lower CL Dif   | -0.03735 | Prob > t  | 0.0489   |
| Confidence   | 0.95     | Prob < t  | 0.9511   |



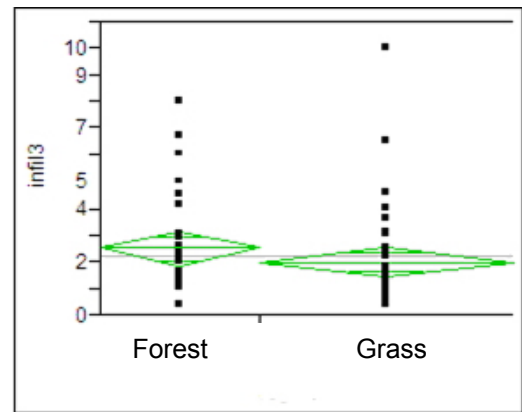
a

| Infiltration (-8) Forest and Grass Group Differences |          |           |          |
|--|----------|-----------|----------|
| Difference   | 0.32388  | t Ratio   | 1.664918 |
| Std Err Dif  | 0.19453  | DF        | 40.72203 |
| Upper CL Dif   | 0.71683  | Prob >  t | 0.1036   |
| Lower CL Dif   | -0.06907 | Prob > t  | 0.0518   |
| Confidence   | 0.95     | Prob < t  | 0.9482   |



b

| Infiltration (-3) Forest and Grass Group Differences |         |           |          |
|--|---------|-----------|----------|
| Difference   | 0.4948  | t Ratio   | 1.185105 |
| Std Err Dif  | 0.4175  | DF        | 57.10111 |
| Upper CL Dif   | 1.3309  | Prob >  t | 0.2409   |
| Lower CL Dif   | -0.3412 | Prob > t  | 0.1204   |
| Confidence   | 0.95    | Prob < t  | 0.8796   |



c

Figure 6.9. T-test (2-tailed) between-group differences for infiltration rates categorized by vegetation types. Group differences are (a) significant at infiltration (-15) at the 95% level, (b) significant at infiltration (-8) as the 90% level, and (c) not significant at infiltration (-3). Tests assume unequal variances. Dark horizontal lines show combined group means for each test. Mean values are indicated by widest lines in diamonds. Height of diamond indicates 95% confidence intervals, and shorter lines are overlap marks. An overlap mark in one diamond which lies closer to the mean of another diamond than the other diamond's overlap mark indicates that the group means are statistically the same.

When divided by depth categories, the individual forest and grass groups have unequal variances and too few cases to support parametric testing. Conservative nonparametric ranking tests that compare forest and grass infiltration and conductivity by depth categories are shown in table 6.7. The composite t-test measures of group infiltration as just described do not appear to adequately reflect changes with depth. However, when forest and grass infiltration and conductivity rates are divided by depths, they also show no statistically significant differences between forest and grass (Table 6.7).

The largest significant difference between forest and grass rates by depths occurs at the 90% level at <10 cm at a -8 infiltration tension. If just the <10 cm readings obtained on the sideslope of the hill (pits 5 through 14) are examined, then significance at the 90% level can also be detected between forest and grass at tensions of both -8 and -3 (Table 6.7). Thus, although the straightforward comparisons of group means shown in table 6.1 indicate that forest infiltration may be somewhat larger than that of grass in upper soil layers under near saturation conditions, this effect is only weakly supported by statistics. Altogether, trends observed in the lumped forest and grass data sets and during examination of infiltration and conductivity means indicate that forest infiltration is slightly higher than that of grass, with a statistically significant tendency for the differences to be greatest at highest tension. In the highest soil layers, this tendency appears to be reversed, so that higher forest than grass infiltration capacity occurs at near saturation. These findings likely tie into the clay and organics influences already discussed, as well as the likelihood of initiating preferential root flow in forest and grass at differing depths and levels of soil saturation.

Other t-tests were run to compare total forest and grass group variables. No difference between vegetation types was noted for the total clay content data set (data not shown in tables). However, a significant difference was found between forest and grass organics, with a mean forest value of 8.727 vs. 6.767 for grass. Most of this difference between forest and grass organic matter content stems from topsoil measurements, and when nonparametric independent groups tests were run for individual soil layers, statistically significant differences between forest and grass organic content were only found in the surface (<10 cm) horizon (Prob >ChiSq 0.0499). This suggests that humus incorporated into the forest topsoil may constitute much of the organics portion detected in this layer, and that forest humus may exceed the humus and root organic content detected in grass topsoil. The difference detected at the 90% level between forest and grass topsoil (<10 cm) infiltration at tensions of -8 and -3 may reflect this higher organic content, in that thoroughly wetted humic soil may provide a somewhat higher infiltration capacity in forest topsoil as opposed to grass.

Table 6.7  
 Probabilities of Differences between Forest and Grass Infiltration and Conductivity by Depths  
 Nonparametric Wilcoxon/Kruskal-Wallis Ranked Sum Tests  
 (yellow indicates statistical significance at 95 % confidence level, green at 90%)

| Depth (cm)        | N             | Prob >ChiSq (1-way test, with Chi Sq Approximation) |                   |                   |         |        |        |
|-------------------|---------------|---|-------------------|-------------------|---------|--------|--------|
|                   |               | Infiltration (-15)                                  | Infiltration (-8) | Infiltration (-3) | K (-15) | K(-8)  | K(-3)  |
| <10               | F = 8, G = 10 | 0.7848  | 0.0983            | 0.1817            | 0.5912  | 0.4772 | 0.7223 |
| 25                | F = 8, G = 15 | 0.6304  | 0.1141            | 0.2448            | 0.6122  | 0.1998 | 0.7429 |
| 55                | F = 7, G = 13 | 0.2162  | 0.2664            | 0.3020            | 0.2342  | 0.2505 | 0.2505 |
| 85                | F = 4, G = 6  | 1.000   | 0.6616            | 0.9244            | 0.4414  | 1.000  | 0.9245 |
| 125               | F = 2, G = 2  | 0.3173  | 0.2207            | 0.1025            | 0.4386  | 0.1213 | 0.1213 |
| <10 (pits 5 to14) | F = 6, G = 7  | 0.1120  | 0.0582            | 0.0713            | 0.1702  | 0.0588 | 0.0588 |

### Grass Surface Infiltration Test Results

Field measurements indicated that some factor other than texture or organic matter influences infiltration rates to a significant extent. A series of supplemental surface tests were taken on the shoulder of the grass slope to address this. Because surface rates were generally found to be somewhat lower at sites lower in elevation, it was first hypothesized that clay builds up through colluvial movements sufficient to obstruct water entry. Test results did not bear this out, however, and a secondary hypothesis was formulated in which the depth of soil to bedrock was considered.

Depths to bedrock varied under even the small 314 cm<sup>2</sup> area covered by the 20 cm infiltrrometer disk, making it difficult to obtain clear soil depth readings. Because water exit from the base of the infiltrrometer disk is essentially vertical, discontinuities in depth would likely have an effect on the speed at which water contacts the rock surface. To compensate for this difficulty, soil depth to rock was measured by probe under the disk after each surface test in at least 6 different locations (Figure 6.10). The mean depth was then used in statistical analysis.

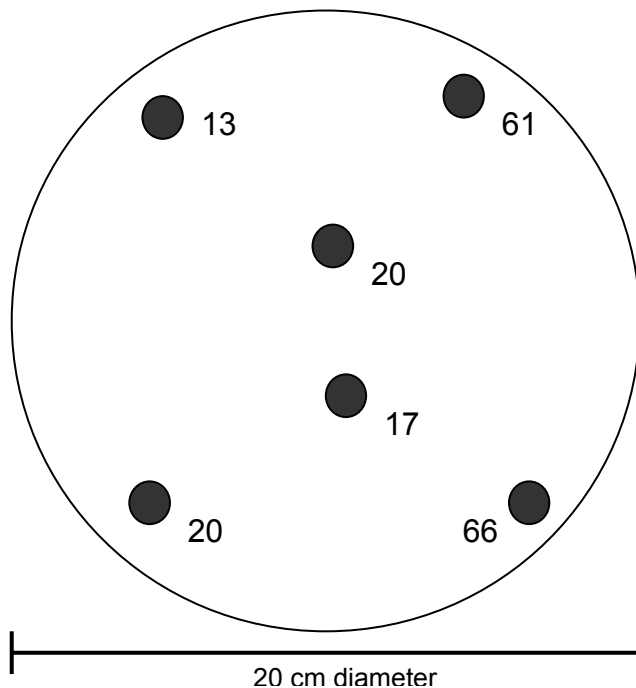
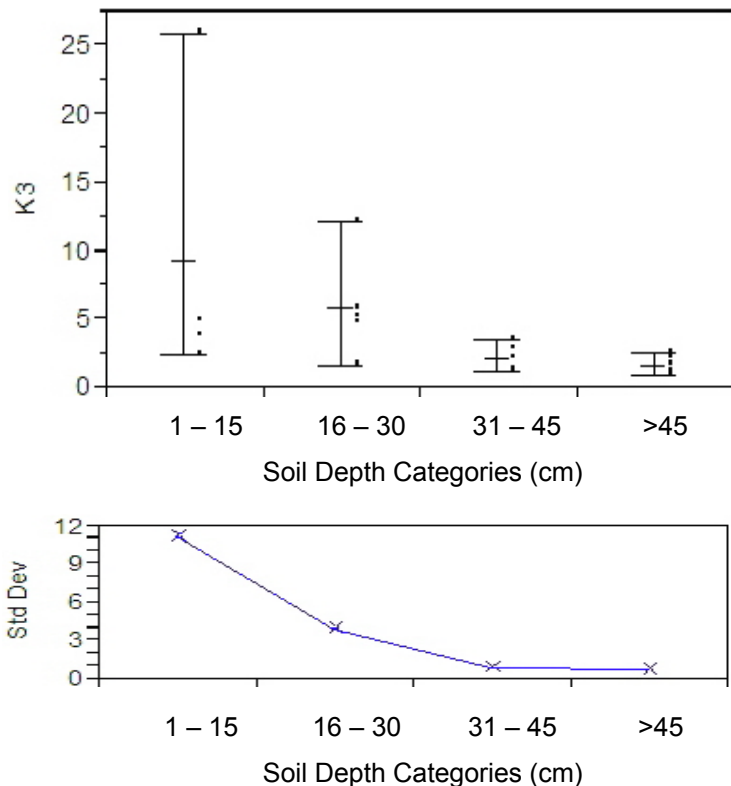


Figure 6.10. Example of soil depths determined under the area of the infiltrrometer disk following surface runs (run 2, October 30, 2005). Depths are measured in centimeters. Mean depth is 32.8 cm.

A total of 21 surface tests, including results from <10 cm from pits 12 through 14, were then categorized by mean soil depths and compared for infiltration and hydraulic conductivity rates. As shown by figure 6.11, analysis of conductivity at K(-3) in relation to soil depth categories shows that the relationship is significant at the 95% level. This is a negative relationship, with increase in soil depth associated with lower infiltration and conductivity rates. Soil depth categories used were 1) 1 to 15 cm, 2) 16 to 30 cm, 3) 31 to 45 cm, and 4) > 45 cm. An abnormally large K(-3) value of 25.92 cm hr<sup>-1</sup> was obtained for one site at 10 cm depth, and even without this outlier, probability that samples come from differing categories remains at 0.0376. Other categorical groupings with 4 or 5 depth classes were used with similar results.

Infiltration rates at -15 were not significantly related to soil depth, but infiltration rates at tensions of -8 and -3 were significantly related. These tests in this thin-soiled area suggest that infiltration is increased by nearness to the bedrock, and that the effect becomes increasingly important as moisture levels rise in the soil. This indicates that rock faces act as preferential flow pathways that function when the soil is nearly saturated. Time constraints did not permit surface tests in the shoulder area of the forest.



| Variable         | Mean     |
|------------------|----------|
| Depth categories | 2.666667 |
| K (-3)           | 4.204762 |
| Correlation      | -0.50575 |
| Signif. Prob     | 0.0193   |
| Number           | 21       |

Figure 6.11. Comparison of surface K(-3) values by soil depth categories (Kruskal/Wallis test) shows a significant correlation between conductivity and depth to bedrock in results of infiltration tests taken at <10 cm depth on the hill shoulder.



## Soil Moisture

### *Observational Evidence for Preferential Tree Root Flow*

During soil sampling and soil depth measurement, saturated soils were discovered at varying depths in some profiles. Only one sample location under grass (site B3, figure 5.24), located above the head of a shallow gully following the forest boundary on Hillslope B, displayed saturation at 2 to 3 cm above bedrock. In forest sites, discrete saturated layers were found in many locations along transects on Hillslopes B, C, and I (Figure 4.1) at varying depths and sometimes at multiple layers within a single profile.

Saturated horizons were always found within a few days of rain events. Under high soil water conditions in the study area, water was able to enter open probe or auger holes to the depth of the temporary water table formed over impervious layers. This occurred at site B5, where the 124 cm deep auger hole was found filled with water to 47 cm below the surface almost two months after the hole was opened. Similarly, if a probe was left in very wet soil for a long time (10 minutes or longer), the probe would often be muddy when it was extracted because of water movement into the low pressure zone created by the hole. The saturated layers revealed after rainstorms differed from these conditions in that they were already present when the probe or auger was inserted.

On Hillslope C, saturated layers were detected on both sides of the tree pictured in figure 6.12 for 3 m in one direction and 5 m in the other following approximately 21 mm rainfall over the prior four days in February 2005. Depths at which saturated layers were detected ranged from 23 to 85 cm, with the deepest saturated layer continuing to bedrock. The transect which explored these saturated layers extended parallel with the contour into the neighboring grassed area, where no saturated layers were found at any depth. Multiple saturated layers were also found in Hillslope I (figure 4.1) forest transects, measured on March 29, 2005 following approximately 27 mm rainfall (Dix Dam data). Saturated layers were particularly prevalent on the Hillslope I knob sideslopes, where soils overlay the top of the Tyrone and its impermeable bentonite layer. Below the elevation of the lowest transect in the grassed area on Hillslope I, water pooled along the grass slope base (figure 5.22), indicating full saturation of the soil. Water did not pond at the equivalent elevation in the nearby forest. Many locations on the lower and middle forest transects on Hillslope I displayed single or multiple discrete saturated soil layers, whereas similar saturated layers were not seen in the grass slope. The concurrence of saturated layers and lack of ponding with forest locations clearly points toward some forest

pathway of preferential flow conduction under high soil moisture conditions. That pathway most likely involves transfer along tree roots.



Figure 6.12. Saturated soil layers were found within an 8 m distance of the central tree. Adjacent soil under grass contained no saturated layers. Photo by author, February 5, 2005.

### *Water Content Data Logging*

Water content dielectric probes were planted on Hillslope C (figure 4.1) in hopes of capturing evidence for preferential flow in the forest pit, which was dug 2 m from the tree shown in figure 6.12. Probes were also placed in a grass pit approximately 30 m away from the forest pit at a matching elevation. Unfortunately, dry conditions prevailed throughout the project's operation period between May 2005 and January 2006. Although a number of storm events were recorded, most at the end of this period, a high percentage of precipitation was lost during early storms because of evapotranspiration and soil storage demands created by the dry antecedent conditions. Preferential flow pathways in soil have been found to often activate only

after near-saturation moisture conditions prevail (Sidle et al., 1995). Such conditions were not created in soil layers surrounding maximum tree root growth until the end of the project. Soil saturation did take place during winter months, but late winter grass data was lost because rodents chewed through wires on the data logging station. Thus direct evidence obtained for preferential flow movement was limited.

However, soil water content readings did provide evidence for differing infiltration and percolation responses at varying depths between forest and grass. Figures 6.13, 6.14, 6.15, and 6.16 graph changes in water content as represented in unprocessed millivolt (mV) data, with precipitation totals graphed at the top to aid in determining response time. Tables 6.8 and 6.9 supply further details that highlight the observed trends in figures 6.13 and 6.14, using changes in mV readings to give initial response times, relative increase or decrease in rates, amounts of rainfall preceding responses, and subsequent measurement patterns. This information can be used to assess differences between water movements into forest and grass soils under both leaf-on and leaf-off conditions.

#### *a) Rains From Hurricane Katrina*

Probes were deployed in late May 2005, after a relatively dry late winter and spring. Hot, dry conditions continued throughout the summer, bringing only 304.8 mm total precipitation to the study area during the period of maximum plant growth between late March and August. When grass pit 10 (Figure 4.5) was dug on August 25, matric pressure as determined by tensiometer was -60 at <10 cm (Appendix 5). Beginning on August 26, a series of storms swept through the region in the aftermath of Hurricane Katrina, depositing 136 mm of rain spread over 6 days. Under these dry antecedent leaf-on conditions, forest and grass infiltration patterns differed substantially.

Loss to evapotranspiration and interception is clearly higher in forest than under grass for the five main events recorded August 26 to 31 (Figure 6.13). Response at the < 10 cm (surface) grass probe occurred within an hour of the beginning of the first event, after delivery of 14.2 mm of precipitation (Table 6.8). The soil moisture increase rate was moderate, and was followed by a very slow increase in grass water content at 25 cm depth five hours later. A <10 cm forest response to the same storm was detected after 15.2 mm rain, but the extremely slow increase rate that was initiated did not change throughout the events of the subsequent 3 days until August 29, after a combined total of 54.3 mm for all events had fallen.

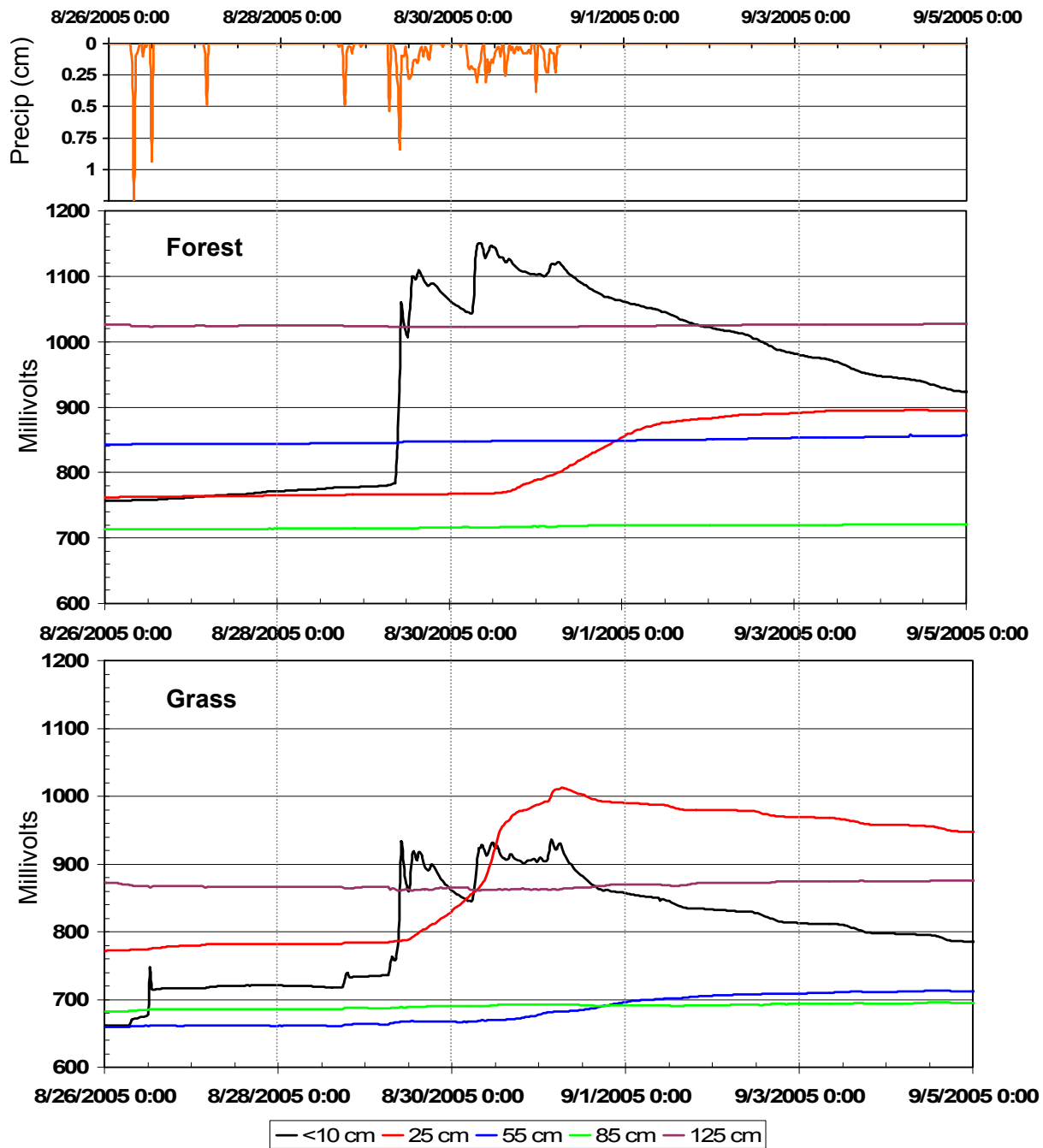


Figure 6.13. Soil water content changes during Hurrican Katrina storms of August 26 though August 31 promoted rapid surface soil moisture increase under grass and more rapid grass movement of water into the 25 cm level.

Table 6.8

Soil Moisture Responses to Hurricane Katrina Events - August 26 – August 31, 2005

| Event                     | Precip (cm) | Site   | <10cm response                                      |   | 25 cm response                           |   | 55 cm response  |                                 |
|---------------------------|-------------|--------|---|---|--|---|---|---------------------------------|
|                           |             |        | Time, preceding rain, and rate                      | Peak time, and rise and/or fall         | Time, preceding rain, and rate           | Peak time, and rise and/or fall         | Time, preceding rain, and rate  | Peak time, and rise and/or fall |
| 8/26<br>6:30 am – 12 noon | 2.69        | Grass  | 7:30 am (1.42 cm); moderate                         | 12:30 pm; then continuous decline       | 1:30 pm; very slow                       | Continuous rise to next event           | Extremely small, slow, fluctuating rise occurs 8/26 thru 9/11 before declining (rises from 659 to 712 mv) |                                 |
|                           |             | Forest | 8 am (1.52 cm); extremely slow                      | Continuous gradual rise                 | 10 pm; extremely slow                    | Continuous gradual, extremely slow rise | -----   | -----                           |
| 8/27<br>3 am – 4 am       | 0.61        | Grass  | 4:30 am (0.61 cm); slow                             | 4:30 pm peak; then continuous decline   | Very slow rise continued thru this event |   | Extremely small, slow, fluctuating rise occurs 8/26 thru 9/11 before declining (rises from 659 to 712 mv) |                                 |
|                           |             | Forest | Extremely slow rise continues                       |   | Extremely slow rise continues            |   | -----   | -----                           |
| 8/28<br>4:30 pm – 11 pm   | 0.91        | Grass  | 6:00 pm (0.18 cm); slow<br>6:30 pm (0.66 cm); rapid | 7 pm peak; then slow continuous decline | Very slow rise continued thru this event |   | Extremely small, slow, fluctuating rise occurs 8/26 thru 9/11 before declining (rises from 659 to 712 mv) |                                 |
|                           |             | Forest | Extremely slow rise continues                       |   | Extremely slow rise continues            |   | -----   | -----                           |

Table 6.8. Soil Moisture Responses to Hurricane Katrina Events - August 26 – August 31, 2005 (continued)

| Event                                       | Precip (cm) | Site   | <10cm response                 |  | 25 cm response  |  | 55 cm response   |                                 |
|---|-------------|--------|--------------------------------|--|---|--|--|---------------------------------|
|   |             |        | Time, preceding rain, and rate | Peak time, and rise and/or fall  | Time, preceding rain, and rate                        | Peak time, and rise and/or fall            | Time, preceding rain, and rate   | Peak time, and rise and/or fall |
| 8/29<br>6:30 am – 6 pm                      | 3.94        | Grass  | 7 am (0.53 cm); rapid          | 10 am peak; then fluctuating decline                                       | Rise continued thru this event, with increase in rate |  | Extremely small, slow, fluctuating rise occurs 8/26 thru 9/11 before declining (rises from 659 to 712 mv)      |                                 |
|   |             | Forest | 9:30 am (1.22 cm); rapid       | 2 pm peak; then decreases to next event                                    | Extremely slow rise continues                         |  | Extremely small, slow, continuous rise occurs 8/29 10 am thru 9/8 before declining ( rises from 846 to 861 mv) |                                 |
| 8/30 – 8/31<br>2 am (8/30) – 6:30 am (8/31) | 5.46        | Grass  | 6 am (0.58); rapid             | Fluctuating peaks, with highest peak 8/31 3:30 am; then continuous decline | Continuous rise; rapid rate                           | 8/31 6:30 am peak; then continuous decline | Extremely small, slow, fluctuating rise occurs 8/26 thru 9/11 before declining (from 659 to 712 mv)            |                                 |
|   |             | Forest | 7 am (0.99 cm); rapid          | 8 am peak; fluctuated with storm until 4:30 pm, then continuous decline    | Continuous rise; moderate rate                        | 9/4 7 am peak, then continuous decline     | Extremely small, slow, continuous rise occurs 8/29 10 am thru 9/8 before declining ( rises from 846 to 861 mv) |                                 |

As shown by the low millivolt readings in the forest at <10 cm depth, most of the early rain for the first four Katrina events did not enter the forest topsoil. This loss of water entry likely reflected the high infiltration and evapotranspiration demands created by the exceptionally dry leaf-on antecedent conditions. Run-off, although not measured in this study, was very unlikely to have taken place considering the degree of vegetation cover and the fact that individual events were relatively short and spaced far enough apart to permit absorption. In contrast to forest response, after an initial large interception loss in the first storm, losses of only 5 to 6 mm occurred at the beginning of each storm before activating rapid water content increases in the grass topsoil. By adding all rain occurring before rapid responses are initiated during each storm event, 27.9% of the total 136 mm precipitation for the entire Katrina storm series did not arrive at the surface soil probes under grass (37.9 mm) and 47.2% was not accounted for by forest probe readings (64.2 mm). For the total combined readings for the entire storm series, forest interception and evapotranspiration demands were thus 59.0% higher than those of grass.

Early storm losses also included water necessary to wet the 10 cm of topsoil covering the probes. By August 30, the topsoil was thoroughly wetted in both forest and grass. With the storm beginning on August 30, the <10 cm probes recorded grass response after 5.8 mm and forest response after 9.9 mm rainfall. Of the total 54.6 mm precipitation recorded for just the August 30-31 event, 10.6% was thus lost to evapotranspiration and interception by the grass and 18.1% was lost under forest. Interception and evapotranspiration demands for this single event were thus 58.6% higher for forest than grass, which is remarkably close to the total percentage of loss found for the entire series of rain events.

Subsoil layers also received water entry differently between forest and grass under the very dry antecedent conditions. Starting almost coincident with the heaviest rains occurring on Aug 29 and 30, an increasing moisture level was detected at 25 cm under grass. As <10 cm grass readings peaked and then fluctuated around a relatively stable value, 25 cm grass readings continued to rise until they exceeded topsoil readings on August 31. In contrast, replenishment of soil storage under forest was delayed far longer than under grass. Forest moisture at the 25 cm level rose only a barely perceptible amount before August 31, when the rate of increase finally began to escalate. As demonstrated in figure 6.13, the forest topsoil held some 20% more moisture at its peak than did the grass, and soil moisture in the forest at 25 cm did not exceed topsoil moisture content until September 7. Detectable movement of small amounts of water into the 55 cm level in the forest did not occur until August 29, and it remained a smaller amount of water than found at 55 cm under grass. Forest water movement into

subsurface layers throughout the series of events was thus much slower, and included lower volumes of water, than did water movements into grass subsoil levels.

*b) Early Winter Rains*

The Katrina rains hit during a leaf-on period. Figure 6.14 shows the forest and grass water content responses recorded between November 12 and December 16 during a leaf-off period under conditions of decreased evapotranspiration and interception. Between September 1 and November 12, the study area received only 57 mm of precipitation, so that conditions were again fairly dry, though soil moisture was above that present at the beginning of the Katrina rains. As recorded in Table 6.9, six moderate events moved through the area in late autumn, eventually replenishing surface moisture. As topsoil moisture was renewed and leaf litter was thoroughly wetted, surface responses in forest and grass became noticeably similar.

During the first three events, on November 13, 15-16, and 28, grass <10 cm responses were faster and rose more rapidly in response to rainfall than forest (Table 6.9). With each event, the amount of rain needed to generate response in the forest soil as compared to grass decreased, so that 67% more on November 13, 45% more on November 15, and only 34% more rain on November 28 was necessary. During both the November 15-16 and November 28 events, an early slow response preceding the rapid rise was detected in the grass. In contrast, rise under forest was rapid, with no preliminary slow increase, indicating that moisture increase around the probe was sudden. These changes in November event response timings show that decreasing amounts of precipitation are lost by the forest as moisture increases in the litter and surface soil. The slow preliminary rise under grass suggests a period of pore channel saturation preceding preferential flow activation. In contrast, the sudden onset of forest <10 cm responses suggests that once fresh leaf litter storage capacity is filled, water may be delivered rapidly to the underlying topsoil.

Beginning in December, as litter and topsoil moisture increased, patterns reversed between forest and grass. Although grass at <10 cm had slow, detectable early soil moisture increases during the events on December 3-4 and December 15, rapid surface response occurred sooner in the forest than it did under grass: after 9.9 mm as opposed to 13.0 mm precipitation for grass on December 3-4, and after 6.6 mm as compared to 7.8 mm on December 15. Under high soil moisture conditions, litter storage was quickly satisfied, allowing a more rapid surface response in forest soils.



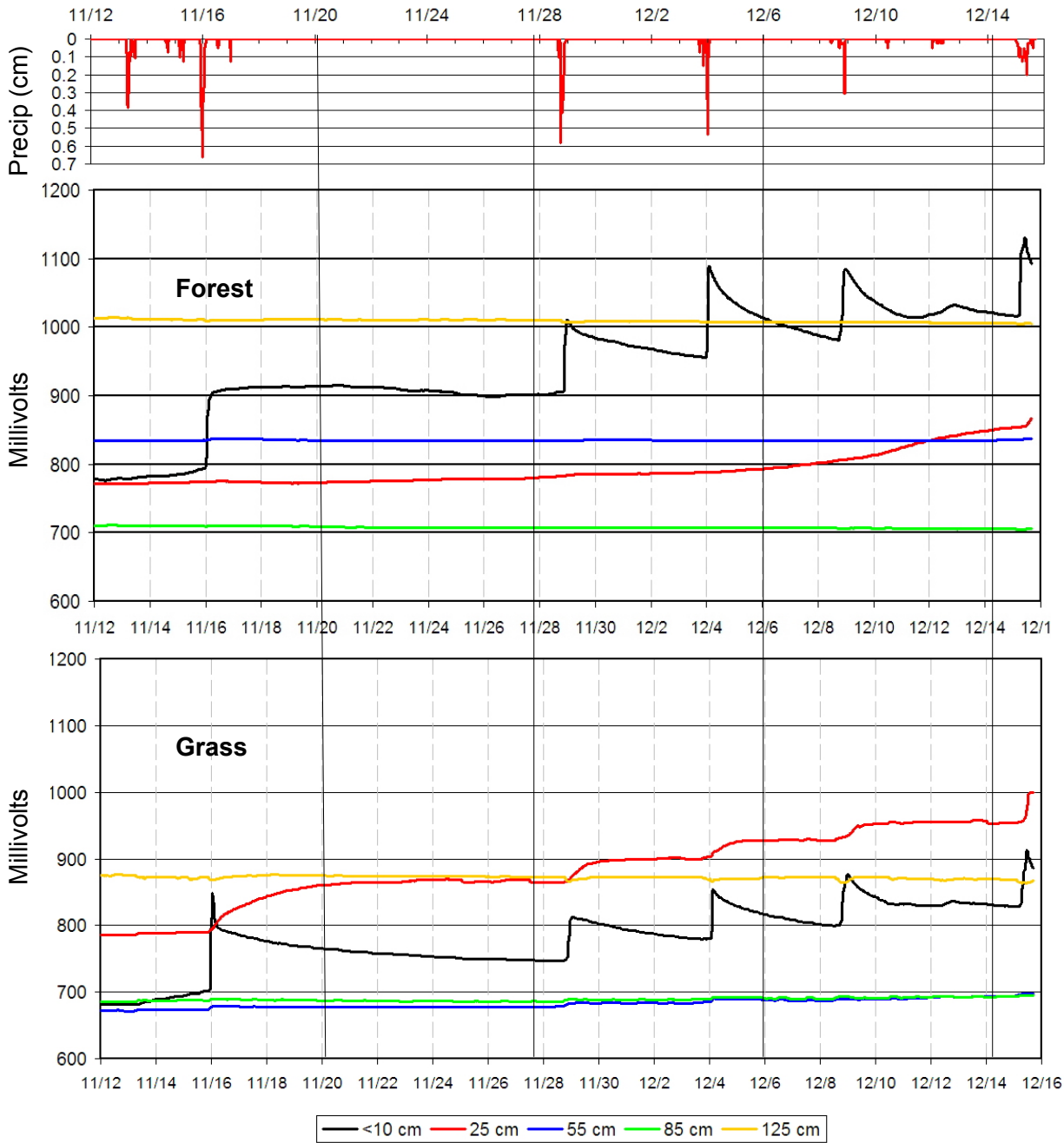


Figure 6.14. Early winter soil water content response to rainfall between November 12 and December 16, 2005. Water again moves more rapidly into the 25 cm level under grass than in the forest.

Table 6.9

Soil Moisture Responses to Storm Events - November 12 to December 15, 2005

| Event                                  | Precip (cm) | Site   | <10cm response  |  | 25 cm response                                   |   | 55 cm response                 |   |
|--|-------------|--------|---|--|--|---|--------------------------------|---|
|  |             |        | Time, preceding rain, and rate                          | Peak time, and rise and/or fall              | Time, preceding rain, and rate                   | Peak time, and rise and/or fall                         | Time, preceding rain, and rate | Peak time, and rise and/or fall         |
| 11/13<br>6:30 am -2 pm                 | 1.57        | Grass  | 8 am (after 0.46 cm); very slow                         | Continuous rise to next event                | 8:30 am; extremely slow                          | Continuous rise to next event                           | -----                          | -----                                   |
|  |             | Forest | 1:30 pm (after 1.40 cm); very slow                      | Continuous rise to next event                | -----  | -----   | -----                          | -----                                   |
| 11/15<br>-<br>11/16<br>10 pm - 2:30 am | 2.54        | Grass  | 10:30 pm (0.05 cm); slow<br>11:30 pm (0.81); rapid      | 1 am peak; then continuous decline           | 10:30 pm; slow                                   | Continuous rise to 11/21 12 noon; then fluctuating rise | 10:30 pm; extremely slow pulse | 1 am peak; decline after 11/18 midnight |
|  |             | Forest | 11/15 midnight (1.47 cm); mod.<br>1 am (2.21 cm); rapid | 11/18 6:30 pm peak; then fluctuations        | 11/16 1 am to 11/19 7:30 am rise and fall pulse, | Slow, fluctuating rise to next event                    | -----                          | -----                                   |
| 11/28<br>4:30 pm - 10 pm               | 2.16        | Grass  | 6:30 pm (0.13 cm); slow<br>8 pm (1.35 cm); rapid        | 11/29 12:30 am peak; then continuous decline | 6 pm; very slow                                  | 12/2 1 pm peak; then fluctuations                       | 6:30 pm; slow pulse            | 11/29 4 am peak; then fluctuations      |
|  |             | Forest | 9 pm (2.032 cm); rapid                                  | 11/28 11:30 pm peak; then continuous decline | 11:30 pm; extremely slow                         | Continuous rise to next event                           | -----                          | -----                                   |

201

Table 6.9 Soil Moisture Responses to Storm Events - November 12 to December 15, 2005 (continued)

| Event                            | Precip (cm) | Site   | <10cm response                                   |  | 25 cm response  |   | 55 cm response                 |                                     |
|----------------------------------|-------------|--------|--|--|---|---|--------------------------------|-------------------------------------|
|                                  |             |        | Time, preceding rain, and rate                   | Peak time, and rise and/or fall        | Time, preceding rain, and rate                                      | Peak time, and rise and/or fall           | Time, preceding rain, and rate | Peak time, and rise and/or fall     |
| 12/3 – 12/4<br><br>5 pm – 2 am   | 1.30        | Grass  | 1:30 am (1.27 cm); slow<br>2 am (1.30 cm); rapid | 3 am peak; then continuous decline     | 1:30 am; slow   | 12/5 10 am peak; then fluctuating decline | 1:30 am; very slow pulse       | 2:30 am peak; then fluctuations     |
|                                  |             | Forest | 12:30 am (0.99 cm); rapid                        | 2 am peak; then continuous decline     | Slow continuous rise from preceding event                           |   | -----                          | -----                               |
| 12/8<br><br>4:30 pm – 10:30 pm   | 0.89        | Grass  | 5:30 pm (0.08 cm); rapid                         | Midnight peak; then continuous decline | 5 pm; slow  | 12/9 9 am peak; then fluctuating rise     | 12/10                          | fluctuating gradual rise thru !2/15 |
|                                  |             | Forest | 6:30 pm (0.10 cm); moderate                      | 11:30 pm peak; then continuous decline | Slow continuous rise from preceding event                           |   | -----                          | -----                               |
| 12/15<br><br>12:30 am – 12:30 pm | 1.78        | Grass  | 4 am (0.38 cm); slow<br>6 am (0.78 cm); rapid    | 11:30 am peak; continuous decline      | 4 am; very slow   | 2:20 pm peak; then decline                | 12/10                          | fluctuating gradual rise thru !2/15 |
|                                  |             | Forest | 5:30 (0.66 cm); rapid                            | 10 am peak; then continuous decline    | Slow continuous rise from preceding event changing to moderate rate |   | -----                          | -----                               |

Surface responses on December 8 appeared much the same between forest and grass, though a peak response was recorded somewhat earlier for forest. Precipitation amounts for December 8 in table 6.9 are not reliable because temperatures hovered around freezing during the early part of the evening, and it is likely that early snow was not recorded by the rain gauge. Both the December 3-4 and December 15 events occurred during above-freezing temperatures, and temperatures throughout the entire data logging recording period never stayed low enough to freeze the soil around the buried soil probes.

During all events recorded, the forest consistently maintained more water in the topsoil layer than the grass. This can be explained by either a higher forest topsoil water storage capacity because of humus content and/or a lower forest ability to promote water entry into underlying soil layers. Soil textural classes are very similar between the probe stations (see Appendix 3, Infiltration pits 1 and 2), suggesting that percolation through the upper horizons should be similar at the two sites. Examination of Figure 6.14 for the November 15-16 event reveals that the grass topsoil reacted after 8.1 mm with a sharp spike that quickly activated entry of water into the 25 cm level and a discernible pulse at 55 cm. This suggests that grass topsoil water retention is not limited by the capacity of the soil, but rather by the fact that moisture over a certain level of soil saturation quickly activates entry into underlying grass soils so that downward withdrawal places an upper cap on topsoil water content.

A consistently greater ability for grass to conduct water into subsoil layers is shown in the early winter storms as both 25 and 55 cm levels responded to events with rapid pulses or rate increases (Figure 6.14). In contrast, forest response to all but the heaviest rains was restricted to an extremely slow, continuous rise in water content at the 25 cm level accompanied by a greater retention of water in the topsoil as subsoil water entry was impeded. This suggests that under dry conditions water movement into forest subsoil layers is restricted to a diffuse movement through the soil matrix, as compared to a greater rate of macropore flow into the 25 and 55 cm depths of grass soils.

### *c) January Events*

Between December 15 and January 17, the study area received 49 mm of rain, with 19.8 mm of rain arriving in the final week. Forest topsoil moisture increased rapidly with each small event (figure 6.15) with soil moisture in deeper layers continuing a slow, steady rise that bridged events with barely perceptible event responses. These subsoil responses at different levels changed abruptly when saturation occurred and preferential flow was established.

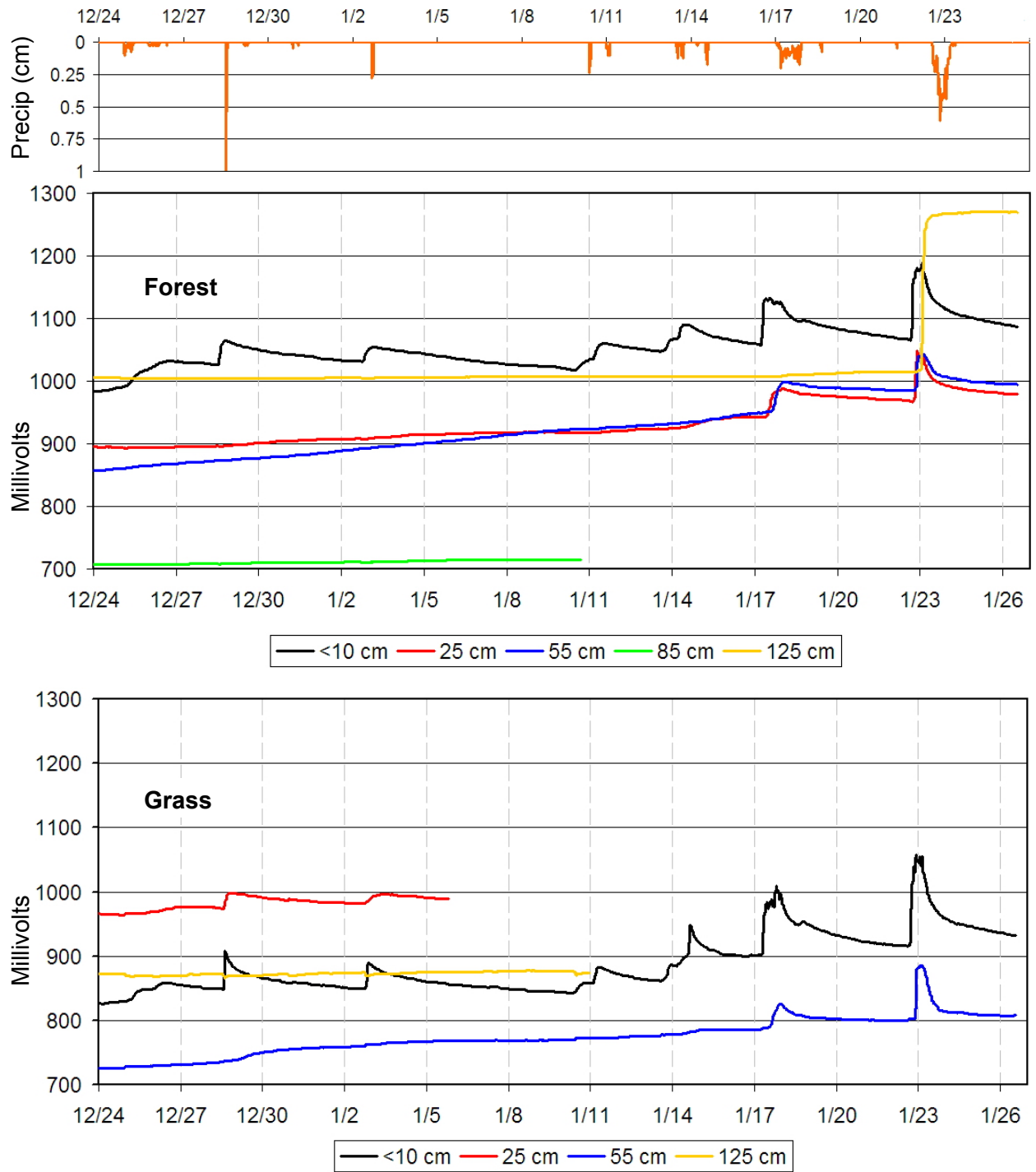


Figure 6.15. Soil moisture changes December 24 through January 26. Water entered deeper forest soil layers slowly until Jan 17, 2006, when precipitation rapidly activated moisture increase at 25 and 55 cm depths. On January 23, a jump in moisture occurred in the forest soil at 125 cm within hours of precipitation. Under grass, water moved to 25 cm with storm events on January 28 and February 3. Forest 85 cm and grass 25, 85, and 125 cm recordings were lost during January.

Direct mV readings along with half hour precipitation amounts are given for forest soil depths in tables 6.10 and 6.11. These tables, giving responses for storm events on January 17-18 and January 22-23, provide a precise way to quickly visualize rates of soil moisture increase with precipitation input over time. Table 6.10 shows both initial detectable responses and peak readings for forest soil depths as measured for the January 17 storm. Precipitation occurring within half hour intervals is shown on the right, and data at 85 cm was not available. As Table 6.10 shows, responses at 25 and 55 cm were first seen approximately 3.5 and 4 hours respectively after the initial <10 cm response. During this event, under moderate antecedent moisture conditions, water collected in the topsoil only briefly under the low intensity rainfall before water began a downward shift to the 25 cm level. There was also little difference between 25 and 55 cm response patterns, indicating that water was moving via some mechanism that allowed rapid movement between soil layers (Figure 6.15).

On January 22 and 23, a steady rainfall totaling 87.6 mm quickly added to the already moderately high antecedent moisture conditions. Responses to this event were initiated at depths down to 125 cm in intervals that followed each other at 1 to 2.5 hour periods (Table 6.11). Soil moisture increase at <10 cm was detected after a total of 9.9 mm rainfall. Rise in moisture content at 25 cm occurred two hours later, with a rise at 55 cm taking place one and a half hours after that. Moisture peaked at <10 cm four and a half hours after the initial response at that level, simultaneous with a peak at 25 cm and the beginning of a rapid rise at 55 cm. Secondary peaks occurred in response to rainfall intensity, and at the same time the <10 cm probe indicated its second peak, the 125 cm probe indicated a very rapid moisture rise at 125 cm (Figure 6.15). This rise continued to January 24, when it stabilized at 1270 mV for a day before beginning to slowly fall.

The rapidity of the 125 cm response on January 23 most likely came from activation of preferential flow. This soil layer is composed of dense clay, and matrix movement would be unlikely to produce the rapid increase in moisture noted at this depth. Bedrock is also at 185 cm, some 60 cm below the probe, making it also unlikely that water table rise above the bedrock was the cause of the rapid climb. In addition, the 55 cm layer shows a much more gradual, extended water content value throughout the time period of the jump at 125 cm, suggesting that flow is bypassing the 55 cm level. The jump at 125 cm actually began an hour prior to the second peak at 10 cm, indicating that water was already entering preferential pathways at that time. As the deep pathways expanded, water was pulled away from upper soil layers.

Table 6.10

Forest Water Content Measurements on January 17-18, 2006 (half-hour intervals)  
 (Measurements are in millivolts: yellow indicates initial response, blue indicates peak)

| Date and Time   | <10  | 25  | 55  | 85  | 125  | Precip (cm) |
|-----------------|------|-----|-----|-----|------|-------------|
| 1/17/2006 5:30  | 1058 | 942 | 949 | --- | 1008 | 0.152       |
| 1/17/2006 6:00  | 1060 | 942 | 949 | --- | 1008 | 0.076       |
| 1/17/2006 6:30  | 1077 | 942 | 949 | --- | 1008 | 0.076       |
| 1/17/2006 7:00  | 1110 | 942 | 950 | --- | 1008 | 0.076       |
| 1/17/2006 7:30  | 1122 | 942 | 950 | --- | 1008 | 0.102       |
| 1/17/2006 8:00  | 1126 | 942 | 950 | --- | 1008 | 0.051       |
| 1/17/2006 8:30  | 1129 | 942 | 950 | --- | 1008 | 0.127       |
| 1/17/2006 9:00  | 1130 | 942 | 950 | --- | 1008 | 0.076       |
| 1/17/2006 9:30  | 1131 | 943 | 950 | --- | 1008 | 0.051       |
| 1/17/2006 10:00 | 1132 | 943 | 951 | --- | 1008 | 0.025       |
| 1/17/2006 10:30 | 1131 | 944 | 951 | --- | 1008 | 0.051       |
| 1/17/2006 11:00 | 1130 | 946 | 951 | --- | 1008 | 0.102       |
| 1/17/2006 11:30 | 1128 | 947 | 951 | --- | 1008 | 0.076       |
| 1/17/2006 12:00 | 1130 | 950 | 951 | --- | 1008 | 0.102       |
| 1/17/2006 12:30 | 1131 | 954 | 951 | --- | 1008 | 0.076       |
| 1/17/2006 13:00 | 1132 | 958 | 952 | --- | 1008 | 0.076       |
| 1/17/2006 13:30 | 1133 | 963 | 952 | --- | 1008 | 0.076       |
| 1/17/2006 14:00 | 1132 | 968 | 952 | --- | 1008 | 0.076       |
| 1/17/2006 14:30 | 1131 | 972 | 952 | --- | 1008 | 0.025       |
| 1/17/2006 15:00 | 1130 | 975 | 953 | --- | 1008 | 0.051       |
| 1/17/2006 15:30 | 1128 | 978 | 954 | --- | 1008 | 0.102       |
| 1/17/2006 16:00 | 1125 | 979 | 955 | --- | 1008 | 0.127       |
| 1/17/2006 16:30 | 1123 | 980 | 958 | --- | 1008 | 0.127       |
| 1/17/2006 17:00 | 1123 | 981 | 962 | --- | 1008 | 0.127       |
| 1/17/2006 17:30 | 1124 | 982 | 967 | --- | 1008 | 0.051       |
| 1/17/2006 18:00 | 1126 | 982 | 971 | --- | 1008 | 0.102       |
| 1/17/2006 18:30 | 1126 | 983 | 975 | --- | 1008 | 0.152       |
| 1/17/2006 19:00 | 1126 | 984 | 979 | --- | 1008 | 0.051       |
| 1/17/2006 19:30 | 1126 | 984 | 982 | --- | 1008 | 0.025       |
| 1/17/2006 20:00 | 1126 | 985 | 985 | --- | 1008 | 0.051       |
| 1/17/2006 20:30 | 1125 | 985 | 988 | --- | 1008 | 0.178       |
| 1/17/2006 21:00 | 1123 | 986 | 990 | --- | 1008 | 0.076       |
| 1/17/2006 21:30 | 1123 | 986 | 991 | --- | 1008 | 0.025       |
| 1/17/2006 22:00 | 1126 | 986 | 993 | --- | 1008 | 0           |
| 1/17/2006 22:30 | 1126 | 986 | 994 | --- | 1008 | 0           |
| 1/17/2006 23:00 | 1125 | 987 | 995 | --- | 1008 | 0           |
| 1/17/2006 23:30 | 1124 | 987 | 996 | --- | 1008 | 0           |
| 1/18/2006 0:00  | 1122 | 988 | 997 | --- | 1009 | 0           |
| 1/18/2006 0:30  | 1120 | 988 | 998 | --- | 1009 | 0           |

Table 6.11

Forest Water Content Measurements on January 22-23, 2006 (half-hour intervals)  
 (Measurements are in millivolts: yellow indicates initial response, blue indicates peak)

| Date and Time   | <10  | 25   | 55   | 85  | 125  | Precip (cm) |
|-----------------|------|------|------|-----|------|-------------|
| 1/22/2006 13:30 | 1066 | 969  | 986  | --- | 1015 | 0.076       |
| 1/22/2006 14:00 | 1066 | 969  | 986  | --- | 1015 | 0.127       |
| 1/22/2006 14:30 | 1066 | 968  | 986  | --- | 1015 | 0.178       |
| 1/22/2006 15:00 | 1066 | 967  | 986  | --- | 1015 | 0.203       |
| 1/22/2006 15:30 | 1065 | 967  | 985  | --- | 1014 | 0.229       |
| 1/22/2006 16:00 | 1065 | 967  | 985  | --- | 1014 | 0.178       |
| 1/22/2006 16:30 | 1070 | 967  | 985  | --- | 1014 | 0.102       |
| 1/22/2006 17:00 | 1112 | 967  | 985  | --- | 1014 | 0.229       |
| 1/22/2006 17:30 | 1144 | 966  | 985  | --- | 1014 | 0.127       |
| 1/22/2006 18:00 | 1158 | 967  | 986  | --- | 1014 | 0.406       |
| 1/22/2006 18:30 | 1159 | 968  | 986  | --- | 1014 | 0.381       |
| 1/22/2006 19:00 | 1165 | 971  | 986  | --- | 1014 | 0.279       |
| 1/22/2006 19:30 | 1165 | 980  | 986  | --- | 1015 | 0.457       |
| 1/22/2006 20:00 | 1168 | 991  | 987  | --- | 1015 | 0.610       |
| 1/22/2006 20:30 | 1177 | 1017 | 989  | --- | 1015 | 0.483       |
| 1/22/2006 21:00 | 1181 | 1048 | 997  | --- | 1015 | 0.406       |
| 1/22/2006 21:30 | 1178 | 1047 | 1020 | --- | 1015 | 0.432       |
| 1/22/2006 22:00 | 1178 | 1045 | 1034 | --- | 1016 | 0.406       |
| 1/22/2006 22:30 | 1178 | 1042 | 1039 | --- | 1016 | 0.406       |
| 1/22/2006 23:00 | 1177 | 1039 | 1040 | --- | 1017 | 0.432       |
| 1/22/2006 23:30 | 1178 | 1039 | 1040 | --- | 1018 | 0.330       |
| 1/23/2006 0:00  | 1180 | 1039 | 1040 | --- | 1018 | 0.356       |
| 1/23/2006 0:30  | 1180 | 1038 | 1040 | --- | 1018 | 0.203       |
| 1/23/2006 1:00  | 1180 | 1039 | 1042 | --- | 1021 | 0.381       |
| 1/23/2006 1:30  | 1183 | 1037 | 1042 | --- | 1041 | 0.432       |
| 1/23/2006 2:00  | 1189 | 1041 | 1042 | --- | 1077 | 0.178       |
| 1/23/2006 2:30  | 1183 | 1043 | 1043 | --- | 1152 | 0.178       |
| 1/23/2006 3:00  | 1174 | 1037 | 1043 | --- | 1189 | 0.127       |
| 1/23/2006 3:30  | 1172 | 1031 | 1042 | --- | 1214 | 0.127       |
| 1/23/2006 4:00  | 1170 | 1028 | 1041 | --- | 1232 | 0.127       |
| 1/23/2006 4:30  | 1166 | 1026 | 1040 | --- | 1242 | 0.051       |
| 1/23/2006 5:00  | 1162 | 1023 | 1037 | --- | 1248 | 0.025       |
| 1/23/2006 5:30  | 1159 | 1021 | 1036 | --- | 1251 | 0           |
| 1/23/2006 6:00  | 1155 | 1019 | 1035 | --- | 1254 | 0           |
| 1/23/2006 6:30  | 1151 | 1018 | 1033 | --- | 1256 | 0.025       |
| 1/23/2006 7:00  | 1148 | 1015 | 1032 | --- | 1258 | 0.025       |
| 1/23/2006 7:30  | 1145 | 1013 | 1029 | --- | 1259 | 0.025       |
| 1/23/2006 8:00  | 1142 | 1012 | 1027 | --- | 1260 | 0           |
| 1/23/2006 8:30  | 1140 | 1010 | 1026 | --- | 1261 | 0.025       |
| 1/23/2006 9:00  | 1138 | 1009 | 1023 | --- | 1262 | 0.076       |



The partial data from grass probes available during this time period show that response at 25 cm was rapid in tandem with topsoil response during the first two events, in contrast to the gradual forest soil moisture increase seen at 25 cm for these small early storms (Figure 6.15). A rapid 55 cm response similar to that seen in the forest also occurred under grass on January 17 and 22. Although no grass data is available for the 125 cm depth during this period, grass data obtained on January 27 revealed a flat line for 125 cm, suggesting that soil moisture increase at 125 cm under grass had not been activated by the January 22-23 storm (Figure 6.16).

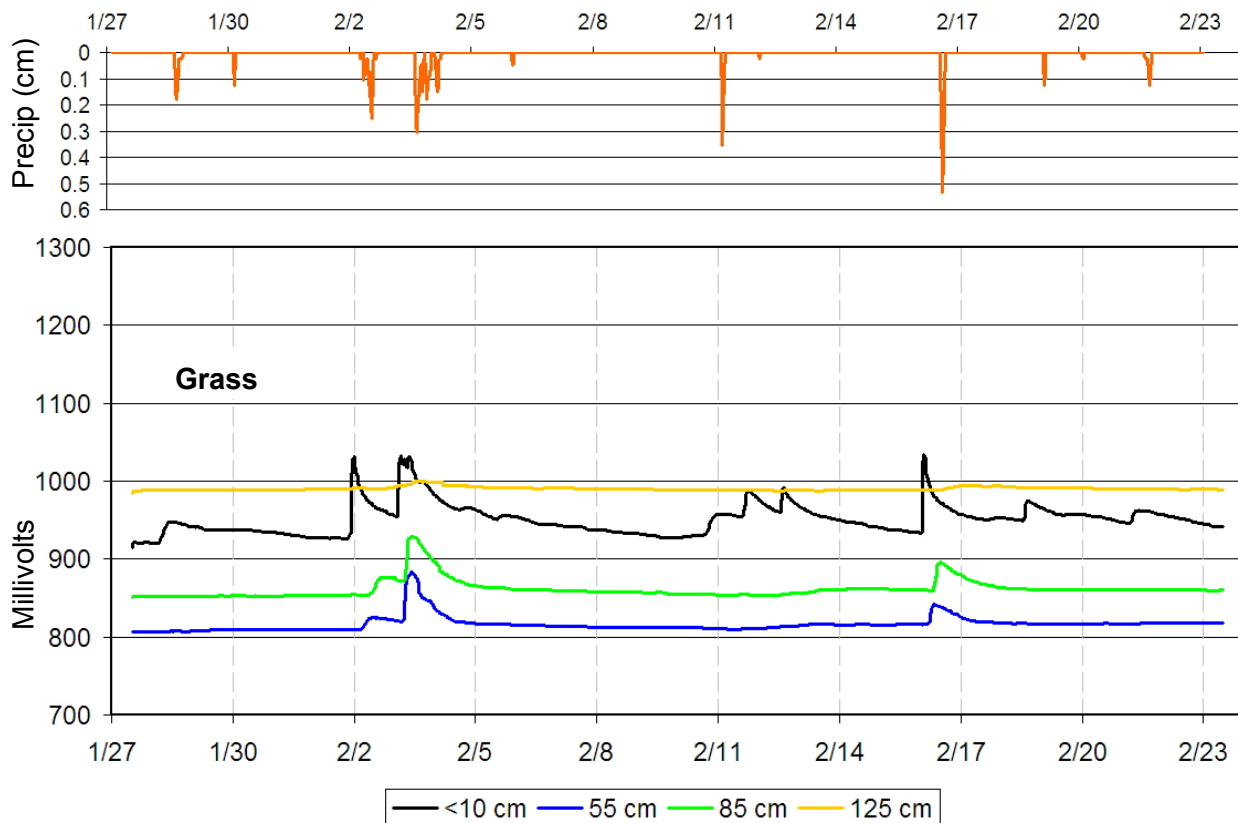


Figure 6.16. Flat grass mV readings at 125 cm on January 27 indicate that water did not move into soil at at this depth following the large rain event of January 22 to 23. Grass responses at depths to 85 cm are rapid following the beginning of intense storm events in February. Forest data for this time period is not available.

*d) Summary of Soil Moisture Information*

Although information from data logging provided only limited evidence for preferential water movement, soil moisture did provide important information on infiltration patterns. In the

study area, high forest evapotranspiration and interception demands moderate the level of moisture that can reach the soil during leaf-on conditions. Loss for single events under dry conditions may reach almost almost 100%. Evapotranspiration and interception loss following thorough wetting during leaf-on conditions was approximately 11% for grass and 18% for forest during the August 30-31 event, making forest loss 59% higher than grass. This percentage of comparative forest loss during this single event is almost identical with the amount calculated for total loss related to the entire series of August events, indicating that it may be a good estimate of the higher rate of evapotranspiration under forest leaf-on conditions in this environment.

During leaf-off periods, evapotranspiration and interception rates become similar in forest and grass when soil and litter moisture are high. The ability of the forest to exceed grass infiltration rates is limited to conditions of very high moisture, and only occurred during this study in early winter after several storms had passed. Leaf litter, at least during the fall when it is largely fresh, has a storage capacity that must be filled before water enters the topsoil, but once thoroughly wetted, it can conduct water rapidly into the forest soil.

Because the records taken in this study do not cover a long enough period of time, annual loss rates for forest or grass can not be determined from the study data. Data from this research does support previous studies that show that annual interception and evapotranspiration rates vary with antecedent conditions on a seasonal basis. Considering that the 18% forest loss observed during the August 30-31 storm represents a best-case scenario in which moist conditions prevailed during leaf-on conditions, most spring and summer storms probably result in forest loss to evapotranspiration well above 18%. Higher infiltration rates under forest than under grass during leaf-on conditions likewise only occur where litter is already wet. Other researchers have determined annual forest loss rates from 12 to 30% (Hewlett, 1982; Fujieda et al., 1997), and forest loss in the study area likely falls somewhere in the high end of the range of these estimates. More important to this study is the fact that grass loss rates in the study area are significantly lower than forest loss rates during the seasons when rainfall is likely to be highest. These findings duplicate studies made by other researchers, who report increased water yield under grass (Reinhart et al., 1963; Sikka et al., 2003; Ziemer and Lisle, 1998).

Water content data also provide good evidence for the existence of a mechanism whereby water can be shunted more rapidly into 25 and 55 cm subsoil layers under low to moderate moisture conditions in the grass than in the forest. Until forest subsoils became thoroughly wetted, forest topsoil consistently retained a higher volume of water during events than grass topsoil, and movement of forest water into the 25 cm level was always slower and of

a lower amount. This better developed ability of grass over forest to shunt water into lower soil levels extended to the 55 cm depth. The grass capacity to move water quickly to deeper soil layers seemed to cap grass topsoil water volume content as further precipitation was routed to lower depths. This direct shunting, along with the known vertical channeling of grass root networks, suggests that root channel macropores provide a significant mechanism for movement of soil water to the depth at which root systems are maintained. The very slow percolation of water into deeper forest layers suggests that early soil moisture derived solely from flow through pores of the soil matrix. The sudden surges of moisture at 25 and 55 cm on January 17 and 22-23 most likely occurred as preferential flow was finally activated at those depths.

Under both grass and forest, gradual rise in soil water content likely indicates a slow rise in moisture from percolation through pores in the soil matrix, as opposed to rapid response with the initiation of preferential flow. The wider distribution of grass root channels and their relative ease of activation in comparison with forest root channels create the differing responses recorded by data logging. Under forest, macropores capable of shunting water from topsoil layers took longer to open, most likely because of the need to saturate soils around larger channels before preferential flow along tree roots could take place. Once saturation is achieved in forest soil, flow to deep layers is rapid, and as under grass, water no longer builds up in higher soil layers. Once tree root pathways are functioning, they can bypass the soil matrix and carry water along the extent of the root network. In the study area, that includes deeper soil layers that are reached by few fescue grass roots.

### **Hillslope Hydrology Summary**

Infiltration and moisture content test results show that forest and grass effects on soil water movements for the most part follow expected patterns based on previous research. In general, measurements found that forest and grass root systems act in this environment as expected, in that both forest and grass roots provide rapid entry to soil layers. However, because forest and grass root systems differ in root size, volume, distribution, and orientation, the pathways for flow they create are very different. In contrast to the rapid movement into grass subsoil that occurs as macropores along grass root channels quickly saturate, forest preferential flow is not seen until the forest soil gains enough moisture through slow matrix percolation to enable the large macropores of tree root channels to function. Forest and grass vegetation thus set up very different patterns of water movement.

Statistical analysis of soil properties in combination with infiltration measurements at various tensions allowed a detailed investigation of interrelationships. Although both clay and organics are negatively correlated to infiltration rates, they moderate each other through their opposing effects on bulk density and thus porosity. Because “organics” as detected in loss on ignition tests for this project include roots, humus, and organic colloids, differences in the development of these factors are detected under forest and grass at varying depths. Because of the more uniform distribution of grass roots, organics in the form of roots are more dispersed in grass subsoils. Subsoils under grass thus tend to have lower bulk density and higher porosity than forest soils. Because clay has a direct negative impact on infiltration, water percolation in clayey forest subsoil is likely to be impeded more than flow in similar soil under grass, which is able to increase porosity without decreasing clay content. In contrast, forest topsoils show a higher organics content than grass because of higher humus levels. Under both forest and grass, surface infiltration is particularly limited at tensions of -15 and -8 by the negative correlation of infiltration to organics.

The negative correlation of organics to infiltration at higher tensions is likely caused by repellency. The effect of this repellency is mediated by the continuity of the porous networks and the decrease in bulk density that roots create in the clay-rich subsoils. Organics resist wetting, but the macropores of grass root channels still provide a much faster mode of water transport than pore movement through clay. Greatest overall infiltration takes place where a moderate to high number of roots are surrounded by a developed structure, rather than on the root mats of the <10 cm layer, and infiltration and conductivity values for the organic-rich topsoil in both forest and grass are thus lower than values at 25 cm. Organics are significantly higher in forest than grass topsoils, but the forest organics distribution as humus does not provide a continuous network into the subsoil. Water instead fills the matric potential of the dry forest topsoil until percolation into the subsoil matrix eventually activates preferential flow.

The initial wetting of grass root channels does not take long, as shown by relatively rapid 25 cm responses during the Katrina rains. Neither clay nor organics are significantly correlated to infiltration at low, near saturation tensions, suggesting that their negative influence is likely to be superseded by the enabling of macropore movement. Thus grass soils are influenced by rapid water movement along vertical channels to more than a meter, although decrease in fescue root volume may limit effectiveness somewhere around 1 m in depth.

Earlier researchers have found that forest soils permit higher infiltration rates than grass (Trimble, 1988; Cheng et al., 2002). Findings from this study give mixed results in support of this supposition. Comparisons of lumped forest and grass sets data (figure 6.9) as well as

mean infiltration and conductivity values at depths of <10 and 25 cm (table 6.1) indicate that forest infiltration rates have a tendency to be slightly higher than grass. However, statistical tests show only topsoil to have a weakly significant difference between forest and grass infiltration rates when measurements are divided by categories. No significant differences between forest and grass infiltration or conductivity values are found at any other depths.

Comparison of forest and grass differences by depths also shows that the weak significant difference (90%) in topsoil that is detected in sideslope data cannot manifest unless the soil is well moistened. Since organics tend to have a negative effect on infiltration until saturation is reached, it is likely the higher humus content of forest topsoil that provides the increased <10 cm infiltration capacity of forest over that of grass when the soil is wet. From soil water content data collected at dielectric probe stations, it was determined that responses to rainfall at <10 cm that were faster in forest than grass did not occur until early winter, when litter and topsoil were both thoroughly wetted.

No increase in infiltration capacity of forest vs. grass was found at 55 cm, and at 85 cm the forest and grass infiltration means are almost identical. The lack of statistical support for larger forest than grass subsoil infiltration rates is likely a reflection of the fact that rapid flow rates in forest subsoils are largely a result of preferential flow. Because of the nature of the infiltrometer test set up, most tests were unable to capture preferential flow along widely-separated tree roots, and data does not likely reflect the full potential of tree root pathways. Tree roots are most frequent at 25 cm depth, and preferential flow along roots was captured in the test results from pits 7 and 8. At these two sites, large infiltration rates in the forest soil were generated by flow connection between the infiltrometer disk and root macropores and fractured rocks under the disk.

The inability of infiltrometer testing to measure preferential tree root flow indicates that although infiltrometer measurement is a good way of gathering site-specific data important in understanding hydrology conditions in the study area, its primary effectiveness lies in picking up flow rates into the soil matrix and smaller macropore channels. Measurements that compare overall forest and grass infiltration rates may be better done by procedures that incorporate evapotranspiration, run-off, and water yield from a larger area than the point-specific coverages measured by an infiltrometer test. However, these test results have revealed that infiltration differences do exist between forest and grass infiltration capacities that are established according to soil depths and antecedent soil moisture. A larger sampling number would provide aid in support of this information, and would likely ease the difficulty created by the limited area coverage of the infiltrometer tests.

The coincidence of high infiltration readings at 85 cm with gravelly clays or layers of limestone fragments above bedrock also points out the importance that rocks play in promoting preferential flow in this thin-soiled environment. Infiltration tests run on the shoulders of the grassed portion of the slopes found a statistically significant relationship between conductivity and the depth to bedrock immediately below the infiltrometer disk. The negative trend of this relationship suggests that in thin soils, pathways of water movement are set up that conduct water along rock faces and fractures, thereby bypassing the soil matrix. It is also likely that clay may be translocated by preferential flow along rock faces, particularly under grass where the grass roots selectively exploit this environment.

Clays derived from *in situ* weathering and translocation build to a highly significant degree with depth in most locations in the study area, but data from this study suggest that fine particles may also be removed from deep layers where freely draining conditions exist at the epikarst surface. Some evidence for translocation of clays along grass roots is also indicated by the study data, as shown by positive correlations of clay content to both organics and porosity at 55 cm depth. Although clay content is statistically the same between forest and grass at equal depths, mechanisms for soil property changes appear to be active under grass in the system, and textural changes are likely to increase slowly over time. This implies that vertical impedance under grass will likely become more accentuated in the future.

In sum, infiltration and soil moisture test results show that differences in water movements originate from a complex web of interactions that change with antecedent moisture and season, and are influenced on a site-specific basis. Under wet leaf-on conditions, about 59% more water is lost to evapotranspiration and interception per storm event by forest than grass, and when leaf-on conditions are dry, essentially no moisture may reach the soil under forest. Under both forest and grass, soil surrounding root channels must become wet before macropore flow can be initiated, but macropore flow is much more easily activated under grass than under forest. Moisture may travel down vertical grass root channels to 55 cm depth with only moderate moisture and rain events, and rapid flow to 85 cm occurs under wetter conditions. Dry forest topsoils trap water, holding it in storage as percolation through soil pores gradually carries it into the subsoil. Once subsoil layers at 25 and 55 cm become saturated, preferential flow pathways under forest activate and rapidly disperse moisture to deep layers. Differences between forest and grass thus lie in their abilities to store moisture in the topsoil, their timings in macropore activation, the depths to which they act, and the possible volumes of flow they might carry.

## CHAPTER 7

### SUMMARY AND SYNTHESIS

#### SYSTEM CONNECTIONS

Understanding erosion on Bowman's Bend, and by extension on other fluviokarst landscapes, requires that its system dynamics be synthesized into a coherent picture. This chapter details system connections, and draws the data together to generate an explanation for the current erosion pattern. In some cases, seemingly disparate pieces of information appear weakly linked, yet these same pieces provide the solid framework of data needed to define system boundaries. Lithology, soil parent material, vegetation cover, and responses to weather events define the system's stage of action. Other pieces of information, such as observed soil or water outflow features, provide direct clues to current processes. Within this background, process measurements define the nature of the system's integrations.

#### Key System Variable Effects

Spatial distributions of the erosion patterns described in this project point to a central factor causing a general shift in upland water fluxes. Erosion correlates most strongly to the grassland/forest boundary line, particularly where the boundary is intersected by karst pathways. Vegetation has thus been the most likely candidate for the cause of changes in hillslope water and sediment movements.

The major variation currently found in vegetation on Bowman's Bend is between grassland, whether fescue or native grasses, and oak-hickory forest. Historical records and aerial photographs provide a means for establishing a time line for land use, and indicate that most slopes were used for agriculture or pasture prior to the native grass introduction by the Nature Conservancy. In the main study area, aerial photographs show that portions of the open area were occupied by forest 40 years ago, allowing those locations to be avoided during sampling, but show that the remaining open area has likely been maintained continuously in fescue since prior to 1937. Areas where samples were taken, whether in forest or grass, represent areas most likely to have been maintained consistently and with as little disturbance as possible under their current vegetation covers since settlement. This permits the comparison of forest and fescue grass effects that forms the central theme in this investigation of erosion on Bowman's Bend.

Variables of climate, geology, and soils determine the way in which plant communities, when left to their natural tendencies, will in turn sponsor shifts in the factors that build the landscape. All of these variables have been explored during the course of this project, both in terms of historical activity and relationship to vegetation influences, and the scope and direction of their influences are summarized briefly here.

### *1. Climate – Establishing When Erosion Occurs*

**Climate acts as an external variable that provides precipitation energy and thus controls the timing and rate of potential erosion, but does not determine the pathways for erosion action.** Dix Dam precipitation records indicate that no changes in rainfall patterns have occurred since 1925 that are sufficient to cause a change in erosion patterns. Climate records show that the last seven years have actually had mostly below average rainfall with somewhat fewer events of >25.4 mm/24 hours, although the numbers of >50.8 mm/24 hours and 101.6 mm/week events have stayed within historical ranges. Although large, high intensity events do activate large erosion episodes, as indicated by correlation of tree core data with the large event occurring in May 1978, low to moderate rainfall under moderately moist antecedent conditions can cause water to collect in flows within the regolith and at the top of the bedrock that are capable of moving particles.

Large events most likely do have a proportionately larger effect on erosion on Bowman's Bend. The one to three large events that occur during a typical year likely set up the current pattern of gullying, and will certainly initiate the seepage, exfiltration, and pipe flows seen at grass slope bases. However, observations of surface water patterns after moderate storm events also show pipe flow in gully heads and ponding at grass slope bases, suggesting that smaller events may maintain scour by preventing vegetation from reestablishing. As shown by vegetated forest gullies, such flow collection after small rain events is far less common in the forest than on grassed slopes. Thus, whereas the current erosion patterns are driven by the occurrence, intensity, and duration of storm events, these do not regulate the emergence of the erosion processes.

The meso-spatial scale of the research area has permitted climate factors to be considered as external to this project, with the expectation that all areas of the bend are receiving more or less the same amount of precipitation and have done so not only over the past 200 years, but throughout the Holocene as well. All soil samples were taken from neighboring slopes of a single hill with northeast, east, or southeast aspects. Differences in insolation and wind patterns should thus be small between the various sites and should certainly



not cause the changes in hydraulics as seen. In other locations on the bend, transects run between matching forest and grass sites always occupied equal elevations on the same slope and thus shared equal aspects. This similarity of climate factors, aspect and the short distance between differently vegetated sites ensures that forest and grass sites have experienced the same microclimate conditions, thus eliminating climate differences as a factor in test results.

## *2. Geology – Where Erosion is Likely to Occur*

**Geology determines bedrock and epikarst pathways of flow collection and solution and thus the placement of erosion features.** Bedrock composition, stratigraphy, and structural conditions along with climate, hydrology, and biota set up the particular weathering environment in which soil develops under the influence of vegetation. In the uplands, the thin limestone beds and shale layers of the Grier, Logana, and Curdsville tend to promote shallow, often curvilinear fracturing and cutter/conduit development, while at the same time promoting rapid dissolution and flagstone release along bedding planes and limestone/shale contacts. Weathering of the members of the lower Lexington Limestones also promotes the formation of benches in the hillslopes where more resistant layers restrict downward solution. The forms taken by these benches and by the various pinnacle, cutter, and solutional cavities in the karren, regulate water movements through the regolith base and into the epikarst. Drainage moves interactively between interconnected cutters and epikarst conduits in the upper slopes, so that flow from some hills converges downslope in soil-covered cutters that cross the grass/forest boundary lines. These cutters, along with high-energy flows dispersed broadly by bedrock surface topography across vegetation boundary lines, form sensitive areas susceptible to sediment loss.

Within all upland geologic members, impervious bedrock layers composed of shale, limy shale, bentonite, or massive micritic limestone, may restrict vertical water entry and guide fracturing and thus affect where weathering occurs. Waters moving within the conduits and cutters of the highest slopes down into the upland hill base are particularly impeded by the thick bentonite layer found five to six meters below the top of the Tyrone. This layer held the historical river channel 1.5 million years ago, and created the terrace that rings the bend today. It acts as a major landscape control unit, and it forms the break line between shallow upslope epikarst solution and deep, vertical shaft and sinkhole development in the High Bridge Group. In the main study area, collection and lateral movement of water through the alluvial sediments on this terrace exacerbate the erosion problem. However, sensitive, high-energy landscape zones are established by convergent topographic and soil conditions in both High Bridge and

lower Lexington Limestone terrains, and erosion is being initiated in the study area by hillslope flux changes in both.

Geology thus supplies the site-specific ability to conduct water over and within the bedrock and to support epikarst forms and karren flow paths. This determines not only bedrock topography, but surface topography as well, as growing solutional features tend to develop their own enlarging zones of influence. As shown by shallow soil depths across the foot of Hillslope A (Figure 5.21), which is bisected by an epikarst conduit, much sediment can move into epikarst pathways. As soil is lost, increased flow is pulled more rapidly into the depression from steepened surrounding terrain. Where flow rates are increased in general, both sediment loss and increase in solutional opening of pre-existing epikarst forms are likely to ensue. Some evidence of soil movement and opening of epikarst channels under grass is provided at certain grass slope bases, where outcrops and swallets appear at convergent zones (Figure 5.17). In general, the cutters and conduits in the shallow epikarst of the uplands are formed by identical processes, making all types of flow pathways susceptible to changes in regolith induced by vegetation.

### *3. Soils – How Vegetation Sets Up Pathways of Water Movement*

**Soils allow the propagation of vegetation effects, in that vegetation interacts with soil properties that are in turn responsible for infiltration rates, movement orientations, and storage capacities.** The effects of vegetation operate through rooting characteristics, sediment and organics movement, and changes in water movement volumes that act over time on soil layers developed under the influences of geology, parent material, and former vegetation community impacts on the landscape.

The basic parent material for soils on the bend is limestone residuum, but disparate inputs occur from bedrock members according to the solution rates and insoluble contents of their various layers. In the uplands, the lower Lexington Limestones, along with likely loess deposits, create high clay content soils with low sand percentages, although sand content is likely to increase directly above bedrock. Although the upland soils are flaggy, a steady increase in clay content typically occurs with depth, with no textural layers that would indicate a change in conductivity by anything other than clay increase itself. Overall, the residuum soils of the higher slopes most likely promote vertical entry that is increasingly impeded at depth. Mean hydraulic conductivity values at 55 cm are much lower than those at 25 cm (Table 6.1), suggesting that development of lateral flow is likely on the slopes.

Alluvium underlies the bottom half of the main study area slopes. These dense, often gravelly clays also show up not only in sideslope pits, but in epikarstal pockets on Hillslope B and in the forest on Hillslope A (figure 4.2), where dense, yellowish brown clays are retained in deep karren forms below the main terrace. Alluvium-based soils have developed in concert with colluvial processes, so that topsoils and AB or B horizons over alluvium often have texture and low gravel characteristics more similar to limestone residuum soils than to the properties of the underlying alluvium. Similar silt loam topsoils with crumb structure compose the relatively loose topsoils across the study area, but as shown by abrupt horizon boundaries in pit 5 and by stone and gravel sorting characteristics in pits at the slope base (Appendix 3), alluvium deposits below 25-50 cm are likely to show little sign of mixing with colluvial materials.

Clay increases with depth in 76% of the sites sampled in this project, but does so in conjunction with both water movements above bedrock and with soil characteristics inherited from parent materials. Continuous clay increase with depth is most likely to occur in “pockets”, where water and sediments are likely trapped. Figure 7.1 shows a cut-away diagram of how lateral water movement in grass pit 13 is likely encouraged with clay buildup to 76% at 55 cm. Conductivity decreases to  $1.51 \text{ cm hr}^{-1}$  at 55 cm, suggesting that water is likely to move sideways through the much more conductive soils at 25 cm.

This project found a significant relationship between clay content of the soil above bedrock and water movement, in that clay percentages often lower than that of overlying soil layers were associated with soils directly above bedrock in sites exhibiting features of flow concentration at the bedrock surface. This typically relates to lateral movement, but can also associate with downward flow into holes in the bedrock. In figure 7.2, a hole >1.6 m deep in pit 12 shows an increase in conductivity with depth to 80 cm at the top of the hole. Since clay content decreases from 59% at 80 cm to 52% at 110 cm, flow is likely conducted easily through the soil-filled hole in the epikarst, quite possibly along the rock walls as preferential flow. The association of lower clay content with concentrated water movement appears to be fairly consistent across the study area, occurring in approximately 20% of the sites, although a decrease in clay content at bedrock was detected in a few locations, such as at 55 cm in pit 14, where sand content increases because of inherited parent material characteristics. Despite the few exceptions, lower clay content above bedrock provides a good line of evidence for collected bedrock flow.

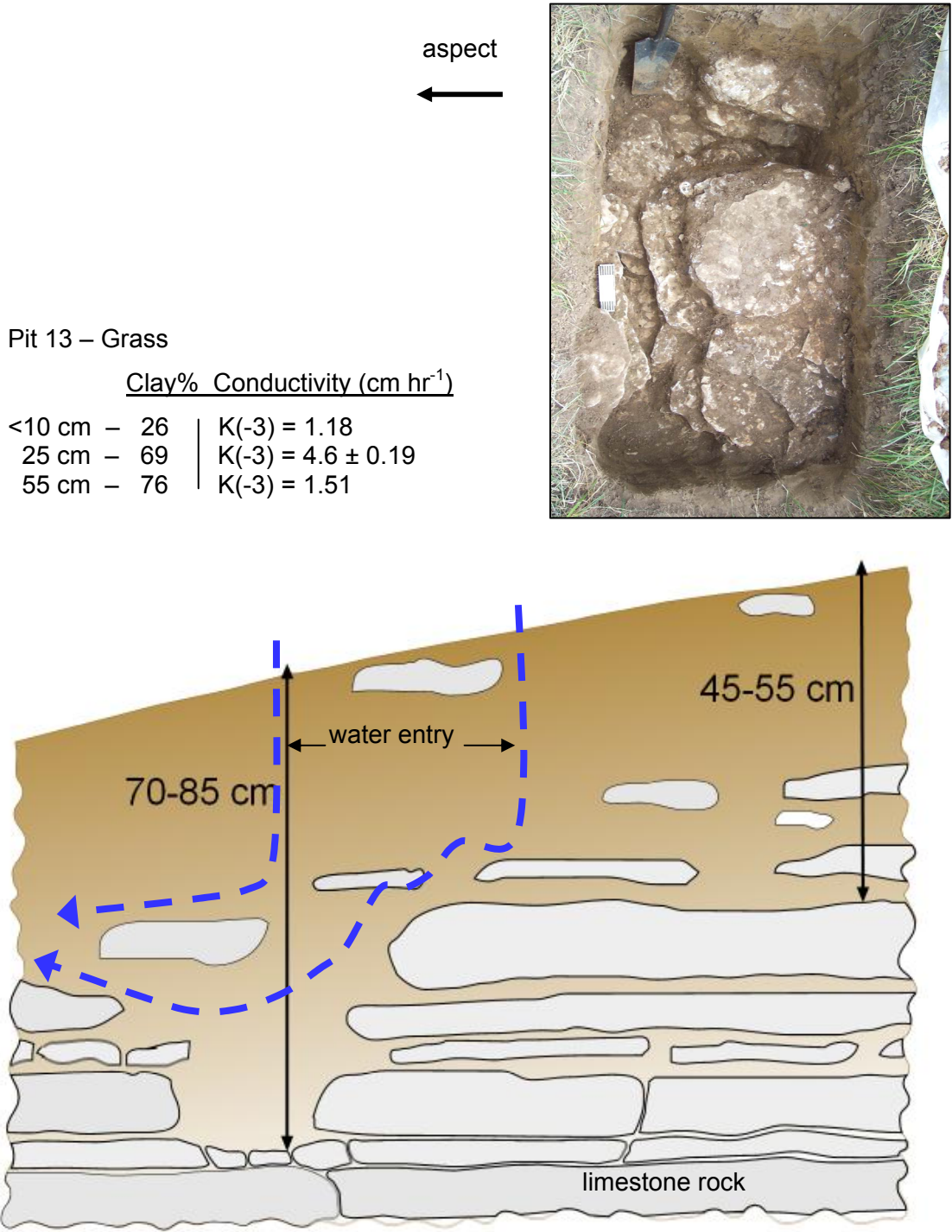


Figure 7.1. Simplified cross-section of soil pit 13, showing that clay build up over consolidated bedrock surfaces will encourage lateral water movement in the soil profile. Here conductivity at 25 cm is much higher than at 55 cm depth.

Pit 12 - Grass

Clay% Conductivity (cm hr<sup>-1</sup>)

|         |      |                     |
|---------|------|---------------------|
| < 10 cm | - 23 | K(-3) = 2.76        |
| 25 cm   | - 38 | K(-3) = 2.89 ± 0.07 |
| 55 cm   | - 56 | K(-3) = 2.88 ± 0.06 |
| 80 cm   | - 59 | K(-3) = 3.15 ± 0.56 |
| 110 cm  | - 52 |                     |

aspect

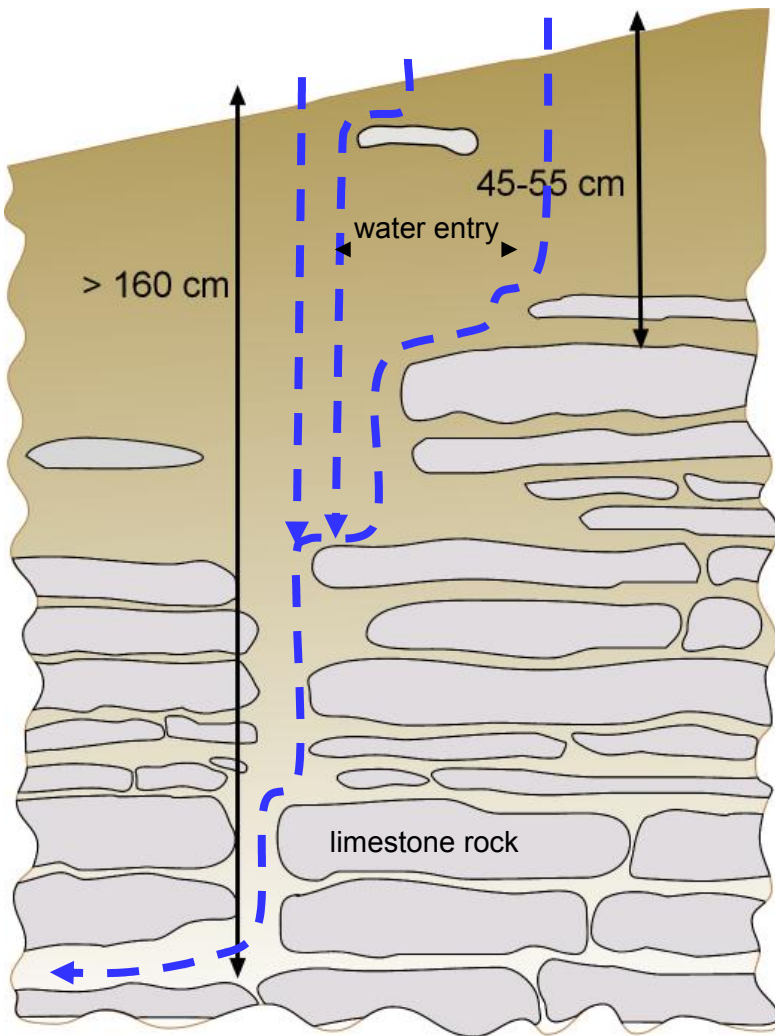


Figure 7.2. Simplified cross-section of epikarstal drainage under pit 12. Water enters a soil-filled solution cavity, as indicated by increase in conductivity at 80 cm and decrease in clay content with increasing depth in the hole.

#### *4. Vegetation Influences – Why Current Patterns of Erosion Have Developed*

**Grass and forest vegetation establish different characteristic growth and rooting patterns that influence water and sediment movements and storage, and thus soil development over time.** Fluviokarst regions are prone to soil loss because of their ability to discharge sediment into both surface and subsurface pathways. Because the fluvio karst landscape develops in conjunction with regolith and epikarst features that tie into the subsurface drainage system, limestone terrains are particularly susceptible to changes in soil that redirect regolith flows. Evidence from this study backs up historical evidence obtained from various other limestone regions of the world (Ford and Drake, 1982; Trudgill, 1985, Drew, 1983, Williams, 1993; Daoxian, 1993), in that it finds that permanent deforestation generates a number of influences that disturb water movement patterns in the regolith and set up processes that encourage soil loss.

Pollen records indicate that this region of the Bluegrass has supported forest growth throughout the Holocene, so that the landscape entered by European settlers was one constructed under forest influence. That landscape contained deep alluvial soils in the north part of the bend that were second only to the current river floodplain in productivity. Agriculture certainly provided the means for sediment loss in these and other slopes on the bend following settlement, but some of the loss may have been a direct effect of loss of tree growth, as shown by bedrock exposures on the shoulder of the main study area. Many currently grassed upland slopes throughout the bend display outcrops that make it unlikely that soil thickness is the same now as it was during deforestation, when settlers were intent on establishing agriculture.

Incidences of root grooving, rock slab lifting by root growth, increase in pitting along forest transects, and bedrock penetration by tree roots in all forest pits indicate that trees are important biogeomorphic agents in this environment. As shown by current conditions on steeper forest slopes, trees actively mine the epikarst through solution and root action in weakened fracture and bedding plane zones. Tree roots likely send preferential flow ever deeper into the epikarst surface as openings are expanded by chemical action expedited by root hair and fungal activity. The final effect of tree root action is a continuous attack on the bedrock surface at numerous points of discrete root entry. Discrete root entry not only provides wicks into the bedrock along which preferential flow can occur, but it also ensures that more storage capacity is generated as pits and pockets are created, and that soils are continuously replenished by residuum materials released from the bedrock (Figure 7.3).

1. Lifted rocks are pushed above thin soil.
2. Surface rock decomposition is encouraged by preferential flow and pressure from lateral roots at the top of the epikarst.
3. Sprouts utilize fractures for early growth.
4. A pit develops within the vicinity of the tree base.
5. Bedding planes provide access for uphill laterals.
6. On steep slopes, thin soil and rock cover sloughes, leaving large roots exposed on the surface.
7. Sinkers exploit weakened zones in the epikarst, opening pathways by root grooving. On slopes, outer rock layers become disconnected from the rock mass.

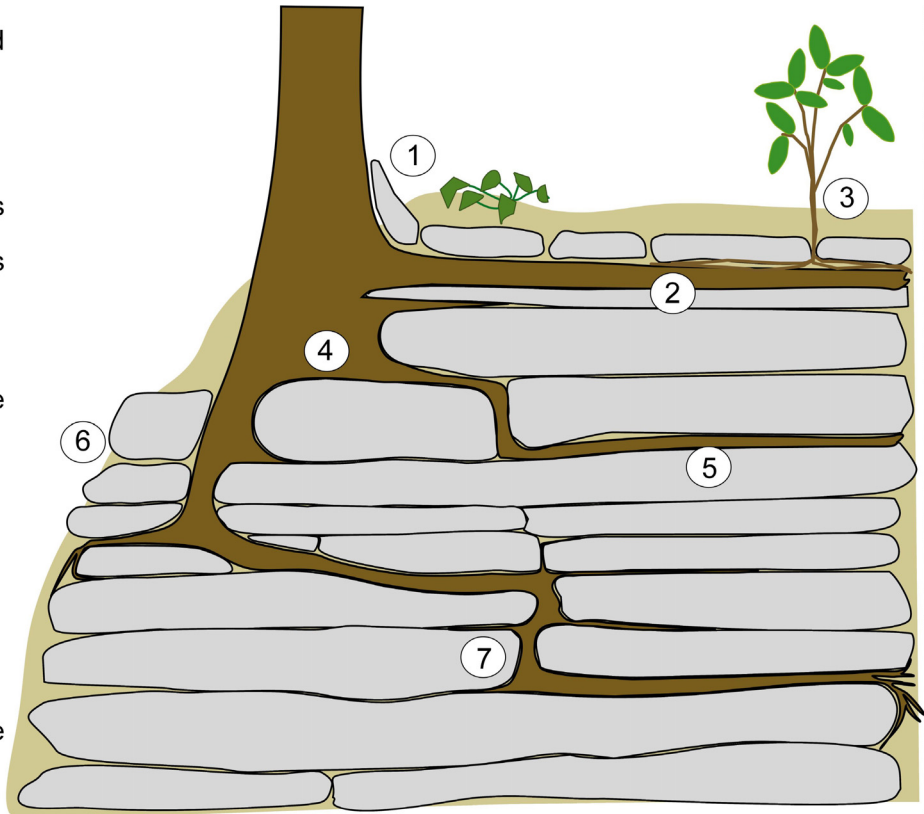


Figure 7.3. Tree roots enter weakened zones in the epikarst, carving solutional pathways with the aid of preferential flow.

Observations of pits and landforms witnessed in the study area suggest that tree roots are undervalued in their effect on epikarst weathering. Part of this underestimation may lie in the fact that most tree growth observed by researchers is that of second growth specimens. As shown by the apparent ability of large roots in pit 7 to decompose thin rock slabs through increased solution and pressure (Figure 5.50), root action clearly increases in impact with tree age and root size. Such effects have most impact in high-energy areas where thin soils offer little resistance to lifting forces created by large roots, so that effects of deforestation are most visible on the steeper eastern slopes of the bend. However, whereas signs of soil loss are less frequent in the north end of the bend, gullying at north bend locations indicates that even deeper-soiled areas are susceptible to changes caused by loss of tree root action.

In contrast to the discrete weathering action sponsored by tree roots, grass roots do not penetrate between bedrock slabs. Although the bulk of the fescue root mass is in the upper 30 cm, vertical networks of roots drop in root channels that permit a moderate infiltration rate in clay-rich soils. Fescue root numbers decrease with depth, so that few to no fine roots will be

present below 125 cm. In the thin soils of the upland, grass roots are easily able to reach the epikarst surface, and they exploit the epikarst by forming mats on rock benches and between plates separated by soil in lower horizons where water is able to enter. Infiltration down the vertical grass networks is amplified where roots connect directly to rock benches and flow can tie in to preferential flow along the rock face. Lack of grass root matting in higher soil layers and on “floaters” suggest that it is the increased water availability related to preferential flow along the walls of the rock benches that encourages the grass matting.

The majority of tree roots were found above one meter, with the largest lateral roots found in mid to upper profile depths (25 to 55 cm). However, small diameter vertical sinkers penetrated the bedrock to at least 1.85 m in one forest pit. Discolorations that follow tree root channels suggest that preferential flow follows the roots throughout their entire lengths, as is also confirmed by the sharp increase in water content seen in the 125 cm responses following the January 22-23 event in 2006. The lateral as well as vertical orientations of tree roots contribute to their versatility in puncturing the epikarst surface. As suggested by the soil-filled pits and shallow channel found near the grassed shoulder of Hillslope H (figure 5.54), laterals likely tend to follow bedding planes. As these roots weather the surrounding bedrock and expand their sphere of contact with increasing age and growth, fractures develop in the overlying rock layers. These fractures in turn provide the means for future generations of trees to become established.

Grass and forest thus support very different root system characteristics. Water and sediment movement responses to these characteristics operate in conjunction with other properties, such as evapotranspiration, soil water storage, and hillslope stability that also have differences sponsored by vegetation, so that final landscape development occurs within a web of vegetation-controlled influences.

### **Water Movement Pathways**

Vegetation creates an overarching influence on hillslope water movements, but it does so based on the inherited characteristics of the landscape. In this section, both pre-existing and currently active variables responsible for water movements are examined with consideration of their interactions.

#### *1. Soil Texture*

**Root actions affect and are affected by existing soil texture and texture variability, which together provide the major overall regulation of hillslope water movement speed**



**and direction.** Clay layers above the limestone contact have been found to induce lateral flow and erosion in other regions (Trudgill, 1985). Increase in clay content with depth, with no layers of intervening texture contrast, occurs in uphill soils developed from Lexington Limestone residuums. Clay impedance of percolation in these soils is likely to have most impact during the wetting phase of storm events, as the negative impact of clay on infiltration decreases as soil approaches saturation. At saturation, heavy clay soils are likely to move water directly to the bedrock in thin-soiled upland locations, activating rapid water movement either across the bedrock surface or into solutional cavities. Thin (2 to 5 cm) layers of unconsolidated rocks and rock fragments in BC horizons in upland soils may help to facilitate bedrock water movement.

High porosity and structural integrity will promote diffuse vertical water penetration in organic-rich horizons with crumb or granular aggregates (Brady and Weil, 1996). Evidence from this study indicates that whereas this is generally true, complex interactions are involved in infiltration processes. Organic matter has a significant negative influence on flow, and both forest humus and organic matter content of grass root mats in topsoils tend to reduce infiltration. At 25 cm, root numbers are less than that of the topsoil, so that the negative influence of organics is reduced, but there are still sufficient roots to increase porosity in the clayey subsoils. Conductivity at 25 cm is thus increased in both forest and grass over that of the topsoil. In general, typical upland soil textures in combination with effects created by vegetation permit low to moderate water entry at the surface, an increasing rate of vertical entry at 25 cm, and a reduced rate at 55 to 85 cm as clay content rises and porosity decreases.

At the slope base, vertical entry is likely encouraged by gravelly and sandy clay alluvial layers, as shown by relatively high near saturation conductivity values at depths of 55 and 85 cm. Because these layers overlie heavy clay layers with low sand content, texture contrast characteristics at the slope base likely set up lateral flow patterns between 55 and 100 cm depth. Where sideslope flow enters alluvial materials, lateral movement within sandy, gravelly layers is likely to increase, carrying water to the edge of the main terrace where alluvial sediments pinch out. Perching of water is common along the outskirts of grass slope bases following moderate rain events (Figure 5.22). The lack of such ponding in the forest at this elevation, despite equal influences created by soil texture and the underlying impervious bentonite layer, indicates that the grass rooting system has increased the volume of water moving along these textural pathways.

Although no significant difference was found between mean clay content percentages of forest and grass soils at any depth, some evidence exists for the establishment of a mechanism whereby such a difference may be developing. Structural ped faces act as pathways for water

entry. Grass root networks are particularly good at exploiting the mesopores passing between ped faces, and clay films discolor vertical root channels formed along the sides of the subangular block structures in the dense soils. This study found evidence that clay translocation along root channels is high enough to generate significant positive relationships between clay content and both organic matter and porosity at 55 cm depth at grass sites. Similar relationships were not evident at this depth under forest, and the clay vs. organics and porosity relationships were actually negative at 85 cm for forest. Thus some evidence is present for increase in clay translocation under grass that causes significant build up in relationship to porosity provided by grass roots.

## *2. Root Pathways*

**Differences between forest and grass root effects on water movements relate to differences in root orientations, sizes, depths, and abilities to enter bedrock.** As evidenced by clay films on both tree and grass root channels, grass root systems encourage diffuse vertical water movement into the soil that contrasts with the lateral and vertical preferential flow generated along discrete tree roots (Figure 7.3). Because few fescue roots are found below 125 cm, fescue roots in this environment are limited in their ability to facilitate percolation into soils below approximately one meter depth at the hill base. The resultant increase of grass water movement in upper soil profile layers within the hill base follows data obtained by researchers who have identified increased flow at higher soil layers under grass in other locations (Burch et al., 1987). Altogether, findings suggest that the depth of grass root penetration plays a large role in setting up water movements that tie into the texture contrast characteristics of the soils in the main study area terrace.

Because grass roots are able to contact the epikarst surface in upland sites, rooting depth is not as important here as it is at the hillslope bottom. However, differences in ability to enter bedrock become critical. Because grass roots cannot penetrate bedrock fractures, their effect on weathering appears to be confined to a general increase in solution of the rock surfaces coated by root mats in hillslope benches. Rock faces typically displayed a micro-scale roughening. Without the penetration of weak epikarst zones by tree roots, bedrock forms under grass become smoother, with less pitting and fracturing, as shown by transects taken in forest and grass at the shoulder of the main study area (Figure 5.49). This smoothing takes time, just as the fracturing of the surface of the epikarst takes time under tree root growth. Reduced bedrock entry following deforestation likely sets up conditions that, along with gradual diffuse

movement of clays to mid-profile depths along grass root channels, leads to increasing lateral water movement in the uphill regolith.

The ability of tree roots to conduct lateral preferential flow also likely plays an important role in the localization of gullying at points where convergent flow under grass contacts the edge of the forest. As shown by the number of sites on the bend where swallet development and conduit unroofing is aided by tree roots (figures 5.36 and 5.37), roots oriented in the direction of the potentiometric gradient permit an increase in preferential flow, which in turn is likely to increase sediment movement. Grass root mats are capable of capturing fines and protecting soil surfaces. Loss of this protection at precisely those locations where tree roots are found 30 to 60 cm below the surface in cutters, creates perfect opportunities for the development of the soil pipes seen in gully heads. Similarly, loss of grass root matting protection most likely sets up conditions for soil loss and eventual erosion at those locations where concentrated flow across the bedrock surface crosses grass/forest boundary lines oriented in an uphill/downhill manner (Figure 2.12). Thus the higher flow depths encouraged by grass roots, coupled with increase in total volume created by lack of bedrock entry, act in concert with tree root preferential flow capabilities to generate soil piping and gullying.

### 3. *Gullies and Conduits*

**Conduits and interconnected cutters funnel much of the water movement on hillslopes, but vegetation controls their characteristic appearances.** Because geologic factors largely limit weathering to shallow depths in the upland slopes, conduits and cutters are interactive, so that conduit roofs break into blocks that are eventually removed by solution, leaving surface cutters in their place. At grass slope bases, epikarst pathways that enter the forest are typically only soil-covered. Such cutters are expressed in both Lexington Limestone and High Bridge Group forest terrains as vegetated and non-scoured gullies one to three meters deep. These forest gullies align perpendicular to the river and are either shallow-soiled (typically <40 cm) or broken by outcrops. Where these gullies are undisturbed, soil removal apparently occurs primarily along subsurface pathways rather than from surface transport. Similar interconnected cutter systems are likely buried under soil on the grassed slopes, as shown by soil depth transects on Hillslope H (Figure 5.16). Differences in the appearances of cutter pathways under forest and grass suggest that soil loss is normal in cutter systems, but that grass sets up different water and sediment movements.

Forest and grass cutter differences most likely derive from the depth of water movements and soil loss promoted by the differing vegetation. Tree roots are able to tap into

the epikarst, and conduits operating beneath the rock in a linear depression would offer prime locations for tree root growth. Such a possibility is shown in Figure 5.19, where a large sink uphill from a vegetated gully has no surface connection to the gully. This lack of surface connection, along with lack of scour in the gully, suggests that primary water movement occurs below the rock surface of the gully base, where soil loss occurs with downward water entry along fractures.

Where forest gullies enter grass downhill from a forest patch, the cutter will become buried, as seen in figure 5.20, showing the ability of the grass root mat to retain soil. Since tree root preferential flow paths would be lost after deforestation, it is possible that sediments entering the drainage below cutters under grass may plug these conduits over time. Field evidence for this is found below Hillslope A in the main study area, where flow issues from a surface gully rather than the vertical fissure visible in the rock wall (Figure 5.15). It is not known if grass-related sediment movement is responsible for plugging this or other conduits, but conditions in exhumed forest cutters all point toward water movements at the bedrock surface that either do not include flow through underlying rocks, or operate at an increased volume that overwhelms existing underlying conduits. Scoured side walls and denuded bedrock floors in the eroded cutters at the grass/forest boundary line contrast sharply with the vegetation and soil present in undisturbed forest gullies.

If grass does tend to promote conduit plugging, water movement and sediment loss on the uphill grassed slopes are likely to concentrate in the bedrock bases of interconnected cutter pathways rather than in conduits within the rock. Under the protective grass root mat, visible evidence for changes in flow concentration in pathways only becomes obvious downhill, where contact is made with the forest root system. Altogether, although evidence for conduit plugging is only circumstantial in this project, a large amount of geomorphic evidence does point to flow under grass that is greater in volume and occurs closer to the surface than conditions under forest. The common effect of grass on uphill cutters is a development of flow at higher soil depths that is disguised by grass root matting, and movement of flow above or at the bedrock surface where cutters pass into downhill forests.

#### *4. Rock Face Pathways*

**Connected rock faces in hillslope benches provide an important, largely unexplored and underestimated route for preferential flow in the limestone benches of the hillslopes.** Determination of a significant relationship between near saturation hydraulic conductivity and the distance measured between the infiltrometer disk and the underlying rock

(Figure 6.11) shows that rock benches can act as viaducts for water movements in thin-soiled areas. This effect increases as the soil becomes more saturated and distance to the disk decreases, thereby increasing the likelihood of establishing a direct preferential flow path between disk and rock face.

Fractures and bench faces were particularly likely to expedite infiltration if roots directly below the infiltrometer tied into the zone of rock preferential flow, so that infiltration capacity created by the integrated effects of roots and rocks exceeded the simple additive effect each might have on its own. Combinations of root and rock effects may be largely responsible for the large outliers in infiltration rates seen at different depths in both forest and grass. During surface infiltration testing on the shoulder of the hill, whereas only 5 out of 21 grass surface infiltration tests generated  $K(-3)$  of more than  $5.0 \text{ cm hr}^{-1}$ , one test at 10 cm above bedrock provided a result of  $25.9 \text{ cm hr}^{-1}$ . This particular site overlay a fractured rock surface.

The activation of rock face preferential flow likely sets up conditions in which particles from shoulder soils are pulled in suspension into water moving along soil-covered rock faces, setting up a pathway for surface rock denudation. Exposures of bedrock expanses in the shoulder of the main study area bear out this concept. As larger areas of flat bedrock are exposed, a feedback mechanism may be set up in which an increasing amount of surface runoff is conducted to the downhill side of the rock where it is able to enter preferential flow lines at the soil/rock interface, thereby setting up the means for increased subsurface sediment movement. At the same time, increased runoff from exposed rock expanses simultaneously heightens the likelihood of excess water movement across the downhill soil surface. It is likely that increases in both surface and subsurface soil loss act together to denude high-energy areas with thin soil cover.

Although statistical evidence for rock face preferential flow was only obtained on the grass slope during this study, connected rocks seem to perform the same action under forest. Infiltration rates were often very high where the tensiometer disk was close to the bedrock in either forest or grass, despite clay-rich soils at depths of 55 or 85 cm. As in the surface tests, such high rates appeared dependent on two things: the existence of fractures in the rock face, so that water was not trapped by the rock, and the presence of roots connecting the soil under the disk to the rock face. Very high infiltration rates were obtained in forest where both circumstances occurred, as shown by the  $K(-3)$  value of  $15.36 \text{ cm hr}^{-1}$  obtained for 25 cm depth in forest pit 8 (Appendix 5). These test results provide evidence for heightened preferential flow activation along root pathways that enter the bedrock surface.

Clay and other sediments may plug conduits. This, and the fact that rock benches in the study area set up preferential flow along their faces, suggest that rock face flow is either limited to where roots contact the rock, or is limited in general by the dissipation of flow with depth. The latter seems more likely, as is indicated by the decrease in conductivity associated with increase in distance to rock shown in surface infiltration tests (Figure 6.11). It is likely that the clay soil is able to pull a portion of the flow away from the rock wall through capillarity induced by matric pressure, so that a film will be dissipated into the surrounding regolith with increasing depth. This would explain why clay may plug conduits at deeper depths, but still permit rapid rock face flow closer to the surface. Although this concept is purely speculative, it is likely that soil may have an increasingly negative impact on rock face flow with depth. Such an impact would be eliminated where conduits were free of sediments.

The effect of this rock face flow was not anticipated, but its existence is most likely important in both bedrock solution and fine sediment transport. Chemical equilibrium between solvents and solutes is likely to take place more quickly where flows are slowest (Trudgill, 1985), suggesting that rapid flows along rock faces are likely to influence solution rates, or at least carry aggressive water into deeper depths and into weakened zones between rock layers in the epikarst surface. Flow along rock faces is also likely to augment water entry in those locations where tree roots penetrate fractures, bedding planes, or along limestone/shale contacts.

In the study area, limestone “floaters” are frequently found in surface horizons, and their presence suggests that solutional attack may be somewhat buffered by the neutralizing effect of the boulders on surrounding soils. Soils become more acid after rainfall as meteoric water percolates downward, but where carbonates are present in the soil, solution will raise the pH level to the alkalinity range (Trudgill, 1976). Such a buffering effect is not possible where rapid flow occurs, indicating that part of the resistance of the “floaters” to decomposition lies in their disconnection from the main rock mass.

Rock preferential flow is maintained where the rock face is continuous, or where separations between layers are very thin so that saturated soils bridge the intervening distance. Once a limestone boulder becomes substantially isolated from the main rock mass, it is much easier for carbonates to chemically equilibrate with the moisture of the surrounding soil matrix. This suggests that the “floaters”, once disconnected from the main limestone mass and its conduction of preferential flow, are able to buffer themselves. This offers a good explanation for why the largest “floaters” are found in upper soil horizons; boulders released from the highest layers of the epikarst are self-maintaining once they disconnect from preferential flow paths in

the driest soil layers, whereas those stones released at lower depths are weathered by more continuously damp soil conditions.

Rock face preferential flow thus seems to be important in solution and sediment movement in the main study area. Where subsurface movement along the bedrock face is high, little surface sediment movement may be detected, but soil loss through subsurface means may still help strip thin soils from high energy areas. Although surface sediment movements were not studied for this project, locations at which evidence for surface water movements were observed were always at mid or lower slope positions where soil depths are deeper. In the forest, rock face flow is likely to percolate into the epikarst along points of root entry, increasing the likelihood of solution along root pathways. Thus, rock face preferential flow is likely firmly tied to the differences in bedrock entry set up by grass and tree root systems.

## INFILTRATION PATTERNS

Vegetation sets up not only characteristic regolith and epikarst water movement patterns, but particular tendencies of evapotranspiration and ease of wetting that must be factored into hydrologic changes. This section summarizes the main differences in these factors between forest and grass as observed in this study.

### Soil Wetting Differences

**Significant differences exist between forest and grass interception and evapotranspiration, initial topsoil wetting, and progressive saturation of soil layers with depth.** These differences varied according to antecedent moisture and seasonal leaf and litter conditions, and are pictured in figures 7.4, 7.5, and 7.6.

Following the drought of summer 2005, near-surface (<10 cm) soil moisture increase was noted under grass within an hour of the beginning of the first heavy shower in August, but interception and evapotranspiration captured 100% of the first four rain events in the forest. Even after foliage had become fully wetted during leaf-on conditions, 59% more precipitation was required by the forest than the grass to initiate soil water increase at <10 cm during each rain event. Thus, in comparison to the forest, a greater volume of water reaches grass soils during growing seasons.

## Forest Water Movements Under Dry, Leaf-on Conditions

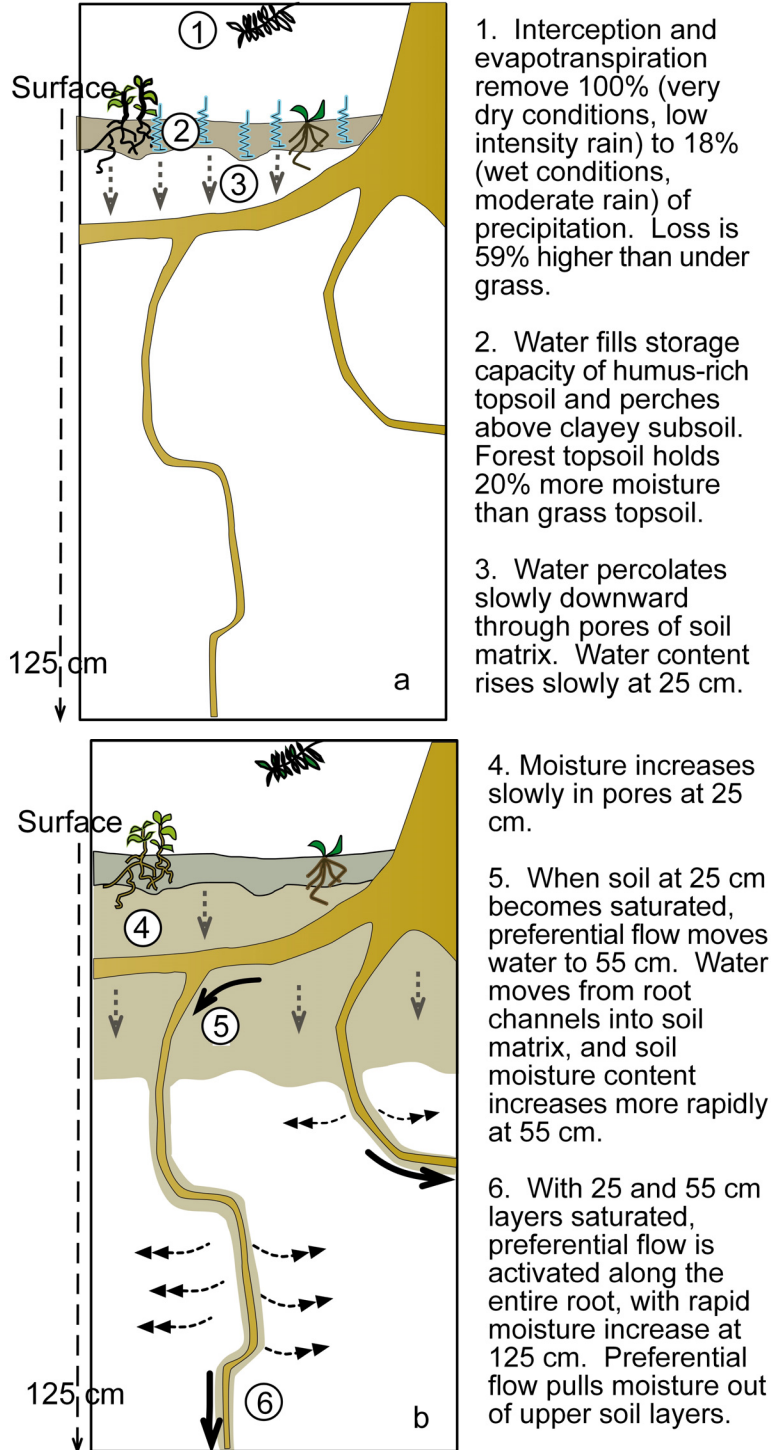


Figure 7.4 Forest water movements during dry, leaf-on conditions. Figures (a) and (b) detail water movements at different soil moisture stages.



## Forest Water Movements Under Wet, Leaf-off Conditions

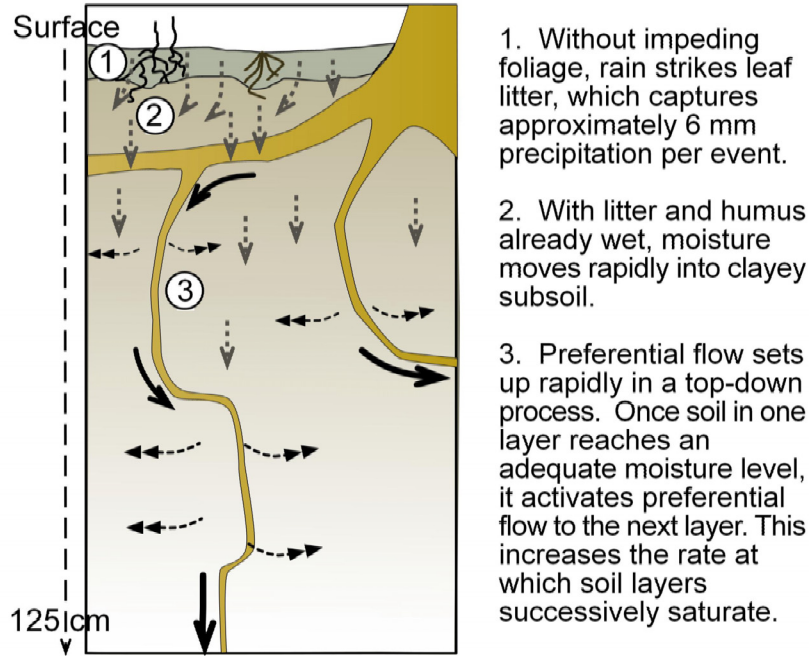


Figure 7.5. Forest water movements during wet, leaf-off conditions.

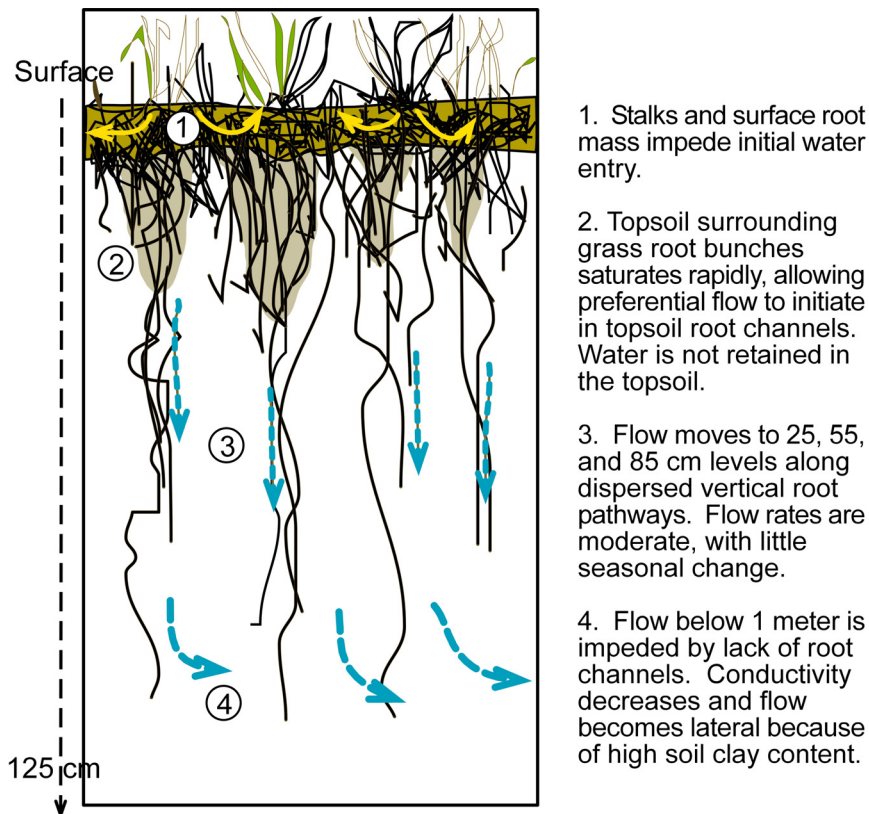


Figure 7.6 Main features of grass water movements.

The water that reaches the forest surface under dry conditions is retained in the humic topsoil, with movement into the subsoil confined to movement through the pores of the soil matrix. Trimble (1988) states that organic layers in forests do not act as 'sponges', and are only able to absorb several mm of water. Data from this study only partially support this statement. The particular infiltration characteristics of the study area are dependent on very high clay content, which tends to restrict water movement between soil pores. Percolation from the topsoil into the 25 cm layer was greatly restricted under dry conditions in the forest (Figure 7.4). Without the vertical root channels of the grass, the organic-rich forest topsoil behaved much like a sponge, holding water and letting it move only gradually into the subsoil matrix.

Once the topsoil became thoroughly wetted under leaf-off conditions, less precipitation was needed under forest than under grass to initiate surface soil moisture increase, and the wetted forest litter and topsoil conducted moisture easily to the probe buried at <10 cm (Figure 7.5). Although litter and topsoil were only able to hold a few mm of water (approximately 6) before moving water to 10 cm, this again shows activity that might be associated with a "sponge", in that it is likely that because the humic topsoil layer retains overall high water content, meteoric water falling at the surface is able to rapidly displace underlying moisture, which then exits the topsoil base. The response pattern in grass at <10 cm under leaf-off conditions shows a development of soil wetting that differs little from that seen in grass during the growing season, though initial topsoil wetting appears to become somewhat slower during the winter. Because less humus is present in the grass topsoil, wetting of the grass root channels during each event is more reliant on wetting of the crumb aggregates composing the soil structure.

Shirmohammadi and Skaggs (1985) found that saturated hydraulic conductivity was increased by fivefold in fine sandy soil with two-year old fescue root systems. They also found it necessary to include seasonal conductivity increases, which they attributed to the ability of growing roots to loosen the soil, within hydrologic models to generate infiltration rate predictions that matched field conditions. This same mechanism may provide an explanation of why more rainfall is required in the winter than in the summer to generate soil moisture increases at <10 cm under grass. Although grass surface moisture increase occurred after approximately 6 mm precipitation during August events, rapid response was delayed until up to 13 mm had fallen in December. During winter seasons, grass roots provide reduced avenues for preferential flow, and the infiltration effectiveness of forest over grass is thus increased not only by equalization of evapotranspiration loss, but by seasonal drop in grass root preferential flow capacity as well. These factors set up circumstances under which the grass slopes must handle a higher volume

of water per event during the growing season, but no difference in volume during leaf-off periods.

In some basins, perching of water and lateral flow in the O horizon may conduct stormflow in forests (Brown et al., 1999). Results from this study verify that this is indeed a likely possibility under some circumstances, such as where high intensity, high duration rains occur under dry antecedent conditions. Under more typical circumstances, forest water movement appears to be more reliant on activation of preferential flow layer-to-layer as saturation proceeds to deeper depths.

### **Comparison of Forest and Grass Infiltration Patterns**

A number of researchers report that forests have a much higher overall infiltration rate than grasslands (Challinor, 1968; Heede, 1975; Burch et al., 1987; Trimble, 1988; Cheng et al., 2002). Other researchers have determined that this higher conductivity capability is largely a result of tree root channels (Sklash et al., 1986), so that once piping sets up, properties of the soil matrix become unimportant in conductance of storm flow (Aubertin, 1971). **Evidence from this study supports the finding that higher forest infiltration capacity is largely related to preferential flow occurring along tree roots under fully saturated conditions.**

Best evidence for preferential flow movement under forest was detected in soil water content responses, which showed rapid preferential flow transfer between forest soil levels and down to 125 cm under saturated soil conditions. The flattening of soil moisture increase in layers overlying those to which water was being preferentially conducted also indicated that relatively large volumes of water may move along tree roots. However, comparison of mean infiltration and hydraulic conductivity values at equal depths found no statistically significant differences (at the 95% level) between forest and grass, even though mean forest values at near saturation were higher than grass at <10 and 25 cm (Table 6.1).

For the most part, forest infiltration tests at deeper depths were unlikely to incorporate readings related to tree root preferential flow, or were likely to reflect other hydraulic effects present at specific depths. This may obscure a possible higher forest infiltration capacity in relation to grass at these depths, but it also indicates that the forest soil matrix alone cannot create the higher infiltration rates often reported for forests. Infiltration rates in both forest and grass were also affected in many locations by site specific influences, most important of which were the proximity of roots and rock bench faces to the disk base. Thus, the differences between forest and grass infiltration capacities measured during this project largely relate to site

specific influences, with the exception of locations such as pits 7 and 8, where preferential tree root flow was captured by infiltrometer testing.

### **Preferential Flow**

**Although preferential flow is not typically associated with grass root systems, this study suggests that different forms of preferential flow form the main mechanism for water entry under both forest and grass.** The infiltration impedance that occurs either because of high clay or organic content diminishes as soil saturation is approached. Preferential flow under both forest and grass likely proceeds once pore pressure lower than that in the surrounding soil matrix has been generated in the soil immediately surrounding the roots (Figures 7.4, 7.5, and 7.6). This suggests that grass infiltration is expedited when the soil surrounding the root mats, either held in aggregates or in soil surrounding grass bunches, is first thoroughly wetted. Saturation of the surface soils surrounding the tops of the grass root channels enables preferential flow in the continuous channel pores, which are then able to wick a detectable level of flow to the 25 cm level fairly rapidly under even the driest circumstances. In the forest, the same saturation of soil must occur before preferential root flow is initiated, but the larger size of tree roots likely delays this process when conditions are dry.

Water content data indicates that once saturation of upper layers has occurred, preferential flow will enter the next lower level, causing rapid responses in successive layers. The rapidity of these responses suggest that preferential flow can enter soil layers that are not saturated, as long as the overlying soil has enough water present to maintain flow. At the same time, preferential flow along either grass or tree roots is likely to move moisture back out into the soils surrounding root channels. The final difference in preferential flow propagation in forest and grass thus lies in the ease with which the flow occurs and the volume of water carried: the diffuse distribution of grass root pores and their relative ease of activation ensure that grass root channel preferential flow response is more rapid when soil is dry. Once the regolith is thoroughly wetted, forest preferential flow along tree roots will be faster, and will likely carry a larger volume of water through the soil.

It is also likely that preferential flow conducted by grass roots creates a positive feedback on conditions conducive to growth along rock faces. It is not known whether grass roots follow rock faces because of increase in moisture, as might occur if the soil in the rock preferential flow zone tends to collect and hold more water, or if the soil/rock interface simply provides an avenue for root growth in the heavy clay soils because of removal of fines at the rock face. In any case, water movement across the rock face would play a role in both effects,

and preferential flow propagated by grass roots would in turn increase flow in this location, creating further capacity for grass root growth.

### **Development of Pathways over Time**

Decaying tree roots are known to support preferential flow pathways that expand during decay, creating zones of loosened soil that are eventually filled (Gaiser, 1952; Challinor, 1968; Noguchi et al., 1999). **During the course of this project, decaying roots approximately 45 years old were discovered in several pits, but no roots or root pathways were found in the soil that could be related to earlier tree growth.** Decaying roots found in pits 6 and 12 were soft but intact, showing that roots may remain in the soil environment for decades. Aerial photographs suggest that these roots belonged to trees that were logged in the early 1960's. However, older evidence for tree roots was restricted to a lump of charcoal mixed with clay that was found at the bedrock surface in pit 13. This charcoal may have resulted from stump burning during early deforestation, but no loose soil features or root remnants were found in the surrounding subsoil. Thus, root decay in this environment may follow a more or less exponential curve; roots are initially resistant to decay, but once preferential flow is set up through the root, translocated clay is likely to rapidly fill the pathway.

Although scant evidence is available to back this speculation, pit walls clearly demonstrated a lack of visible older root pathways. This shows that the current conditions of grass water movement are evolving minus the ameliorative effects of decaying tree root preferential zones. Any increased conductivity to deeper depths provided in the decades after deforestation has now been lost. Hillslope water movements in open portions of the main study area are now solely regulated by the slowly evolving soil and flow characteristics created by grass.

## **FUTURE CONSIDERATIONS**

Despite (or possibly because of) the scope of this study, a number of questions remain unanswered. Some result from work that could not be completed because of time constraints. Because this study touched on a large number of geomorphic issues, other issues arise concerning observed variable interactions. Some of these issues involve considerations particular to the bend itself, such as detailed information on the Kentucky River's historical path or patterns of karst development in certain geologic units, but other issues revolve around topics with wider significance to all limestone terrains. Some of the later are discussed in this section.

## **Native Grass Influence and Future Management**

All grass samples and infiltration test results in this study came solely from areas vegetated mainly by fescue. Whereas factors such as disturbance and historical land use were the main determinants in study area selection, this leaves the question of native grass influence unanswered. However, information gained during this study does provide some material for speculation on their long-term effects on soil retention.

Native grass species planted on most slopes in the bend have rooting depths of up to 6 m, which would certainly reach the bedrock surface in even the deepest soils of the main terrace. However, it is unlikely that these deep roots will be able to penetrate the bedrock surface as tree roots do. It thus seems unlikely that native grasses will provide any increased protection over that provided by fescue against eventual soil loss in high energy areas, or from regions in which flow is activated over broad areas of the bedrock surface.

Historical evidence indicates that it is quite likely that native grasses once occupied portions of the upland in savanna communities. As shown by this study, very large, old growth trees have a correspondingly large influence on bedrock decomposition. In any savanna, the widely-spaced trees likely had lateral root extensions >30 m in length (Stone and Kalisz, 1991), and possibly up to as much as one and a half times their height (McQuilkin, 1935), so that epikarst penetration operated in tandem with and underneath grass growth. This would have established ideal patterns for water retention, with rapid vertical grass transmission into the soil under dry conditions and preferential flow carried into the epikarst by tree roots during wetter periods. Native grasses by themselves are likely to set up lateral water movement along the epikarst surface, and although this may occur at a deeper level than the lateral flow set up above 125 cm depth under fescue, it seems likely to also generate increased sediment loss.

Repellency of organics and humic materials was noted in this study during infiltration testing. Burning also makes soils repellent, which ties into surface sediment movements noted on native grass slopes burned seasonally. Repellency, along with the exposure of soil between grass root bunches, creates good conditions for erosion during high intensity events occurring in the period following burns and prior to spring growth. Although sediment movement from this source appears to be minimal at this time, the native grasses have been present for only six years, and with increasing time the likelihood of high rainfall and thus major erosion during the critical post-burn stage also increases.

Infiltration and bedrock penetration capabilities of the native grasses are worth continued investigation. However, based on the findings of this study, management for long term soil retention in these or similar slopes elsewhere likely necessitates bringing high-energy zones

under forest cover. This could be done on a very piecemeal basis, with young trees planted on shoulders and steeper slopes, and with special consideration given to those areas where cutters and conduits can be identified from aerial photographs and the ground. Deeper soils provide a great deal of protection against soil loss even in steeper areas, making this factor important in land cover decisions. Thin-soiled locations, such as exist over the Tyrone in some of the northern slopes on the bend, should also be considered for eventual savanna or forest management. In these locations, flow passes downhill across broad expanses of the bedrock.

Management for localized conditions would thus be reliant on determination of soil depths, slope, and bedrock and epikarst drainage. One important line of investigation generated by this study could be GIS analysis of an enlarged area of study with ground truthing to determine if these factors mesh to induce soil removal elsewhere. Spatial analysis could provide a soil cover management tool pertinent to not only steeper Bluegrass slopes, but other fluviokarst regions.

### **Importance of Rock Pathways**

Although the literature acknowledges that rocks provide pathways for preferential flow, little research has been done into either the mechanisms or effects of such flow. Research on preferential vadose flow concentrates on movements through pathways in the soil matrix (Stephens, 1996), or through fractured flow in rock mediums (Bear et al., 1993; National Research Council, 2001; Neuman, 2005). Flows along rock/soil interfaces are largely unexplored, but they appear to be very important in the study area. The ability of rocks to channel bypass flow in the dense clay soils, their support of root systems with their possible subsequent effect on solution, and the likelihood that preferential flows induce sediment transport all suggest that rock preferential flows play a key role in limestone soil loss from high-energy, thin-soiled zones. Although rock face films are recognized as important modes of water movement in open shafts, films or preferential flows at the rock/soil interface may have a large bearing on water movement into soil-filled solutional cavities where soil depth is relatively shallow. Drawdown in such situations is likely related to rock face flow rather than simple movement through the soil matrix. Altogether, rock face preferential flow should provide a rich arena for future investigations.

### **Organic Influence on Surface Movements**

Statistical tests indicate that soil organic matter is negatively related to infiltration, whether present as humus or roots. The reduction of this effect with saturation suggests the

possibility that root mats may be responsible for some of the intermittent infiltration excess flows that operate on grass hillslopes during storm events. Such flows are commonly attributed to shallow build-up of thin clay layers (Bowden et al., 2001; Srinivasan et al., 2002; Swiechowicz, 2002a,b), but they may be related at least in part to the resistance peaks shown by unsaturated grass root systems. Where organic content is high and bulk density is low, a resistance period would be created during a storm event as soil moisture grew in upper soil layers, thereby delaying infiltration in localized spots. Although not critical to this study, this would also be a fruitful area for future research.

### **Surface Sediment Movement**

Surface sediment movements were not studied for this project, although observations were made of highly visible incidences. Although observations indicate little to no surface sediment movements in grass shoulder areas, more accurate information is needed before it is possible to state unequivocally that shoulder soils are being moved through subsurface flows along rock faces. Future research should couple rock face flow study to surface sediment movement detection, and should incorporate both forest and grass areas in that research.

### **Preferential Flow**

Evidence in this study indicates that preferential flow may be underappreciated in its effects on water movements, whether under grass or forest. It appears that vertical movement of water under either type of vegetation occurs as a sequential activation of macropores, in which near saturation of a soil layer causes preferential flow along root channels to the next depth, which in turn generates increased soil moisture at this level. This process continues with each level, with main difference between forest and grass lying in the size of root channels and thus the proportionately greater difficulty in activating root preferential flow along tree roots. Preferential flow thus appears to be an integral part of soil water movement, rather than only an overflow mechanism as suggested by other authors (Trimble, 1988).

This stepped mechanism may be more important during dry conditions, as observed during wetting of forest soils in August in this study. The high clay content of the study area soils also likely played a role in setting up conditions in which the stepped preferential flow process could be observed. In coarser soils, and where soil moisture is higher, the rapidity at which the matrix/preferential flow transfers at each layer would cause the mechanism to be easily missed. Although researchers have found that most stormflow emerges from subsurface soil matrix movement (Sidle et al., 1995), the process of moving water to that level may involve



preferential flow. This suggests that studies of preferential flow should incorporate considerations of texture as well as matrix pressure, and points out another area for future investigation.

This study also found a great deal of evidence for preferential flow conduction into the epikarst via tree roots, but did not actually measure that flow. Difficulties in doing this are numerous, but results would prove interesting.

## **CONCLUSIONS**

The major contribution of this study is its integration of biogeomorphic effects on hillslope water movements into a coherent systems picture. From this perspective, as shown in table 7.1, it can be seen that deforestation creates a wide range of effects, and that it is the composite of these effects, rather than any single or multiple influence, that makes forest growth critical in maintaining soil cover in high-energy limestone terrains.

Forest roots enter bedrock, whereas grass roots do not. This factor is probably most critical in erosion development. As tree roots tap into weakened zones in the rock, preferential flow is carried along their lengths and into the epikarst surface at a myriad number of points. Water is thus dispersed directly into epikarst storage. As solution opens pits and epikarst pathways along tree roots, more storage capacity is continuously generated along with new sediment from limestone decomposition. Under grass, this mode of storage and supply provision shuts down. Without the continuous generation of new solutionally opened pathways between bedding planes and fractures, water movement under grass remains a property of the regolith or bedrock surface.

In the regolith, water under grass is rapidly conducted to mid-profile via root channels and rock surfaces. Where thin soils exist, deeper soil layers offer two avenues for continued movement: lateral flow as clay builds up in sealed pockets over consolidated rock layers, and flow into epikarst conduits. These same conditions also operate under forest, but dispersed root entry into bedrock limits the amount of water stored in pockets or moving through the soil matrix or along the bedrock. In addition, where lateral water movement is generated within the forest slope regolith, downslope tree roots are likely able to deflect that flow by drawing water from saturated pores into vertical preferential pathways. Lack of epikarst storage and flow deflection, plus the overall increase in grass water yield caused by reduced growing season evapotranspiration all work together to raise the amount of water moving downslope under grass.

Table 7.1. Spatial and Temporal Factors Regulating Hillslope Hydrology

|                     | Forest   |  |   |  | Grass   |  |   |  |  |   |
|---------------------|--|--|---|--|---|--|---|--|--|---|
|                     | Wet  |  | Dry   |  | Wet   |  | Dry   |  |  |   |
| Shoulder (convex)   | Leaf-on  | Leaf-off   | Leaf-on   | Leaf-off   | Leaf-on   | Leaf-off   | Leaf-on   | Leaf-off   | Lexington Limestones Residuum soils form from thin limestones with shale interbeds.  |   |
| Sideslope           | Lifted and tilted flagstones only supply limited direct runoff into fractures and pits.  |  |   |  | Runoff from large rock expanses enters downhill soil and joins rock face preferential flow.                       |  |   |  | <ol style="list-style-type: none"> <li>1. Clay increases with depth.</li> <li>2. No textural contrast.</li> <li>3. Impedence of infiltration with depth because of clay.</li> <li>4. Thin BC horizon permits flow at bedrock surface.</li> </ol> |   |
|                     | <p>Canopy - I&amp;E is 59% higher than grass</p> <p>Litter - almost none present; effects limited.</p> <p>Canopy - I&amp;E limited</p> <p>Litter - absorbs appx. 6 mm/event, then rapid movement to topsoil.</p> <p>Topsoil saturation occurs rapidly.</p> | <p>Canopy - I&amp;E is high, up to 100% of events</p> <p>Litter -almost none present; effects limited.</p> <p>Topsoil retains moisture. Releases water slowly to pores of underlying subsoil.</p> <p>Saturation of successive layers takes place over many events.</p> | <p>Canopy - I&amp;E is high, up to 100% of events</p> <p>Litter -fills storage first (appx. 14 mm).</p> <p>Topsoil retains moisture. Releases water slowly to pores of underlying subsoil.</p> <p>Saturation of successive layers takes place over many events.</p> | <p>Canopy - I&amp;E limited</p> <p>Litter - fills storage first (appx. 14 mm).</p> <p>Topsoil retains moisture. Releases water slowly to pores of underlying subsoil.</p> <p>Saturation of successive layers takes place over many events.</p> | <p>Organics - little effect on infiltration</p> <p>Soil around root channels saturates after appx. 6 mm rain.</p> | <p>Organics - little effect on infiltration</p> <p>Root channels less conductive. Takes app. 8 mm rain to initiate flow.</p> | <p>Organics - impede water entry.</p> <p>Surrounding soil saturates after app. 14 mm. rain.</p> | <p>Organics - impede water entry</p> <p>Root channels less conductive. Takes app. 13 mm rain to initiate flow.</p>   |  | <p>Preferential flow drops along vertical root channels to 25 cm.</p> <p>Saturation at 25 cm initiates flow to 55 cm.</p> |
| Terrace (concave)   | As top soil layers are saturated, preferential flow to underlying layers is initiated. All soil layers saturate. Significant flow conducted into epikarst storage in fractures and bedding planes.   |  |   |  | Saturated clay permits percolation to the bedrock. Flow is initiated in the BC horizon.                           |  |   |  | High intensity entry is impeded at >55 cm. Lateral movement through the regolith is generated.   |   |
|                     | As soil layers saturate in deeper soils, preferential flow moves moisture to >125 cm. Lateral soil water movements are deflected to the epikarst by low pore pressure root channels.   |  |   |  | Bedrock flow enters epikarst conduits.  |  |   |  | Lateral slope movements enter coarse textured alluvium subsoils. Lateral flow increases.   |   |
| Escarpment (convex) | Large roots stabilize hillslopes during high intensity events. Forest roots carry preferential flow into epikarst conduits, creating vegetated forest gullies. Most water leaves forest through deep subsurface pathways.                                  |  |   |  | Bedrock flow continues across broad slope areas.  |  |   |  | Water ponds at grass slope base where alluvium pinches out.  |   |
|                     | Increased bedrock surface flow volume generates more energy.   |  |   |  | Conduits are overwhelmed by increased flow volume. Saturated soils lose cohesion.                                 |  |   |  | At the grass/forest boundary, grass root mat protection is lost where tree roots provide pathways for preferential flow.   |   |
|                     |  |  |   | Gullying, conduit exhumation.  |   |  |   |  |  |   |
|                     |  |  |   |  |   |  |   | Alluvium Heavy clay soils with gravelly layers at 55 to > 100 cm depth. "Pencil Cave" bentonite supports main terrace.   |  |   |
|                     |  |  |   |  |   |  |   | Tyrone Uphill forest - sand content high from silica grains in bentonite layers Lower forest - thin residuum soil with low sand content from thick, micritic limestone beds. |  |   |

I&E - Interception and Evapotranspiration

The effects are foreseeable. As clay gradually fills decaying tree root paths and builds along the pores of grass root channels, lateral movement in the upper soil layers increases. Much of that increase in throughflow enters preexisting epikarst cutter and conduit pathways, with the greatest effect after large storm events, when the regolith has reached field capacity. At those times the preexisting cutters, with subsurface fissures possibly blocked, are overwhelmed. Saturation excess flow initiates where water is pushed into thinner soils, such as occurs at the grass slope base in the main study area. Where converging flow enters preexisting cutters, positive pore pressure creates lift and destabilizes the oversaturated soil, allowing particles to be moved during surface flow. Within the saturated soils, pipes are also able to organize at depths where clay content resistance causes the hydraulic gradient to become lateral. As turbulent pipe flow conducts water and sediment through destabilized soils at 30 to 60 cm depth, conditions become ripe for gully opening.

Pipe flow is more common in soil layers that include tree root pathways. Grass root mats strongly resist surface erosion, but where the grass root mat can no longer maintain coherency, its protection is lost. At the grass/forest boundary line in the study area, the loss of the grass root mat protection coincides with saturated soils caused by increased water convergence under the grass mat. This is simultaneously coupled to the presence of tree roots and increase in clay content with depth. Under these conditions, the exhumation of cutters and development of gullies headed at the grass/forest boundary become inexplicable only in terms of why more of them do not occur.

The answer to this lies in the sensitivity of the landscape. Flow in the landscape is controlled mostly by the topography of the epikarst surface, and the best examples of gullying occur where epikarst cutters/conduits pass from grass to forest. These pathways through the decomposed top 1 to 3 m of the bedrock collect flow from the surrounding slopes and cause the oversaturated conditions downslope that lead to exfiltration and pipe flow generation. Sites sensitive to erosion may also resolve from flow along the bedrock that is not associated with conduits, such as seen in the shallow gully development along the vertical forest/grass boundary of Hillslope B. Erosion takes place outside the forest edge at the bottom of this slope, where loss of grass root mat protection coincides with tree root ability to concentrate preferential flow. Here, at the edge of the forest, tree roots oriented with the hydraulic gradient will promote downward flow within the regolith.

The sensitivity of Hillslope B and others like it on Bowman's Bend increases with gain in slope, so that the effects of loss of grass root mat protection and gain in tree root preferential flow concentration are directly dependent on the degree of energy held by the water moving

downhill over the bedrock surface. In steep, high energy locations, flow from only limited source areas are capable of causing erosion along vertical grass/forest boundary lines. Thus, in sites such as Hillslope B, erosion does not appear to be associated with flow convergence, except as occurs as flow speed increases with preferential flow conductance by tree roots at the forest edge. Gain in volume of water descending across the bedrock from grassed slopes is likely, however, showing that although the factors creating sensitivity in these types of locales are somewhat different from that creating gully heads, grass-related changes in water movement are responsible for the activation of both.

This study shows that the changes in hillslope water movements leading to the observed erosion patterns are created by the combined effects of all of these factors. These effects will vary seasonally and with antecedent conditions, but still create overall tendencies that are shifting system responses over time. Since vegetation effects accumulate slowly, the current patterns are likely to increase under grass, with continued hill shoulder thinning and movement of sediments to mid and base slope positions via subsurface movements, exposure of outcrops where flows cross broad areas of the bedrock or concentrate in linear depressions, and continued gullying. Because root pathways from 200 years ago are not visible in soils on the grass slopes, and because some statistical evidence of clay movement to 55 and 85 cm under grass is already detectable, these findings suggest that conditions conducive to erosion are already well established on the upland slopes. Management to minimize the effects of vegetation change on soil loss should focus on defining zones of high slope, thin soil depth, and topography related to epikarst drainage or bedrock flow above vertical forest/grass boundary lines. In these locations, long term soil retention can be assured by planting forest.

### **Implications for Soil Retention in Other Fluviokarst Regions**

Although sampling for this study was done in areas overlying bedrock units composed of thin limestones with shale interbeds, tree root exploitation of bedding planes and fractures, root grooving, development of forest gully systems, and opening of swallets and gullies along roots entering cutters were all observed in the study area in the massive, micritic beds of the Tyrone Formation. Geology and steepening topography at the escarpment edge generate increasing outcrop height and conduit depth in the High Bridge Group units, but forest growth maintains thin soil layers in all but the sheerest locations. Findings from this study indicate that it is the large trees that flourish in even precipitous sites that are responsible for soil generation and stabilization at the escarpment edge. Thus, although this project developed a detailed picture of factors responsible for soil loss in a particular location, these findings concerning vegetation

influences should be largely applicable across a wide spectrum of temperate carbonate environments.

Despite the many spatial and temporal specifics identified for the study area, its key elements are driving forces in other fluviokarst landscapes. By nature, fluviokarst environments are influenced by similar solutional weathering and subsurface water movement processes and thus changes in hillslope hydrology. Because of their composition, limestones typically generate soils high in clay content, providing particulate matter that can be easily moved in suspension as well as soil texture that delays percolation. Dependent on topography and types of insolubles present in particular limestone residuums, the same factors responsible for fluviokarst landscape evolution in the study area are common to other limestone regions.

Trees by nature tend to exploit any supporting terrain for water and nutrients; grass does the same, but to the best of its own, quite differing abilities. Tree and grass roots thus utilize the preferential flow routes of limestone rock faces differently, thereby producing different results, with one producing increased bedrock entry and the other producing increased flow along the epikarst surface. Translocation occurs during preferential flow along root channels in any temperate location, aiding in clay build up that impedes water entry at depths of maximum root extent. Seasonal variations in soil moisture uptake will be regulated in similar fashions by forest and grass across varying temperate regions. In short, the overall influence of grass as compared to forest in any temperate limestone environment will likely be an increase in total water volume moving downslope during growing season, a movement of water through higher subsoil layers over time, an increased movement of water over the bedrock surface in thinner soils, and a subsurface loss of fines in high-energy locations.

Within any particular carbonate landscape, vegetation effects will be played out within a web of interacting influences caused by storm events, human impact, pre-existing karren forms, inherited soils, geologic composition, slope steepness, and so on. These factors determine the sensitivity of the landscape, and thus the final effects of the overriding influences created by forest or grass. As with all landscapes, fluviokarst earth surface systems operate contingent on a number of more or less locally dependent conditions. To manage fluviokarst terrains for soil retention thus demands first, that vegetation effects be properly credited for their critical influence, and secondly, that their effects be considered in spatial and temporal context with the supporting landscape variables. If the fluviokarst landscape is acknowledged as a process mosaic, rather than as a homogenous, uniform surface, then vegetation effects can be used advantageously to ensure the best possible long-term soil, hydrology, and environmental conditions.

## **Broader Implications**

All landscapes are mosaics. Researchers tend to forget or at least ignore this critical fact because of the overwhelming mass of detail needed to even partially define the landscape system. Yet many important questions related to understanding the earth and our impact on it can only be answered from within the context of an integrated system perspective.

This study creates a geomorphic picture of the collective variables leading to and generated by one small area of space, caught at one specific point in time. At this point in time, only 200 years after deforestation, the trajectories of influence created by forest and grass have only just become visible to a measurable degree. System divergence has just begun, and as conceptualized by chaos theory, more accurate early measurements permit increased prediction of the future (Williams, 1997). It is still possible to weigh the biogeomorphic effects against a common landscape background that has only been slightly disturbed by subsequent landscape development. Once a geomorphic evolutionary branch is taken, the transfers of material and energy creating the divergence sponsor increasingly singular system responses.

Biogeomorphic effects are shown by this study to have a dominant effect on system divergence. However, this research also shows that vegetation is only one player in the landscape field. It can only act within the particular boundaries and relationships imposed by lithology, soils, climate, and land use, and the historically recombinant properties of those variables. The myriad chemical and physical processes that connect these variables are inseparable, plus the actions of vegetation are also part of the very system that they are impacting. By pulling on one strand of the web, however, we can bend the entire network. A change to grass bends the network, sets a new trajectory, and eventually reshapes the landscape.

This thus brings into question the concept of process dominance as explored by geomorphologists. Biogeomorphic effects on this fluviokarst landscape are dominant because they are not mere perturbations subject to dampening by other processes. The nature of fluviokarst subsurface sediment movement precludes dampening, but it does so based on the energy propagating abilities of the landscape. A flat topography with deep soils that do not provide rock face preferential flow pathways is likely to negate the erosive effects noted on Bowman's Bend. In such a case, topography and soil, and the historical and lithologic factors that lead to their development, would take precedence in landscape formation. Topography and soil in this scenario would thus be dominant in terms of process control and landscape development, and yet the strands of biogeomorphic interaction and effect must still be present and active. Topography and soil, or any of the other innumerable variables we can define, can

only operate within the web. Dominance is thus totally contingent on the form of the web. It is not just lithology, or soils, or vegetation that is critical – it is how they are seated within each other at a point in time.

By specifying the system parameters, and by defining process tendencies, it is possible to outline the web structure and thus the particular factors that are dominant in one situation. This allows for extrapolation to wider areas supporting similar web variable relationships, and this tactic forms the necessary basis of most geomorphic work. Extrapolation must be done with caution, however, with the constant thought that it is the web that is in control. Grass effects may be rapidly devastating throughout one fluviokarst region, detrimental in spots in another, and have negligible or even beneficial effects in a third location if surface soil capture is desired in a flat terrain. It is quite important to understand variable processes and likely effects, but it is equally necessary to remember that the web redistributes those effects spatially and temporally, and does so on a continuing basis even within a single system. Geomorphologists all seem to grasp the integrated nature of landscape dynamics; it is less certain that we manage to retain a conceptualization that truly gives credit to the ubiquitous power of the web. This project has derived its answers from within the fluviokarst landscape web on Bowman's Bend. Answers to other geomorphic process questions, in all their complexity, may lie in their landscape webs as well.

**APPENDIX 1**  
**AERIAL PHOTOGRAPHS UTILIZED IN THIS STUDY**



## APPENDIX 1 – AERIAL PHOTOGRAPHS

|              |   |
|--------------|---|
| Date         | September 14, 1937  |
| Scale        | 1:20,000  |
| Source       | National Archives, College Park, Maryland                       |
| Type         | 10X10 rolled aerial negative                                    |
| Record Group | RG 145, Can 2114  |
| Frames       | AFX-33-2973, AFX-33-2975, AGD-32-2937                           |
| Date         | April 4, 1949   |
| Scale        | 1:20,000  |
| Source       | National Archives, College Park, Maryland                       |
| Type         | 10X10 rolled aerial negative                                    |
| Record Group | RG 145, Can 4413  |
| Frames       | AFS-2F-22   |
| Date         | April 9, 1949   |
| Scale        | 1:20,000  |
| Source       | National Archives, College Park, Maryland                       |
| Type         | 10X10 rolled aerial negative                                    |
| Record Group | RG 145, Can 4414  |
| Frames       | AFS-4F-148  |
| Date         | April 7, 1950   |
| Scale        | 1:20,000  |
| Source       | USGS, Earth Science Information Center, Rolla, Missouri         |
| Type         | B&W negative  |
| Record Group | AB1KS0000000001   |
| Frames       | 4 120, 4 121  |
| Date         | July 10, 1953   |
| Scale        | 1:20,000  |
| Source       | National Archives, College Park, Maryland                       |
| Type         | 10X10 rolled aerial negative                                    |
| Record Group | RG 145, Can ON38238   |
| Frames       | AFS-4X-52   |
| Date         | August 23, 1956   |
| Scale        | 1:20,000  |
| Source       | USDA-CFSA, Aerial Photograph Field Office, Salt Lake City, Utah |
| Type         | B&W negative  |
| Record Group | 1R  |
| Frames       | AFS-1R-97   |
| Date         | October 6, 1960   |
| Scale        | 1:20,000  |
| Source       | USDA-CFSA, Aerial Photograph Field Office, Salt Lake City, Utah |
| Type         | B&W negative  |
| Record Group | 3AA   |
| Frames       | AFS-3AA-98  |

## APPENDIX 1 – AERIAL PHOTOGRAPHS (CONTINUED)

Date September 24, 1966  
Scale 1:20,000  
Source USDA-CFSA, Aerial Photograph Field Office, Salt Lake City, Utah  
Type B&W negative  
Record Group 2GG  
Frames AFS-2GG-113

Date October 18, 1973  
Scale 1:40,000  
Source USDA-CFSA, Aerial Photograph Field Office, Salt Lake City, Utah  
Type B&W negative  
Record Group 21079, roll 173  
Frames A 40 21079-173-60

Date April 10, 1974  
Scale 1:24,000  
Source Kentucky Transportation Cabinet, Frankfort, Kentucky  
Type B&W negative  
Record Group 712 R432  
Frames 29, 31

Date March 24, 1977  
Scale 1:40,000  
Source USDA-CFSA, Aerial Photograph Field Office, Salt Lake City, Utah  
Type B&W negative  
Record Group 21113, roll 176  
Frames S48 21113-176-22

Date April 17, 1985  
Scale 1:40,000  
Source USGS, Earth Science Information Center, Rolla, Missouri  
Type B&W negative  
Record Group AB1NHAP82000364  
Frames 364-102

Date January 11, 1986  
Scale 1:12,000  
Source Kentucky Transportation Cabinet, Frankfort, Kentucky  
Type B&W negative  
Record Group L10 R 727C  
Frames 10, 12

Date March 23, 1988  
Scale 1:20,000  
Source Kentucky Transportation Cabinet, Frankfort, Kentucky  
Type B&W negative  
Record Group 1 R714C  
Frames 57

## APPENDIX 1 – AERIAL PHOTOGRAPHS (CONTINUED)

Date April 8, 1990  
Scale 1:40,000  
Source USGS, EROS Data Center, Sioux Falls, South Dakota  
Type Color Infrared positive  
Record Group AB1NAPP00000054  
Frames 54-032

Date April 18, 1993  
Scale 1:20,000  
Source USGS, EROS Data Center, Sioux Falls, South Dakota  
Type B&W negative  
Record Group AB1NAPPW0006064  
Frames 6064-97

Date March 21, 1997  
Scale 1:20,000  
Source USGS, EROS Data Center, Sioux Falls, South Dakota  
Type B&W negative  
Record Group AB1NAPPW0009797  
Frames 9797-155

Date March 21, 1997  
Scale 1:20,000  
Source USGS, EROS Data Center, Sioux Falls, South Dakota  
Type B&W negative  
Record Group AB1NAPPW0009798  
Frames 9798-188

**APPENDIX 2**  
**DIGITAL DATA SETS UTILIZED IN THIS STUDY**

## APPENDIX 2 – DIGITAL DATA SETS

Theme: Regional aerial photographs  
Title: Wilmore (L40) Digital Ortho Quarter Quad Images (DOQQ)  
NW , NE, SE  
Format: JPEG formatted raster images, taken spring 1997 by NREPC  
Scale: 1 meter grayscale  
Database size: 310 KB/file  
Produced by: Kentucky Geological Survey  
Acquired from: Kentucky Geographic Explorer  
Website: <http://kymartian.ky.gov/dogq/>

Theme: Bedrock and quaternary geology  
Title: Wilmore (L40) 7.5 minute Geologic Quadrangle Map (DVGQ)  
Format: digitally vectorized (point/line/polygon)  
Scale: 1:24,000  
Database Size: 2.2 MB  
Produced by: Kentucky Geological Survey  
Acquired from: Kentucky Geological Survey  
Website: <http://www.uky.edu/KGS/gis/DVGQ/homepage.htm>

Theme: Land-surface elevation  
Title: Wilmore (L40) 7.5 minute Digital Elevation Model (DEM)  
Format: raster/grid  
Scale: 1:24,000  
Database Size: 4.08 MB  
Produced by: Kentucky Division of Geographical Information (DGI)  
Acquired from: Kentucky Geographic Explorer  
Website: <http://kymartian.ky.gov/demweb/index.html>

Theme: Soils  
Title: Soil Survey Geographic (SSURGO) Database for Garrard and Lincoln Counties, Kentucky, 2001  
Format: digitally vectorized (point/line/polygon)  
Scale: 1:24,000  
Database Size: 17.5 MB  
Produced by: U.S.D.A., Natural Resources Conservation Services  
Acquired from: U.S.D.A., National Resources Conservation Services  
Website: <http://soildatamart.nrcs.usda.gov>

Theme: Garrard County basemap data  
Title: Census 2000 Tiger/Line data for Garrard County, Kentucky  
Format: digitally vectorized (point/line/polygon)  
Scale: 1:24,000  
Database Size: 3 to 750 KB/file  
Produced by: U.S. Bureau of the Census  
Acquired from: Esri® GIS Software and Mapping  
Website: [http://arcdata.esri.com/data/tiger2000/tiger\\_statelayer.cfm](http://arcdata.esri.com/data/tiger2000/tiger_statelayer.cfm)

**APPENDIX 3**  
**SOIL PROFILE DESCRIPTIONS**



Water Probe Setup Site #1  
Grass area, Hillslope C

5/21/2005

Slope 15°, Aspect 200°

Large earthworms present down to 80 cm. One 1.5 cm wide vertical macropore found at 85 cm.

Limestone pinnacle obstructed digging on the north side of the pit at 70 cm.

Grass, raspberry (medium roots extend 1m), herbs

Matrix colors are for moist soil.

- Oi < 1 cm. Scant liter; moss or soil visible on 1/3 of surface
- A 0-15 cm (0-6 in). Dark yellowish brown (10YR 3/4) silt loam; moderate fine granular structure; friable (moist), slightly sticky and slightly plastic (wet); abundant fine roots, few medium roots; pores > 5%; clear smooth boundary.
- B1 15-30 cm (6-12 in). Dark yellowish brown (10YR 4/6) silt loam; moderate fine to medium subangular blocky structure; firm (moist), slightly sticky and slightly plastic (wet); many very fine and abundant fine roots, few medium roots; gradual wavy boundary.
- Bt1 30-65 cm (12-26 in). Yellowish brown (10YR 5/6) silty clay loam, common very fine faint dark yellowish brown (10YR 4/4) mottles, <5% rounded geodes 100 to 250 mm in diameter; moderate fine and medium subangular blocky structure; very firm (moist), sticky and slightly plastic (wet); common fine and few medium roots; clear wavy boundary.
- Bt2 65-75 cm (26-30 in). Yellowish brown (10YR 5/6) extremely gravelly clay; rounded geodes 100 to 250 mm in diameter, rounded pebbles and subangular chert pebbles 2 to 50 mm in length; moderate fine subangular blocky structure; very firm (moist), sticky and plastic (wet); common fine and few medium roots; clear wavy boundary.
- Bt3 75-126 cm (30-50 in). Brown (7.5YR 4/4) gravelly clay with common very fine to medium black concretions, rounded pebbles and subangular chert pebbles 2 to 50 mm in length, rounded geodes 100 to 250 mm in diameter; weak fine and medium subangular blocky structure; very firm (moist), sticky and plastic (wet); few fine and medium roots; abrupt wavy boundary.
- Bt4 126-185 cm (50-73 in). Olive yellow (2.5Y 6/6) gravelly clay with many very fine to medium concretions and many very fine to fine distinct brown (2.5Y 5/3) mottles; rounded pebbles and subangular chert pebbles 2 to 50 mm in length, rounded geodes 100 to 250 mm in diameter; weak medium subangular blocky structure; extremely firm, sticky, plastic; few fine roots; abrupt smooth boundary.
- R 185 cm (73 in). Hard, gray limestone.



Water Content Probe Site #2  
Forest area, Hillslope C

5/22/2005

Slope 15°, Aspect 214°

Network of small to 1 cm roots present from surface to > 1 m. Roots >2 cm common between 10 and 50 cm depths. Black concretions appear in subsoil as in probe pit #1, but the surrounding matrix is darker colored. Organic coatings are present along root pathways.

Pit was dug between an ash and a maple tree (2 m from each). Shrubs, violets, wild rose, various herbs present.

Matrix colors are for moist soil.

- Oi 0.5 cm. Very scant litter; mostly bare soil on surface
- A 0-15 cm (0-6 in). Dark grayish brown (10YR 4/2) silt loam; moderate fine granular structure; hard (dry), slightly sticky and slightly plastic (wet); many very fine to coarse roots, roots >2 cm common below 10 cm; pores >5%; clear, wavy boundary.
- B1 15-30 cm (6-12 in). Dark yellowish brown (10YR 4/4) silt loam with many distinct very dark grayish brown (10YR 3/2) films on root channels; moderate fine subangular blocky structure; firm (moist), slightly sticky, slightly plastic (wet); many fine roots, common medium to very coarse tree roots, pores fine to coarse > 5%; gradual wavy boundary.
- B2 30-50 cm (12-20 in). Brown (7.5YR 4/4) silt loam with common distinct very dark grayish brown (10YR 3/2) clay films on root channel and wormholes; <5% rounded pebbles 2 to 30 mm in length; moderate fine to medium subangular blocky structure; very firm (moist), slightly sticky, slightly plastic (wet); many fine to coarse roots, pores fine to coarse 2-5%; gradual wavy boundary.
- Bt 50-90 cm (20-35 in). Brown (7.5YR 5/4) silty clay loam with common very fine to fine black concretions increasing in frequency with depth; common distinct dark grayish brown (10YR 4/2) clay films on root channels; <5% rounded pebbles and cobbles 2 to 250 mm in length; weak fine to medium subangular blocky structure, very firm (moist), sticky, plastic (wet); many fine to coarse roots; pores fine to coarse 2%; clear irregular boundary.
- Bt2 90-185 cm (35-73 in). Reddish yellow (7.5YR 6/6) gravelly clay with abundant fine to medium dark brown (7.5YR 3/4) and brown (7.5 YR 5/4) mottles, abundant very fine to fine prominent black concretions; rounded pebbles and cobbles 2 to 250 mm in length; weak coarse subangular blocky structure; extremely firm (moist), sticky and plastic (wet); few fine to coarse roots; abrupt wavy boundary.
- R 185 cm (73 in). Hard, gray limestone.



Infiltration Test Pit #1  
Forest, Hillslope C

6/19/2005

Site is 4 m SW of the forest probe pit at the same elevation.

Slope 15°, Aspect 214°

Full pit only dug to 125 cm because of hard, dry soil. Partial hole opened to bedrock. Coarse roots present at bedrock, but root entry into bedrock could not be determined.

Pit dug 2 m from maple tree.

Matrix colors are for moist soil.

- Oi < 0.5 cm (0.2 in). Scant litter, mostly dried leaves; soil visible >1/2 of area
- A 0-10 cm (0-4 in). Dark brown (10YR 3/3) silt loam, common very fine to fine distinct dark yellowish brown (10YR 4/6) and faint very dark gray (10YR 3/1) films on peds and root channels; moderate fine granular structure; hard (dry), slightly sticky and slightly plastic (wet); abundant fine to medium roots, common coarse roots (up to 88 mm diameter) beginning at 7 cm depth; pores very fine to very coarse >5%; clear, wavy boundary.
- B1 10-45 cm (4-18 in). Brown (10YR 4/3) silt loam with many fine to medium very dark grayish brown (10YR 3/2) clay films on ped faces; <5% rounded pebbles 2 to 50 mm in length; moderate fine subangular blocky structure; firm (moist), slightly sticky and slightly plastic (wet); many fine to coarse roots; clear, wavy boundary.
- B2 45-60 cm (18-24 in). Dark yellowish brown (10YR 4/4) silt loam with common fine to medium very dark grayish brown (10YR 3/2) clay films on ped faces; <5% rounded pebbles 2 to 50 mm in length; moderate fine to medium subangular blocky structure; firm (moist), slightly sticky, slightly plastic (wet); common fine to coarse roots; gradual, irregular boundary.
- Bt1 60-75 cm (24-30 in). Strong brown (7.5YR 4/6) very gravelly clay; rounded pebbles 2 to 60 mm in length and rounded geodes 100 to 250 mm in diameter; weak medium subangular blocky structure; very firm (moist), sticky and plastic (wet); common fine to coarse roots; gradual, irregular boundary.
- Bt2 75-106 (30-42 in). Strong brown (7.5YR 4/6) gravelly silty clay loam with common fine dark brown (7.5YR 3/2) films on root channels; rounded pebbles 2 to 60 mm in length; weak coarse subangular blocky structure, very firm (moist), sticky and plastic (wet); common fine to coarse roots; earthworms to 85 cm; clear, irregular boundary.
- Bt3 106-115 cm (26-45 in). Yellowish brown (10YR 5/6) very gravelly clay with common fine very dark grayish brown (10YR 3/2) mottles, many very fine to fine prominent black concretions; rounded pebbles 2 to 60 mm in length, <5% rounded geodes 100 to 250 mm in diameter; weak coarse subangular blocky structure, extremely firm (moist), very sticky and very plastic (wet); common fine to medium roots; distinct smooth boundary.
- Bt4 115-145 (45-57 in). Yellowish brown (10YR 5/6) gravelly clay with common fine very dark grayish brown (10YR 3/2) mottles, many very fine to fine prominent black concretions; rounded pebbles and cobbles 2 to 250 mm in length; weak coarse subangular blocky structure, extremely firm (moist), very sticky and very plastic (wet); common fine to medium roots; distinct wavy boundary.
- R 145 cm (57 in). Hard, gray limestone.



Infiltration Test Pit #2  
Grass, Hillslope C

6/21/2005

Site 3 m NE of grass probe pit along same contour elevation.

Slope 15°, Aspect 200°

Pit only opened to 125 cm because of hard, dry soil.  
Bedrock depth not determined.

Grass (fescue), raspberry, wild grape, herbs.

Matrix colors are for moist soil.

- Oi <1.0 cm. Grass leaf litter, broken stalks, some moss
- A 0-15 cm (0-6 in). Brown (7.5YR 4/3) silt loam, <5% rounded pebbles 2 to 50 mm in length, moderate fine to medium granular structure; slightly hard (dry), slightly sticky and slightly plastic (wet); abundant fine to medium and common coarse roots; fine root mat forms top 5 cm; pores very fine to coarse >5%; clear, smooth boundary.
- B1 15-30 cm (6-12 in). Dark yellowish brown (10YR 4/6) silt loam with common fine to medium distinct dark brown (10YR 3/3) films on pore and ped faces; <5% rounded pebbles 2 to 50 mm in length; moderate fine to medium subangular blocky structure; firm (moist), slightly sticky and slightly plastic (wet); abundant very fine to fine roots, many medium and coarse roots; few grub holes up to 15 mm diameter, diffuse wavy boundary.
- Bt 30-73 (12-29 in). Yellowish brown (10 5/6) silty clay loam with common fine to medium dark brown (10YR 3/3) films on ped faces and root channels, <5% rounded pebbles 2 to 50 mm in length; weak fine to medium subangular blocky structure; very firm (moist), sticky and slightly plastic (wet); common fine and medium and few coarse roots; gradual wavy boundary.
- Bt2 73- 85 cm (29-33 in). Yellowish brown (10YR 5/6) very gravelly clay with common fine distinct yellowish red (5YR 5/8) mottles; rounded pebbles 2 to 60 mm in length, 5-10% rounded geodes 100 to 250 mm in diameter; weak coarse subangular blocky structure; very firm (moist), sticky and plastic (wet); few fine and medium roots; gradual wavy boundary.
- Bt3 85-100 (33-39 in). Yellowish brown (10YR 5/6) gravelly clay with common fine distinct yellowish red (5YR 5/8) mottles and common very fine to medium prominent black concretions; rounded pebbles 2 to 60 mm in length, <5% rounded geodes 100 to 250 mm in length; weak coarse subangular blocky structure; very firm (moist), sticky and plastic (wet); few fine and medium roots; gradual wavy boundary.
- Bt4 110->125 cm (43->49 in). Yellowish brown (10YR 5/8) very gravelly clay with common distinct brown (10YR 4/2) films on ped faces, common very fine to medium prominent black concretions; 25-35% rounded pebbles and cobbles 2 to 250 mm in length; weak coarse subangular blocky structure; extremely firm (moist), very sticky and very plastic (wet); few fine roots to 2 mm diameter; bedrock depth not determined.



Infiltration Test Pit #3  
Forest, Hillslope H bottom

6/30/2005

Slope 11°, Aspect 170°

Site is at the 22 m mark of the forest/grass transect measured across the Hillslope H bottom, and is about 20 m from the forest/grass boundary line.

Site is 2 m from a maple tree. Hackberry and shag-barked hickory common in immediate area. Many small saplings (<1m high), open undergrowth. Sparse vegetation, violets, few grass bunches

- Oi 1-2 cm (0.4-0.8 in). Dried leaf litter
- A 0-10 cm (0-4 in). Dark reddish brown (5YR 2.5/2) silt loam, <5% rounded pebbles 2 to 20 mm in length; moderate fine to medium granular structure; slightly hard (dry), slightly sticky, slightly plastic (wet); many fine to coarse roots, common large roots up to 70 mm in diameter in lateral and vertical network; pores very fine to very coarse >5%; clear, wavy boundary.
- B1 10-35 cm (4-14 in). Dark yellowish brown (10YR 4/4) silt loam with common very fine to fine distinct very dark grayish brown (10YR 3/2) films on root channels, <5% rounded pebbles 2 to 20 mm in length; moderate fine to medium subangular blocky structure; firm (moist), slightly sticky and slightly plastic (wet); common fine to coarse roots, very coarse roots up to 70 mm in diameter; diffuse wavy boundary.
- B2 35-60 cm (14-24 in). Strong brown (7.5YR 4/6) silty clay loam with dark yellowish brown (10YR 4/4) films on root channels, <5% rounded pebbles and cobbles 2 to 250 mm in length; weak medium subangular blocky structure; very firm (moist), sticky and slightly plastic (wet); common fine to coarse roots, very coarse roots up to 30 mm in diameter; pores fine to medium 2-5%; gradual wavy boundary.
- Bt 60-65 cm (24-26 in). Strong brown (7.5YR 4/6) very gravelly clay; 50-60% rounded pebbles and subangular chert pebbles 2 to 60 mm in length, 5-10% rounded geodes 100 to 250 mm in diameter; weak medium subangular blocky structure; very firm (moist), sticky and plastic (wet); common fine to coarse roots; gradual wavy boundary.
- Bt2 65-90 cm (26-35 in). Strong brown (7.5YR 4/6) gravelly clay with very dark brown (7.5YR 2.5/2) root and pore coatings, 10-15% rounded pebbles and cobbles 2 to 200 mm in length; weak coarse subangular blocky structure; extremely firm (moist), sticky and very plastic (wet); common fine to coarse roots, largest root 15 mm diameter; abrupt wavy boundary.
- Bt3 90-100 cm (35-39 in). Yellowish brown (10YR 5/4) very gravelly clay; 50-60% rounded pebbles and cobbles 2 to 250 mm in length, weak coarse subangular blocky structure; extremely firm (moist), very sticky and very plastic (wet); common fine to coarse roots, gradual wavy boundary.
- Bt4 92-140 cm (35/37-52/57 in). Yellowish brown (10YR 5/4) clay with common very fine brownish yellow (10YR 6/6) films on peds, <5% rounded pebbles 2 to 20 mm in length; weak very coarse subangular blocky structure; extremely firm (moist), very sticky and very plastic (wet); common fine to coarse roots, roots 14 and 6 mm in diameter extended into bedrock; abrupt irregular boundary.
- R 140 cm (55 in). Hard gray limestone.

Infiltration Test Pit #4  
Grass, Hillslope H bottom

7/4/2005

Slope 11°, Aspect 170°

Site is about 25 m past the forest boundary on the same transect as site #3.

Grass (fescue) and herbaceous growth is thick, mixed. Young locust, ash, and elm (1-2 cm DBH) have sprouted in the open area but nearest sapling is 5 m from site.

Matrix colors are for moist soil.

- Oi 1-2 cm (0.4-0.8 in). Dried plant matter, soil not visible
- A 0-15 cm (0-6 in). Dark yellowish brown (10YR 4/4) silt loam with <5% rounded pebbles 2 to 20 mm in length; moderate fine to medium granular structure; friable (moist), non-sticky and non-plastic (wet); abundant very fine to medium and few coarse roots, largest 8 mm across; gradual wavy boundary.
- AB 15-28 cm (6-11 in). Dark yellowish brown (10YR 3/4) silt loam with dark yellowish brown (10YR 4/6) films on peds and root channels, <5% rounded pebbles 2 to 20 mm in length; moderate fine to medium subangular blocky structure; firm (moist), non-sticky and slightly plastic; many fine and common medium roots; gradual, wavy boundary,
- B1 28-58 cm (11-23 in). Dark yellowish brown (10YR 4/6) silty clay loam with few very fine yellowish brown (10YR 5/6) mottles, common fine to medium yellowish brown (10YR 5/4) films on peds, common very fine to fine prominent black concretions increasing with depth, <5% rounded pebbles and cobbles 2 to 250 mm in length; moderate fine to medium subangular blocky structure; very firm (moist), sticky and slightly plastic; common fine to medium roots, largest root 2mm diameter; macropores <2%; gradual wavy boundary.
- B2 58-65 cm (23-26 in). Dark yellowish brown (10YR 4/6) very gravelly clay; 40-50% rounded pebbles and stones 2 to 250 mm in length; weak medium subangular blocky structure; very firm (moist), sticky and plastic (wet); common fine to medium roots; gradual wavy boundary.
- Bt1 65-80 cm (26-31 in). Dark yellowish brown (10YR 4/6) gravelly silty clay loam with common medium yellowish brown (10YR 5/4) films on peds, common fine prominent black concretions; 20-35% rounded pebbles and subangular chert 2 to 60 mm in length, <5% rounded geodes 100 to 150 mm in size; weak medium subangular blocky structure; very firm (moist), sticky and slightly plastic (wet); common fine to medium roots; clear wavy boundary.
- Bt2 80-90 cm (31-35 in). Yellowish brown (10YR 5/8) very gravelly clay with many fine to medium black concretions; >50% rounded pebbles, subangular chert, and cobbles 2 to 250 mm in size, weak coarse subangular blocky structure; very firm (moist), sticky and plastic (wet); few fine roots, largest 1mm diameter; gradual wavy boundary.
- Bt3 90-138 cm (35-54 in). Yellowish brown (10YR 5/6) gravelly clay with abundant pale brown (10YR 6/3) mottles, many fine to medium black concretions; pebbles coarsen upward in size and frequency; weak coarse subangular blocky structure; very firm (moist), very sticky and very plastic; few to no roots; abrupt wavy boundary.
- R 138 cm (54 in). Hard, gray limestone.



Infiltration Test Pit #5  
Forest, Hillslope H

7/21/2005

Slope 9° (15%), Aspect 170°

Site is approximately 30 m uphill from pit #3.

Pit is approximately 2 m from elm and shag-bark hickory trees. Poison ivy and small tree sprouts are predominant ground cover.

Irregularities in the AB/B horizon boundary were reflected in irregularities in the bedrock shape.

Matrix colors are for moist soil.

- Oi 1 cm (0.4 in). Scant liter from decomposing leaves
- A 0-10 cm (0-4 in). Very dark brown (10YR 2/2) gravelly silt loam; rounded pebbles 2 to 60 mm in length, <5% rounded geodes 100 to 250 mm in length; moderate fine to medium subangular blocky structure; firm (moist), non-sticky and slightly plastic (wet); many very fine to coarse roots; clear wavy boundary.
- AB 10-21 cm (4-8 in). Dark yellowish brown (10YR 3/4) silty clay with common dark grayish brown (10YR 4/2) films on ped faces and 6-15% fine to coarse rounded pebbles, <5% rounded geodes 100 to 250 mm in length; moderate granular structure; very firm (moist), sticky and slightly plastic (wet); many very fine to coarse roots, very coarse roots form lateral and vertical network with largest root 8 cm in diameter; macropores fine to coarse 5%; clear irregular boundary (10 to 20 cm thick).
- Bt 21-45 cm (8-18 in). Yellowish brown (10YR 5/6) clay with common distinct fine to medium brown (10YR 4/4) films on root channels, few prominent very fine black concretions, <5% 2 to 20 mm rounded pebbles ; weak medium to coarse subangular blocky structure; extremely firm (moist), sticky and plastic (wet); common fine to coarse roots; abrupt wavy boundary, to bedrock or to
- Bt2 45-78 cm (18-31 in). Dark yellowish brown (10YR 4/6) clay with few very fine to fine faint dark yellowish brown (10YR 4/3) films on peds, common prominent very fine to fine black flecks, common fine yellowish red (5YR 5/8) mottles localized below the dip in the AB/B boundary; <5% rounded pebbles 2 to 20 mm in length; weak medium subangular blocky structure; extremely firm (moist), very sticky and plastic (wet); common fine to medium and few coarse roots, sharp irregular boundary.
- 2BC 78-80 cm (31-32 in). Grayish brown (10YR 5/2) flaggy clay; extremely firm, very sticky and plastic; common fine to medium and few coarse roots; sharp irregular boundary.
- R 80 cm (32 in). Hard, gray limestone



Infiltration Test Pit #6  
Forest, Hillslope H

7/24/2005

Slope 11° (19%), Aspect  
175°

Located approximately 30  
m uphill from  
pit #5.

Poison ivy main ground  
cover. Ash and hackberry  
in vicinity. Outcrop and  
large decayed stump  
uphill.

Matrix colors are for moist soil.

- Oi 1 cm (0.4 in). Scant litter from decomposing leaves
- A 0-11 cm (0-4 in). Very dark grey (10YR 3/1) and very dark grayish brown (10YR 3/2) flaggy silty clay loam; moderate fine to coarse granular structure; friable (moist), slightly sticky and slightly plastic (wet); many very fine to coarse roots, very coarse roots form lateral network; macropores very fine to very coarse >5%; gradual wavy boundary.
- B 11-26 cm (4-10 in). Very dark grayish brown (10YR 3/2) stony silty clay; <5% rounded pebbles 6 to 20 mm in length, limestones to 650 mm in length; moderate fine to medium subangular blocky structure; firm (moist), sticky and plastic (wet); many fine to coarse roots, very coarse vertical and lateral roots 10 to 20 mm in diameter common (both living and decomposing); clear wavy boundary.
- Bt 26-60 cm (10-24 in). Yellowish brown (10YR 5/8) clay with very many distinct coarse dark yellowish brown (10YR 4/4) films on ped faces and few distinct very fine black concretions; <5 % limestones 6 to 60 mm in length; weak coarse subangular blocky structure; very firm (moist), sticky and plastic (wet); common fine to coarse roots; sharp irregular boundary, to bedrock or to
- Bt2 60-88 (24-35 in). Brownish yellow (10YR 6/6) clay with very many distinct coarse dark yellowish brown (10YR 4/4) films on ped faces and few distinct very fine black concretions; weak coarse subangular blocky structure; very firm (moist), sticky and plastic (wet); common fine to coarse roots; sharp irregular boundary.
- 2BC 88-90 cm (35-36 in). Grayish brown (10YR 5/2) very flaggy clay; very firm (moist), sticky and plastic (wet); common fine to coarse roots, coarse roots enter bedrock fractures; sharp irregular boundary.
- R 90 cm (36 in). Hard, gray limestone.



Infiltration Test Pit #7  
Forest, Hillslope H

8/12/2005

Slope 14° (24%), Aspect 180°

Site lies approximately 20 m uphill and slightly NW of pit 6.

Nearest tree is a red cedar 2.5 m from pit. Many young (1-4 m high) elm, maple, and hackberry saplings are found in the vicinity. A 1.15 m DBH chinquapin oak lies 7 m uphill. Thick poison ivy ground cover.

The entire pit is essentially filled with layers of limestone fragments separated by soil layers supporting numerous coarse roots. Bedrock is at 15/20 cm in half the pit. Decomposed bedrock plates surround two large roots in the other half of the pit.

Matrix colors are for moist soil.

- Oi 1 cm (0.4 in). Scant litter from decomposing leaves
- A 0-10 cm (0-4 in). Very dark brown (10YR 2/2) very flaggy silty clay loam; moderate medium to very coarse granular structure; firm (moist), sticky and slightly plastic (wet); many very fine to coarse roots, very coarse roots up to 2 cm form lateral network; gradual wavy boundary.
- B 10-17 cm (4-7 in). Very dark grayish brown (10YR 3/2) very flaggy silty clay; limestones 10 to 60 mm thick and up to 500 mm in length; many fine to coarse roots, medium to very coarse roots up to 9 cm in diameter form vertical and lateral network between stones; moderate fine to medium subangular blocky structure; firm (moist), sticky and plastic (wet); clear irregular boundary, to bedrock or to
- Bt 17-50 cm (7-20 in). Yellowish brown (10YR 5/6) very flaggy clay with dark brown (10YR 3/3) stains below roots; limestones 6 to 200 mm in length; weak medium to coarse subangular blocky structure; very firm (moist), very sticky and plastic (wet); common fine to coarse roots, very coarse roots (9 cm and 6 cm in diameter) enter bedding plane laterally at pit base; abrupt irregular boundary.
- R 50 cm (20 in). Hard brownish gray limestone.



Infiltration Test Pit #8  
Forest, Hillslope H

8/13/2005

Slope 12° (21%),  
Aspect 170°

Site lies 15 m uphill  
from pit 7.

Nearest large trees are  
an ash sited 2 m uphill  
and a shag-bark hickory  
1.5 m to the east.  
Walnut, sugar maple,  
and red oak are found  
in the vicinity and a  
dead cedar lies 2 m  
downhill. Stones  
outcrop at the bases of  
all trees.

Matrix colors are for moist soil.

- Oi 1 cm (0.4 in). Scant litter from decomposing leaves
- A 0-15 cm (0-6 in). Very dark grayish brown (10YR 3/2) very flaggy silty clay loam; limestones 6 to 600 mm in length; moderate medium to very coarse granular structure; extremely hard (dry), hydrophobic when water is applied, firm (moist), slightly sticky and slightly plastic (wet); many very fine to coarse roots; gradual wavy boundary.
- Bt 15- 30 cm (6-12 in). Very dark grayish brown (10YR 3/2) very flaggy silty clay with abundant dark grayish brown (10YR 4/2) films on ped faces; limestones up to 20-80 mm thick and 500 mm in length; moderate coarse to very coarse granular structure; extremely hard (dry), hydrophobic when water is applied, very firm (moist), sticky and plastic (wet); common fine to coarse roots, medium to coarse roots up to 10 mm in diameter form vertical and lateral network between stones; abrupt wavy boundary, to bedrock or to
- Bt2 30-60 cm (12-24 in). Dark yellowish brown (10YR 4/4) very flaggy clay; limestones 7 to 200 mm in length; moderate coarse subangular blocky structure; very hard (dry), very firm (moist), sticky and very plastic (wet); common fine to coarse roots, medium to coarse roots up to 10 mm in diameter form vertical and lateral network between stones and enter bedrock fractures; abrupt irregular boundary.
- R 60 cm (24 in). Hard, brownish gray limestone.





Infiltration Test Pit #9  
Grass, center backslope

8/21/2005

Slope 12° (21%), Aspect 95°

Fescue grass forms a solid mat, several horse nettle plants also present.

Matrix colors are for moist soil.

- Oi 1-2 cm (0.4-0.8 in). Dried grass liter. Not highly decomposed.
- A 0-8 cm (0-3 in). Very dark grayish brown (10YR 3/2) flaggy silty clay loam; 5-15% rounded pebbles 6 to 60 mm in length, limestones 20-50 mm thick and up to 350 mm in length, few geodes up to 100 mm in length; strong fine to coarse granular structure; friable (moist), slightly sticky and slightly plastic (wet), hydrophobic aggregate reaction to water, dense fine roots hold aggregates; abundant very fine and fine roots, common medium roots up to 4 mm in diameter; gradual, wavy boundary.
- Bt 8-20 cm (3-8 in). Dark grayish brown (10YR 4/2) very flaggy clay with many very dark grayish brown (10YR 3/2) films on ped faces, 15-35% chert and limestone pebbles 6 to 60 mm in length, 36-60% limestones 20-200 mm in length in layers; moderate medium to very coarse subangular blocky structure; very hard (dry), sticky and very plastic (wet); abundant very fine and fine vertical roots up to 2 mm in diameter; macropores very fine to coarse 2-5%; abrupt wavy boundary.
- Bt2 20-40 cm (8-16 in). Strong brown (7.5YR 5/6) gravelly clay with few very fine to fine reddish yellow (7.5YR 6/8) distinct mottles and many fine to medium very dark grayish brown (10YR 3/2) films on peds and root channels; 15-35% subangular chert and rounded pebbles 2-60 mm in length and limestones 60 to 250 mm in length; moderate medium to very coarse subangular blocky structure; hard (dry), sticky and plastic (wet), gradual wavy boundary.
- Bt3 40-60 cm (16-24 in). Yellowish brown (10YR 5/6) very gravelly clay with many fine to medium prominent dark grayish brown (10YR 4/2) films on peds and common prominent very fine to fine black concretions; 35-45% rounded pebbles 2 to 60 mm in length; weak coarse subangular blocky structure; firm (moist), sticky and plastic (wet), few very fine and fine roots up to 1 mm in diameter; macropores <0.5%, vertical cracks pass through entire horizon, small earthworms found curled up in balls, diffuse smooth boundary.
- Bt4 60->135 cm (24->53 in). Yellowish brown (10YR 5/8) very gravelly clay with many fine to medium prominent very dark grayish brown (10YR 3/2) films on ped faces, common medium distinct light brownish gray (10YR 6/2) mottles, many fine prominent reddish yellow (7.5YR 6/8) mottles, and common prominent very fine to fine black concretions; 35-40% subangular chert and rounded pebbles 2 to 60 mm in length, 5-10% geodes 100 to 200 mm in length; weak very coarse subangular blocky structure; firm (moist), sticky and plastic (wet); few fine roots at higher levels; macropores 0.1%; occasional earthworms found down to 80 cm; bedrock depth not determined.



Infiltration Test Pit #10  
Grass, hill shoulder

8/25/2005

Slope 11° (19%), Aspect 95°

Site lies approximately 10 m uphill from pit #9.

Vegetation is 90% fescue, with several herbaceous white snakeroot (*Eupatorium rugosum*) plants. Fescue roots form a solid mat through the A horizon.

Tilted limestone slabs indicate subsidence in this location, likely within a sinkhole.

Matrix colors are for moist soil.

- Oi 1-2 cm (0.4-0.8 in). Dried grass stems over decomposing humus
- A 0-8 cm (0-3 in). Very dark grayish brown (10YR 3/2) flaggy silt loam; limestones, 10-40 mm thick and up to 230 mm in length; strong fine to coarse granular structure; friable (moist), non-sticky, non-plastic (wet); abundant very fine to medium roots orient vertically, roots up to 4 mm in diameter under snakeroot; macropores >5%; gradual wavy boundary.
- Bt1 8-40 cm (3-16 in). Dark brown (10YR 3/3) bouldery silty clay loam with many medium distinct dark gray (10YR 4/1) films on root channels; limestones tilted at approximately 45° angle with uphill dip; moderate fine to medium subangular blocky structure; firm (moist), non-sticky and slightly plastic (wet); abundant fine roots decreasing with depth, roots up to 2 mm in diameter, fine roots form a mat 5 mm thick on upper and lower sides of tilted limestones; gradual wavy boundary.
- B2t 40->80 cm (16->32 in). Yellowish brown (10YR 5/4) very bouldery silty clay with very many medium to coarse distinct dark grayish brown (10YR 4/2) films on peds and root channels; many tilted limestone boulders continue from horizon above; weak medium to coarse subangular blocky structure; firm (moist), sticky and plastic (wet); common fine roots decreasing with depth, fine roots form mats on upper and lower sides of tilted limestones; bedrock depth not determined.



Infiltration Test Pit #11  
Grass, Hillslope A upper shoulder

9/2/2005

Slope 12° (21%), Aspect 30°

Site is on the hill shoulder approximately 18 m downhill and NW of a single mature locust tree.

Vegetation is predominantly fescue grass, with snakeroot, horse nettle, and garlic also represented. The fescue creates a thick root mat for the top 10 cm of the A horizon.

Matrix colors are for moist soil.

- Oi 2-3 cm (0.8-1.2 in) Dried grass stalks
- A 0-18 cm (0-7 in). Dark grayish brown (10YR 4/2) silty clay loam; <5% limestones 6-60 mm in length; strong fine to coarse granular structure; friable (moist), non-sticky and non-plastic (wet); abundant very fine to medium roots; clear, wavy boundary.
- B 18-45 cm (7-18 in). Dark yellowish brown (10YR 4/4) silty clay with many fine to medium very dark grayish brown (10YR 3/2) films on root channels, <5% limestones <20 mm in length; moderate medium to coarse subangular blocky structure; firm (moist), sticky and plastic (wet); many very fine and fine roots up to 1 mm in diameter; abrupt irregular boundary, to bedrock or to
- Bt 45-55 cm (18-22 in). Dark yellowish brown (10YR 4/4) very flaggy silty clay; moderate medium to coarse subangular blocky structure; firm (moist), sticky and plastic (wet); many very fine and fine roots up to 1 mm in diameter, fine root mat found on top of rock at 45 cm with no discoloration; abrupt irregular boundary, to bedrock or to
- Bt2 55-110 cm (22-43 in). Yellowish brown (10YR 5/4) flaggy clay with common medium distinct brown (10YR 4/3) films on peds, limestones 20-200 mm covering bedrock and hole in bedrock; weak coarse subangular blocky structure; very firm (moist), sticky and very plastic (wet); common fine roots decreasing to few with depth; soil continues in bedrock hole to 110 cm, abrupt irregular boundary.
- R 110 cm (43 in). Hard, gray limestone.



Infiltration Test Pit #12  
Grass, Hillslope A

9/4/2005

Slope 12° (21%), Aspect 35°

Site lies approximately 8-10 m below  
pit #11.

Vegetation is 80% fescue grass with  
a small coralberry (*Symphoricarpos  
orbiculatus*) shrub on the south end  
and several large snakeroot plants on  
the north end.

Matrix colors are for moist soil.

- Oi 2 cm (0.8 in). Dried grass stalks
- A 0-22 cm (0-9 in). Dark brown (10YR 3/3) silt loam; <5% limestones 30-80 mm in length; strong fine to medium granular structure; friable (moist), non-sticky and slightly plastic; abundant very fine to medium vertical roots; macropores >0.5%; clear wavy boundary.
- B 22-50 cm (9-20 in). Dark yellowish brown (10YR 4/6) silty clay loam with many distinct medium dark grayish brown (10YR 4/2) films on root channels decreasing in frequency with depth; <5% limestones 20-200 mm in length; moderate medium to coarse subangular blocky structure; firm (moist), sticky and plastic (wet); many very fine to fine vertical roots, few medium roots up to 4 mm in diameter; abrupt irregular boundary, to bedrock or to
- Bt 50-70 cm (20-28 in). Dark yellowish brown (10YR 4/6) silty clay with very many coarse distinct brown (10YR 4/3) and many fine distinct very dark grayish brown (10YR 3/2) films on ped faces, and few (2%) very fine black concretions; <5% limestones 20 to 200 mm in length; weak coarse subangular blocky structure; very firm (moist), sticky and plastic (wet); common very fine to fine roots, two lateral decayed roots 2 cm in diameter at 50 cm; abrupt irregular boundary, to bedrock or to
- Bt2 70->160cm (28->63 in). Very dark grayish brown (10YR 3/2) clay with common (20%) fine distinct dark yellowish brown (10YR 4/4) films; <5% limestones 20 to 200 mm in length; weak very coarse subangular blocky structure; few very fine to fine roots in matrix, many very fine to fine roots along limestone plates to >100 cm, decayed root 2 cm in diameter at 85 cm; partial abrupt boundary at 100 cm bedrock, bedrock depth in hole not determined.



Infiltration Test Pit #13  
Grass, Hillslope A

9/12/2005

Slope 13° (23%), Aspect 35°

Site lies approximately 10 m downhill and SW of pit 12.

Vegetation is mostly fescue with a few herbs and several small raspberries at the pit's north end.

A large clump of charcoal was found in the north end of the pit on the top of the bedrock at 40 cm depth.

Matrix colors are for moist soil.

- Oi 1-2 cm (0.4-0.8 in). Dried grass stems
- A 0-8 cm (0-3 in). Dark yellowish brown (10YR 4/4) silt loam; <5% limestones 20 to 80 mm in length; strong fine granular structure; friable (moist), non-sticky and slightly plastic (wet); abundant very fine to medium roots, with solid root mat in top 5 cm; clear wavy boundary.
- Bt 8-22 cm (3-9 in). Brown (10YR 4/3) silty clay loam with very many faint dark grayish brown (10YR 4/2) films on root channels; <5% limestones 20 to 80 mm in length; moderate fine to coarse subangular blocky structure; firm (moist), sticky and plastic (wet); many very fine to medium roots, raspberry roots up to 4 mm in diameter; earthworms; abrupt wavy boundary.
- Bt2 22- 40 cm (9-16 in). Yellowish brown (10YR 5/4) clay with very many distinct dark grayish brown (10YR 4/2) films on peds and root channels and common faint grayish brown (10YR 5/2) mottles; weak fine to medium subangular structure; very firm (moist), very sticky and very plastic (wet); common very fine to medium roots; abrupt irregular boundary, to bedrock or to
- Bt3 40-70 cm (16-28 in). Strong brown (7.5YR 4/6) flaggy clay with very many faint dark brown (7.5YR 3/2) films on peds and very many light yellowish brown (2.5Y 6/4) mottles above bedrock; 16-35% limestones 20-200 mm in length; weak very coarse subangular blocky structure; very firm (moist), extremely sticky and very plastic (wet); common fine roots, many fine roots form mats on upper sides of bedrock stones; abrupt irregular boundary, to bedrock or to
- BC 70-82 cm (28-32 in). Strong brown (7.5YR 4/6) very flaggy clay with very many faint dark brown (7.5YR 3/2) films on peds; limestones 60 to 250 mm in length; common fine roots, many fine roots form mats on upper sides of bedrock stones; abrupt irregular boundary.
- R 82 cm (32 in). Hard, gray limestone.



Infiltration Test Pit #14  
Grass, Hillslope A

9/21/2005

Slope 10° (18%), Aspect 15°

Site lies approximately 8 m downhill from pit #13.

Vegetation cover is mostly fescue, with horse nettle, snakeroot and coralberry (*Symphoricarpos orbiculatus*) shrub. Lower soil is of alluvial origin and grades upwards into a residuum/fluvial mix. Mottling at bedrock may be related to decomposition of the particular limestone layer.

Matrix colors are for moist soil.

- Oi 1-2 cm (0.4-0.8 in). Dried grass stems
- A 0-10 cm (0-4 in). Brown (10YR 4/3) silt loam; <5% rounded pebbles 2 to 30 mm in length; strong fine to medium granular structure; friable (moist), non-sticky and slightly plastic (wet); abundant very fine to medium roots, grass roots form mat; clear wavy boundary.
- Bt 10-22 (4-9 in). Brownish yellow (10YR 6/6) clay with very many prominent fine to coarse brown (10YR 4/3) and very many distinct fine to coarse yellowish brown (10YR 5/6) films on root channels; <5% rounded and subangular chert pebbles 6 to 30 mm in length; moderate fine to coarse subangular blocky structure; very firm (moist), sticky and plastic (wet); abundant very fine to fine roots decreasing with depth, common medium roots (up to 2 mm), few coarse roots (up to 10 mm); small earthworms; gradual irregular boundary.
- Bt2 22-50 (9-20 in). Yellowish brown (10YR 5/6) clay with many fine to coarse distinct dark yellowish brown (10YR 4/4) films on peds and root channels, <5% rounded and subangular chert pebbles 6 to 30 mm in length; weak medium subangular blocky structure; very firm (moist), very sticky and very plastic (wet), many very fine to fine roots; clear smooth boundary
- Bt2C 50-85 cm (20-33 in). Brown (10YR 5/3) very flaggy clay with very many prominent coarse dark brown (10YR 3/3) films on peds, common prominent very fine to medium black (10YR 2/1) concretions increasing with depth, common very fine distinct yellowish brown (10YR 5/6 and 10YR 5/8) mottles, very many prominent medium to coarse yellow (10YR 7/6) mottles, few very fine distinct strong brown (7.5YR 5/6) mottles and few very fine light yellowish brown (10YR 6/4) mottles; < 5% rounded pebbles 6 to 20 mm in length, 35-60% limestones 40 to 300 mm in length; coarse subangular blocky structure; very firm (moist), very sticky and very plastic (wet); common very fine to fine roots, abundant roots in mats on bedrock surfaces; abrupt irregular boundary .
- R 85 cm (33 in). Hard, gray limestone.

**APPENDIX 4**  
**PARTICLE SIZE PERCENTAGES AND TEXTURE CLASSES**

#### APPENDIX 4 – HILLSLOPE A SOIL SAMPLES

| No. | Depth<br>(cm) | Particle Size<br>Percentages |      |      | USDA<br>Texture Class               | Slope Position             |
|-----|---------------|------------------------------|------|------|-------------------------------------|----------------------------|
|     |               | Sand                         | Silt | Clay |                                     |                            |
| A1  | <10           | 18.0                         | 66.0 | 16.0 | silt loam                           | grass field, midslope.     |
|     | 20-30         | 15.0                         | 55.0 | 30.0 | silty clay loam                     | App. 50 m above            |
|     | 40-50         | 8.3                          | 20.0 | 71.7 | clay                                | and NE of large sink.      |
|     | 60-70         | 6.1                          | 21.5 | 72.4 | clay                                |                            |
|     | 85-95         | 3.7                          | 23.8 | 72.5 | clay                                |                            |
| A2  | <10           | 20.0                         | 64.0 | 16.0 | silt loam                           | grass field, midslope.     |
|     | 20-30         | 12.5                         | 65.9 | 21.6 | silt loam                           | 1 m E of site 1.           |
|     | 40-50         | 13.0                         | 64.0 | 23.0 | silt loam                           |                            |
|     | 60-70         | 8.0                          | 36.0 | 56.0 | clay                                |                            |
|     | 78-85         | 4.2                          | 28.7 | 67.0 | clay                                |                            |
| A3  | <10           | 15.0                         | 66.0 | 19.0 | silt loam                           | grass field, midslope.     |
|     | 20-30         | 10.0                         | 64.0 | 26.0 | silt loam                           | App.10 m E of site 2       |
|     | 40-50         | 12.0                         | 58.0 | 30.0 | silty clay loam<br>silty clay-silty | and 1.5 m from a small     |
|     | 60-70         | 15.0                         | 45.0 | 40.0 | clay loam                           | linear depression; slight  |
|     | 110-115       | 6.0                          | 22.0 | 72.0 | clay                                | slope to depression.       |
| A4  | <10           | 11.3                         | 69.7 | 19.1 | silt loam                           | grass field, midslope.     |
|     | 20-30         | 9.2                          | 64.3 | 26.5 | silt loam                           | 1.5 m E of site 3.         |
|     | 40-50         | 13.8                         | 39.4 | 46.8 | clay                                | Center of very shallow     |
|     | 60-70         | 8.1                          | 15.7 | 76.3 | clay                                | linear depression.         |
|     | 110-114       | 5.8                          | 23.3 | 70.9 | clay                                |                            |
| A5  | <10           | 11.0                         | 67.3 | 21.8 | silt loam                           | grass field, midslope.     |
|     | 20-30         | 8.4                          | 69.2 | 22.4 | silt loam                           | Directly above large sink. |
|     | 40-50         | 10.0                         | 62.0 | 28.0 | silt loam-silty<br>clay loam        | Surface slopes to a        |
|     | 60-70         | 13.2                         | 53.7 | 33.1 | silty clay loam                     | linear depression that     |
|     | 75-83         | 17.6                         | 51.3 | 31.0 | silty clay loam                     | leads to the sink.         |
| A6  | <10           | 15.2                         | 62.2 | 22.5 | silt loam                           | grass field above sink.    |
|     | 20-30         | 11.1                         | 34.1 | 54.8 | clay                                | 2 m from center of the     |
|     | 40-47         | 12.4                         | 21.1 | 66.5 | clay                                | linear depression.         |
| A7  | <10           | 8.6                          | 65.0 | 26.4 | silt loam                           | grass field above sink.    |
|     | 20-30         | 13.0                         | 53.0 | 34.0 | silty clay loam                     | Small flat area within     |
|     | 40-50         | 11.0                         | 28.6 | 60.4 | clay                                | the larger slope.          |
|     | 60-70         | 10.1                         | 15.5 | 74.4 | clay                                |                            |
|     | 110-120       | 6.0                          | 28.0 | 66.0 | clay                                |                            |
| A8  | <10           | 9.0                          | 68.5 | 22.5 | silt loam                           | grass field above sink.    |
|     | 20-30         | 7.9                          | 64.8 | 27.3 | silt loam                           | E of site 7, also on the   |
|     | 40-50         | 9.0                          | 33.0 | 58.0 | clay                                | small flat area.           |
|     | 60-70         | 9.1                          | 18.6 | 72.3 | clay                                |                            |
|     | 110-117       | 4.4                          | 30.2 | 65.4 | clay                                |                            |



**APPENDIX 4 – HILLSLOPE A SOIL SAMPLES (CONTINUED)**

| No. | Depth   | Sand | Silt | Clay | Texture Class             | Slope Position   |
|-----|---------|------|------|------|---------------------------|--|
| A9  | <10     | 9.1  | 66.6 | 24.4 | silt loam                 | grass field above sink.  |
|     | 20-30   | 12.1 | 51.7 | 36.1 | silty clay loam           | On a slight rise E of sites 7 and 8.   |
|     | 40-50   | 11.0 | 32.0 | 57.0 | clay                      |  |
|     | 60-70   | 12.0 | 20.0 | 68.0 | clay                      |  |
|     | 110-120 | 8.5  | 18.5 | 73.0 | clay                      |  |
| A10 | <10     | 12.4 | 70.1 | 17.5 | silt loam                 | grass field.   |
|     | 20-30   | 15.8 | 56.8 | 27.4 | silt loam                 | Below sink elevation.  |
|     | 40-50   | 17.0 | 47.0 | 36.0 | silty clay loam           | Crest of slope nose.   |
|     | 60-75   | 24.0 | 33.9 | 42.1 | clay                      |  |
| A11 | <10     | 13.2 | 72.0 | 14.8 | silt loam                 | grass field.   |
|     | 20-30   | 12.2 | 69.3 | 18.5 | silt loam                 | Center of nose sideslope.  |
|     | 40-50   | 11.0 | 66.0 | 23.0 | silt loam                 | 8 m from site 10 in a line normal to the linear                                  |
|     | 60-70   | 11.0 | 65.0 | 24.0 | silt loam                 |  |
|     | 70-80   | 12.0 | 60.1 | 28.0 | silt loam-silty clay loam | depression below the sink..  |
| A12 | <10     | 15.6 | 70.2 | 14.2 | silt loam                 | grass field.   |
|     | 20-30   | 11.9 | 69.9 | 18.2 | silt loam                 | Lower nose sideslope.  |
|     | 40-50   | 9.0  | 71.0 | 20.0 | silt loam                 | 26 m from site 10 in a line normal to the linear                                 |
|     | 60-70   | 8.2  | 67.5 | 24.3 | silt loam                 |  |
|     | 85-95   | 9.1  | 64.5 | 26.4 | silt loam                 | depression below the sink..  |
| A13 | <10     | 10.6 | 71.1 | 18.3 | silt loam                 | grass field.   |
|     | 20-30   | 8.0  | 66.0 | 26.0 | silt loam                 | Center of linear depression below sink.  |
|     | 40-50   | 5.0  | 70.3 | 24.8 | silt loam                 |  |
|     | 60-70   | 4.2  | 65.3 | 30.5 | silty clay loam           |  |
|     | 110-118 | 6.5  | 65.1 | 28.4 | silty clay loam           |  |
| A14 | <10     | 13.5 | 65.4 | 21.2 | silt loam                 | grass; 30 m above fence.   |
|     | 20-28   | 16.8 | 61.5 | 21.8 | silt loam                 | Linear depression center.  |
| A15 | <10     | 17.9 | 66.5 | 15.7 | silt loam                 | grass field.   |
|     | 20-30   | 12.0 | 66.0 | 22.0 | silt loam                 | App. 10 m NE from site 14 in a line normal to the path of the linear depression. |
|     | 40-50   | 15.8 | 58.0 | 26.1 | silt loam                 |  |
|     | 60-70   | 18.0 | 49.0 | 33.0 | silty clay loam           |  |
|     | 70-82   | 20.5 | 46.5 | 33.1 | clay loam                 |  |
| A16 | <10     | 17.4 | 65.9 | 16.7 | silt loam                 |  |
|     | 20-30   | 19.7 | 54.2 | 26.1 | silt loam                 | Center nose side slope in line with sites 14 and 15.                             |
|     | 40-50   | 24.0 | 35.0 | 41.0 | clay                      |  |
|     | 60-70   | 22.1 | 30.3 | 47.6 | clay                      |  |
|     | 80-86   | 22.9 | 26.0 | 51.1 | clay                      |  |
| A17 | <10     | 20.1 | 54.5 | 25.4 | silt loam                 | grass field.   |
|     | 20-30   | 15.2 | 61.4 | 23.4 | silt loam                 | Nose crest.  |
|     | 30-37   | 13.4 | 63.7 | 22.8 | silt loam                 | In line with sites 14-16.  |
| A18 | <10     | 14.5 | 70.5 | 15.0 | silt loam                 | grass, opposite hillslope from 14-17; 30 m from path of linear depression.       |
|     | 20-30   | 10.0 | 66.0 | 24.0 | silt loam                 |  |
|     | 30-36   | 13.0 | 62.0 | 25.0 | silt loam                 |  |

**APPENDIX 4 – HILLSLOPE A SOIL SAMPLES (CONTINUED)**

| No. | Depth | Sand | Silt | Clay | Texture Class   | Slope Position   |
|-----|-------|------|------|------|-----------------|--|
| A19 | <10   | 11.0 | 73.0 | 16.0 | silt loam       | forest, 8 m below fenceline.<br>SW of the incision that starts at the fence.                             |
|     | 20-30 | 14.3 | 62.3 | 23.4 | silt loam       |  |
|     | 40-50 | 13.0 | 63.5 | 23.5 | silt loam       |  |
|     | 60-70 | 13.0 | 66.0 | 21.0 | silt loam       |  |
|     | 70-80 | 15.0 | 63.0 | 22.0 | silt loam       |  |
| A20 | <10   | 12.1 | 67.1 | 20.8 | silt loam       | forest, about 5 m from site 19<br>in a shallow concavity that collects flow from site 19 and from above. |
|     | 20-30 | 11.5 | 66.6 | 21.9 | silt loam       |  |
|     | 40-50 | 10.1 | 65.7 | 24.2 | silt loam       |  |
|     | 60-70 | 10.8 | 66.2 | 23.0 | silt loam       |  |
| A21 | <10   | 14.4 | 64.0 | 21.6 | silt loam       | forest, app. 20 m from site 20<br>in a line paralleling the fence<br>Immediate site area is flat.        |
|     | 20-30 | 13.1 | 64.7 | 22.2 | silt loam       |  |
|     | 40-50 | 13.0 | 60.0 | 27.0 | silt loam       |  |
|     | 60-70 | 8.0  | 38.0 | 54.0 | clay            |  |
|     | 90-98 | 4.0  | 24.0 | 72.0 | clay            |  |
| A22 | 0-10  | 16.2 | 61.9 | 21.9 | silt loam       | forest, app. 20 m from site 21<br>in a line paralleling the fence<br>Local site is flat.                 |
|     | 20-30 | 13.1 | 37.3 | 49.7 | clay            |  |
|     | 40-50 | 2.2  | 20.5 | 77.3 | clay            |  |
|     | 50-58 | 6.6  | 27.4 | 66.1 | clay            |  |
| A23 | <10   | 16.7 | 61.1 | 22.2 | silt loam       | Channel center, 3 m below fence.   |
|     | 10-20 | 17.9 | 60.0 | 22.1 | silt loam       |  |
| A24 | <10   | 16.3 | 59.5 | 24.2 | silt loam       | forest, app. 35 m below fence  |
|     | 20-30 | 14.7 | 47.1 | 38.2 | silty clay loam |  |
|     | 34-44 | 15.3 | 38.4 | 46.3 | clay            |  |
| A25 | <10   | 16.9 | 62.5 | 20.5 | silt loam       | forest, 5 m W of site 24.<br>Local small slope; lies slightly lower than site 24.                        |
|     | 20-30 | 12.7 | 62.1 | 25.2 | silt loam       |  |
|     | 30-38 | 12.8 | 56.6 | 30.6 | silty clay loam |  |
| A26 | <10   | 18.3 | 58.6 | 23.1 | silt loam       | forest, app 20 m E of site 24.<br>Site 24 slopes toward 26.  |
|     | 20-29 | 14.8 | 55.1 | 30.2 | silty clay loam |  |
| A27 | <10   | 15.8 | 64.7 | 19.5 | silt loam       | forest, channel bank edge.   |
|     | 20-30 | 11.1 | 47.1 | 41.8 | silty clay      |  |
|     | 30-36 | 11.8 | 50.8 | 37.4 | silty clay loam |  |
| A28 | <10   | 20.1 | 60.2 | 19.7 | silt loam       | forest, channel bank slope.<br>Channel 1.5 m from site.  |
|     | 20-31 | 12.1 | 64.8 | 23.1 | silt loam       |  |
| A29 | <10   | 14.9 | 66.2 | 18.9 | silt loam       | forest<br>Crest of peninsula between channels entering the shaft.  |
|     | 20-30 | 12.8 | 64.7 | 22.5 | silt loam       |  |
|     | 40-48 | 13.7 | 65.9 | 20.4 | silt loam       |  |
| A30 | <10   | 13.4 | 66.9 | 19.8 | silt loam       | forest; Peninsula side slope<br>app. 2 m below site 29.<br>Small depression lies directly downhill.      |
|     | 20-30 | 12.0 | 35.0 | 53.0 | clay            |  |
|     | 40-50 | 5.0  | 17.0 | 78.0 | clay            |  |
|     | 60-70 | 4.7  | 11.7 | 83.6 | clay            |  |
|     | 80-90 | 9.0  | 13.0 | 78.0 | clay            |  |
| A31 | <10   | 16.2 | 63.8 | 20.0 | silt loam       | forest; app. 50 m below fence<br>In a slight circular depression in a clump of trees.                    |
|     | 20-30 | 4.0  | 37.0 | 59.0 | clay            |  |
|     | 40-50 | 3.0  | 24.0 | 73.0 | clay            |  |
|     | 55-65 | 5.0  | 18.0 | 77.0 | clay            |  |

#### APPENDIX 4 – HILLSOPE A SOIL SAMPLES (CONTINUED)

| No. | Depth | Sand | Silt | Clay | Texture Class             | Slope Position  |
|-----|-------|------|------|------|---------------------------|---|
| A32 | <10   | 15.5 | 62.9 | 21.6 | silt loam                 | forest, crest of slight rise.   |
|     | 20-30 | 10.0 | 46.0 | 44.0 | silty clay                |   |
|     | 45-54 | 10.0 | 30.0 | 60.0 | clay                      |   |
| A33 | <10   | 17.3 | 61.6 | 21.1 | silt loam                 | forest, in a slight downhill trending depression.   |
|     | 20-30 | 7.3  | 20.1 | 72.6 | clay                      |   |
|     | 40-50 | 6.1  | 15.7 | 78.3 | clay                      |   |
|     | 55-61 | 6.0  | 11.6 | 82.3 | clay                      |   |
| A34 | <10   | 20.9 | 57.9 | 21.1 | silt loam                 | forest; E of 33 in a line normal with the channel. Crest of a small linear rise angling downhill. |
|     | 20-30 | 22.5 | 54.2 | 23.4 | silt loam                 |   |
|     | 40-50 | 15.6 | 56.6 | 27.8 | silt loam                 |   |
|     | 60-69 | 14.7 | 54.3 | 31.0 | silty clay loam           |   |
| A35 | <10   | 10.0 | 67.7 | 22.3 | silt loam                 | forest, lies 10 m E of 34 in a slight depression.   |
|     | 20-27 | 10.7 | 67.2 | 22.1 | silt loam                 |   |
| A36 | <10   | 11.7 | 66.7 | 21.6 | silt loam                 | forest, 4 m from channel.   |
|     | 20-30 | 15.1 | 58.5 | 26.4 | silt loam                 |   |
|     | 33-43 | 13.9 | 58.0 | 28.1 | silty clay loam           |   |
| A37 | <10   | 9.6  | 71.2 | 19.2 | silt loam                 | forest, app. 80 m below fence   |
|     | 20-30 | 6.0  | 67.0 | 27.0 | silt loam                 |   |
|     | 34-44 | 7.0  | 55.0 | 38.0 | silty clay loam           |   |
| A38 | <10   | 7.0  | 73.0 | 20.0 | silt loam                 | forest, app. 15 m E of 37.  |
|     | 20-30 | 7.0  | 66.0 | 27.0 | silt loam                 |   |
|     | 40-53 | 11.8 | 48.8 | 39.4 | silty clay loam           |   |
| A39 | <10   | 11.0 | 69.0 | 20.0 | silt loam                 | forest, center of a clump of 6 trees.   |
|     | 20-30 | 7.0  | 69.0 | 24.0 | silt loam                 |   |
|     | 40-47 | 7.0  | 62.0 | 31.0 | silty clay loam           |   |
| A40 | <10   | 9.4  | 67.3 | 23.4 | silt loam                 | forest, app 10 m E of site.39. Site starts sloping to channel.                                    |
|     | 25-37 | 8.2  | 65.5 | 26.2 | silt loam                 |   |
| A41 | <10   | 9.3  | 62.4 | 28.4 | silty clay loam           | forest, app. 10 m from channel.   |
|     | 20-30 | 8.2  | 60.9 | 30.9 | silty clay loam           |   |
|     | 34-44 | 8.3  | 58.6 | 33.1 | silty clay loam           |   |
| A42 | <10   | 19.1 | 55.8 | 25.1 | silt loam                 | grass, in mown path 2 m above fence. Fairly level   |
|     | 20-30 | 20.0 | 56.2 | 23.8 | silt loam                 |   |
|     | 40-52 | 15.0 | 59.8 | 25.2 | silt loam                 |   |
| A43 | <10   | 18.4 | 62.6 | 19.0 | silt loam                 | grass; app. 3-4 m above fence at the crest of hill nose within the path area; sloping.            |
|     | 20-30 | 13.0 | 59.0 | 28.0 | silt loam-silty clay loam |   |
|     | 30-42 | 16.0 | 56.0 | 28.0 | silt loam-silty clay loam |   |

#### APPENDIX 4 – HILLSOPE B SOIL SAMPLES

| No.   | Depth (cm) | Particle Size Percentages |      |      | USDA Texture Class         | Slope Position   |
|-------|------------|---------------------------|------|------|----------------------------|--|
|       |            | Sand                      | Silt | Clay |                            |  |
| B1    | 0-10       | 11                        | 63   | 26   | silt loam                  | open grass and brush area. Sideslope, below a concave slump.                                     |
|       | 20-30      | 9                         | 54   | 38   | silty clay loam            |  |
|       | 40-50      | 6                         | 59   | 36   | silty clay loam            |  |
|       | 60-70      | 5                         | 55   | 40   | silty clay-silty clay loam |  |
|       | 80-90      | 7                         | 29   | 65   | clay                       |  |
| B2    | 0-10       | 12                        | 63   | 25   | silt loam                  | open grass and brush area. Sideslope; 5 m SE of site 1, parallel with contours.                  |
|       | 20-30      | 6                         | 57   | 37   | silty clay loam            |  |
|       | 40-50      | 4                         | 39   | 57   | clay                       |  |
| B3    | 0-10       | 12                        | 59   | 29   | silt loam-silty clay loam  | open grass and brush area. Sideslope, below slump. 4-5 m SE of site 2, parallel with contours.   |
|       | 20-30      | 8                         | 54   | 38   | silty clay loam            |  |
|       | 40-50      | 6                         | 49   | 45   | silty clay                 |  |
|       | 60-70      | 6                         | 47   | 46   | silty clay                 |  |
|       | 72-82      | 8                         | 40   | 53   | silty clay-clay            |  |
| B4    | 0-10       | 10                        | 61   | 29   | silty clay loam            | forest, sideslope. In line with sites 1-3.   |
|       | 20-30      | 10                        | 57   | 34   | silty clay loam            |  |
|       | 40-50      | 5                         | 58   | 37   | silty clay loam            |  |
|       | 60-70      | 5                         | 65   | 31   | silty clay loam            |  |
|       | 80-90      | 5                         | 65   | 30   | silty clay loam            |  |
|       | 101-111    | 9                         | 55   | 36   | silty clay loam            |  |
| B5    | 0-10       | 9                         | 65   | 26   | silt loam                  | forest, sideslope. Large outcrop 30 cm away.   |
|       | 20-30      | 7                         | 60   | 34   | silty clay loam            |  |
|       | 40-50      | 5                         | 66   | 29   | silt loam-silty clay loam  |  |
|       | 60-70      | 5                         | 64   | 31   | silty clay loam            |  |
|       | 80-90      | 8                         | 52   | 39   | silty clay loam            |  |
|       | 114-124    | 7                         | 25   | 68   | clay                       |  |
|       | B6         | 0-10                      | 8    | 64   | 28                         |  |
| 20-30 |            | 7                         | 60   | 33   | silty clay loam            |  |
| 40-50 |            | 8                         | 59   | 33   | silty clay loam            |  |
| 64-74 |            | 13                        | 36   | 51   | clay                       |  |
| B7    | 0-10       | 14                        | 68   | 18   | silt loam                  | forest, within 2 m of 2 large trees. Slope below sites 1-6, at base of regenerating forest area. |
|       | 20-30      | 11                        | 62   | 27   | silt loam                  |  |
|       | 40-50      | 11                        | 63   | 26   | silt loam                  |  |
|       | 63-73      | 15                        | 59   | 27   | silt loam                  |  |
| B8    | 0-10       | 11                        | 67   | 22   | silt loam                  | forest. Slope below sites 1-6 at base of regenerating forest area.                               |
|       | 20-30      | 9                         | 65   | 26   | silt loam                  |  |
|       | 40-50      | 10                        | 60   | 30   | silty clay loam            |  |
|       | 50-60      | 12                        | 55   | 33   | silty clay loam            |  |

**APPENDIX 4 – HILLSLOPE B SOIL SAMPLES (CONTINUED)**

| No  | Depth   | Sand | Silt | Clay | Texture Class             | Slope Position                |
|-----|---------|------|------|------|---------------------------|-------------------------------|
| B9  | 0-10    | 11   | 68   | 20   | silt loam                 | forest.                       |
|     | 20-30   | 11   | 65   | 25   | silt loam                 | Slope below sites 1-6         |
|     | 40-50   | 13   | 61   | 27   | silt loam                 | at base of regenerating area. |
| B10 | 0-10    | 14   | 68   | 18   | silt loam                 | forest.                       |
|     | 20-30   | 12   | 58   | 31   | silty clay loam           | Slope below sites 1-6         |
|     | 40-50   | 15   | 47   | 38   | silty clay loam           | at base of regenerating area. |
|     | 60-70   | 15   | 47   | 38   | silty clay loam           |                               |
|     | 95-105  | 15   | 28   | 57   | clay                      |                               |
| B11 | 0-10    | 11   | 69   | 20   | silt loam                 | grass and brush.              |
|     | 20-30   | 11   | 67   | 22   | silt loam                 | Slope below sites 1-6         |
|     | 30-40   | 14   | 58   | 28   | silt loam-silty clay loam | slope slants to nearby gully. |
| B12 | 0-10    | 11   | 62   | 27   | silt loam                 | grass and brush               |
|     | 20-30   | 10   | 60   | 29   | silty clay loam           | Slope below sites 1-6.        |
|     | 40-50   | 13   | 58   | 29   | silty clay loam           |                               |
| B13 | 0-10    | 12   | 61   | 26   | silt loam                 | grass and brush               |
|     | 20-30   | 12   | 51   | 37   | silty clay loam           | Slope below sites 1-6.        |
|     | 60-70   | 13   | 39   | 48   | clay                      |                               |
|     | 104-114 | 16   | 22   | 62   | clay                      |                               |
| B14 | 40-50   | 12   | 64   | 24   | silt loam                 | forest, beginning of revised  |
|     |         |      |      |      | silt loam-silty clay loam | transect.                     |
|     | 60-70   | 15   | 57   | 28   | clay loam                 |                               |
|     | 80-90   | 23   | 42   | 35   | clay loam                 |                               |
|     | 110-120 | 21   | 16   | 63   | clay                      |                               |

#### APPENDIX 4 – HILLSOPE C SOIL SAMPLES

| No. | Depth (cm) | Particle Size Percentages |      |      | USDA Texture Class        | Slope Position                         |
|-----|------------|---------------------------|------|------|---------------------------|--|
|     |            | Sand                      | Silt | Clay |                           |  |
| C1  | <10        | 13                        | 71   | 17   | silt loam                 | grass and brush area.                  |
|     | 20-30      | 10                        | 68   | 22   | silt loam                 | Straight sideslope.                    |
|     | 40-50      | 13                        | 60   | 27   | silt loam                 |  |
|     | 60-70      | 19                        | 51   | 31   | silty clay loam           |  |
|     | 90-101     | 20                        | 36   | 44   | clay                      |  |
| C2  | <10        | 14                        | 69   | 17   | silt loam                 |  |
|     | 20-30      | 10                        | 69   | 21   | silt loam                 | Elevation parallel to site C1.         |
|     | 40-50      | 13                        | 59   | 28   | silt loam-silty clay loam |  |
|     | 60-70      | 18                        | 51   | 32   | silty clay loam           |  |
|     | 80-90      | 22                        | 33   | 45   | clay                      |  |
| C3  | <10        | 16                        | 64   | 20   | silt loam                 |  |
|     | 20-30      | 10                        | 64   | 26   | silt loam                 | Elevation parallel to sites C1 and C2. |
|     | 40-50      | 10                        | 62   | 28   | silt loam-silty clay loam |  |
|     | 60-70      | 12                        | 55   | 34   | silty clay loam           |  |
|     | 100-110    | 20                        | 44   | 36   | clay loam                 |  |
| C4  | 20-30      | 11                        | 68   | 21   | silt loam                 |  |
|     | 40-50      | 13                        | 60   | 27   | silt loam                 | Elevation parallel to sites C1 and C2. |
|     | 60-70      | 20                        | 50   | 30   | clay loam-silty clay loam |  |
|     | 80-87      | 24                        | 35   | 41   | clay                      |  |

#### APPENDIX 4 – HILLSOPE F SOIL SAMPLES

| No. | Depth<br>(cm) | Particle Size<br>Percentages |      |      | USDA<br>Texture Class        | Slope Position   |
|-----|---------------|------------------------------|------|------|------------------------------|--|
|     |               | Sand                         | Silt | Clay |                              |  |
| F1  | <10           | 21                           | 61   | 19   | silt loam                    | forest; between two large trees sited next to gully.         |
|     | 20-30         | 16                           | 60   | 24   | silt loam                    |  |
|     | 40-50         | 19                           | 53   | 28   | silt loam-silty<br>clay loam |  |
|     | 60-70         | 17                           | 28   | 55   | clay                         |  |
|     | 80-90         | 9                            | 18   | 73   | clay                         |  |
|     | 150-161       | 7                            | 15   | 78   | clay                         |  |
| F2  | <10           | 19                           | 65   | 17   | silt loam                    | forest; near top of transect.                                |
|     | 20-30         | 8                            | 68   | 24   | silt loam                    |  |
|     | 40-50         | 5                            | 68   | 27   | silt loam                    |  |
|     | 60-70         | 8                            | 55   | 37   | silty clay loam              |  |
|     | 80-90         | 8                            | 44   | 48   | silty clay                   |  |
|     | 95-114        | 10                           | 38   | 52   | clay                         |  |
| F5  | <10           | 10                           | 66   | 23   | silt loam                    | grass, steep mid-slope area. Matches forest elevation at F2. |
|     | 20-30         | 6                            | 66   | 28   | silt loam-silty<br>clay loam |  |
|     | 40-50         | 4                            | 61   | 35   | silty clay loam              |  |
|     | 60-70         | 6                            | 57   | 37   | silty clay loam              |  |
|     | 80-91         | 11                           | 51   | 38   | silty clay loam              |  |
| F6  | <10           | 8                            | 66   | 26   | silt loam                    | grass, steep mid-slope area. Matches forest elevation at F1. |
|     | 20-30         | 6                            | 62   | 33   | silty clay loam              |  |
|     | 40-50         | 7                            | 51   | 42   | silty clay                   |  |
|     | 60-70         | 9                            | 34   | 56   | clay                         |  |
|     | 80-90         | 10                           | 25   | 65   | clay                         |  |
|     | 90-99         | 19                           | 21   | 60   | clay                         |  |

## APPENDIX 4 – INFILTRATION TEST PIT SOIL SAMPLES

| No. | Depth (cm)  | Particle Size Percentages |      |      | USDA Texture Class         | Slope Position                                  |
|-----|-------------|---------------------------|------|------|----------------------------|---|
|     |             | Sand                      | Silt | Clay |                            |   |
| 1   | <10         | 15                        | 68   | 17   | silt loam                  | forest, Hillslope C                             |
|     | 25          | 12                        | 63   | 24   | silt loam                  | Site is just inside forest edge in a mid-bottom |
|     | 55          | 10                        | 65   | 25   | silt loam                  |   |
|     | 85          | 20                        | 44   | 36   | clay loam-silty clay loam  | slope position.                                 |
|     | 125         | 19                        | 19   | 61   | clay                       |   |
| 2   | <10         | 14                        | 70   | 16   | silt loam                  | grass, Hillslope C                              |
|     | 25          | 10                        | 66   | 24   | silt loam                  | Site is just inside forest edge in a mid-bottom |
|     | 55          | 13                        | 59   | 28   | silt loam-silty clay loam  |   |
|     | 85          | 21                        | 36   | 43   | clay                       | slope position. Matches elevation with site 1.  |
|     | 125         | 19                        | 17   | 64   | clay                       |   |
| 3   | <10         | 21                        | 69   | 11   | silt loam                  | forest, Hillslope H.                            |
|     | 25          | 9                         | 69   | 22   | silt loam                  | App; 5 m inside forest edge in a mid-bottom     |
|     | 55          | 7                         | 54   | 39   | silty clay loam            |   |
|     | 85          | 13                        | 39   | 48   | clay                       | slope position.                                 |
|     | 125         | 5                         | 26   | 69   | clay                       |   |
| 4   | <10         | 16                        | 73   | 11   | silt loam                  | grass, Hillslope H.                             |
|     | 25          | 10                        | 68   | 22   | silt loam                  | App. 30 m from forest edge. Matches             |
|     | 55          | 14                        | 50   | 36   | silty clay loam            |   |
|     | 85          | 18                        | 32   | 50   | clay                       | elevation with site 3.                          |
|     | 125         | 6                         | 22   | 72   | clay                       |   |
| 5   | <10         | 12                        | 61   | 28   | silt loam-silty clay loam  | forest, Hillslope H.                            |
|     | 25 (yellow) | 8                         | 21   | 71   | clay                       | Site is uphill from pit 3.                      |
|     | 25 (brown)  | 11                        | 49   | 40   | silty clay-silty clay loam |   |
|     | 55          | 10                        | 18   | 73   | clay                       |   |
|     | 75-80       | 7                         | 21   | 73   | clay                       |   |
| 6   | <10         | 11                        | 59   | 30   | silty clay loam            | forest, Hillslope H.                            |
|     | 11-25       | 8                         | 42   | 50   | silty clay                 | Site is uphill from Pit 5.                      |
|     | 25          | 8                         | 36   | 56   | clay                       |   |
|     | 55          | 18                        | 19   | 62   | clay                       |   |
|     | 70          | 10                        | 18   | 71   | clay                       |   |
| 7   | <10         | 12                        | 53   | 35   | silty clay loam            | forest, Hillslope H                             |
|     | 25          | 12                        | 40   | 48   | silty clay-clay            | 7 m downhill                                    |
|     | 40-45       | 14                        | 23   | 62   | clay                       | from 1.15 m DBH oak.                            |
| 8   | <10         | 10                        | 58   | 33   | silty clay loam            | forest. Hillslope H                             |
|     | 11-30       | 7                         | 47   | 46   | silty clay                 | 15 m uphill from pit #7.                        |
|     | >30         | 6                         | 37   | 57   | clay                       |   |



**APPENDIX 4 – INFILTRATION TEST PIT SOIL SAMPLES (CONTINUED)**

| No. | Depth | Sand | Silt | Clay | Texture Class   | Slope Position  |
|-----|-------|------|------|------|-----------------|---|
| 9   | <10   | 7    | 60   | 32   | silty clay loam | grass, midslope<br>Hillslope H.                                 |
|     | 10-25 | 5    | 31   | 64   | clay            |   |
|     | 25    | 14   | 26   | 60   | clay            |   |
|     | 55    | 27   | 26   | 47   | clay            |   |
|     | 85    | 31   | 24   | 45   | clay            |   |
| 10  | <10   | 6    | 69   | 24   | silt loam       | Hillslope H grass<br>10 m uphill from Pit 9.                    |
|     | B     | 4    | 60   | 36   | silty clay loam |   |
|     | 55    | 4    | 48   | 48   | silty clay      |   |
| 11  | <10   | 5    | 65   | 30   | silty clay loam | Hillslope A grass.<br>Low shoulder of hill.                     |
|     | 25    | 4    | 46   | 50   | silty clay      |   |
|     | 55    | 5    | 28   | 67   | clay            |   |
|     | 85    | 5    | 27   | 68   | clay            |   |
| 12  | <10   | 11   | 66   | 23   | silt loam       | Hillslope A grass.<br>Downhill from pit 11.                     |
|     | 25    | 5    | 57   | 38   | silty clay loam |   |
|     | 55    | 4    | 40   | 56   | silty clay-clay |   |
|     | 75-80 | 4    | 37   | 59   | clay            |   |
|     | 110   | 3    | 45   | 52   | silty clay      |   |
| 13  | < 10  | 13   | 61   | 26   | silt loam       | Hillslope A grass.<br>Site is 10 m below and SW<br>of pit 12.   |
|     | 8-22  | 5    | 56   | 39   | silty clay loam |   |
|     | 25    | 7    | 24   | 69   | clay            |   |
|     | 55    | 7    | 17   | 76   | clay            |   |
|     | 82    | 6    | 15   | 79   | clay            |   |
| 14  | < 10  | 11   | 64   | 26   | silt loam       | Hillslope A grass.<br>Site is app. 8 m downhill<br>from pit 13. |
|     | 10-25 | 11   | 21   | 69   | clay            |   |
|     | 25    | 11   | 22   | 67   | clay            |   |
|     | 55    | 22   | 18   | 60   | clay            |   |

**APPENDIX 5**  
**DATA USED IN STATISTICAL ANALYSES**

**APPENDIX 5 – DATA INCLUDED IN STATISTICAL COMPARISONS OF HYDROLOGICAL CHARACTERISTICS**

(NM – No Measurement) K(h) is unsaturated hydraulic conductivity at designated tensions.

282

| Site         | Depth (cm) | Steady State Infiltration Rates (cm <sup>3</sup> /hr) |      |     | K(h) (cm/hr) |       |       | Matric Potential | Clay % | Bulk Density (g/cm <sup>3</sup> ) | Pore Space (%) |
|--------------|------------|---|------|-----|--------------|-------|-------|------------------|--------|-----------------------------------|----------------|
|              |            | -15   | -8   | -3  | K(-15)       | K(-8) | K(-3) |                  |        |                                   |                |
| 1<br>Forest  | < 10       | 0.5   | 0.5  | 1   | 0.00         | 0.77  | 1.55  | -62              | 17     | 1.19                              | 51.00          |
|              | 25         | 1   | 3    | 8   | 1.64         | 5.40  | 14.41 | -58              | 24     | 1.21                              | 51.29          |
|              | 55         | 2   | 5    | 6   | 3.01         | 3.31  | 3.97  | -47              | 25     | 1.31                              | 48.02          |
|              | 85         | 0.2   | 0.8  | 2   | 0.36         | 1.40  | 3.51  | -48              | 36     | 1.34                              | 48.11          |
|              | 125        | 0.07  | 0.2  | 1   | 0.11         | 0.43  | 2.13  | -46              | 61     | 1.35                              | 48.40          |
| 2<br>Grass   | < 10       | 0.3   | 0.5  | 0.8 | 0.32         | 0.63  | 1.01  | -68              | 16     | 1.16                              | 52.55          |
|              | 25         | 1.1   | 2    | 4   | 1.31         | 3.10  | 6.19  | -73              | 24     | 1.32                              | 46.90          |
|              | 55         | 1   | 3    | 10  | 1.64         | 5.83  | 19.43 | -72              | 28     | 1.49                              | 40.68          |
|              | 85         | 0.4   | 1    | 1.6 | 0.60         | 1.26  | 2.02  |                  | 43     | 1.45                              | 43.93          |
|              | 125        | 0.1   | 0.2  | 0.4 | 0.13         | 0.31  | 0.62  |                  | 64     | 1.43                              | 44.95          |
| 3A<br>Forest | < 10       | 1   | 1.3  | 1.6 | 0.68         | 0.95  | 1.17  |                  | 11     | 1.11                              | 52.54          |
|              | 25         | 2   | 2.1  | 2.9 | 0.31         | 2.10  | 2.90  |                  | 22     | 1.26                              | 49.61          |
|              | 55         | 1.1   | 1.6  | 3   | 0.97         | 2.36  | 4.43  |                  | 39     | 1.41                              | 44.64          |
|              | 85         | 0.4   | 1    | 2   | 0.60         | 1.55  | 3.10  |                  | 48     | 1.37                              | 47.44          |
|              | 125        | 0.14  | 0.29 | 1   | 0.19         | 0.57  | 1.96  |                  | 69     | 1.33                              | 49.40          |
| 3B           | < 10       | 1.2   | 1.3  | 1.4 | 0.29         | 0.40  | 0.43  |                  | 11     | 1.11                              | 52.54          |
|              | <10        | 0.6   | 0.75 | 1   | 0.36         | 0.69  | 0.92  |                  | 11     | 1.11                              | 52.54          |
|              | 25         | 1.6   | 1.7  | 2.6 | 0.30         | 2.02  | 3.09  |                  | 22     | 1.26                              | 49.61          |
|              | 55         | 1   | 2    | 4.5 | 1.30         | 3.33  | 7.49  |                  | 39     | 1.41                              | 44.64          |
|              | 85         | 0.5   | 1    | 1.5 | 0.65         | 1.16  | 1.73  |                  | 48     | 1.37                              | 47.44          |
|              | 125        | NM  |      |     |              |       |       |                  |        |                                   |                |
| 4A<br>Grass  | < 10       | 0.6   | 1    | 1.7 | 0.65         | 1.35  | 2.30  |                  | 11     | 0.97                              | 59.85          |
|              | 25         | 0.4   | 0.5  | 1.1 | 0.24         | 0.82  | 1.81  |                  | 22     | 1.27                              | 49.47          |
|              | 55         | 0.01  | 0.3  | 0.8 | 0.02         | 0.54  | 1.44  |                  | 36     | 1.51                              | 40.77          |
|              | 85         | 0.2   | 1    | 2.5 | 0.38         | 1.75  | 4.38  |                  | 50     | 1.43                              | 44.43          |
|              | 125        | 0.1   | 0.13 | 0.5 | 0.06         | 0.25  | 1.02  |                  | 72     | 1.32                              | 49.42          |

**APPENDIX 5 – DATA INCLUDED IN STATISTICAL COMPARISONS OF HYDROLOGICAL CHARACTERISTICS  
(CONTINUED)**

(NM – No Measurement) K(h) is unsaturated hydraulic conductivity at designated tensions.

283

| Site         | Depth (cm)  | Steady State Infiltration Rates (cm <sup>3</sup> /hr) |      |     | K(h) (cm/hr) |       |       | Matric Potential | Clay % | Bulk Density (g/cm <sup>3</sup> ) | Pore Space (%) |
|--------------|-------------|---|------|-----|--------------|-------|-------|------------------|--------|-----------------------------------|----------------|
|              |             | -15   | -8   | -3  | K(-15)       | K(-8) | K(-3) |                  |        |                                   |                |
| 4B           | < 10        | 0.7   | 1.5  | 6.5 | 0.96         | 3.11  | 13.46 |                  | 11     | 0.97                              | 59.85          |
|              | 25          | 0.6   | 1    | 2.3 | 0.65         | 1.68  | 3.87  |                  | 22     | 1.27                              | 49.47          |
|              | 55          | 0.35  | 0.6  | 1.2 | 0.39         | 0.93  | 1.86  |                  | 36     | 1.51                              | 40.77          |
|              | 85          | 0.4   | 1    | 2.4 | 0.60         | 1.72  | 4.13  |                  | 50     | 1.43                              | 44.43          |
|              | 125         | NM  |      |     |              |       |       |                  |        |                                   |                |
| 5A<br>Forest | < 10        | 0   | 0.5  | 4.1 |              | 1.14  | 9.35  | -14              | 28     | 0.82                              | 64.77          |
|              | 25 (yellow) | 0.03  | 0.1  | 0.4 | 0.05         | 0.20  | 0.81  | -12              | 71     | 1.34                              | 46.59          |
|              | 25 (brown)  | 0.04  | 0.53 | 2.1 | 0.09         | 1.08  | 4.37  | -12              | 40     | 1.28                              | 48.40          |
|              | 55          | 0.14  | 0.4  | 1   | 0.22         | 0.70  | 1.75  | -42              | 73     | 1.29                              | 48.64          |
| 5B           | < 10        | NM  |      |     |              |       |       |                  |        |                                   |                |
|              | 25 (yellow) | NM  |      |     |              |       |       |                  |        |                                   |                |
|              | 25 (brown)  | NM  |      |     |              |       |       |                  |        |                                   |                |
|              | 55          | 0.2   | 0.4  | 1.1 | 0.26         | 0.73  | 2.01  | -42              | 73     | 1.29                              | 48.64          |
| 6A<br>Forest | < 10        | 0.13  | 0.39 | 2.3 | 0.21         | 0.85  | 5.08  | -32              | 30     | 0.82                              | 63.39          |
|              | 25          | 0.2   | 0.8  | 1.6 | 0.36         | 1.22  | 2.37  | -42              | 56     | 1.29                              | 50.14          |
|              | 55          | 0.4   | 0.78 | 1.5 | 0.51         | 1.17  | 2.26  | -56              | 62     | 1.40                              | 46.79          |
|              | 70          | 0.45  | 1    | 3   | 0.63         | 1.88  | 5.64  | -65              | 71     | 1.48                              | 44.86          |
| 6B           | < 10        | NM  |      |     |              |       |       |                  |        |                                   |                |
|              | 25          | 0.4   | 1.1  | 2.3 | 0.63         | 1.73  | 3.54  | -42              | 56     | 1.29                              | 50.14          |
|              | 55          | 0.35  | 1    | 2   | 0.56         | 1.55  | 3.10  | -56              | 62     | 1.40                              | 46.79          |
|              | 70          | NM  |      |     |              |       |       |                  |        |                                   |                |
| 7<br>Forest  | <10         | 0.15  | 0.5  | 1.3 | 0.26         | 0.89  | 2.32  | -58              | 35     | 0.75                              | 67.94          |
|              | 25          | 0.5   | 1.2  | 5   | 0.74         | 2.46  | 10.27 | -62              | 48     | 1.10                              | 55.63          |
| 8<br>Forest  | <10         | 0.2   | 0.64 | 1.3 | 0.34         | 1.00  | 2.03  | -52              | 33     | 0.79                              | 66.27          |
|              | 25          | 0.22  | 0.78 | 6.7 | 0.38         | 1.79  | 15.36 | -66              | 46     | 1.23                              | 50.92          |

**APPENDIX 5 – DATA INCLUDED IN STATISTICAL COMPARISONS OF HYDROLOGICAL CHARACTERISTICS  
(CONTINUED)**

(NM – No Measurement) K(h) is unsaturated hydraulic conductivity at designated tensions.

284

| Site         | Depth (cm) | Steady State Infiltration Rates (cm <sup>3</sup> /hr) |      |     | K(h) (cm/hr) |       |       | Matric Potential | Clay % | Bulk Density (g/cm <sup>3</sup> ) | Pore Space (%) |
|--------------|------------|---|------|-----|--------------|-------|-------|------------------|--------|-----------------------------------|----------------|
|              |            | -15   | -8   | -3  | K(-15)       | K(-8) | K(-3) |                  |        |                                   |                |
| 9A<br>Grass  | <10        | 0.24  | 0.38 | 0.9 | 0.24         | 0.64  | 1.46  | -57              | 32     | 0.88                              | 63.16          |
|              | 25         | 0.27  | 0.65 | 2.5 | 0.40         | 1.31  | 5.09  | -60              | 60     | 1.36                              | 47.91          |
|              | 55         | 0.48  | 1.15 | 3.6 | 0.71         | 2.19  | 6.81  | -60              | 47     | 1.55                              | 40.51          |
|              | 85         | ----  | 0.55 | 1.1 |              | 0.84  | 1.65  |                  | 45     | 1.56                              | 39.90          |
| 9B           | <10        | 0.12  | 0.22 | 0.5 | 0.14         | 0.37  | 0.84  | -57              | 32     | 0.88                              | 63.16          |
|              | 25         | 0.33  | 0.77 | 2.5 | 0.48         | 1.48  | 4.82  | -60              | 60     | 1.36                              | 47.91          |
|              | 55         | 0.36  | 0.9  | 1.8 | 0.54         | 1.40  | 2.84  | -60              | 47     | 1.55                              | 40.51          |
|              | 85         | 0.4   | 1    | 3   | 0.60         | 1.88  | 5.64  |                  |        | 1.56                              | 39.90          |
| 10A<br>Grass | <10        | 0.2   | 0.31 | 0.6 | 0.20         | 0.46  | 0.85  | -60              | 24     | 0.94                              | 60.23          |
|              | 25         | 0.44  | 1.13 | 3.1 | 0.67         | 2.06  | 5.65  |                  | 36     | 1.15                              | 52.60          |
|              | 55         | 0.6   | 1    | 1.4 | 0.65         | 1.08  | 1.56  |                  | 48     | 1.50                              | 41.37          |
| 10B          | <10        | NM  |      |     |              |       |       |                  |        |                                   |                |
|              | 25         | 0.6   | 1.28 | 4.5 | 0.82         | 2.53  | 8.95  |                  | 36     | 1.15                              | 52.60          |
|              | 55         | 1.9   | 2.1  | 3   | 0.57         | 2.24  | 3.20  |                  | 48     | 1.50                              | 41.37          |
| 11A<br>Grass | <10        | 0.2   | 0.6  | 2.3 | 0.33         | 1.21  | 4.69  | -24              | 30     | 0.99                              | 57.90          |
|              | 25         | 0.13  | 0.27 | 1.1 | 0.17         | 0.55  | 2.20  | -10              | 50     | 1.30                              | 48.17          |
|              | 40         | 0.08  | 0.34 | 1   | 0.15         | 0.64  | 1.87  |                  | 67     | 1.21                              | 52.68          |
| 11B          | <10        | NM  |      |     |              |       |       |                  |        |                                   |                |
|              | 25         | 0.16  | 0.52 | 1.5 | 0.27         | 0.97  | 2.88  | -7               | 50     | 1.30                              | 48.17          |
|              | 40         | NM  |      |     |              |       |       |                  |        | 1.21                              | 52.68          |
| 12A<br>Grass | <10        | 0.18  | 0.4  | 1.4 | 0.25         | 0.79  | 2.76  | -32              | 23     | 1.13                              | 54.10          |
|              | 25         | 0.15  | 0.36 | 1.5 | 0.22         | 0.73  | 2.96  | -12              | 38     | 1.42                              | 43.51          |
|              | 55         | 0.29  | 0.7  | 1.7 | 0.43         | 1.21  | 2.94  | -22              | 56     | 1.28                              | 50.16          |
|              | 80         | 0.4   | 0.9  | 2.2 | 0.57         | 1.55  | 3.71  | -60              | 59     | 1.34                              | 48.13          |

**APPENDIX 5 – DATA INCLUDED IN STATISTICAL COMPARISONS OF HYDROLOGICAL CHARACTERISTICS  
(CONTINUED)**

(NM – No Measurement) K(h) is unsaturated hydraulic conductivity at designated tensions.

285

| Site         | Depth<br>(cm) | Steady State Infiltration Rates<br>(cm <sup>3</sup> /hr) |      |     | K(h) (cm/hr) |       |       | Matric<br>Potential | Clay<br>% | Bulk<br>Density<br>(g/cm <sup>3</sup> ) | Pore Space<br>(%) |
|--------------|---------------|--|------|-----|--------------|-------|-------|---------------------|-----------|---|-------------------|
|              |               | -15  | -8   | -3  | K(-15)       | K(-8) | K(-3) |                     |           |   |                   |
| 12B          | <10           | NM   |      |     |              |       |       |                     |           |   |                   |
|              | 25            | 0.2  | 0.38 | 1.4 | 0.25         | 0.76  | 2.87  | -12                 | 38        | 1.42                                    | 43.51             |
|              | 55            | 0.26   | 0.66 | 1.6 | 0.39         | 1.15  | 2.82  | -22                 | 56        | 1.28                                    | 50.16             |
|              | 80            | 0.52   | 0.94 | 1.8 | 0.62         | 1.39  | 2.59  | -60                 | 59        | 1.34                                    | 48.13             |
| 13A<br>Grass | <10           | 0.2  | 0.33 | 0.7 | 0.21         | 0.54  | 1.18  | -62                 | 26        | 1.00                                    | 58.78             |
|              | 25            | 0.25   | 0.69 | 2.4 | 0.40         | 1.36  | 4.79  | -32                 | 69        | 1.27                                    | 50.59             |
|              | 55            | 0.14   | 0.25 | 0.8 | 0.16         | 0.48  | 1.51  | -22                 | 76        | 1.27                                    | 51.56             |
| 13B          | <10           | NM   |      |     |              |       |       |                     |           |   |                   |
|              | 25            | 0.3  | 0.72 | 2.3 | 0.44         | 1.38  | 4.41  | -32                 | 69        | 1.27                                    | 50.59             |
|              | 55            | NM   |      |     |              |       |       |                     |           |   |                   |
| 14A<br>Grass | <10           | 0.22   | 0.26 | 0.5 | 0.10         | 0.41  | 0.86  | -54                 | 26        | 1.11                                    | 55.40             |
|              | 25            | 0.41   | 0.93 | 2.3 | 0.58         | 1.61  | 3.91  | -54                 | 67        | 1.23                                    | 55.80             |
|              | 55            | 0.23   | 0.45 | 1   | 0.29         | 0.74  | 1.65  | -56                 | 60        | 1.36                                    | 50.14             |
| 14B          | <10           | NM   |      |     |              |       |       |                     |           |   |                   |
|              | 25            | 0.3  | 0.68 | 1.4 | 0.43         | 1.07  | 2.21  | -54                 | 67        | 1.23                                    | 55.80             |
|              | 55            | 0.25   | 0.4  | 1.3 | 0.26         | 0.77  | 2.48  | -56                 | 60        | 1.36                                    | 50.14             |

**APPENDIX 5 – DATA INCLUDED IN STATISTICAL COMPARISONS OF HYDROLOGICAL CHARACTERISTICS  
(CONTINUED)**

**SURFACE MEASUREMENTS ON HILL SHOULDER**

| Site   | Depth<br>to Rock (cm) | Steady State Infiltration Rates<br>(cm <sup>3</sup> /hr) |      |     | K(h) (cm/hr) |       |       | Matric<br>Potential |
|--------|-----------------------|--|------|-----|--------------|-------|-------|---------------------|
|        |                       | -15  | -8   | -3  | K(-15)       | K(-8) | K(-3) |                     |
| Grass  | 27                    | 0.31   | 1.17 | 5.8 | 0.55         | 2.48  | 12.20 | -2                  |
| Grass  | 23                    | 0.2  | 0.56 | 2.5 | 0.32         | 1.16  | 5.11  | -18                 |
| Grass  | 35                    | 0.2  | 0.32 | 0.7 | 0.21         | 0.54  | 1.25  | -49                 |
| Grass  | 75                    | 0.41   | 0.51 | 1   | 0.24         | 0.78  | 1.53  | -48                 |
| Grass  | 17                    | 0.37   | 0.8  | 2.9 | 0.51         | 1.59  | 5.74  | -58                 |
| Grass  | 20                    | 0.31   | 0.75 | 2.4 | 0.46         | 1.45  | 4.71  | -58                 |
| Grass  | 10                    | 0.44   | 1.68 | 12  | 0.78         | 3.75  | 25.92 |                     |
| Grass  | 26                    | 0.5  | 0.73 | 1.2 | 0.44         | 0.95  | 1.56  |                     |
| Grass  | 38                    | 0.35   | 0.5  | 1.2 | 0.30         | 0.86  | 2.04  |                     |
| Grass  | 32.6                  | 0.24   | 0.3  | 0.7 | 0.14         | 0.52  | 1.26  |                     |
| Grass  | 32.8                  | 0.25   | 0.46 | 1.2 | 0.30         | 0.81  | 2.04  |                     |
| Grass  | 31.2                  | 0.18   | 0.37 | 1.7 | 0.24         | 0.77  | 3.44  |                     |
| Grass  | 59.8                  | 0.19   | 0.36 | 1.1 | 0.23         | 0.68  | 2.08  |                     |
| Grass  | 50.8                  | 0.21   | 0.31 | 0.7 | 0.19         | 0.51  | 1.14  |                     |
| Grass  | 8.2                   | 0.22   | 0.57 | 1.9 | 0.34         | 1.11  | 3.72  |                     |
| Grass  | 10.6                  | 0.24   | 0.69 | 2.5 | 0.39         | 1.37  | 4.87  |                     |
| Grass  | 11                    | 0.13   | 0.36 | 1.2 | 0.21         | 0.70  | 2.36  |                     |
| Grass  | 46                    | 0.11   | 0.36 | 1.3 | 0.19         | 0.71  | 2.53  |                     |
| Forest | 18                    | 0.26   | 0.44 | 1   | 0.29         | 0.75  | 1.75  | -60                 |
| Forest | 10.5                  | 0.26   | 0.36 | 0.8 | 0.21         | 0.58  | 1.24  | -62                 |

## REFERENCES

- Ahmed, S. and Carpenter, P.J., 2003. Geophysical response of filled sinkholes, soil pipes and associated bedrock fractures in thinly mantled karst, east-central Illinois. *Environmental Geology*, 44: 705-716.
- Anderson, M. and Burt, T.P., 1982. Throughflow and pipe monitoring in the humid temperate environment. In: R. Bryan and A. Yair (Editors), *Badland Geomorphology and Piping*. GEO Books, Norwich, England, pp. 337-355.
- Anderson, W.H. and Barron, L.S., 1995. High-carbonate, low-silica, high-calcium stone in the High Bridge Group (Upper Ordovician) Mason County, North-Central Kentucky. *Information Circular 53*, Kentucky Geological Survey, Lexington, Ky., 33 pp.
- Ahnert, F., 1994. Randomness in geomorphological process response models. In: M.J. Kirkby (Editor), *Process Models and Theoretical Geomorphology*. John Wiley and Sons, Chichester, England, pp. 3-21.
- Andrews, W.M.Jr., 2004. *Geologic Controls on Plio-Pleistocene Drainage Evolution of the Kentucky River in Central Kentucky*. PhD Thesis, University of Kentucky, Lexington, Ky., 216 pp.
- Arthur, M.A., Coltharp, G.G. and Brown, D.L., 1998. Effects of best management practices on forest streamwater quality in eastern Kentucky. *Journal of the American Water Resources Association*, 34(3): 481-495.
- Atkinson, T.C. and Smith, D.I., 1976. The erosion of limestones. In: T.D. Ford and C.H.D. Cullingford (Editors), *The Science of Speleology*. Academic Press, London, England, pp.151-177.
- Aubertin, G.M., 1971. Nature and extent of macropores in forest soils and their influence on subsurface water movement. *USDA Forest Service Research Paper, NE-192*, Upper Darby, Pa.
- Barnhisel, R.I., Bailey, H.H. and Matondang, S., 1971. Loess distribution in central and eastern Kentucky. *Soil Science Society of America Proceedings*, 35: 483-487.
- Bear, J., Tsang, C.-F. and de Marsily, G., 1993. *Flow and Contaminant Transport in Fractured Rock*. Academic Press, Inc., San Diego, 560 pp.
- Bell, M. and Limbrey, S. (Editors), 1982. *Archaeological Aspects of Woodland Ecology*. Symposia of the Association for Environmental Archaeology No. 2. B.A.R. International Series 146, Oxford, England.
- Betson, R.P., 1964. What is watershed runoff? *Journal of Geophysical Research*, 69: 1541-1552.
- Birkeland, P.W., 1984. *Soils and Geomorphology*. Oxford University Press, Oxford, 372 pp.
- Black, D.F.B., Cressman, E.R. and MacQuown, W.C.J., 1965. The Lexington limestone (middle Ordovician) of central Kentucky. *Geological Survey Bulletin 1224-C*. United States Department of the Interior, Washington, D.C., 29 pp.
- Boardman, J., 1993. The sensitivity of downland arable land to erosion by water. In: D.S.G. Thomas and R.J. Allison (Editors), *Landscape Sensitivity*. John Wiley and Sons Ltd, New York, pp. 211-228.
- Bogli, A., 1989. *Karst Hydrology and Physical Speleology*. Springer, Berlin.
- Bond, B.J., Jones, J.A., Moore, G., Phillips, N., Post, D., McDonnell, J.J., 2002. The zone of vegetation influence on baseflow revealed by diel patterns of streamflow and vegetation water use in a headwater basin. *Hydrological Processes*, 16: 1671-1677.
- Bowden, W.B., Fahey, B.D., Ekanayake, J. and Murray, D.L., 2001. Hillslope and wetland hydrodynamics in a tussock grassland, South Island, New Zealand. *Hydrological Processes*, 15: 1707-1730.
- Brady, N.C. and Weil, R.R., 1996. *The Nature and Properties of Soils*. Prentice Hall, Upper Saddle River, New Jersey, 740 pp.



- Brooks, K. and V., 2003. Personal interview, Bowman's Bend, Ky.
- Brooks, K., 2005. Personal Interview, Bowman's Bend, Ky.
- Brown, L., 1997. Grasslands. National Audubon Society Nature Guides. Alfred A. Knopf, New York, N.Y., 606 pp.
- Brown, V.A., McDonnell, J.J., Burns, D.A. and Kendall, C., 1999. The role of event water, a rapid shallow flow component, and catchment size in summer stormflow. *Journal of Hydrology*, 217: 171-190.
- Bryan, R.B. and Jones, J.A.A., 1997. The significance of soil piping processes: inventory and prospect. *Geomorphology*, 20: 209-218.
- Bull, L.J. and Kirkby, M.J., 1997. Gully processes and modelling. *Progress in Physical Geography*, 21(3): 354-374.
- Bull, P.A. and Laverty, M., 1982. Observations on phytokarst. *Zeitschrift fur Geomorphologie*, 26(4): 437-457.
- Burch, G.J., Bath, R.K., Moore, I.D. and O'Loughlin, E.M., 1987. Comparative hydrological behaviour of forested and cleared catchments in southeastern Australia. *Journal of Hydrology*, 90: 19-42.
- Burt, J.E. and Barber, G.M., 1996. *Elementary Statistics for Geographers*, 2nd Ed. The Guilford Press, New York, 640 pp.
- Burt, T.P., 1992. The hydrology of headwater catchments. In: P. Calow (Editor), *The Rivers Handbook, Hydrological and Ecological Principles*. Blackwell Scientific Publications, Oxford, pp. 3-29.
- Burt, T.P., 2001. Integrated management of sensitive catchment systems. *Catena*, 42: 275-290.
- Burt, T.P. and Swank, W.T., 1992. Flow frequency responses to hardwood-to-grass conversion and subsequent succession. *Hydrological Processes*, 6: 179-188.
- Byrnes, W.R. and Kardos, L.T., 1963. Hydrologic characteristics of three soils supporting natural hardwoods, planted red pine, and old field plant communities. *Soil Science Society of America Proceedings*, 27: 468-473.
- Cambridge Department of Geography, 2004. Loss On Ignition Physical Geography lab protocol. University of Cambridge, Cambridge, UK. [Online WWW]. Available URL: "<http://www-labs.geog.cam.ac.uk/protocols/>" [last accessed 12/5/2005].
- Campbell, J.J.N., 1980. Present and Presettlement Forest Conditions in the Inner Bluegrass of Kentucky. PhD dissertation Thesis, University of Kentucky, Lexington, Kentucky, 208 pp.
- Canton, Y., Domingo, F., Sole-Benet, A. and Puigdefabregas, J., 2002. Influence of soil-surface types on the overall runoff of the Tabernas badlands (south-east Spain): field data and model approaches. *Hydrological Processes*, 16: 2621-2643.
- Carey, D.I. and Stickney, J.F., 2001. *Ground-Water Resources of Garrard County, Kentucky*. Kentucky Geological Survey, University of Kentucky, Lexington, Ky., 25 pp.
- Casper, B.B., Schenk, H.J., and Jackson, R.B., 2003. Defining a plant's belowground zone of influence. *Ecology* 84(9): 2313-2321.
- Challinor, D., 1968. Alteration of surface soil characteristics by four tree species. *Ecology*, 49(2): 286-290.
- Chaplot, V. and Walter, C., 2003. Subsurface topography to enhance the prediction of the spatial distribution of soil wetness. *Hydrological Processes*, 17: 2567-2580.
- Cheng, J.D., Lin, L.L. and Lu, H.S., 2002. Influences of forests on water flows from headwater watersheds in Taiwan. *Forest Ecology and Management*, 165: 11-28.
- Clemens, T., Huckinghaus, D., Liedl, R. and Sauter, M., 1999. Simulation of the development of karst aquifers: role of the epikarst. *International Journal of Earth Sciences*, 88: 157-162.
- Clothier, B.E., 2002. Rapid and far-reaching transport through structured soils. *Hydrological Processes*, 16: 1321-1323.

- Conacher, A.J. and Dalrymple, J.B., 1977. The nine unit land surface model: An approach to pedogeomorphic research. *Geoderma*, 18: 1-154.
- Conkin, J.E. and Dasari, M.R., 1986. Capitol Metabentonite in the Trenton Curdsville Limestone of central Kentucky, University of Louisville, Louisville, Ky. 15 pp.
- Cooley, T., 2002. Geological and geotechnical context of cover collapse and subsidence in mid-continent US clay-mantled karst. *Environmental Geology*, 42: pp. 469-475.
- Crabtree, K., 1982. Evidence for the Burren's forest cover. In: M. Bell and S. Limbrey (Editors), *Archaeological Aspects of Woodland Ecology*. Symposia of the Association for Environmental Archaeology No. 2. BAR International Series 146, Oxford, England, pp. 105-113.
- Cressman, E.R. and Hrabar, S.V., 1970. Geologic map of the Wilmore quadrangle, central Kentucky. U.S. Geological Survey, Washington, D.C.
- Currens, J.C., 2002. Changes in groundwater quality in a conduit-flow-dominated karst aquifer, following BMP implementation. *Environmental Geology*, 42: 525-531.
- Daniels, R.B. and Hammer, R.D., 1992. *Soil Geomorphology*. John Wiley and Sons, Inc., New York, 236 pp.
- Daoxian, Y., 1993. Environmental change and human impact on karst in southern China. In: P.J. Williams (Editor), *Karst Terrains: Environmental Changes and Human Impact*. Springer-Verlag, Cremlingen-Destedt, Germany, pp. 99-107.
- Day, P.R., 1965. Particle fractionation and particle-size analysis. In: C.A. Black (Editor), *Methods of soil analysis, Part I. Agronomy 9*. American Society of Agronomy, Inc., Madison, Wisconsin, pp. 545-567.
- Daily climatological data, 1925-2005, Dix Dam and Burgin Dix Dam, Ky. NOAA National Climate Data Center. <http://lwf.ncdc.noaa.gov/oa/climate>. Accessed 5/16/05 and 10/23/05.
- Decagon Device, Inc., 2005. Pullman, Wa. [Online WWW]. Available URL: "<http://www.decagon.com>" [last accessed 12/5/2005].
- Deike, R.G., 1969. Relations of jointing to orientation or solution cavities in limestones of central Pennsylvania. *American Journal of Science*, 267: 1230-1248.
- Dekker, L.W., 1998. *Moisture Variability Resulting From Water Repellency in Dutch Soils*. Doctoral Thesis. Wageningen Agricultural University, The Netherlands, 240 pp.
- Delcourt, P.A., Delcourt, H.R., Ison, C.R., Sharp, W., E. and Henderson, A.G., 1999. *The Story of Cliff Palace Pond, Jackson County, Ky*. Ed. Series No.4, Ky. Archaeological Survey, Ky. Heritage Council, Lexington, Ky.
- Drew, D.P., 1982. Environmental archaeology and karstic terrains: the example of the Burren, Co. Claire, Ireland. In: M. Bell and S. Limbrey (Editors), *Archaeological Aspects of Woodland Ecology*, Symposia of the Association for Environmental Archaeology No. 2. B.A.R., Oxford, England, pp. 115-127.
- Drew, D.P., 1983. Accelerated soil erosion in a karst area: the Burren, western Ireland. *Journal of Hydrology*, 61: 113-124.
- Dreybrodt, W., 1990. The role of dissolution kinetics in the development of karst aquifers in limestone: a model simulation of karst evolution. *The Journal of Geology*, 98(5): 639-655.
- Dreybrodt, W., 1996. Principles of early development of karst conduits under natural and man-made conditions revealed by mathematical analysis of numerical models. *Water Resources Research*, 32(9): 2923-2935.
- Dunne, T., 1978. Field studies of hillslope flow processes. In: M.J. Kirkby (Editor), *Hillslope Hydrology*. John Wiley and Sons, Chichester, pp. 227-294.
- Dunne, T. and Black, R.D., 1970. Partial are contributions to storm runoff in a small New England watershed. *Water Resources Research*, 6: 1296-1311.

- Egerton-Warbuton, L.M., Graham, R.C., and Hubbert, K.R., 2003. Spatial variability in mycorrhizal hyphae and nutrient and water availability in a soil-weathered bedrock profile. *Plant and Soil* 249: 331-342.
- Eisenbeer, H., 2001. Hydrologic flowpaths in tropical rainforest soils - a review. *Hydrological Processes*, 15: 1751-1759.
- Ela, S.D., Gupta, S.C. and Rawls, W.J., 1992. Macropore and surface seal interactions affecting water infiltration into soil. *Soil Science Society America Journal*, 56: 714-721.
- Elam, A.B., 1973. Meteorological drought in Kentucky 1929-71. University of Kentucky Collections, Agricultural Expansion Station Progress Report 209. 20 pp.
- Elvrum, C.D., 1994. Relationship of Fracture Traces and Sinkholes to Stratigraphy and Groundwater in the Inner Bluegrass Karst Region, Kentucky. Master's Thesis, University of Kentucky, Lexington, Kentucky, 138 pp.
- Embleton, C. and Thornes, J.B., 1979. Sub-surface processes. In: C. Embleton and J. Thornes (Editors), *Process in Geomorphology*. John Wiley and Sons, New York, pp. 187-205.
- Ford, D.C. and Drake, J.J., 1982. Spatial and temporal variations in karst solution rates: the structure of variability. In: C.E. Thorn (Editor), *Space and Time in Geomorphology*. George Allen and Unwin, London, pp. 147-170.
- Ford, D.C. and Williams, P.W., 1989. *Karst Geomorphology and Hydrology*. Unwin Hyman, London, 601 pp.
- Fujieda, M., Kudoh, T., de Cicco, V. and de Calvarcho, J.L., 1997. Hydrological processes at two subtropical forest catchments: the Sierra do Mar, Sao Paulo, Brazil. *Journal of Hydrology*, 196: 26-46.
- Gabrovsek, F. and Dreybrodt, W., 2001. A model of the early evolution of karst aquifers in limestone in the dimensions of length and depth. *Journal of Hydrology*, 240: 206-224.
- Gagarina, E.I., 1968. Weathering of calcareous rock debris in soil. *Soviet Soil Science*, 7: 1300-1307.
- Gaiser, R.N., 1952. Root channels and roots in forest soils. *Soil Science Society Proceedings*, 16(1): 62-65.
- Gams, I., Nicod, J., Julian, M., Anthony, E. and Sauro, U., 1993. Environmental change and human impacts on the Mediterranean karsts of France, Italy and the Dinaric region, *Karst Terrains: Environmental Changes and Human Impact*. Catena-Verlag, Cremlingen-Destedt, Germany, pp. 59-98.
- Gardner, W.R., 1958. Some steady state solutions of unsaturated moisture flow equations with application to evaporation from a water table. *Soil Science*, 85: 228-232.
- Gee, G.W. and Bauder, J.W., 1986. Particle-size Analysis. In: A. Klute (Editor), *Methods of soil analysis Part 1 Physical and Mineralogical Methods*, 2nd Ed. Soil Science Society of America, Inc., Madison, Wisconsin, pp. 383-411.
- Gersper, P.L. and Holwaychuk, N., 1971. Some effects of stem flow from forest canopy trees on chemical properties of soils. *Ecology*, 52: 691-702.
- Green, A.J., 1978. Particle-size analysis. In: J.A. McKeague (Editor), *Manual on Soil Sampling and Methods of Analysis*, 2nd Edition. Canadian Society of Soil Science, Ottawa, pp. 4-29.
- Grossnickle, E.A., 1985. Tempestites and depositional interpretations of the middle Ordovician Curdsville Limestone of central Kentucky. Master of Science Thesis, University of Kentucky, Lexington, Ky., 106 pp.
- Groves, C.G. and Howard, A.D., 1994a. Early development of karst systems 1. Preferential flow path enlargement under laminar flow. *Water Resources Research*, 30(10): 2837-2846.
- Groves, C.G. and Howard, A.D., 1994b. Minimum hydrochemical conditions allowing limestone cave development. *Water Resources Research*, 30(3): 607-615.
- Gunn, J., 1981. Hydrological processes in karst depressions. *Zeitschrift fur Geomorphologie*, 25(3): 313-331.

- Gunn, J., 1983. Point-recharge of limestone aquifers - a model from New Zealand karst. *Journal of Hydrology*, 61: 19-29.
- Gutierrez, M., Sancho, C., Benito, G., Sirvent, J. and Desir, G., 1997. Quantitative study of piping processes in badland areas of the Ebro Basin, NE Spain. *Geomorphology*, 20: 237-253.
- Gyssels, G. and Poesen, J., 2003. The importance of plant root characteristics in controlling concentrated flow erosion rates. *Earth Surface Processes and Landforms*, 28: 371-384.
- Hagee, J., 2000-2004. A detailed history of High Bridge, Ky. [Online WWW]. Available URL: <http://www.worldtimezone.com/railtrail/highbridge/> [Accessed 11/11/2005].
- Halihan, T., Wicks, C.M. and Engeln, J.F., 1998. Physical response of a karst drainage basin to flood pulses: example of the Devil's Icebox cave system (Missouri, USA). *Journal of Hydrology*, 204: 24-36.
- Hamilton, D.K., 1946. Some solutional features of the limestone near Lexington, Kentucky. Master of Arts Thesis, University of Kentucky, Lexington, Ky., 36 pp.
- Harvey, A.M., 2001. Coupling between hillslopes and channels in upland fluvial systems: Implications for landscape sensitivity, illustrated from the Howgill Fells, northwest England. *Catena*, 42: 225-250.
- Heede, B.H., 1975. Stages of development of gullies in the West, Proc. Sediment-Yield Workshop. U.S. Dept. Agric., Oxford, Mississippi, 11-1972, pp. 285.
- Hein, O., Lotter, A.F. and Lemcke, G., 2001. Loss on ignition as a method for estimating organic and carbonate content in sediments: reproducibility and comparability of results. *Journal of Paleolimnology*, 25: 101-110.
- Herak, M., 1972. Karst of Yugoslavia. In: M. Herak and V.T. Stringfield (Editors), *Karst. Important Karst Regions of the Northern Hemisphere*. Elsevier Publishing Co., Amsterdam, pp. 24-83.
- Hewlett, J.D., 1961. Watershed management, report for 1961 Southeastern Forest Experiment Station. U.S. Forest Service, Asheville, North Carolina, pp. 62-66.
- Hewlett, J.D., 1982. *Principles of Forest Hydrology*. The University of Georgia Press, Athens, Georgia, 176 pp.
- Hewlett, J.D. and Hibbert, A.R., 1967. Factors affecting the response of small watersheds to precipitation in humid areas, *Proceedings of the First International Symposium on Forest Hydrology*, pp. 253-275.
- Hinsinger, P., Barros, O.N.F., Benedetti, M.F., Noack, Y. and Callot, G., 2001. Plant-induced weathering of a basaltic rock: Experimental evidence. *Geochimica et Cosmochimica Acta*, 65(1): 13-152.
- Holmes, J.W. and Colville, J.S., 1970. Grassland hydrology in a karstic region of southern Australia. *Journal of Hydrology*, 10: 38-58.
- Hopmans, J.W., Hendrickx, J.M.H. and Selker, J.S., 1999. Emerging Measurement Techniques for Vadose Zone Characterization. In: M.B. Parlange and J.W. Hopmans (Editors), *Vadose Zone Hydrology, Cutting Across Disciplines*, pp. 279-316.
- Howard, A.D. and Groves, C.G., 1995. Early development of karst systems 2. Turbulent flow. *Water Resources Research*, 31(1): 19-26.
- Huff, W.D., 1963. A Study of Middle Ordovician K-Bentonites in Kentucky and Southern Ohio. PhD Dissertation Thesis, University of Cincinnati, Cincinnati, 120 pp.
- Huggett, R.J., 1985. *Earth Surface Systems*. Springer-Verlag, Berlin, 270 pp.
- Huggett, R.J., 1997. *Environmental Change, The evolving ecosphere*. Routledge, New York, 378 pp.
- Hussen, A.A. and Warrick, A.W., 1995. Tension infiltrometers for the measurement of vadose zone hydraulic properties. In: L.G. Wilson, L. Everett, G. and S.J. Cullen

- (Editors), Handbook of Vadose Zone Characterization and Monitoring. Lewis Publishers, Boca Raton, Fl., pp. 189-201.
- Jackson, R.B., Moore, L.A., Hoffman, W.A., Pockman, W.T. and Linder, C.R., 1999. Ecosystem rooting depth determined with caves and DNA. Proc. Nat. Acad. Sci. USA, 96(Ecology): 11387-11392.
- Jackson, R.B., Schenk, H.J., Jobbagy, E.G., Canadell, J., Colello, G.D., Dickinson, R.E., Field, C.B., Friedlingstein, P., Heimann, M., Hibbard, K., Kicklighter, D.W., Kleidon, A., Neilson, R.P., Parton, W.J., Sala, O.E., Sykes, M.T., 2000. Belowground consequences of vegetation change and their treatment in models. Ecological Applications, 10(2): 470-483.
- Jacobson, R.B., 1995. Spatial controls on patterns of land-use induced stream disturbance at the drainage-basins scale--an example from gravel-bed streams of the Ozark Plateaus, Missouri, Natural and Anthropogenic Influences in Fluvial Geomorphology. American Geophysical Union, pp. 219-239.
- Jacobson, R.B. and Pugh, A.T., 1996. Riparian vegetation controls on the spatial pattern of stream-channel instability, Little Piney Creek, Missouri. U.S. Geological Survey Water-Supply Paper 2494, 62 pp.
- Jardine, P.M., Wilson, G.V. and Luxmoore, R.J., 1990. Unsaturated solute transport through a forest soil during rain storm events. Geoderma, 46: 103-118.
- Jennings, J.N., 1983. Karst landforms. American Scientist, 71: 578-586.
- Jennings, J.N., 1985. Karst Geomorphology. Basil Blackwell, Inc., New York, New York.
- Jessamine County Kentucky River Task Force, 2005. Kentucky River Guidebook, [Online WWW]. Available URL: <http://www.jessamineco.com/tourism/guidebook/guidebook3.htm> [Accessed 11/13/2005].
- Johnson, D.L., 1994. Reassessment of early and modern soil horizon designation frameworks and associated pedogenetic processes: Are midlatitude A E B-C horizons equivalent to tropical M S W horizons? Soil Science (Trends in Agricultural Science), 2: 77-91.
- Jones, D. L., 1998. Organic acids in the rhizosphere – a critical review. Plant and Soil 205: 25-44.
- Jones, J.A., 1997. The role of natural pipeflow in hillslope drainage and erosion: extrapolation from the Maesnant data. Physical Chemistry of the Earth, 22: 303-308.
- Julian, H.E. and Young, S.C., 1995. Conceptual model of groundwater flow in a mantled karst aquifer and effects of the epikarst zone. In: B.F. Beck (Editor), Karst Geohazards, Engineering and Environmental Problems in Karst Terrane. A.A.Balkema, Rotterdam, pp. 131-139.
- Kaddah, M.T., 1974. The hydrometer method for detailed particle-size analysis: 1. Graphical interpretation of hydrometer readings and test of method. Soil Science, 118(2): 102-108.
- Kaufmann, G. and Braun, J., 1999. Karst aquifer evolution in fractured rocks. Water Resources Research, 35(11): 3223-3238.
- Kaufmann, G. and Braun, J., 2000. Karst aquifer evolution in fractured, porous rocks. Water Resources Research, 36(6): 1381-1391.
- Kendall, C., McDonnell, J.J. and Gu, W., 2001. A look inside 'black box' hydrograph separation models: a study at the Hydrohill catchment. Hydrological Processes, 15: 1877-1902.
- Kirkby, M.J., 1994. Threshold and instability in stream head hollows: a model of magnitude and frequency for wash processes. In: M.J. Kirkby (Editor), Process Models and Theoretical Geomorphology. John Wiley and Sons, Chichester, England, pp. 295-314.
- Kishel, H.F. and Gerla, P.J., 2002. Characteristics of preferential flow and groundwater discharge to Shingobee Lake, Minnesota, USA. Hydrological Processes, 16: 1921-1934.
- Klimchouk, A., 2000. The formation of epikarst and its role in vadose speleogenesis. In:

- A.B. Klimchouk, D.C. Ford, A.N. Palmer and W. Dreybrodt (Editors), *Speleogenesis, Evolution of Karst Aquifers*. National Speleological Society, Inc., Huntsville, Alabama, pp. 91-99.
- Klimchouk, A. and Ford, D.C., 2000a. Lithologic and structural controls of dissolutional cave development. In: A. Klimchouk, D.C. Ford, A.N. Palmer and W. Dreybrodt (Editors), *Speleogenesis, Evolution of Karst Aquifers*. National Speleological Society, Inc., Huntsville, Al., pp. 54-64.
- Klimchouk, A. and Ford, D.C., 2000b. Types of karst and evolution of hydrogeologic setting. In: A. Klimchouk, D.C. Ford, A.N. Palmer and W. Dreybrodt (Editors), *Speleogenesis, Evolution of Karst Aquifers*. National Speleological Society, Inc., Huntsville, Alabama, pp. 45-53.
- Knapp, B., 1979. *Elements of Geographical Hydrology*. Leighton Park School, Reading, Great Britain.
- Knox, J.C., 2001. Agricultural influence on landscape sensitivity in the Upper Mississippi River Valley. *Catena*, 42: 193-224.
- Kochenderfer, J.N., 1973. Root distribution under some forest types native to West Virginia. *Ecology*, 54(2): 445-448.
- Kuhnhenh, G.L. and Haney, D.C., 1986. Middle Ordovician High Bridge Group and Kentucky River fault system in central Kentucky, *Geological Society of America Centennial Field Guide - Southeastern Section*, pp. 25-29.
- LaMoreaux, P., Wilson, B.M. and Memon, B.A., 1984. *Guide to the hydrology of carbonate rocks*. UNESCO, Paris, France, 347 pp.
- Landeweert, R., Hoffland, E., Finlay, R.D., Kuyper, T.W., and van Breeman, N., 2001. Linking plants to rocks: ectomycorrhizal fungi mobilize nutrients from minerals. *Trends in Ecology and Evolution* 16(5): 248-253.
- Lastennet, R. and Mudry, J., 1997. Role of karstification and rainfall in the behavior of a heterogeneous karst system. *Environmental Geology*, 32(2): 114-123.
- L.-F.U.C.G. (Lexington-Fayette Urban County Government), 2005. *Stormwater Manual*, Lexington-Fayette Co., Kentucky.
- Likens, G.E., Bormann, F.H., Johnson, N.M., and Pierce, R.S., 1967. The calcium, magnesium, potassium and sodium budgets for a small forested ecosystem. *Ecology* 48(5): 773-785.
- Luxmoore, R.J., Jardine, P.M., Wilson, G.V., Jones, J.R. and Zelazny, L.W., 1990. Physical and chemical controls of preferred path flow through a forested hillslope. *Geoderma*, 46: 139-154.
- MacQuown, W.C.J., 1967. Factors controlling porosity and permeability in the Curdsville member of the Lexington limestone. Research Report No. 7, University of Kentucky Water Resources Institute, Lexington, Kentucky. 80 pp
- McCarthy, B.C., 1997. *Lab Protocols for the Testing of Eastern Deciduous Forest Soils*. Department of Environmental and Plant Biology, Ohio University, Athens, Ohio. [Online WWW]. Available URL: "<http://www.plantbio.ohiou.edu/epb/soils.soils.htm>" [last accessed 5/10/2005].
- McGlynn, B.L., McDonnell, J.J. and Brammer, D.D., 2002. A review of the evolving perceptual model of hillslope flowpaths at the Maimai catchments, *New Zealand Journal of Hydrology*, 257: 1-26.
- McIntosh, J., McDonnell, J.J. and Peters, N.E., 1999. Tracer and hydrometric study of preferential flow in large undisturbed soil cores from the Georgia Piedmont, USA. *Hydrological Processes*, 13: 139-155.
- McKeague J.A., 1978. Bulk density and particle density. In: J.A. McKeague (Editor), *Manual on Soil Sampling and Methods of Analysis*, 2nd Edition. Canadian Society of Soil Science, Ottawa, pp 29-38.

- McKnight, T.L. and Hess, D., 2002. *Physical Geography, A Landscape Appreciation*. Prentice Hall, Upper Saddle River, New Jersey, 629 pp.
- McQuilkin, W.E., 1935. Root development of pitch pine, with some comparative observations on short-leaf pine. *Journal of Agricultural Research*, 51: 983-1016.
- McRae, S.G., 1988. *Practical Pedology Studying Soils in the Field*. John Wiley and Sons, Chichester, England, 253 pp.
- Midwest Regional Climate Center, Cooperative Illinois State Water Survey and National Climate Data Center (NCDC) program [Online WWW]. Available URL: [http://mcc.sws.uiuc.edu/climate\\_midwest/mwclimate\\_data\\_summaries.htm#](http://mcc.sws.uiuc.edu/climate_midwest/mwclimate_data_summaries.htm#). [Accessed 11/11/2005].
- Mitchell, P., 1988. The influences of vegetation, animals and micro-organisms on soil processes. In: H.A. Viles (Editor), *Biogeomorphology*. Basil Blackwell, Oxford, pp. 43-81.
- Miyashita, H., Sakura, Y., Shindo, S. and Nishio, K., 1994. A study on the mechanism of infiltration and runoff in a small forest watershed, Inuyama, Central Japan; the role of humic layer in hydrologic cycle, *Proceedings of the International Symposium on Forest Hydrology*, Tokyo, Japan, pp. 323-330.
- Mizuyama, T., Kosugi, K.i., Sato, I. and Kobashi, S., 1994. Runoff through underground pipes in hollows, *Proceedings of the International Symposium on Forest Hydrology*, Tokyo, Japan, pp. 233-240.
- Montgomery, D.R. and Dietrich, W.E., 1994. Landscape Dissection and Drainage Area-Slope Thresholds. In: M.J. Kirkby (Editor), *Process Models and Theoretical Geomorphology*. John Wiley and Sons, Chichester, England, pp. 221-246.
- Moulton, K.L. and Berner, R.A., 1999. Quantitative effects of plants on weathering forest sinks for carbon. In H. Armannsson (ed.) *Geochemistry of the Earth's Surface*, Balkema, Rotterdam.
- National Research Council, Commission on Geosciences, Environment, and Resources, Panel on Conceptual Models of Flow and Transport in the Fractured Vadose Zone, 2001. *Conceptual Models of Flow and Transport in the Fractured Vadose Zone*. National Academy Press, Washington, D.C., 373 pp.
- Nature Conservancy Kentucky River Palisades Ecosystem Project [Online WWW]. Available URL: <http://nature.org/wherewework/northamerica/states/kentucky/preserves>. [Accessed 11/11/2005].
- Navar, J., Turton, D.J. and Miller, E.L., 1994. Observed and estimated soil moisture content of an experimental forest plot of Arkansas, *Proceedings of the International Symposium on Forest Hydrology*. University of Tokyo, Tokyo, Japan, pp. 99-106.
- Neuman, S.P., 2005. Trends, prospects and challenges in quantifying flow and transport through fractured rocks. *Hydrogeology Journal*, 13: 124-147.
- Noguchi, S., Tsuboyama, Y., Sidle, R.C. and Hosoda, I., 1999. Morphological characteristics of macropores and the distribution of preferential flow pathways in a forested slope segment. *Soil Science Society of America Journal*, 63: 1413-1423.
- Official Soil Series Descriptions (OSD), USDA National Resources Conservation Service (NRCS) Technical Resources [Online WWW]. Available URL: ["http://soils.usda.gov/technical/classification/"](http://soils.usda.gov/technical/classification/) [last accessed 12/12/2005].
- Onda, Y., Komatsu, Y., Tsujimura, M. and Fujihara, J.-i., 2001. The role of subsurface runoff through bedrock on storm flow generation. *Hydrological Processes*, 15: 1693-1706.
- Onset Computer Corporation, 2005. Bourne, MA [Online WWW]. Available URL: ["http://www.onsetcomp.com"](http://www.onsetcomp.com) [last accessed 12/5/2005].
- Owoputi, L.O. and Stolte, W.J., 2001. The role of seepage in erodibility. *Hydrological Processes*, 15: 13-22.
- Pagano, R.R., 1994. *Understanding Statistics in the Behavioral Sciences*, 4th Ed. West Publishing Company, Minneapolis/St. Paul, 498 pp.

- Palmer, A.N., 1991. Origin and morphology of limestone caves. *Geological Society of America Bulletin*, 103: 1-21.
- Palmer, A.N., 2002. Karst in Paleozoic rocks: how does it differ from Florida? In: J.B. Martin, C.M. Wicks and I.D. Sasowsky (Editors), *Hydrogeology and Biology of Post-Paleozoic Carbonate Aquifers*. Karst Waters Institute, Inc., Gainesville, Florida, pp. 185-191.
- Panno, S.V., Wiebel, C.P., Heigold, P.C. and Reed, P.C., 1994. Formation of regolith-collapse sinkholes in southern Illinois: Interpretation and identification of associated buried cavities. *Environmental Geology*, 23: 214-220.
- Paton, T.R., Humphreys, G.S. and Mitchell, P.B., 1995. *Soils, A New Global View*. New Haven, Yale University Press, 213 pp.
- Penn State Cooperative Extension, Geospatial Technology Program (GTP) Land Analysis Lab, 2005. Using Soils Data Tutorial. [Online WWW]. Available URL: "<http://lal.cas.psu.edu/software/index.htm>" [last accessed 12/11/2005].
- Perrin, J., Jeannin, P.-Y. and Zwahlen, F., 2003. Epikarst storage in a karst aquifer: a conceptual model based on isotopic data, Milandre test site, Switzerland. *Journal of Hydrology*, 279: 106-124.
- Peterson, E.W., Davis, R.K., Brahana, J.V. and Orndorff, H.A., 2002. Movement of nitrate through regolith covered karst terrane, northwest Arkansas. *Journal of Hydrology*, 256: 35-47.
- Pettapiece, W.W., 1969. The forest-grassland transition, Pedology and Quaternary research: symposium held at Edmonton. National Research Council of Canada, Edmonton, Alberta, pp. 103-113.
- Petts, G.E. and Amoros, C., 1996. *Fluvial Hydrosystems*. Chapman and Hall, London, 306 pp.
- Phillips, J.D., 1992a. The end of equilibrium? *Geomorphology*, 5: 195-201.
- Phillips, J.D., 1992b. Nonlinear dynamical systems in geomorphology: revolution or evolution. *Geomorphology*, 5: 219-229.
- Phillips, J.D., 1996. Deterministic complexity, explanation, and predictability in geomorphic systems. In: B.L. Rhoads and C.E. Thorn (Editors), *The Scientific Nature of Geomorphology: Proceedings of the 27th Binghamton Symposium in Geomorphology*. John Wiley and Sons Ltd., New York, pp. 315-335.
- Phillips, J.D., 1997a. A short history of a flat place: three centuries of geomorphic change in the Croatan National Forest. *Annals of the Association of American Geographers*, 87(2): 197-216.
- Phillips, J.D., 1997b. Humans as geological agents and the question of scale. *American Journal of Science*, 297(January): 98-115.
- Phillips, J.D., 1998. On the relations between complex systems and the factorial model of soil formation (with discussion). *Geoderma*, 86: 1-42.
- Phillips, J.D., 2000. Signatures of divergence and self-organization in soils and weathering profiles. *Journal of Geology*, 108: 91-102.
- Phillips, J.D., 2001a. The relative importance of intrinsic and extrinsic factors in pedodiversity. *Annals of the Association of American Geographers*, 9(14): 609-621.
- Phillips, J.D., 2001b. Contingency and generalization in pedology, as exemplified by texture-contrast soils. *Geoderma*, 102: 347-370.
- Phillips, J.D., 2002. Global and local factors in earth surface systems. *Ecological Modelling*, 149: 257-272.
- Phillips, J.D., 2003. Sources of nonlinearity and complexity in geomorphic systems. *Progress in Physical Geography*, 27(1): 1-23.
- Phillips, J.D., 2004. Divergence, sensitivity, and nonequilibrium in ecosystems. *Geographical Analysis*, 36(4): 369-383.
- Phillips, J.D. and Marion, D.A., 2004. Pedological memory in forest soil development. *Forest Ecology and Management*, 188: 363-380.



- Phillips, J.D., Martin, L.L., Nordberg, V.G. and Andrews, W.A., 2004. Divergent evolution in fluviokarst landscapes of central Kentucky. *Earth Surface Processes and Landforms*, 29: 799-819.
- Plagnes, V. and Bakalowicz, M., 2002. The protection of a karst water resource from the example of the Larzac karst plateau (south of France): a matter of regulations or a matter of process knowledge? *Engineering Geology*, 65: 107-116.
- Post, D.A. and Jones, J.A., 2001. Hydrologic regimes of forested, mountainous, headwater basins in New Hampshire, North Carolina, Oregon, and Puerto Rico. *Advances in Water Resources*, 24: 1195-1210.
- Prawito, P., 1996. Pedogenesis on Karst Toposequences of Kentucky. PhD Thesis, University of Kentucky, Lexington, Ky., 351 pp.
- Prosser, I.P., Dietrich, W.E. and Stevenson, J., 1995. Flow resistance and sediment transport by concentrated overland flow in a grassland valley. *Geomorphology*, 13: 71-86.
- Prosser, I.P. and Soufi, M., 1998. Controls on gully formation following forest clearing in a humid temperate environment. *Water Resources Research*, 34(12): 3661-3671.
- Reinhart, K.G., Eschner, A.R. and Trimble Jr., G.R., 1963. Effect on streamflow of four forest practices in the mountains of West Virginia, U.S. Forest Service Research Paper. USDA, Upper Darby, Pa., pp. 79.
- Ritter, E., Vesterdal, L. and Gundersen, P., 2003. Changes in soil properties after afforestation of former intensively managed soils with oak and Norway spruce. *Plant and Soil*, 249: 319-330.
- Robinson, D., Hodge, A. and Fitter, A., 2003. Constraints on the form and function of root systems. In: H. de Kroon and E.J.W. Visser (Editors), *Root Ecology*, Berlin, pp. 1-31.
- Rockwell, D.L., 2002. The influence of groundwater on surface flow erosion processes during a rainstorm. *Earth Surface Processes and Landforms*, 27: 495-514.
- Rowell, D.L., 1994. *Soil Science: Methods and Applications*. Longman Scientific and Technical, Essex, UK, 350 pp.
- Ruhe, R.V. and Walker, P.H., 1968. Hillslope models and soil formation. I. Open systems. *Transactions 9<sup>th</sup> International Congress of Soil Science*, 4: 551-560.
- Schoeneberger, P. and Amoozegar, A., 1990. Directional saturated hydraulic conductivity and macropore morphology of a soil-saprolite sequence. *Geoderma* 46: 31-49.
- Shimohammadi, A., Gish, T.J., Sadeghi, A. and Lehman, D.A., 1991. Theoretical representation of flow through soils considering macropore effect. In: T.J. Gish, Sadeghi, A. and Shirmohammadi, A. (Editors), *Preferential Flow*. Proceedings of the National Symposium 16-17 December 1991, Chicago, Illinois. American Society of Agricultural Engineers, St. Joseph, Michigan, pp. 233-243.
- Shirmohammadi, A. and Skaggs, R.W., 1985. Predicting infiltration for shallow water table soils with different surface covers. *Transactions of the American Society of Agricultural Engineers*, 28(6): 1829-1837.
- Sidele, R.C., Pearce, A.J. and L., O.L.C., 1985. *Hillslope Stability and Land Use*. American Geophysical Union, Washington, D.C., 140 pp.
- Sidele, R.C., Tsuboyama, Y., Noguchi, S. and Hosoda, I., 1994. Subsurface flow through the soil matrix and macropores: Results of tracer tests at Hitachi Ohta, Japan, Proceedings of the International Symposium on Forest Hydrology, Tokyo, Japan, pp. 225-232.
- Sidele, R.C., Tsuboyama, Y., Noguchi, S., Hosoda, I., Fujieda, M., Shimizu, T., 1995. Seasonal hydrologic response at various spatial scales in a small forested catchment, Hitachi Ohta, Japan. *Journal of Hydrology*, 168: 227-250.
- Sidele, R.C., Noguchi, S., Tsuboyama, Y. and Laursen, K., 2001. A conceptual model of preferential flow systems in forested hillslopes: evidence of self-organization. *Hydrological Processes*, 15: 1675-1692.

- Sikka, A.K., Samra, J.I., Sharda, V.N., Samraj, P. and Lakshmanan, V., 2003. Low flow and high flow responses to converting natural grassland into bluegum (*Eucalyptus globulus*) in Nigris watersheds of South India. *Journal of Hydrology*, 270: 12-26.
- Singer, M.J. and Munns, D.N., 1996. *Soils; an Introduction*. Prentice Hall, Upper Saddle River, New Jersey, 480 pp.
- Sklash, M.G., Stewart, M.K. and J., P.A., 1986. Storm runoff generation in humid headwater catchments 2. A case study of hillslope and low-order stream response. *Water Resources Research*, 22(8): 1273-1282.
- Smakhtin, V.U., 2002. Some early Russian studies of subsurface storm-flow processes. *Hydrological Processes*, 16: 2613-2620.
- Smith, R.T. and Atkinson, K., 1975. *Techniques in Pedology*. Elek Science, London, 213 pp.
- Smith, D.I., Atkinson, T.C. and Drew, D.P., 1976. The hydrology of limestone terrains. In: T.D. Ford and C.H.D. Cullingford (Editors), *The Science of Speleology*. Academic Press, London, pp. 179-212.
- Soil Conservation Service, 1972. Soil survey laboratory methods and procedures for collecting soil samples. Soil Survey Investigations Report No. 1, U.S. Department of Agriculture, Washington, D.C., 63 pp.
- Soil Measurement Systems, LLC., 2005. Tucson, Az. [Online WWW]. Available URL: "<http://www.soilmeasurement.com>" [last accessed 12/5/2005].
- Soil Survey Staff, Natural Resources Conservation Service, United States Department of Agriculture, Soil Survey Geographic (SSURGO) Database for Garrard and Lincoln Counties, Ky. [Online WWW]. Available URL: "<http://soildatamart.nrcs.usda.gov>" [last accessed 10/20/2005].
- Sokal, R.R. and Rohlf, F.J., 1997. *Biometry, The Principles and Practice of Statistics in Biological Research*. W.H. Freeman and Co., New York, N.Y., 887 pp.
- Spang, B., 2004. Water97\_v13.xla (version 1.3). Cheresources Online Eight Chemical Engineering Information. <http://www.cheresources.com/iapwsif97.shtml#addin> [last accessed 11/27/2005].
- Spyridakis, D.E., Chesters, G. and Wilde, S.A., 1967. Kaolinization of biotite as a result of coniferous and deciduous seedling growth. *Soil Sci. Soc. Amer. Proc.*, 31: 203-210.
- Srinivasan, M.S., Gburek, W.J. and Hamlett, J.M., 2002. Dynamics of stormflow generation - A hillslope-scale field study in east-central Pennsylvania, USA. *Hydrological Processes*, 16: 649-665.
- Stephens, D.B., 1996. *Vadose Zone Hydrology*. CRC Press, Inc., Lewis Publishers, New York, N.Y., 339 pp.
- Sterflinger, K., 2000. Fungi as geologic agents. *Geomicrobiology Journal* 17: 97-124.
- Stone, E.L. and Comerford, N.B., 1994. Plant and animal activity below the solum. *SSSA Special Publication*, 34: 57-74.
- Stone, E.L., and Kalisz, P.J., 1991. On the maximum extent of tree roots. *Forest Ecology and management* 46: 59-102.
- Stout, B.B., 1956. Studies of the root systems of deciduous trees. *Black Rock Forest Bulletin No. 15*. Harvard University, Cambridge, Massachusetts, 45 pp.
- Strafford, T.F., Jr., 1962. Features of Jointing in the Inner Bluegrass of Kentucky. Master of Science Thesis, University of Kentucky, Lexington, Ky., 72 pp.
- Sweeting, M.M., 1973. *Karst Landforms*. Columbia University Press, New York, New York, 362 pp.
- Swiechowicz, J., 2002a. The influence of plant cover and land use on slope-channel decoupling in a foothill catchment: a case study from the Carpathian foothills, southern Poland. *Earth Surface Processes and Landforms*, 27: 463-479.

- Swiechowicz, J., 2002b. Linkage of slope wash and sediment and solute export from a foothill catchment in the Carpatian foothills of south Poland. *Earth Surface Processes and Landforms*, 27: 1389-1413.
- Taborosi, D., 2002. Biokarst on a tropical carbonate island: Guam, Mariana Islands. *Theoretical and Applied Karstology*, 15: 73-91.
- Tan, K.H., 1996. *Soil Sampling, Preparation, and Analysis*. Marcel Dekker, Inc., New York, N.Y.
- Tani, M., 1997. Runoff generation processes estimated from hydrological observations on a steep forested hillslope with a thin soil layer. *Journal of Hydrology*, 200: 84--109.
- Taylor, C.J., 1992. *Ground-Water Occurrence and Movement Associated with Sinkhole Alignments in the Inner Bluegrass Karst Region of Central Kentucky*. Master of Science Thesis, University of Kentucky, Lexington, Kentucky.
- Teller, J.T. and Goldthwait, R.P., 1991. The Old Kentucky River: A major tributary to the Teays River, *Geology and Hydrogeology of the Teays-Mahomet Bedrock Valley System*. Geological Society of America, Boulder, Co., pp. 29-41.
- Teragina, T., Sakamoto, T. and Shirai, T., 2000. Morphology, structure, and flow phases in soil pipes developing in forested hillslope underlain by a Quaternary sand-gravel formation, Hokaido, northern main island in Japan. *Hydrological Processes*, 14: 713-726.
- Thomas, D.S.G. and Goudie, A., 2000. *The Dictionary of Physical Geography*. Blackwell Publishers Ltd, Oxford, 610 pp.
- Thomas, M.F., 2001. Landscape sensitivity in time and space - an introduction. *Catena*, 42: 83-98.
- Thornes, J.B., 1979. Fluvial processes. In: C. Embleton and J. Thornes (Editors), *Process in Geomorphology*. John Wiley and Sons, New York, pp. 384.
- Thornes, J.B., 1985. The ecology of erosion. *Geography*: 222-235.
- Thornes, J.B., 1990. *Vegetation and Erosion*. John Wiley and Sons, Chichester, England, 290 pp.
- Thrailkill, J., 1982. *Groundwater in the Inner Bluegrass Karst Region, Kentucky*. Research Report No.136, Water Resources Institute, University of Kentucky, Lexington, Kentucky. 105 pp.
- Thrailkill, J., 1984. Hydrogeology and environmental geology of the inner Bluegrass karst region, Kentucky, Field Guide for the Annual Meeting of the Southeastern and North Central Sections of the Geological Society of America, Lexington, Ky., 29 pp.
- Thrailkill, J. and Robl, T.L., 1981. Carbonate geochemistry of vadose water recharging limestone aquifers. *Journal of Hydrology*, 54: 195-208.
- Tindall, J.A., Kunkel, J.R. and Anderson, D.E., 1999. *Unsaturated Zone Hydrology for Scientists and Engineers*. Prentice Hall, Upper Saddle River, New Jersey, 624 pp.
- Trimble, S.W., 1988. The impact of organisms on overall erosion rates within catchments in temperate regions. In: H.A. Viles (Editor), *Biogeomorphology*. Basil Blackwell, Oxford, pp. 83-142.
- Trimble, S.W., 1990. Geomorphic effects of vegetation cover and management: Some time and space considerations in prediction of erosion and sediment yield. In: J.B. Thornes (Editor), *Vegetation and Erosion*. John Wiley and Sons, Chichester, England, pp. 55-65.
- Trimble, S., W., 1997. Stream channel erosion and change resulting from riparian forests. *Geology*, 25(5): 467-469.
- Trudgill, S.T., 1976a. Limestone erosion under soil. In: V. Panos (Editor), *Proceedings of the 6<sup>th</sup> International Congress of Speleology*. Academia, pp. 409-422.
- Trudgill, S.Y., 1976b. The erosion of limestones under soil and the long term stability of soil-vegetation systems on limestones. *Earth Surface Processes and Landforms*, 1: 31-41.
- Trudgill, S., 1985. Limestone geomorphology. In: K.M. Clayton (Editor), *Geomorphology Texts 8*. Longman, pp. 53-70.

- Tsuboyama, Y., Hosoda, I., Noguchi, S. and Sidle, R.C., 1994. Piezometric response in a zero-order basin, Hitachi Ohta, Japan.
- Turnage, K.M., Lee, S.Y., Foss, J.E., Kim, K.H. and Larsen, I.L., 1997. Comparison of soil erosion and deposition rates using radiocesium, RUSLE, and buried soils in dolines in East Tennessee. *Environmental Geology*, 29 (1/2): 1-10.
- Uchida, T., Kosugi, K. and Mizuyama, T., 1999. Runoff characteristics of pipeflow and effect of pipeflow on rainfall-runoff phenomena in a mountainous watershed. *Journal of Hydrology*, 222: 18-36.
- Uchida, T., Kosugi, K. and Mizuyama, T., 2001. Effects of pipeflow on hydrological process and its relation to landslide: a review of pipeflow studies in forested headwater catchments. *Hydrological Processes*, 15: 2151-2174.
- Van Stiphout, T.P.J., Van Lannen, H.A.J., Boersma, O.H. and Bouma, J., 1987. The effect of bypass flow and internal catchment of rain on the water regime in a clay loam grassland soil. *Journal of Hydrology*, 95: 1-11.
- Viles, H.A., 1984. Biokarst: review and prospect. *Progress in Physical Geography*, 8: 523-542.
- Viles, H.A., 1988. Organisms and karst geomorphology. In: H.A. Viles (Editor). Basil Blackwell, Oxford, pp. 265.
- Walker, P.H. and Ruhe, R.V., 1968. Hillslope models and soil formation. II. Closed systems. *Transactions 9<sup>th</sup> International Congress of Soil Science*, 4: 561-568.
- Wall, J.R.D. and Wilford, G.E., 1966. Two small-scale solution features of limestone outcrops in Sarawak, Malaysia. *Zeitschrift fur Geomorphologie*, 10: 91-94.
- Watson, P.V., 1982. Man's impact on the Chalklands: Some new pollen evidence. In: M. Bell and S. Limbrey (Editors), *Archaeological Aspects of Woodland Ecology*. Symposia of the Association for Environmental Archaeology No. 2. B.A.R. International Series 146, Oxford, England, pp. 75-91.
- Watts, W.A., 1979. Late Quaternary vegetation of central Appalachia and the New Jersey coastal plain. *Ecological Monographs*, 49(4): 427-466.
- Weiler, M. and McDonnell, J.J., 2004. Virtual experiments: a new approach for improving process conceptualization in hillslope hydrology. *Journal of Hydrology*, 285: 3-18.
- Weiler, M. and Naef, F., 2003. An experimental tracer study of the role of macropores in infiltration in grassland soils. *Hydrological Processes*, 17: 477-493.
- Whaley, P.W., 1964. A Petrographic Study of the Tyrone Limestone. Master of Science Thesis, University of Kentucky, Lexington, Ky., 45 pp.
- White, W.B., 1988. *Geomorphology and Hydrology of Karst Terrains*. Oxford University Press, New York, New York, 464 pp.
- White, W.B., 2002. Karst hydrology: recent developments and open questions. *Engineering Geology*, 65: 85-105.
- White, W.B. and White, E.L., 1995. Thresholds for soil transport and the long term stability of sinkholes. In: B.F. Beck (Editor), *Karst Geohazards Engineering and Environmental Problems in Karst Terrane*. A.A. Balkema, Rotterdam, pp. 73-78.
- Wierenga, P., J., 1995. Water and Solute Transport and Storage. In: L.G. Wilson, L. Everett, G. and S.J. Cullen (Editors), *Handbook of Vadose Zone Characterization and Monitoring*. Lewis Publishers, Boca Raton, Fl., pp. 41-60.
- Wijdenes, D.J.O. and Bryan, R., 2001. Gully-head erosion processes on a semi-arid valley floor in Kenya: a case study into temporal variation and sediment budgeting. *Earth Surface Processes and Landforms*, 26: 911-933.
- Wilkins, G.R., Delcourt, P.A., Delcourt, H.R., Harrison, F.W. and Turner, M.R., 1991. Paleoecology of central Kentucky since the last glacial maximum. *Quaternary Research*, 36: 224-239.
- Williams, G.P., 1997. *Chaos Theory Tamed*. Joseph Henry Press/National Academy Press, Washington, D.C., 499 pp.

- Williams, P.J., 1993. Environmental change and human impact on karst terrains: an introduction. In: P.J. Williams (Editor), *Karst Terrains: Environmental Changes and Human Impact*. Catena Verlag, Cremlingen-Destedt, Germany, pp. 1-19.
- Williams, P.W., 1966. Limestone pavements with special reference to Western Ireland. *Transactions of the Institute of British Geographers*, 40: 155-172.
- Williams, P.W., 1972. The analysis of spatial characteristics of karst terrains. In: R.J. Chorley (Editor), *Spatial Analysis in Geomorphology*. Harper and Row, New York, N.Y.
- Williams, P.W., 1983. The role of the subcutaneous zone in karst hydrology. *Journal of Hydrology*, J61: 45-67.
- Wilson, G.V., Jardine, P.M., Luxmoore, R.J. and Jones, J.R., 1990. Hydrology of a forested hillslope during storm events. *Geoderma*, 46: 119-138.
- Wooding, R.A., 1968. Steady infiltration from a shallow circular pond. *Water Resources Research*, 4: 1259-1273.
- Woods, A.J., Omernik, J.M., Martin, W. H., Pond, G.J., Andrews, W.M. Jr., Call, S.M., Comstock, J.A., Taylor, D.D., 2002. Ecoregions of Kentucky (color poster with map, descriptive text, summary tables, and photographs). U.S. Geological Survey (map scale 1:1,000,000), Reston, VA.
- Wyseure, G.C.L., Sattar, M.G.S., Adey, M.A. and Rose, D.A. 2005. Determination of unsaturated hydraulic conductivity in the field by a robust tension infiltrometer. Department of Agriculture and Environmental Science, University of Newcastle, UK. [Online WWW]. Available URL: "<http://www.agr.kuleuven.ac.be/facdid/guidow/Tensio.htm>" [last accessed 1/18/2005].
- Zambo, L. and Ford, D.C., 1997. Limestone dissolution processes in Beke doline, Aggtelek National Forest, Hungary. *Earth Surface Processes and Landforms*, 22: 531-543.
- Ziemer, R.R. and Lisle, T.E., 1998. Hydrology. In: R.J. Naiman and B.B. Bilby (Editors), *River Ecology Management: lessons from the Pacific coastal ecoregion*. Springer Co., New York, pp. 43-68.
- Zinke, P.J., 1962. The pattern of influence of individual forest trees on soil properties. *Ecology*, 43(1): 130-133.
- Zhu, X.-Y., Xu, S.-H., Zhu, J.-J., Zhou, N.-Q. and Wu, C.-Y., 1997. Study on the contamination of fracture-karst water in Boshan District, China. *Groundwater*, 35(3): 538-545.
- Zseni, A., 2002. The role of soil cover in the evolution of karrenfelds. In: F. Gabrovsek (Editor), *Evolution of Karst: From Prekarst to Cessation*. Littera picta, Ljubljana-Postojna, pp. 299-306.

# VITA

Linda Leann Martin

## Date and Place of Birth

August 6, 1952, Pottstown, Pennsylvania

## Education

2001, M.S., Interdisciplinary Resource Planning/Biology Program. Missouri State University (former Southwest Missouri State University), Springfield, Missouri. Thesis title: "Geomorphic Adjust of Ozark Stream Channels to Urbanization, Southwest Missouri"

1998, B.S., Geography, Environmental Science Emphasis. Missouri State University (former Southwest Missouri State University), Springfield, Missouri

1994, A.S., Environmental Science. Drury University (former Drury College), Springfield, Missouri

## Professional Experience

2003-2004 Teaching Assistant, Department of Geography, University of Kentucky, Lexington, Kentucky

2001-2002 Research Assistant, and Assistant Physical Geography Lab Manager, Department of Geography, University of Kentucky, Lexington, Kentucky

2002 (summer) Interpreter, Lake Roosevelt National Recreation Area, Coulee Dam, Washington

2001 (summer) Instructor, Department of Geography, Geology and Planning, Southwest Missouri State University, Springfield, Missouri

2000-2001 Teaching Assistant, Department of Geography, Southwest Missouri State University, Springfield, Missouri

## Scholastic and Professional Honors

2004-2006 U.S. Environmental Protection Agency STAR Fellowship

2004 and 2005 University of Kentucky Graduate School Incentive Award

2004 Geological Society of America Student Research Award for dissertation research

March 2004 Best Student Paper, Association of American Geographers Geomorphology Specialty Group Student Paper Session, Philadelphia, Pennsylvania

2001-2003 Daniel R. Reedy Quality Achievement academic year fellowship award, University of Kentucky, Lexington, Kentucky

April 2001 Best Presentation, Interdisciplinary Graduate Forum of Southwest Missouri State University, Springfield, Missouri

April 2000 Best Presentation, Interdisciplinary Graduate Forum of Southwest Missouri State University, Springfield, Missouri

April 2000 Best Masters Thesis Proposal, Geomorphology Specialty Group, Association of American Geographers Annual Meeting, Pittsburgh, Pennsylvania

**Professional Publications**

Phillips, J.D., Martin, L.L., Nordberg, V.G., Andrews, W.A., 2004. Divergent evolution in fluviokarst landscapes of central Kentucky." *Earth Surface Processes and Landforms* 29: 799-819.

Linda Leann Martin